ELUCIDATING THE CALCIUM OXIDE DERIVED FROM THE WASTE SHELLS OF MUD CLAM (GELOINA EXPANSA) AS A CATALYST FOR BIODIESEL PRODUCTION

ARTICLES FOR FACULTY MEMBERS

Biodiesel production from waste cooking oil using calcium oxide derived from scallop shell waste / Puspitasari, P., Pramono, D. D., Fiansyah, D. N., Permanasari, A. A., Mufti, N., & Razak, J. A.

Clean Energy
Volume 8 Issue 2 (2024) Pages 113–126
https://doi.org/10.1093/CE/ZKAE005
(Database: Oxford University Press)

Calcium oxide waste-based catalysts for biodiesel production and depollution: A review / Teo, C. K., Chia, P. W., Nordin, N., Kan, S. Y., Ismail, N. M., Zakaria, Z., Liew, R. K., Wu, L., & Yong, F. S. J.

Environmental Chemistry Letters
Volume 22 Issue 4 (2024) Pages 1741–1758
https://doi.org/10.1007/s10311-024-01740-4
(Database: Springer Nature Link)

Efficient conversion of leather tanning waste to biodiesel using crab shell-based catalyst: Waste-to-energy approach / Yuliana, M., Santoso, S. P., Soetaredjo, F. E., Ismadji, S., Ayucitra, A., Gunarto, C., Angkawijaya, A. E., Ju, Y. H., & Truong, C. T.

Biomass and Bioenergy
Volume 151 (2021) 106155 Pages 1-9
https://doi.org/10.1016/J.BIOMBIOE.2021.106155
(Database: ScienceDirect)

ELUCIDATING THE CALCIUM OXIDE DERIVED FROM THE WASTE SHELLS OF MUD CLAM (GELOINA EXPANSA) AS A CATALYST FOR BIODIESEL PRODUCTION

ARTICLES FOR FACULTY MEMBERS

Exploration of efficiency of nano calcium oxide (CaO) as catalyst for enhancement of biodiesel production / Malek, M. N. F. A., Pushparaja, L., Hussin, N. M., Embong, N. H., Bhuyar, P., Rahim, M. H. A., & Maniam, G. P.

Journal of Microbiology, Biotechnology and Food Sciences
Volume 11 Issue 1 (2021) e3935 Pages 1-4
https://doi.org/10.15414/JMBFS.3935
(Database: Faculty of Biotechnology and Food Sciences, Universiti Malaysia Pahang)

From waste to catalyst: Transforming mussel shells into a green solution for biodiesel production from jatropha curcas oil / Alsabi, H. A., Shafi, M. E., Almasoudi, S. H., Mufti, F. A. M., Alowaidi, S. A., Sharawi, S. E., & Alaswad, A. A.

Catalysts
Volume 14 Issue 1 (2024) 59 Pages 1-18
https://doi.org/10.3390/catal14010059
(Database: MDPI)

Preparation and characterization of shell-based CaO catalysts for ultrasonication-assisted production of biodiesel to reduce toxicants in diesel generator emissions / Chong, N. S., Nwobodo, I., Strait, M., Cook, D., Abdulramoni, S., & Ooi, B. G.

Energies
Volume 16 Issue 14 (2023) 5408 Pages 1-20
https://doi.org/10.3390/en16145408
(Database: MDPI)

ELUCIDATING THE CALCIUM OXIDE DERIVED FROM THE WASTE SHELLS OF MUD CLAM (GELOINA EXPANSA) AS A CATALYST FOR BIODIESEL PRODUCTION

ARTICLES FOR FACULTY MEMBERS

Progress on modified calcium oxide derived waste-shell catalysts for biodiesel production / Ooi, H. K., Koh, X. N., Ong, H. C., Lee, H. V., Mastuli, M. S., Taufiq-Yap, Y. H., Alharthi, F. A., Alghamdi, A. A., & Mijan, N. A.

Catalysts
Volume 11 Issue 2 (2021) 194 Pages 1–26
https://doi.org/10.3390/catal11020194
(Database: MDPI)

Snail shells as a heterogeneous catalyst for biodiesel fuel production / Gaide, I., Makareviciene, V., Sendzikiene, E., & Kazancev, K.

Processes
Volume 11 Issue 1 (2023) 260 Pages 1-13
https://doi.org/10.3390/pr11010260
(Database: MDPI)

Synthesis of green biodiesel using heterogeneous catalyst derived from snail shells / Chaib, A., Benammar, S., Hamitouche, A. E., Bachari, K., & Boudjemaa, A.

Environmental Progress and Sustainable Energy
(2025) e70084 Pages 1- 13
https://doi.org/10.1002/ep.70084
(Database: Wiley Online Library)

ARTICLES FOR FACULTY MEMBERS

ELUCIDATING THE CALCIUM OXIDE DERIVED FROM THE WASTE SHELLS OF MUD CLAM (GELOINA EXPANSA) AS A CATALYST FOR BIODIESEL PRODUCTION

Biodiesel production from waste cooking oil using calcium oxide derived from scallop shell waste / Puspitasari, P., Pramono, D. D., Fiansyah, D. N., Permanasari, A. A., Mufti, N., & Razak, J. A.

Clean Energy
Volume 8 Issue 2 (2024) Pages 113–126
https://doi.org/10.1093/CE/ZKAE005
(Database: Oxford University Press)

Clean Energy, 2024, Vol. 8, No. 2, 113–126
https://doi.org/10.1093/ce/zkae005
Advance access publication 6 March 2024
Research Article

Biodiesel production from waste cooking oil using calcium oxide derived from scallop shell waste

Poppy Puspitasari[1,2,*], Diki Dwi Pramono[1], Davi Nur Fiansyah[1] Avita Ayu Permanasari[1,2], Nandang Mufti[2,3] and Jeefferie Abd Razak[4]

[1]Department of Mechanical and Industrial Engineering, Universitas Negeri Malang, Malang, Indonesia
[2]Centre of Advanced Material and Renewable Energy, Universitas Negeri Malang, Malang, Indonesia
[3]Department of Physics, Faculty of Mathematics and Natural Sciences, Universitas Negeri Malang, Malang, Indonesia
[4]Fakulti Kejuruteraan Pembuatan, Universiti Teknikal Malaysia Melaka, Melaka, Malaysia
*Corresponding author. E-mail: poppy@um.ac.id

Abstract

Biodiesel is one of the alternative forms of diesel fuel and can be obtained using the transesterification process of waste cooking oil with a catalyst to accelerate the reaction. The heterogeneous catalyst from waste scallop shells is used due to its potential for being reused in the subsequent transesterification reactions. Heterogeneous catalysts can also be recycled, contributing to their environmentally friendly nature. This study aims to identify the performance of recycling a calcium oxide (CaO) catalyst from scallop shell waste on synthesis biodiesel. The method used is the transesterification method with the basic ingredients of waste cooking oil using a CaO catalyst. Then, after the transesterification process is complete, the catalyst is separated from the biodiesel and recycled to be reused in the transesterification process up to five times. The biodiesel samples obtained are identified for yield value, physico-chemical properties, thermal properties and performance. X-ray diffraction characterization results for the CaO catalyst show that it has a crystal size of 67.83 nm. Scanning electron microscope characterization shows that it has spherical particle shapes. Fourier transform infrared characterization shows the presence of Ca–O bonds. The highest biodiesel yield value of 74.23% is obtained in biodiesel Cycle 1. The flash point value of biodiesel samples ranges from 141.2°C to 149°C. Further, all of the biodiesel samples exhibit a cetane number of 75. The highest lower heating value of 38.22 MJ/kg is obtained in biodiesel Cycle 1 and the viscosity of the biodiesel samples ranges from 5.65 to 5.88 cSt. The density of the biodiesel samples ranges from 881.23 to 882.92 kg/m^3. Besides, ester functional groups (C=O) and methyl functional groups have been successfully formed in all samples, with the methyl oleate compound observed as dominating the biodiesel samples. The cloud point value of the biodiesel samples ranges from 12°C to 13°C, and their pour point value ranges from 10°C to 12°C. The lead content in biodiesel is 0.8826 mg/kg. The lowest sulphur content is obtained from biodiesel Cycles 1 and 2 at 0.005%. Performance tests show that biodiesel has lower torque and brake power values than commercial diesel fuel and higher specific fuel consumption values than commercial diesel fuel.

Graphical Abstract

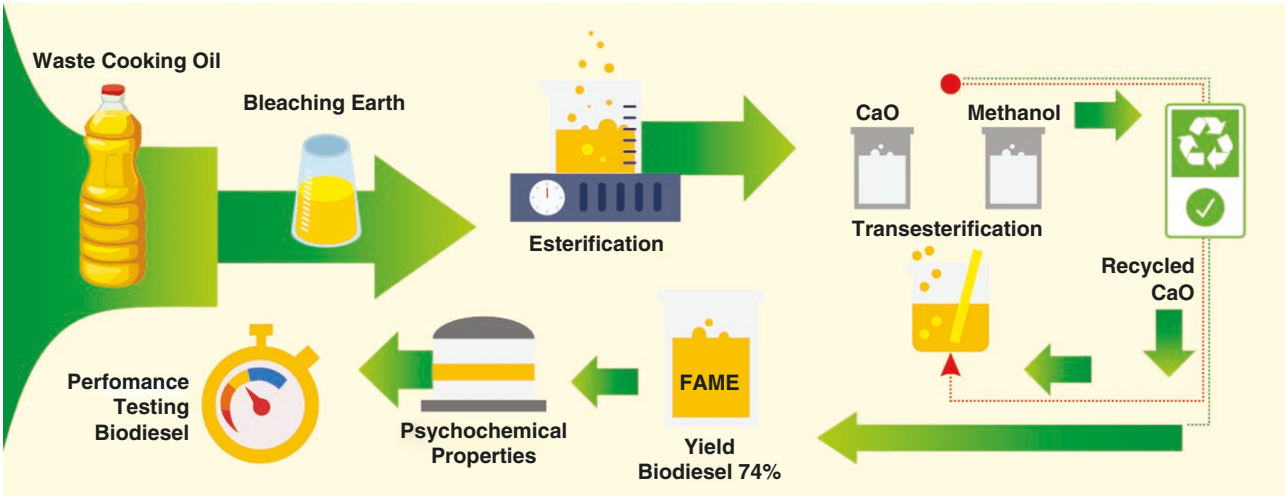

Keywords: biodiesel; CaO catalyst; waste cooking oil; scallop shell

Received: 2 October 2023. **Accepted:** 11 January 2024

Introduction

The industrial sector mostly utilizes gas, coal and electricity as energy sources, apart from diesel oil and fuel oil [1]. Consequently, fossil fuels are depleting at a concerning rate, suggesting the need to formulate alternative fuel sources to meet the continuously rising energy demand [2]. By 2050, energy consumption is expected to accelerate further as it replaces the consumption of costlier oil fuels, necessitating a focus on reducing the use of fossil fuels [1].

The increasing use of fossil energy has led to the addition of greenhouse gases, resulting in climate instability and rising global temperatures [3, 4]. This has brought a series of environmental challenges, such as the energy crisis and the greenhouse effect, which have seriously affected the environment on which humans depend [5]. Efforts to prevent the greenhouse effect are to replace alternative fossil fuels [6].

Biodiesel is a type of biofuel that can be used as an alternative fuel for diesel engines [7]. Biodiesel is produced from raw materials obtained from vegetable oils, animal fats and used cooking oil [1]. Its production is easy to adjust to the needs, environmentally friendly, non-toxic, biodegradable, has low viscosity and has a high cetane number [8, 9].

Biodiesel consists of fatty acid alkyl esters and can be produced by a method called transesterification, which is by reacting renewable oils such as oils from soybean [10], palm oil [11], sunflower oil [12], Jatropha curcas [13], Moringa oleifera [14] and waste cooking oil [15], and it can be produced from animal fats using alcohol as primary substance into the esters [16].

The transesterification reaction has the disadvantage of being a slow process; therefore, the addition of a catalyst is needed to accelerate the transesterification reaction. Homogeneous catalysts and heterogeneous catalysts can be used in the transesterification process. The catalysts commonly used in the transesterification reaction process on biodiesel are NaOH and KOH, which are classified as homogeneous base catalysts [17]. Homogeneous catalysts used in the biodiesel transesterification process have the disadvantage of costing more because the biodiesel purification process is more complex [18]. Another disadvantage of homogeneous catalysts is the characteristic that they can dissolve in biodiesel and glycerol, so water is needed to remove the dissolved catalyst content [19]. The main disadvantage of homogeneous catalysts is that they cannot be reused [20].

Catalyst reuse is an advantage of heterogeneous catalysts. One of the reusable catalysts comes from heterogeneous catalysts. Heterogeneous catalysts are more advantageous than homogeneous catalysts because heterogeneous catalysts can be recycled so that they are more environmentally friendly. The use of heterogeneous catalysts in biodiesel transesterification can reduce production costs because they are easily separated from the product medium, can be recycled and are less saponification in the reaction medium during the biodiesel purification process [21]. One of the materials included in the heterogeneous catalyst type is calcium oxide (CaO). CaO is the most sustainable and cost-effective heterogeneous catalyst [22]. CaO-based catalysts are heterogeneous, inexpensive and abundant in nature. CaO-based catalysts can also be obtained from the waste of living things such as scallop shells [23].

Scallop shells are 97–99% composed of calcium carbonate ($CaCO_3$) [24]. The calcium contained in scallop shell waste that can be used as a catalyst for transesterification reactions must go through a calcination process at high temperatures [23]. The high level of calcium contained in the scallop shell has the potential to be the basic material for making CaO as a biodiesel catalyst; on the other hand, this can also be a breakthrough in overcoming problems related to the utilization of waste from the processing of scallop shells that are happening in Indonesia.

1 Novelty

Previous studies have successfully found that shell waste can be used as an alternative heterogeneous catalyst for biodiesel synthesis using a transesterification reaction [1, 25, 26]. However, some studies have not found much catalyst recycling performance from shell waste. The research of Degfie *et al.* successfully optimized biodiesel synthesis parameters using CaO catalysts [27] but the CaO used did not come from shell waste. In this study, the catalyst base material used is scallop shell waste and the biodiesel base material used is used cooking oil; this study also identifies the effect of recycling CaO catalysts that have previously been used in the biodiesel transesterification process and reused in the biodiesel transesterification process up to five times on the physico-chemical and thermal properties of each biodiesel produced.

2 Materials and methods

2.1 Materials

Waste cooking oil was obtained from several local fried chicken sellers. The chemicals used were methanol, sulphuric acid (H_2SO_4), n-Hexane and phenolphthalein, and were of analytical reagent grade from Smart Lab (Indonesian). The catalyst used in this study came from scallop shell waste obtained from Kampung Nelayan, Gresik, East Java, Indonesia. Bleaching earth was purchased from a local seller.

2.2 Instrument and apparatus

Three neck flasks, Allihn Condenser glass, a glass funnel, beaker glass, a pycnometer and a separating funnel were purchased form Iwaki Glass, Indonesia. A digital stick probe thermometer was purchased from TENMA, Japan and a hotplate magnetic stirrer came from Thermo Fisher Scientific, USA. Whatman filter paper was from SigmaAldrich, USA and a Muffle Furnace KSL-1750X-KA3 was from MTI Corporation, China. A Centrifuge LC-04R came from Oregon, China and a WANT Analytical Balance Model 2204H with Readability 0.1 mg came from WANT Balance Instrument Company, China. Paraffin Film PM-996 was obtained from Parafilm, USA and a Vacuum-Desiccator NOVUS DN 150 clear, with a porcelain plate, thread lid GL32 MOBILEX, with PBT came from Duran Wheaton Kimble, USA.

2.3 Experimental procedures

2.3.1 *Preparation of cooking oil*

Waste cooking oil was obtained from several local fried chicken sellers. The collected oil was purified through mixing using bleaching earth at a ratio of 10:1 for the used cooking oil and bleaching earth [28]. The mixing of the bleaching earth and the cooking oil was carried out at 80°C, then it was set aside for 24 hours [29]. The resulting sediment was separated and filtered to remove the residue.

2.3.2 *Preparation of the CaO catalyst*

The $CaCO_3$ sample from scallop shells was synthesized using the wet ball milling method through a 'planetary ball mill' [30]. This process was performed using a water medium with

a 3:1 mass fraction from the $CaCO_3$ micro powder sample [31]. In this study, four differently sized balls were employed, with three balls for each size [32]. The sample mass ratio was 1:20 from the mass of the total ball being used in the process [32, 33]. The milling process was carried out for 40 hours, with the rotation of the milling machine alternating between clockwise and counterclockwise every 15 minutes [31]. The suspension resulting from the ball milling was subsequently filtered using filter paper and the obtained sediment was dried at 110°C using an oven [34, 35]. The dried sediment was then crushed [34], followed by calcination at a temperature of 900°C for 2 hours [36]. After calcination, the catalyst was stored in a vacuum desiccator.

2.3.3 *Preparation of biodiesel using waste cooking oil and catalyst recycling*

The prepared waste cooking oil was be used in the transesterification process as shown in Fig. 1. The transesterification process of used cooking oil into biodiesel was carried out by adding 1 wt% of CaO with oil to methanol at a 1:8 molar ratio. The mixture was then stirred at 60°C with a speed of 1400 r.p.m. for 90 minutes [27]. After the transesterification process was complete, the mixture was then centrifuged for 5 minutes at 3000 r.p.m. to separate the CaO catalyst [37].

In the CaO catalyst recycling stage, the catalyst that had been successfully separated was then washed using n-Hexane [38] and then a filtration process was carried out to filter the CaO catalyst. The filtrated catalyst was then dried using an oven at 100°C for 12 hours [39]. To achieve an optimal level of fineness, the catalyst underwent a crushing process for 1 hour. The catalyst was then calcined at 900°C for 2 hours [36]. After calcination, the crucible containing the CaO catalyst was sealed using paraffin film and stored in a vacuum desiccator. The pulverized catalyst would be reused in the next cycle of biodiesel synthesis. The process was repeated for up to five cycles.

In the separation process using glycerol, the mixture was allowed to stand overnight so that the biodiesel and glycerol were separated using a separating funnel [40]. The mixture that had been separated using glycerol produced biodiesel [40]. The biodiesel was then washed using warm water to remove the remaining glycerol that was still contained in the biodiesel [41]. Biodiesel that had been washed using warm water was then heated to 110°C for 1 hour to reduce the water content [41].

2.4 Instrumental characterization

2.4.1 *Test for phase and crystallite size of the CaO catalyst*

The phase and crystallite size of the biocatalyst CaO was measured using X-ray diffraction (XRD) [42]. The XRD test was conducted at the Laboratory of Minerals and Advanced Materials of Universitas Negeri Malang, utilizing a Pananaltyical Expert Pro X-ray.

2.4.2 *Test for morphology of the CaO catalyst*

The surface morphology of the CaO biocatalyst was examined using a scanning electron microscope (SEM) [43]. The test was conducted at the Laboratory of Minerals and Advanced Materials of Universitas Negeri Malang, utilizing an FEI Japan Inspect-S50.

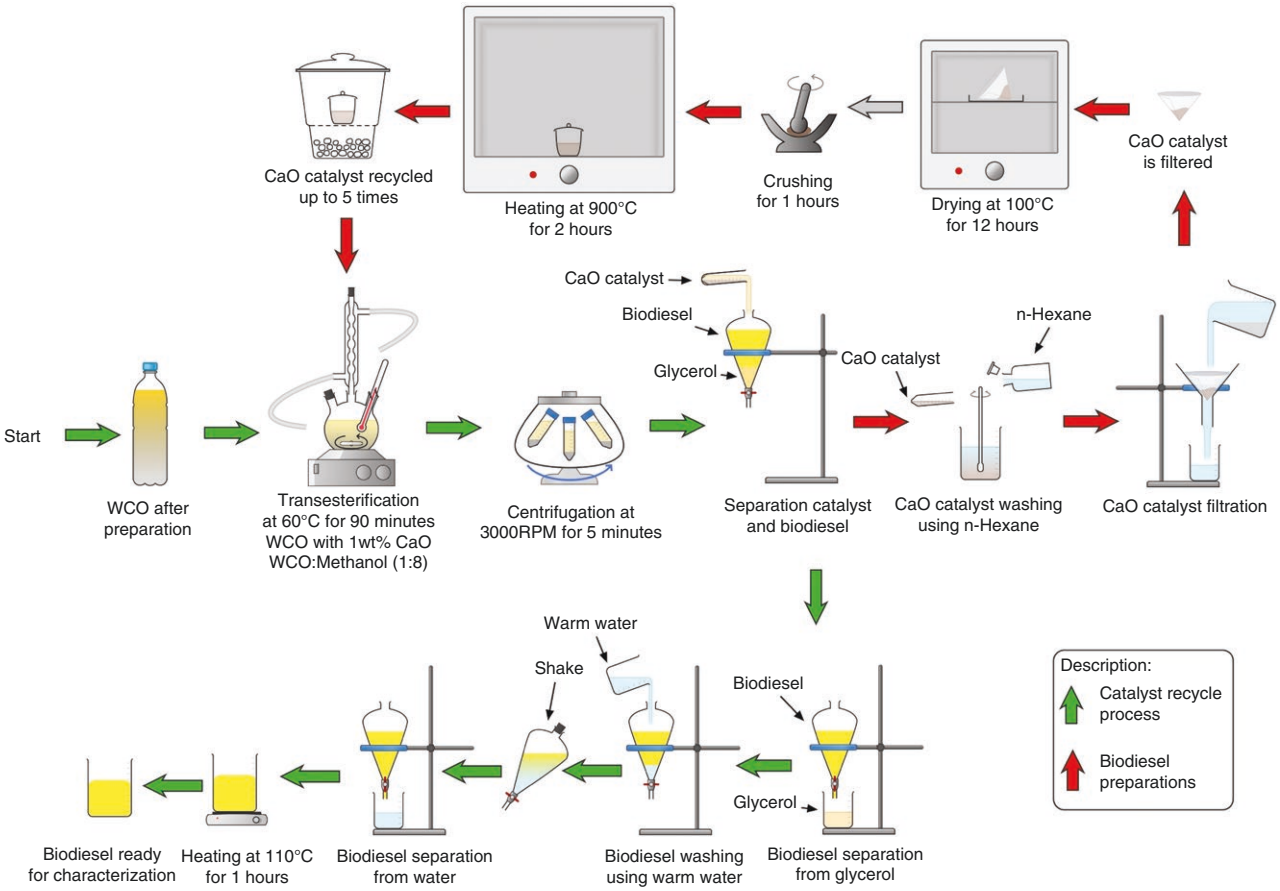

Fig. 1 : Schematic diagram of biodiesel preparation using waste cooking oil and recycling catalysts

2.4.3 Test for functional groups of the CaO catalyst and biodiesel

The functional groups of the CaO biocatalyst and biodiesel were determined using Fourier transform infrared (FTIR) spectroscopy [40, 43]. The FTIR test was conducted at the Laboratory of Minerals and Advanced Materials, Universitas Negeri Malang, using a Shimadzu instrument, IR Prestige 21 model.

2.4.4 Test for biodiesel yield

The biodiesel yield test was performed to identify the performance and efficiency of the catalyst recycling during the transesterification process. The quantity and type of catalyst significantly influence the biodiesel yield. Meanwhile, the presence of a catalyst made a substantial impact on the rate of the transesterification reaction. The biodiesel yield test was conducted for each cycle of catalyst recycling. The percentage of biodiesel yield was estimated using Equation (1) [44]:

$$\text{Yield } \% = \text{Weight of methyl ester/weight of oil} \quad (1)$$

The mass of the methyl ester was obtained from the result of the transesterification of the used cooking oil, while the mass of the oil refers to the initial mass of the sterilized used cooking oil that had not yet undergone the transesterification process [45]. Biodiesel yield was calculated for each cycle to assess the catalyst recycling performance. Thus, since there were five cycles, five biodiesel yields were calculated.

2.4.5 Test for compound composition of biodiesel

The compound composition was observed using the gas chromatography–mass spectrometry (GC–MS) method [40]. The GC–MS test was conducted at the Integrated Laboratory, Universitas Islam Indonesia and the GC–MS Shimadzu QP 2010 SE was used.

2.4.6 Test for flash point of biodiesel

The flash point of the fuel was measured using a flash point tester instrument [40]. Flash point tests necessitate a source of ignition. Biodiesel that meets the established standards can be categorized as suitable for being used. The flash point test was conducted using the Flash Point Tester SYD-3536 with the ASTM D93 collection method.

2.4.7 Test for cetane number of biodiesel

The cetane number indicates the ignition delay and quality of the diesel fuel. In a particular diesel engine, higher-cetane fuels will have shorter ignition delay periods than lower-cetane fuels [46]. The cetane number from the samples was analysed using the ASTM D 4737-11 standardization at the Energy and Environment Laboratory, Institut Teknologi Sepuluh Nopember, Surabaya.

2.4.8 Test for caloric value of biodiesel

The calculation parameters were obtained using an oxygen bomb calorimeter of XRY-1A type [47]. The calorific value testing in the research was conducted at the Laboratory of Mineral and Advanced Materials, Universitas Negeri Malang. The calorific value represents the amount of energy released when a substance is completely burned. It is typically measured in units of energy per unit mass, such as joules per gram (J/g) or calories per gram (cal/g). The calorific value test was carried out to determine the amount of energy generated by the biodiesel during the combustion process. A high heating value (HHV) and a low heating value (LHV) could also be determined from the calorific value testing. The formulas to calculate HHV and LHV are shown in Equations (2) and (3):

$$\text{HHV} = ((\Delta T \times E)40)/G \quad (2)$$

$$\text{LHV} = \text{HHV}3,052\,\text{MJ/kg} \quad (3)$$

2.4.9 Test for density of biodiesel

The density test was performed at the standard test temperature of 40°C [48]. The mass parameter was obtained from the analytic digital balance, while the volume was measured using a pycnometer of 25 ml [49].

The density of the biodiesel was estimated using Equation (4):

$$\rho = \text{m/v} \quad (4)$$

2.4.10 Test for viscosity of biodiesel

The obtained viscosity test represents the dynamic viscosity, which illustrates the ability of a fluid to resist shear flow, while kinematic viscosity can be considered as the resistance to fluid momentum [50]. Therefore, in this study, the kinematic viscosity was examined using Equation (5):

$$\vartheta = \mu/\rho \quad (5)$$

2.4.11 Test for cloud point of biodiesel

The cloud point is the temperature at which crystallization occurs and it starts when the solid crystal becomes visible when the fuel cools down [51]. There are no international standards for specifying the cloud point value [52] but lower cloud points represent a greater quality of biodiesel. In this study, the cloud point was analysed using the D2500 ASTM standardization in the Laboratorium Energy dan Lingkungan, Institut Sepuluh Nopember, Surabaya.

2.4.12 Test for pour point of biodiesel

The pour point is the temperature at which a significant amount of crystal aggregates has formed, causing the fuel to be non-flowable even when pumped [51]. Similar to the cloud point, there is no standard for the pour point specified on ASTM D6571 and EN 14214 [53]. The pour point test was conducted following the ASTM D97-02 standard at the Laboratorium Energy dan Lingkungan, Institut Sepuluh Nopember, Surabaya.

2.4.13 Test for lead content of biodiesel

The lead content test in biodiesel is crucial as it guarantees the safety of the biodiesel for utilization and adherence to established environmental regulations [52]. The lead content test was conducted using the Inductively Coupled Plasma Optical Emission Spectrometry (ICP OES) instrument at the Energy and Environmental Laboratory, Sepuluh Nopember Institute of Technology, Surabaya.

2.4.14 Test for sulphuric content of biodiesel

High sulphur content in fuel will result in sulphur-derived pollution after the combustion process [54]. For example, sulphur dioxide (SO_2) contributes to respiratory illnesses and aggravates heart and lung diseases, and it also contributes to acid rain [55]. A sulphuric content test was conducted following the ASTM D129 standard at the Laboratorium Energy dan Lingkungan, Institut Sepuluh Nopember, Surabaya.

2.4.15 Test for performance of biodiesel

The biodiesel performance test was carried out involving the B35 biodiesel samples and D100 diesel, specifically on torque, brake power and brake-specific fuel consumption. The frequency of performance test data collection was carried out three times. The

test was conducted using the Nissan Mazda R2 diesel engine. The specifications of the diesel engine for this test are presented in Table 1.

Further, the torque, brake power and brake-specific fuel consumption were estimated using Equations (6–8).

Calculation of torque:

$$T = W \times l \tag{6}$$

Calculation of brake power [56]:

$$BP = (2\pi \times n \times T)/(60.000) \tag{7}$$

Estimation of brake-specific fuel consumption [56]:

$$BFSC = FC/BP \tag{8}$$

$$FC = (v/t) \times \rho \times (3600/1000) \tag{9}$$

3 Results and discussion

3.1 Catalyst characterization

3.1.1 Phase and crystallite size of the CaO catalyst

The XRD test on the CaO catalyst was carried out to identify the phase and crystallite size of the scallop shell powder [57]. The crystallite size was calculated using the Scherrer [58] formula shown in Equation (10):

$$d = \frac{k \times \lambda}{\beta \cos\theta} \tag{10}$$

The obtained calculated XRD results are summarized in Table 2.

Table 2 shows that the CaO catalyst synthesized from scallop shell material has a crystal size of 67.83 nm. As illustrated in Fig. 2, the synthesized and sintered catalyst from scallop shell material at 900°C for 120 minutes exhibits CaO peaks at 32.28° (111), 37.45° (200), 53.96° (220), 64.47° (311), 67.74° (222), 79.82° (022) and 88.92° (400), consistently with the International Centre for Diffraction Data (ICDD) database No. 00-004-0777 [59–62]. In other words, $Ca(OH)_2$ was also observed on the catalyst at 18.28° (001), 34.11° (101), 47.17° (102) and 51.82° (110) [60–62]. The $Ca(OH)_2$ is characterized by the peaks comparable to ICDD database No. 00-004-0733. The $Ca(OH)_2$ is formed due to the reaction between CaO and H_2O in the air [63]. The $Ca(OH)_2$ phases originate from water molecules absorbed on the surface of the CaO, which has been widely acknowledged as hygroscopic, allowing the absorption of moisture from the air [64]. Analysis using the MATCH software also yielded information about the crystal structure of the CaO from the scallop shell powder. The CaO catalyst has a crystal shape with a cubic structure [65].

Table 1: Specifications of diesel engine

Technical item	Data
Type	Nissan Mazda R2
Number of cylinders	4 Cylinder 2184 cc OHV indirect injection
Pressure injection	100–130 bar
Valve slit	In 0.45 mm
	Ex 0.45 mm
Capacity bore/stroke	86/94 mm
Max output (din hp)/rpm	>64/4000
Max torque Nm/rpm	140/2000

Table 2: Intensity, full width half maximum (FWHM), d-spacing and crystallite size of the CaO catalyst

Sample	XRD Peak			
	Intensity (counts)	FWHM (rad)	d-spacing (Å)	Crystallite size (nm)
CaO catalyst	889	0.001 373 574	2.40 163	67.83

3.1.2 Morphology of the CaO catalyst

The SEM was used to identify the morphology of the CaO catalyst from the scallop shell waste.

Fig. 3 illustrates that the particle morphology of the CaO catalyst derived from the waste scallop shell has a spherical shape and is non-uniform in size [66–68]. The test results also indicated the presence of agglomeration, which can be attributed to several factors, such as the calcination temperature, calcination time, uneven crushing and the duration of the crushing process [30, 67, 69].

3.1.3 Functional groups of the CaO catalyst

FTIR characterization was conducted to find the functional group of the CaO catalyst from the scallop shell waste. The results of the FTIR are illustrated in Fig. 4.

Fig. 4 depicts the FTIR spectrum of the CaO catalyst derived from scallop shell waste. The peak at 3643.53 cm^{-1} indicates the presence of an OH stretching band during the water absorption by the CaO [70]. Meanwhile, the 'bands' of 1415.18, 1132.21 and 875.68 cm^{-1} correlate with the asymmetrical C–O with vibration from the carbonate groups [71, 72]. The peak at 875.68 cm^{-1} signifies the Ca–O bond [73].

3.2 Biodiesel characterization

Table 3 shows the test results on biodiesel synthesized using a CaO catalyst made from scallop shell waste. The test results were compared with the characteristics of diesel fuel and ASTM standards.

3.2.1 Yield of biodiesel

Reusing catalysts is a sign of catalyst stability, which is very important in lowering biodiesel production costs [74]. It demonstrates efficiency in resource use and can contribute to environmental safety by reducing the chemical waste generated. By effectively

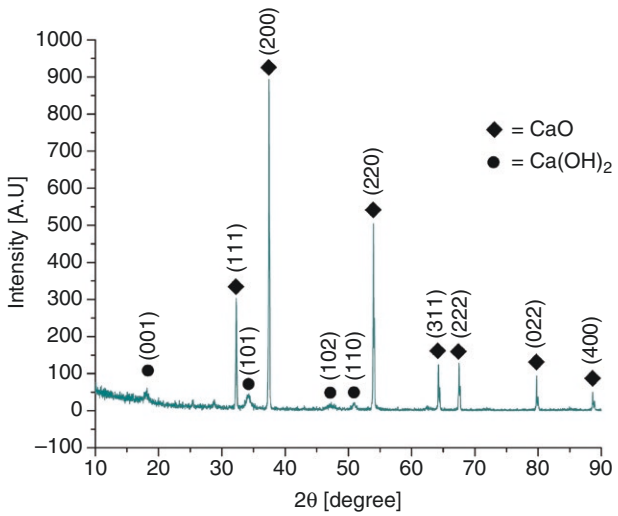

Fig. 2: XRD results for CaO catalyst from scallop shell

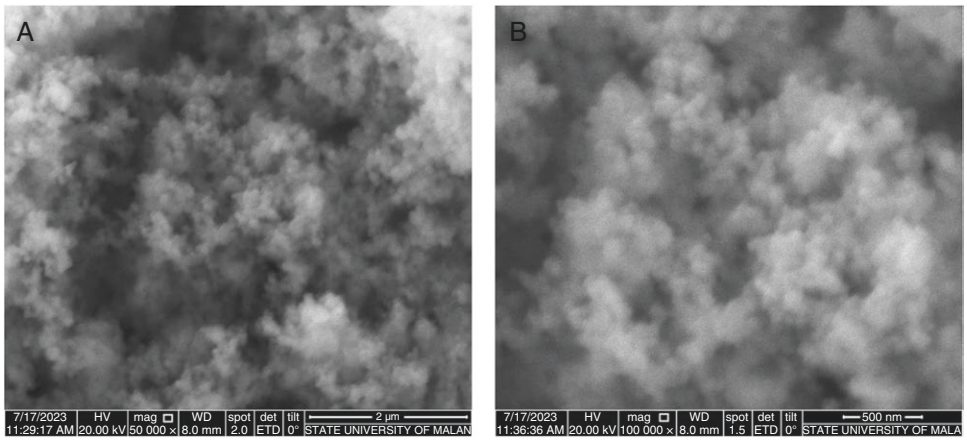

Fig. 3: Morphology CaO catalyst from scallop shell with (a) ×50 000 and (b) ×100 000 magnification

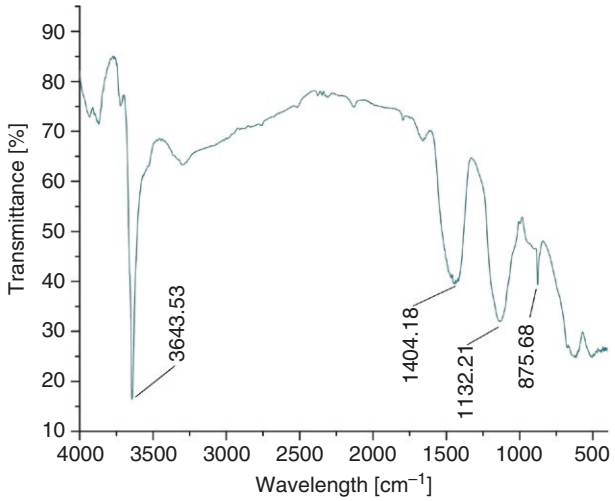

Fig. 4: FTIR results of CaO catalyst from scallop shell

reusing catalysts, the biodiesel production process can become more economically and ecologically sustainable. The value of the fatty acid methyl ester (FAME) generated from used cooking oil can be observed through the percentage yield of the biodiesel. Biodiesel yield is determined through the ratio of the biodiesel produced from the transesterification to the initial amount of used cooking oil. As depicted in Fig. 5, the highest biodiesel yield is obtained in the first cycle, reaching 74.23%. The yield gradually decreases in each subsequent cycle. Consequently, the lowest yield is recorded in the fifth cycle, at 57.04%. The effectiveness of the biocatalyst diminishes as the number of catalyst recycling cycles in the biodiesel transesterification process increases.

The decelerated biodiesel yield is attributed to the influence of catalyst recycling, in which the catalyst initially separates free fatty acids present in the feedstock and, subsequently, it is reused in subsequent cycles, repeating up to the fifth cycle. The lower biodiesel yield can also be caused by the diminished contact area between the reactants and the active catalytic sites [75], the decreasing stability of the biocatalyst CaO in subsequent cycles [76] and the reaction between the catalyst with CO_2 and H_2O, as well as the other impurities in the air [77].

In addition, the lower yield following the cycle indicates that the catalyst is contaminated by the air, forming $Ca(OH)_2$, which affects the reaction power in separating glycerol or free fatty acids in the used cooking oil. This aligns with the findings of a study conducted by Widayat *et al.* [38] in which the biodiesel yield value decreased as the recycling cycles of the CaO catalyst increased, owing to the formation of CaO and diglycerides.

3.2.2 *Flash point of biodiesel*

Based on Table 3, the highest flash point value of the biodiesel was obtained in the second cycle, measuring 149.7°C, while the lowest value was observed in the fourth cycle, at 141.2°C. The flash point value can be influenced by the density of the fuel. As shown in Fig. 2, the fourth cycle exhibited a low flash point value, which aligns with the lower density observed in that cycle. This observation is in line with the findings of Elangovan *et al.* [78], who reported that the flash point of the fuel is affected by density. Meanwhile, the lower flash point is affected by the alcohol residue in the biodiesel [79].

Following the standard, the flash point of biodiesel should be ≥100°C [48]. As illustrated in Fig. 6, the obtained flash point is in accordance with the Indonesian National Standard (SNI) 7182:2015 and ASTM D93. The higher flash point indicates the greater fuel resistance to ignition. In general, the flash point of biodiesel tends to be higher compared with fossil-derived diesel fuels, with biodiesel produced in the second cycle exhibiting a higher resistance to ignition, as shown in Fig. 6. This is because fossil diesel consists of molecules with lower molecular weight and branched compounds, leading to a lower flash point value [80].

3.2.3 *Cetane number of biodiesel*

The cetane number functions as the delay in ignition time between fuel injection and the start of combustion in an engine [81]. Table 3 presents the results of the cetane number test using the octane–cetane analyser method. The cetane number of the biodiesel is estimated based on the composition of FAMEs [82]. Noushabadi *et al.* [82] reported that a more significant cetane number signifies higher FAME content.

Fuels with higher cetane numbers tend to be more responsive to ignition under high pressure and have a shorter interval between the ignition moment and the onset of combustion [83]. This characteristic is crucial for optimizing the efficiency and performance of internal combustion engines. Besides, biodiesel produced from diverse sources exhibits variations in chemical composition and structure [83]. These variations lead to different fuel properties, particularly in cetane number and compression–ignition characteristics. The cetane number value of biodiesel

Table 3: Properties of biodiesel synthesized using recycled CaO catalyst

Sample	B100 Cycle 1	B100 Cycle 2	B100 Cycle 3	B100 Cycle 4	B100 Cycle 5	SNI	ASTM
Flash point (°C)	148.7 ± 2.34	149.7 ± 1.11	145.6 ± 3.13	141.2 ± 4.51	147.1 ± 5.52	Min. 100	Min. 130 (ASTM D93)
Cetane number	75	75	75	75	75	Min. 51	Min. 51 (ASTM D613)
Density (kg/m^3)	882.93 ± 0.46	882.11 ± 1.11	881.38 ± 0.46	881.23 ± 0.46	881.33 ± 0.46	850–890	860–900 (ASTM D1298)
Kinematic viscosity (cSt)	5.65 ± 0.73	5.7 ± 0.69	5.88 ± 0.83	5.68 ± 0.70	5.73 ± 0.78	2.3–6	1.9–6 (ASTM D445)
Cloud point (°C)	13	16	12	15	16	Max. 18	-3–19 (ASTM D2500)
Pour point (°C)	10	12	10	11	10	–	-4–16 (ASTM D97)
Lead content (mg/kg)	0.8826	0.9315	0.9617	0.9234	1.0378	–	–
Sulphur content (%)	0.005	0.005	0.006	0.007	0.007	Max. 0.05	Max. 0.05 (ASTM D5453)

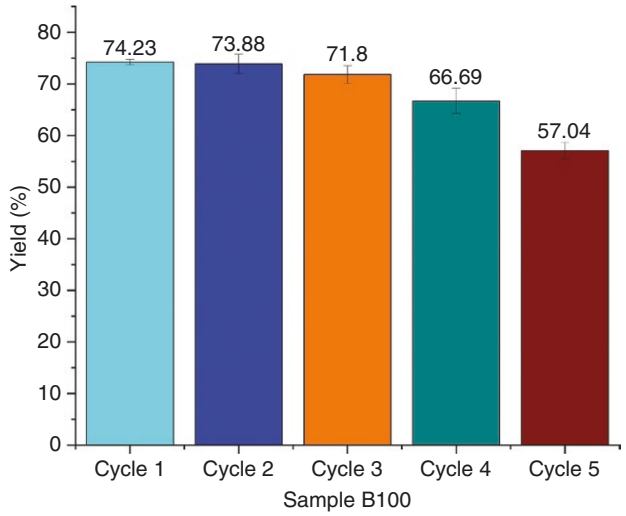

Fig. 5: Results of biodiesel yield from each cycle

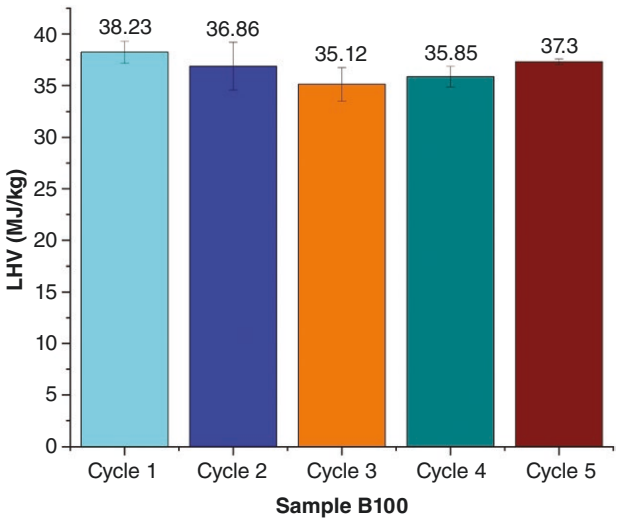

Fig. 6: Calorific value biodiesel from each cycle

can also indicate the fatty acid content of the biodiesel [25]. The higher the cetane number value of the diesel fuel, the more difficult it is to start a diesel engine, requiring a diesel engine with higher compression specifications.

3.2.4 *Calorific value of biodiesel*

The calorific value test was conducted to identify the energy content of the produced fuel [84]. Fig. 6 presents the LHV of the biodiesel from each cycle. The highest LHV is found in the biodiesel from the first cycle, at 38.23 MJ/kg, while the lowest value is observed in the biodiesel of the third cycle, at 35.12 MJ/kg. Biodiesel in the third cycle suggests a lower degree of saturation whereas biodiesel in the first cycle exhibits a higher degree of saturation. This aligns with the report from Van Gerpen *et al.* [85] that fuels with a higher degree of unsaturation tend to have slightly lower energy content per unit weight, while fuels with a higher degree of saturation tend to have higher energy content.

Universally, biodiesel presents a lower calorific value than pure diesel fuel [17]. The lower calorific value produced by biodiesel than pure diesel is also attributed to its lower carbon content [86]. The heating value of biodiesel fuel will affect the performance of diesel engines during performance testing [87, 88]. As the calorific value influences the specific fuel consumption, the higher calorific value corresponds to a lower specific fuel consumption [89].

3.2.5 *Density of biodiesel*

Density is obtained by dividing the mass of the biodiesel by its volume, while biodiesel volume was measured using a 25-ml pycnometer. Table 3 shows the consistent density values of biodiesel, with the highest and lowest recorded densities of 882.93 and 881.23 kg/m^3, respectively. The obtained density values shown in Table 3 conform to SNI 7182:2015, which specifies that biodiesel density should fall within the range of 850–890 kg/m^3 at a temperature of 40°C [48]. Further, a different density for each cycle is induced by fluctuation of the temperature and humidity during the density test.

According to [90], biodiesel that complies with SNI 7182:2015 generates complete combustion. Meanwhile, the density values exceeding the standard can lead to incomplete combustion reactions, thus affecting the emissions emitted by diesel engines [90]. Besides, high biodiesel density also significantly impacts the injector pump, fuel filter and ignition process of the diesel engine during the compression phase [91, 92]. Additionally, the variation in density values from each cycle can also be influenced by the

temperature during the transesterification reaction. As described by [90], different density values obtained from the biodiesel density test can be attributed to the fluctuating transesterification temperature.

3.2.6 *Kinematic viscosity of biodiesel*

Viscosity represents the resistance of a liquid to flow or the shear resistance of a liquid [90]. Table 3 shows the kinematic viscosity of the biodiesel across each cycle. The data indicate that the highest kinematic viscosity value is obtained in the third cycle, measuring 5.88 cSt, while the lowest kinematic viscosity value is observed in the first cycle, at 5.65 cSt. Ideally, biodiesel viscosity values should be within the range of 2.3–6.0 cSt at 40°C. Therefore, the obtained kinematic viscosity in this study has met the requirements for biodiesel. The first cycle has the lowest viscosity value, where the biodiesel in the first cycle has a more intense collision intensity between particles than the other cycles. A higher frequency of contact between particles will increase the efficiency, which in turn will significantly reduce the viscosity of the biodiesel [25].

Wahyuni observed that higher viscosity corresponds to a thicker and more resistant flow of liquid [93]. The fifth cycle of the transesterification process produces biodiesel that is more sluggish to flow compared with the biodiesel from other cycles due to its higher kinematic viscosity value. As presented in Table 3, we observed increasing viscosity in the biodiesel from the third cycle, indicating the exceeding boiling amount of methanol used in the transesterification process, which is 64.7°C [90]. High viscosity can cause an excess of smoke in the exhaust during combustion because it hinders the efficient atomization of fuel in the combustion chamber [94]. Evaporating methanol can impact viscosity values, thus resulting in variations in the kinematic viscosity across the cycles.

3.2.7 *Functional group of biodiesel*

The composition of biodiesel can be identified through the Fourier transform infrared (FTIR) test [95]. The results of the FTIR test in the biodiesel are illustrated in Fig. 7. The FTIR test is performed to detect the chemical bonds in a molecule, detected through infrared absorption spectra, which indicate different functional groups.

Fig. 7 show the results of the FTIR testing with a wavelength range of 500–4000 cm^{-1}. Based on Fig. 7, biodiesel samples from the first cycle to the fifth cycle have identical FTIR graphs. The

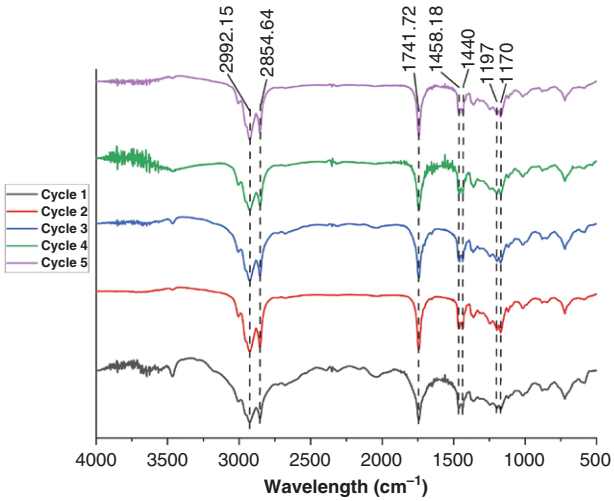

Fig. 7: FTIR spectrum for biodiesel sample from each cycle

wavelengths of 2922.15 and 2854.64 cm^{-1} indicate CH stretching in the CH_2 and CH_3 groups. This is in accordance with the research of Emma *et al.* [96], who said that CH stretching is shown in the absorption regions of 2922.87 and 2854.56 cm^{-1}. CH stretching is in the absorption region of 2800 cm^{-1} [37]. Rosset *et al.* [95] also explained that the CH bond is in the absorption region of 2800–3000 cm^{-1}. Referring to the research of Emma *et al.* [96], the ester (C=O) functional group is shown in the absorption region of 1741.72 cm^{-1} and the methyl functional group is shown in the absorption region of 1458.18 cm^{-1}. The presence of methyl ester compounds proven by using FTIR testing indicates that used cooking oil has been successfully synthesized into biodiesel [97].

3.2.8 *Compound composition of biodiesel*

Compound composition can be identified through using the GC–MS test. The results of the GC–MS test for the biodiesel in each cycle are summarized in Table 4.

Table 4 and Fig. 8 show the results of the GC–MS test, which show the compound components present in biodiesel samples from the first to the fifth cycles. The results indicate the dominating methyl oleate compound with a peak area of 53.7%. This is consistent with the findings of Zayed *et al.* [98] that the transesterification process of coconut oil produces FAMEs, with methyl oleate being the primary compound. Methyl oleate in biodiesel is associated with a lower calorific value and a high cetane number, contributing to reduced ignition delay and improved thermal efficiency [99].

As shown in Table 4, biodiesel samples from the first to the fifth cycles exhibit identical compound compositions. However, differences emerge in the biodiesel produced from the third to fifth cycles. Unlike the biodiesel from the first and second cycles, the biodiesel from the third cycle displays nine peaks, with the last peak indicating the presence of the $C_{30}H_{50}$ squalene compound. Squalene is a by-product compound that may be detected during biodiesel manufacturing [100]. The identified squalene compound indicates the presence of impurities within the produced biodiesel [100].

3.2.9 *Cloud point of biodiesel*

The cloud point of biodiesel can be determined through a test performed following the ASTM D2500 method. The cloud point represents the temperature at which small solid or crystal formation in the biodiesel occurs [101]. Table 3 presents the results of the cloud point test for biodiesel in each cycle. The highest cloud point is observed from the biodiesel in the second and fifth cycles at 16°C, while the lowest cloud point value is observed in the third cycle at 12°C. In general, the produced biodiesel complies with standards, as the maximum cloud point value is at 18°C [48].

There has been no international standard for the cloud point of biodiesel [52]. Barabás *et al.* reported that the cloud point of biodiesel ranges between –5°C and 17°C [102]. Biodiesel has a higher cloud point than fossil diesel fuel [102]. The saturation level of the fuel can affect the cloud point value and viscosity [37]. Meanwhile, a lower cloud point in biodiesel implies a lower operational temperature range, thereby indicating higher biodiesel quality [53]. Further, the formation of crystal aggregates can potentially clog the filters and precipitate in fuel tanks when the cloud point temperature is reached [103]. The biodiesel from the third cycle has a lower temperature at which crystal aggregates form.

3.2.10 *Pour point of biodiesel*

The pour point was observed using the ASTM D97-02 test and the results are summarized in Table 3. The pour point signifies

Table 4: Results of GC–MS on biodiesel samples from each cycle

Peak	Sample									
	B100 Cycle 1		B100 Cycle 2		B100 Cycle 3		B100 Cycle 4		B100 Cycle 5	
	Compound name	Formula	Compound name	Formula	Compound name	Formula	Compound name	Formula	Compound name	Formula
1	Methyl dodecanoate	$C_{13}H_{26}O_2$	Methyl dodecanoate	$C_{13}H_{26}O_2$	Methyl dodecanoate	$C_{13}H_{26}O_2$	Methyl dodecanoate	$C_{13}H_{26}O_2$	Methyl dodecanoate	$C_{13}H_{26}O_2$
2	Methyl tetradecanoate	$C_{15}H_{30}O_2$	Methyl tetradecanoate	$C_{15}H_{30}O_2$	Methyl tetradecanoate	$C_{15}H_{30}O_2$	Methyl tetradecanoate	$C_{15}H_{30}O_2$	Methyl tetradecanoate	$C_{15}H_{30}O_2$
3	Methyl palmitoleinate	$C_{17}H_{32}O_2$	Methyl palmitoleinate	$C_{17}H_{32}O_2$	Methyl palmitoleinate	$C_{17}H_{32}O_2$	Methyl palmitoleinate	$C_{17}H_{32}O_2$	Methyl palmitoleinate	$C_{17}H_{32}O_2$
4	Methyl hexadecanoate	$C_{17}H_{34}O_2$	Methyl hexadecanoate	$C_{17}H_{34}O_2$	Methyl hexadecanoate	$C_{17}H_{34}O_2$	Methyl hexadecanoate	$C_{17}H_{34}O_2$	Methyl hexadecanoate	$C_{17}H_{34}O_2$
5	Methyl octadec-9-enoate	$C_{19}H_{36}O_2$	Methyl octadec-9-enoate	$C_{19}H_{36}O_2$	Methyl octadec-9-enoate	$C_{19}H_{36}O_2$	Methyl octadec-9-enoate	$C_{19}H_{36}O_2$	Methyl octadec-9-enoate	$C_{19}H_{36}O_2$
6	Methyl octadecanoate	$C_{19}H_{38}O_2$	Methyl octadecanoate	$C_{19}H_{38}O_2$	Methyl octadecanoate	$C_{19}H_{38}O_2$	Methyl octadecanoate	$C_{19}H_{38}O_2$	Methyl octadecanoate	$C_{19}H_{38}O_2$
7	Methyl oleate	$C_{19}H_{36}O_2$	Methyl oleate	$C_{19}H_{36}O_2$	Methyl oleate	$C_{19}H_{36}O_2$	Methyl oleate	$C_{19}H_{36}O_2$	Methyl oleate	$C_{19}H_{36}O_2$
8	Methyl arachate	$C_{21}H_{42}O_2$	Methyl arachate	$C_{21}H_{42}O_2$	Methyl arachate	$C_{21}H_{42}O_2$	Methyl arachate	$C_{21}H_{42}O_2$	Methyl arachate	$C_{21}H_{42}O_2$
9					Squalene	$C_{30}H_{50}$	Squalene	$C_{30}H_{50}$	Squalene	$C_{30}H_{50}$

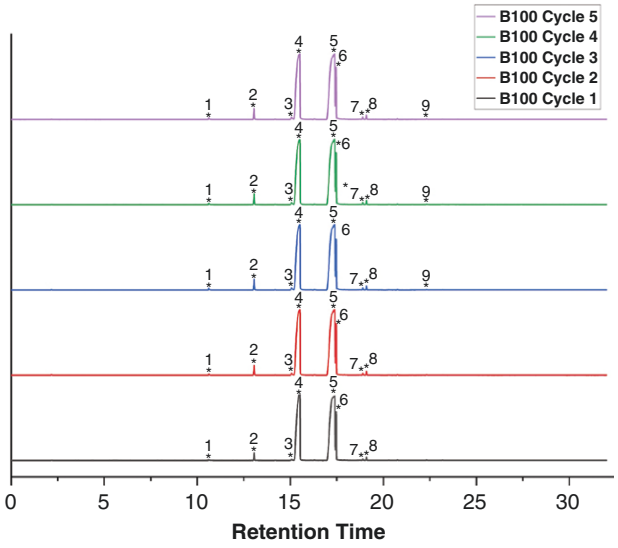

Fig. 8: Results of mass chromatography of biodiesel from each cycle

the temperature at which crystal aggregates form to a notable degree, resulting in the fuel becoming non-flowable even under pumping conditions [51]. The highest pour point is found from the second cycle at 12°C. Meanwhile, the biodiesel samples from the first, third and fifth cycles present the lowest pour point of 10°C. The pour point is generally lower than the cloud point [103].

The international standard for the pour point of biodiesel is given in ASTM D97 and EN 14214 [53]. Isioma *et al.* described that the pour point ranges from 0°C to 12°C [104]. As illustrated in Table 3, the biodiesel from the third cycle has better cold flow than the other cycles. A low pour point can enhance the performance of a diesel engine during cold weather by facilitating better acceleration [105]. This capability is crucial for optimal engine function, especially in frigid conditions, ensuring smoother operation and improved responsiveness.

3.2.11 *Lead content of biodiesel*

Based on Table 3, the highest lead content is observed in the fifth-cycle biodiesel at 1.0378 mg/kg, while the lowest lead content is found in the first-cycle biodiesel, at 0.8826 mg/kg. This trend indicates the increase in lead content following the progression of catalysis cycles during the biodiesel transesterification process. Excessive lead content in fuel can have adverse environmental effects, as lead is released through exhaust emissions from vehicle engines, which results in environmental pollution [106]. As per the resolution of the European Economic Community, the upper limit for lead content in fuel is established at 0.4% [52].

3.2.12 *Sulphur content of biodiesel*

Table 3 presents the sulphur content from the synthesized biodiesel using a CaO catalyst derived from the scallop shell. The lowest sulphur content was observed in the biodiesel sample from the first and second cycles, measuring 0.005%. In contrast, the highest sulphur content was found in the biodiesel samples from the fourth and fifth cycles, measuring 0.007%. The sulphur content from the synthesized biodiesel samples meets the requirements of SNI 718:2015 and ASTM D5453 standards [48]. The sulphur content exceeding the permissible amount carries detrimental effects on vehicle engines. In line with the research, Sirviö *et al.* [107] also state that the lower the sulphur content, the better the fuel quality. Fayad *et al.* [108] also mentioned that high sulphur content in fuel can cause combustion problems and increase combustion emissions. High sulphur content in fuel can increase soot and particulate emissions in the exhaust of all types of internal combustion engines, cause corrosion and have a damaging effect on advanced treatment systems used for CO, HC, NOx and particulate reduction [109]. Fuel sulphur also causes corrosion in the engine cylinder. In combustion, it is oxidized into sulphur dioxide. SO_2 will be further oxidized into SO_3 and then react again with water. The formed sulphuric acid, H_2SO_4, will condense on metal surfaces and cause corrosion [110].

3.3 Test of performance of biodiesel

3.3.1 *Torque*

Fig. 9 presents the decreasing torque as the engine speed increases from 1500 to 1900 r.p.m. in both the Biodiesel B35 sample and the D100 diesel fuel. Maximum loading is found at an engine speed of 1500 r.p.m., resulting in the highest torque of 33.72 Nm for Diesel D100 and 30.69 Nm for Biodiesel B35. Besides, Fig. 9 also indicates that Diesel D100 produces higher

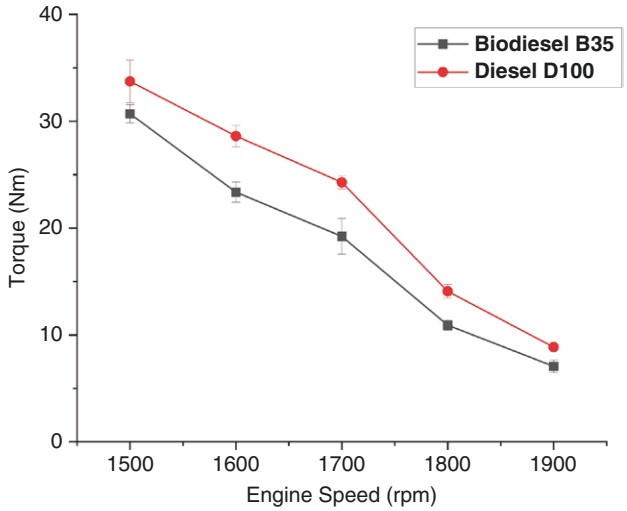

Fig. 9: Torque test results of Biodiesel B35 and Diesel D100 fuel samples at various engine speeds

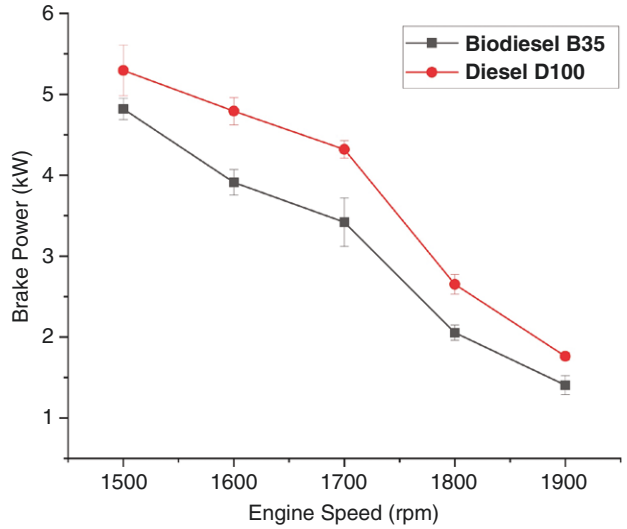

Fig. 10: Brake power test result of Biodiesel B35 and Diesel D100 fuel samples at various engine speeds

torque values compared with Biodiesel B35. The lower calorific value and higher viscosity of biodiesel compared with diesel contribute to poor combustion outcomes [111]. This is in accordance with the research of El-Adawy *et al.*, who said that the higher the calorific value of the fuel, the higher the torque produced [112]. Also, the purity of diesel fuel compared with biodiesel also affects the obtained torque values [113], thereby leading to higher torque values in Diesel D100 compared with Biodiesel B35.

The results demonstrate decreasing torque as the engine speed increases. This reduction in torque is attributed to the decreasing load generated as the engine speed increases. This finding is in line with Equation (6), in which the torque is directly proportional to the load and lever arm length. The lower engine speeds result in greater load values due to the torque test conducted using a braking system [114, 115].

3.3.2 *Brake power*

Fig. 10 illustrates a reduction in the brake power following the increase in engine speed, observed for both Biodiesel B35 and

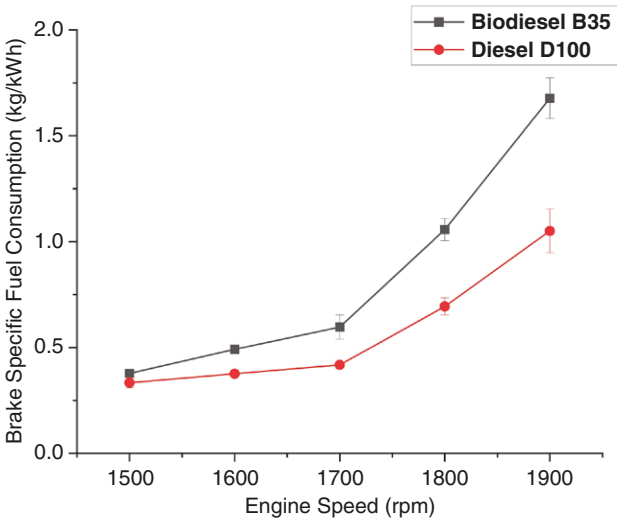

Fig. 11: Brake-specific fuel consumption test results of Biodiesel B35 and Diesel D100 fuel samples at various engine speeds

Diesel D100. The decline in brake power occurs within the range of engine speeds of 1500–1900 r.p.m. At an engine speed of 1500 r.p.m., a higher load is encountered. The peak of brake power is also recorded at an engine speed of 1500 r.p.m., amounting to 4.81 kW for Biodiesel B35 and 5.29 kW for Diesel D100. The brake power correlates directly with the torque, in agreement with Equation (7). Both the torque and the brake power will increase with escalating load conditions [116]. This is in line with the research of Dwivedi *et al.* [117], which states that the power generated from biodiesel fuel tends to be lower because biodiesel has a lower calorific value than diesel fuel.

The psychochemical properties also influence the generated brake power. As biodiesel contains less oxygen and possesses a lower calorific value compared with pure diesel fuel [118], it produces a lower brake power value for Biodiesel B35 as opposed to Diesel D100.

3.3.3 *Brake-specific fuel consumption*

The graph in Fig. 11 depicts an increase in the value of the brake-specific fuel consumption (BSFC) with the rise in engine speed. This rise occurs between the engine speeds of 1500 and 1900 r.p.m. for both Biodiesel B35 and Diesel D100. As per Fig. 11, Biodiesel B35 exhibits a higher value of BSFC compared with Diesel D100.

BSFC represents the fuel flow rate per unit of output power [119]. Fig. 11 shows an increase in BSFC following the higher engine speed. This greater BSFC is observed between the engine speeds of 1500 and 1900 r.p.m. for both Biodiesel B35 and Diesel D100. Besides, Fig. 11 also suggests that Biodiesel B35 has a higher BSFC than Diesel D100. At an engine rotation rate of 1500 r.p.m., Biodiesel B35 exhibits a BSFC of 0.38 kg/kWh, whereas Diesel D100 registers a BSFC of 0.33 kg/kWh.

The higher calorific value of pure diesel than biodiesel leads to a lower BSFC in pure diesel [116]. The lower BSFC value suggests better thermal efficiency [116]. The volumetric effects of a constant fuel injection rate, along with the high viscosity of biodiesel, also contribute to fuel consumption variations [120, 121].

4 Conclusion

Based on the results, the highest yield of biodiesel synthesized using the recycled CaO catalyst was obtained from the first cycle,

at 74.23%. However, as the recycling cycle progressed, the yield value gradually decreased. The physico-chemical and thermal properties (density, kinematic viscosity, functional groups, compound composition, cloud point, pour point, lead content, sulphur content, flash point) of the biodiesel synthesized using the recycled CaO catalyst met the requirements of the ASTM and SNI standards. The performance test results of the biodiesel synthesized using the recycled CaO catalyst showed lower torque and brake power values compared with Pertamina Dex. On the other hand, the BSFC value was higher than that of Pertamina Dex.

Biodiesel synthesized from used cooking oil using a CaO catalyst made from scallop shell waste has the potential to replace diesel fuel because the research that has been done shows that the biodiesel that has been synthesized has properties that meet international standards. The process of recycling and reusing CaO catalysts also shows positive results because the catalyst is still effectively used in the transesterification process up to three times.

Nomenclature

HHV, higher heating value (MJ/kg);
LHV, lower heating value (MJ/kg);
ΔT, differential temperature in the calorimetry system (°C);
E, heat capacity benzoic acid (12 460,2840 J/°C);
40, addition of ignition wire heat during the calibration (J);
G, sample mass (g);
ρ, biodiesel density (kg/m^3);
m, biodiesel mass (kg);
V, biodiesel volume (m^3);
ϑ, biodiesel kinematic viscosity (cSt);
μ, biodiesel dynamic viscosity (cP);
T, torque (Nm);
W, load (N);
L, sleeve length (m);
BP, brake power (kW);
n, engine rotation (r.p.m.);
BSFC, brake-specific fuel consumption (kg/kWh);
FC, fuel consumption (kg/jam);
v, fuel volume (ml);
t, fuel consumption time (s);
ρ, fuel density (g/ml);
k, constant (0.9);
β, full-width half maximum;
λ, XRD wavelength (1.5406 Å).

Author contributions

Poppy Puspitasari: Conceptualization, Methodology, Supervision, Reviewing and Editing; Diki Dwi Pramono: Data curation, Writing-Original draft preparation; Davi Nur Fiansyah: Data curation, Writing; Avita Ayu Permanasari: Methodology, Supervision; Nandang Mufti: Reviewing and Editing, Investigation; Jeefferie Abd Razak: Reviewing and Editing.

Conflict of interest statement

None declared.

Funding

This work was supported by Universitas Negeri Malang for the PUI CAMRY 2023 Research Grant (5.4.862/UN32.20.1/LT/2023).

Data Availability

The data underlying this article are available in Zenodo, at https://doi.org/10.5281/zenodo.10409069.

References

[1] Susvira D. Synthesis of biodiesel from waste cooking oil using heterogeneous catalyst (CaO) based on duck eggshell with transesterification reaction. *Jurnal Kartika Kimia*, 2022, 5:40–43.
[2] Premkumar S, Radhakrishnan K, Kalidoss R, *et al*. Synthesis, characterization and application of SnO_2 @ rGO nanocomposite for selective catalytic reduction of exhaust emission in internal combustion engines. *Catalyst*, 2023, 13:381.
[3] Martins F, Felgueiras C, Smitkova M, *et al*. Analysis of fossil fuel energy consumption and environmental impacts in European countries. *Energies*, 2019, 12:964.
[4] Lamb WF, Wiedmann T, Pongratz J, *et al*. A review of trends and drivers of greenhouse gas emissions by sector from 1990 to 2018. *Environ Res Lett*, 2021, 16:073005.
[5] Li W, Ma J, Liu H, *et al*. Investigations on combustion system optimization of a heavy-duty natural gas engine. *Fuel*, 2023, 331:125621.
[6] Papież M, Śmiech S, Frodyma K, *et al*. Decoupling is not enough: evidence from fossil fuel use in over 130 countries. *J Clean Prod*, 2022, 379:134856.
[7] Espootin S, Sameti M, Zaker S. Biodiesel from fish waste oil: synthesis via supercritical methanol and thermodynamic optimization. *Clean Energy*, 2021, 5:187–195.
[8] Sulaiman NF, Hashim ANN, Toemen S, *et al*. Biodiesel production from refined used cooking oil using co-metal oxide catalyzed transesterification. *Renew Energy*, 2020, 153:1–11.
[9] Thangaraj B, Solomon PR. Biodiesel production by the electrocatalytic process: a review. *Clean Energy*, 2021, 5:19–31.
[10] Gobikrishnan S, Park J-H, Park S-H, *et al*. Sonication-assisted production of biodiesel using soybean oil and supercritical methanol. *Bioprocess Biosyst Eng*, 2013, 36:705–712.
[11] Asri NP, Machmudah S, Wahyudiono, *et al*. Palm oil transesterification in sub- and supercritical methanol with heterogeneous base catalyst. *Chem Eng Process*, 2013, 72:63–67.
[12] Tchuessa EBH, Ouédraogo IWK, Richardson Y, *et al*. Production of biodiesel by ethanolic transesterification of sunflower oil on lateritic clay-based heterogeneous catalyst. *Catal Lett*, 2023, 153:2443–2455.
[13] Wang Y-T, Fang Z, Yang X-X. Biodiesel production from high acid value oils with a highly active and stable bifunctional magnetic acid. *Appl Energy*, 2017, 204:702–714.
[14] Boulal A, Atabani AE, Mohammed MN, *et al*. Integrated valorization of Moringa oleifera and waste Phoenix dactylifera L. dates as potential feedstocks for biofuels production from Algerian Sahara: an experimental perspective. *Biocatal Agric Biotechnol*, 2019, 20:101234.
[15] Joshi S, Gogate PR, Moreira PF, *et al*. Intensification of biodiesel production from soybean oil and waste cooking oil in the presence of heterogeneous catalyst using high speed homogenizer. *Ultrason Sonochem*, 2017, 39:645–653.

[16] Ndiaye M, Arhaliass A, Legrand J, *et al*. Reuse of waste animal fat in biodiesel: biorefining heavily-degraded contaminant-rich waste animal fat and formulation as diesel fuel additive. *Renew Energy*, 2020, 145:1073–1079.

[17] Ramirez J, Buest L, Lopez-Maldonado EA. Preparation and physicochemical characterization of biodiesel from recycled vegetable oil in Cuenca, Ecuador by transesterification catalyzed by KOH and NaOH. *Eng*, 2023, 4:954–963.

[18] Barros S, Pessoa Junior WAG, Sá ISC, *et al*. Pineapple (Ananás comosus) leaves ash as a solid base catalyst for biodiesel synthesis. *Bioresour Technol*, 2020, 312:123569.

[19] Li S, Cheng S, Cross JS. Homogeneous and heterogeneous catalysis impact on pyrolyzed cellulose to produce bio-oil. *Catalysts*, 2020, 10:178.

[20] Junior WAGP, Takeno ML, Nobre FX, *et al*. Application of water treatment sludge as a low-cost and eco-friendly catalyst in the biodiesel production via fatty acids esterification: process optimization. *Energy*, 2020, 213:118824.

[21] Mendonça IM, Paes OARL, Maia PJS, *et al*. New heterogeneous catalyst for biodiesel production from waste tucumã peels (Astrocaryum aculeatum Meyer): parameters optimization study. *Renew Energy*, 2019, 130:103–110.

[22] Zhang Y, Niu S, Han K, *et al*. Synthesis of the SrO–CaO–Al_2O_3 trimetallic oxide catalyst for transesterification to produce biodiesel. *Renew Energy*, 2021, 168:981–990.

[23] Mazaheri H, Ong HC, Amini Z, *et al*. An overview of biodiesel production via calcium oxide based catalysts: current state and perspective. *Energies*, 2021, 14:3950.

[24] Srichanachaichok W, Pissuwan D. Micro/Nano structural investigation and characterization of mussel shell waste in Thailand as a feasible bioresource of CaO. *Materials (Basel)*, 2023, 16:805.

[25] Azzahro UL, Broto W. Utilization of waste shells as CaO catalyst in biodiesel production from used cooking oil. *Acta Chimica Asiana*, 2022, 5:147–152.

[26] Ooi HK, Koh XN, Ong HC, *et al*. Progress on modified calcium oxide derived waste-shell catalysts for biodiesel production. *Catalysts*, 2021, 11:194.

[27] Degfie TA, Mamo TT, Mekonnen YS. Optimized biodiesel production from waste cooking oil (WCO) using calcium oxide (CaO) nano-catalyst. *Sci Rep*, 2019, 9:18982.

[28] Akbar T, Hendro A. Pemurnian Minyak Goreng Bekas dengan Menggunakan Adsorbent Zeolit dan Bleaching Earth. *Indonesian J Halal*, 2022, 4:16–24.

[29] Trisnaliani L, Ridwan KA, Fitriyanti D. Pretreatment Minyak Jelantah Dengan Menggunakan Adsorben Sebagai Bahan Baku Biodiesel. *KINETIKA*, 2019, 10:19–24.

[30] Puspitasari P, Fauzi AF, Susanto H *et al*. Synthesis and characterization of $CaCO_3$/CaO from Achatina fulica in various sintering time. In: *International Conference on Mechanical Engineering Research and Application (iCOMERA 2020)*, Vol. 2, Malang, Indonesia, 7–9 October, 2020, 012093.

[31] Gbadeyan OJ, Adali S, Bright G, *et al*. Optimization of milling procedures for synthesizing Nano-$CaCO_3$ from *Achatina fulica* shell through mechanochemical techniques. *J Nanomater*, 2020, 2020:4370172.

[32] Sargheini J, Ataie A, Salili SM, *et al*. One-step facile synthesis of $CaCO_3$ nanoparticles via mechano-chemical route. *Powder Technol*, 2012, 219:72–77.

[33] Dulian P, Bąk W, Wieczorek-Ciurowa K, *et al*. Controlled mechanochemical synthesis and properties of a selected perovskite-type electroceramics. *Mater Sci Poland*, 2013, 31:462–470.

[34] Camargo ILD, Lovo JFP, Erbereli R, *et al*. Influence of media geometry on wet grinding of a planetary ball mill. *Mater Res*, 2019, 22:e20190432.

[35] Ozkan A, Yekeler M, Calkaya M. Kinetics of fine wet grinding of zeolite in a steel ball mill in comparison to dry grinding. *Int J Miner Process*, 2009, 90:67–73.

[36] Boey P-L, Maniam GP, Hamid SA, *et al*. Utilization of waste cockle shell (Anadara granosa) in biodiesel production from palm olein: optimization using response surface methodology. *Fuel*, 2011, 90:2353–2358.

[37] Kedir WM, Wondimu KT, Weldegrum GS. Optimization and characterization of biodiesel from waste cooking oil using modified CaO catalyst derived from snail shell. *Heliyon*, 2023, 9:e16475.

[38] Widayat W, Darmawan T, Rosyid RA, *et al*. Biodiesel production by using CaO catalyst and ultrasonic assisted. *J Phys Conf Ser*, 2017, 877:012037.

[39] Fung S, Brahma S, Hoque M, *et al*. Advances in CaO-based catalysts for sustainable biodiesel synthesis. *Green Energy Resources*, 2023, 1:100032.

[40] Ameen M, Zafar M, Nizami A-S, *et al*. Biodiesel synthesis from Cucumis melo var. Agrestis seed oil: toward non-food biomass biorefineries. *Front Energy Res*, 2022, 10:830845.

[41] Wahyuni S, Kadarwati S, Latifah L. Sintesis Biodiesel Dari Minyak Jelantah Sebagai Sumber Energi Alternatif Solar. *Sainteknol: Jurnal Sains dan Teknologi*, 2011, 9:51–63.

[42] Pramono DD, Puspitasari P, Permanasari AA *et al*. Effect of sintering time on porosity and compressibility of calcium carbonate from Amusium Pleuronectes (Scallop Shell). In: *International Conference on Renewable Energy (I-CoRE 2021)*, Vol. 2, Malang, Indonesia, 7–8 October, 2021, 050003.

[43] Puspitasari P, Pramono DD. Phase identification, morphology, and compressibility of scallop shell powder (Amusium Pleuronectes) for bone implant materials. In: Karim SAA (ed). *Nanotechnologies in Green Chemistry and Environmental Sustainability*. Boca Raton: CRC Press, 2022, 5–25.

[44] Sinha P, Madavi AS. Study on yield percentage of biodiesel from waste cooking oil using transesterification. *Int J Appl Eng Res*, 2021, 16:154–160.

[45] Usaku C, Yahya AB, Daisuk P, *et al*. Enzymatic esterification/transesterification of rice bran acid oil for subsequent γ-oryzanol recovery. *Biofuel Res J*, 2023, 10:1830–1843.

[46] Ng J-H, Ng HK, Gan S. Development of emissions predictor equations for a light-duty diesel engine using biodiesel fuel properties. *Fuel*, 2012, 95:544–552.

[47] Permanasari AA, Ramadani R, Sukarni S *et al*. Fuel properties and chemical characterizations of waste cooking oil biodiesel-diesel (B20) with lemongrass essential oil bioadditive. In: *International Conference on Condensed Matters and Advanced Materials (IC2MAM)*, Vol. 2, Malang, Indonesia, 27 October 2020, 020049.

[48] Badan Standardisasi Nasional. *Biodiesel*, Vol. 7182. Jakarta, Indonesia: Standar Nasional Indonesia, 2015.

[49] Puspitasari P, Ayu Permanasari A, Ilman Hakimi Chua Abdullah M, *et al*. Tribology characteristic of ball bearing SKF RB-12.7/G20W using SAE 5W-30 lubricant with carbon-based nanomaterial addition. *Tribol Ind*, 2023, 45:664–675.

[50] Simpson DA. Surface engineering concepts. In: Simpson DA (ed). *Practical Onshore Gas Field Engineering*. Amsterdam: Elsevier Science, 2017, 221–272.

[51] Mejía JD, Salgado N, Orrego CE. Effect of blends of diesel and palm-castor biodiesels on viscosity, cloud point and flash point. *Ind Crops Prod*, 2013, 43:791–797.

[52] Prankl H, Körbitz W, Mittelbach M, *et al*. Review on biodiesel standardization world-wide. *IEA Bioenergy Task*, 2004, 39:38–46.
[53] Suzihaque MUH, Syazwina N, Alwi H *et al*. A sustainability study of the processing of kitchen waste as a potential source of biofuel: biodiesel production from waste cooking oil (WCO). *Mater Today Proc*, 2022, 63:S484–9.
[54] Ali OM, Mamat R, Rasul MG *et al*. Potential of biodiesel as fuel for diesel engine. In: Rasul MG, Azad AK, Sharma SC (eds). *Clean Energy for Sustainable Development: Comparisons and Contrasts of New Approaches*. Amsterdam: Elsevier, 2017, 557–590.
[55] Hoekman SK, Gertler AW, Broch A, *et al*. Biodistillate transportation fuels 1. Production and properties. *SAE Int J Fuels Lubr*, 2009, 2:185–232.
[56] Nagwan H, Rana N, Kumar A, *et al*. Performance and emission characteristics of diesel engine using karanja oil methyl ester and eucalyptus oil fuel blends. *Proc Environ Sci Eng Manage*, 2019, 6:553–563.
[57] Bunaciu AA, Udriştioiu E, Aboul-Enein HY. X-ray diffraction: instrumentation and applications. *Crit Rev Anal Chem*, 2015, 45:289–299.
[58] Puspitasari P, Putra CS, Permanasari AA *et al*. Physical and magnetic properties of nickel cobalt oxide ($NiCo_2O_4$) as synthesized by self-combustion method. In: Karim SAA, Puspitasari P (eds). *Advanced Materials towards Energy Sustainability*. 1st edn. Boca Raton: CRC Press, 2023, 5–35.
[59] Rujitanapanich S, Kumpapan P, Wanjanoi P. Synthesis of hydroxyapatite from oyster shell via precipitation. *Energy Procedia*, 2014, 56:112–117.
[60] Sahadat Hossain M, Jahan SA, Ahmed S. Crystallographic characterization of bio-waste material originated $CaCO_3$, green-synthesized CaO and $Ca(OH)_2$. *Results Chem*, 2023, 5:100822.
[61] Bano S, Pillai S. Green synthesis of calcium oxide nanoparticles at different calcination temperatures. *World J Sci Technol Sustain Dev*, 2020, 17:283–295.
[62] Alobaidi YM, Ali MM, Mohammed AM. Synthesis of calcium oxide nanoparticles from waste eggshell by thermal decomposition and their applications. *Jordan J Biol Sci*, 2022, 15:269–274.
[63] Linggawati A. Preparation and characterization of calcium oxide heterogeneous catalyst derived from Anadara Granosa shell for biodiesel synthesis. *KnE Eng*, 2016, 1:1–8. https://doi.org/10.18502/keg.v1i1.494.
[64] Puspitasari P, Iftiharsa MA, Zhorifah HFN, *et al*. Analysis of physical properties and compressibility of avian eggshell nanopowders in solid state reaction. *EUREKA: Phys Eng*, 2021, 5:110–120.
[65] Supriyanto NSW, Sukarni S, Puspitasari P *et al*. Synthesis and characterization of $CaO/CaCO_3$ from quail eggshell waste by solid state reaction process. In: *International Conference on Biology and Applied Science (ICOBAS)*, Vol. 1, Malang, Indonesia, 13–14 March 2019, 040032.
[66] Ningrum RA, Humaidi S, Sihotang S, *et al*. Synthesis and material characterization of calcium carbonate ($CaCO_3$) from the waste of chicken eggshells. *J Phys Conf Ser*, 2022, 2193:012009.
[67] Puspitasari P, Utomo DM, Zhorifah HFN, *et al*. Physicochemical determination of calcium carbonate ($CaCO_3$) from chicken eggshell. *Key Eng Mater*, 2020, 840:478–483.
[68] Kosanović C, Fermani S, Falini G, *et al*. Crystallization of calcium carbonate in alginate and xanthan hydrogels. *Crystals*, 2017, 7:355.
[69] Puspitasari P, Chairil M, Sukarni S, *et al*. Physical properties and compressibility of quail eggshell nanopowder with heat treatment temperature variations. *Mater Res Express*, 2021, 8:055008.
[70] Ahmad R, Rohim R, Ibrahim N. Properties of waste eggshell as calcium oxide catalyst. *Appl Mech Mater*, 2015, 754–755:171–175.
[71] Tizo MS, Blanco LAV, Cagas ACQ, *et al*. Efficiency of calcium carbonate from eggshells as an adsorbent for cadmium removal in aqueous solution. *Sustainable Environ Res*, 2018, 28:326–332.
[72] Doostmohammadi A, Monshi A, Salehi R, *et al*. Bioactive glass nanoparticles with negative zeta potential. *Ceram Int*, 2011, 37:2311–2316.
[73] Tangboriboon N, Kunanuruksapong R, Sirivat A. Preparation and properties of calcium oxide from eggshells via calcination. *Mater Sci Poland*, 2012, 30:313–322.
[74] Saad M, Siyo B, Alrakkad H. Preparation and characterization of biodiesel from waste cooking oils using heterogeneous catalyst (Cat. TS-7) based on natural zeolite. *Heliyon*, 2023, 9:e15836.
[75] Roschat W, Phewphong S, Thangthong A, *et al*. Catalytic performance enhancement of CaO by hydration-dehydration process for biodiesel production at room temperature. *Energy Convers Manage*, 2018, 165:1–7.
[76] Pandit PR, Fulekar MH. Biodiesel production from microalgal biomass using CaO catalyst synthesized from natural waste material. *Renew Energy*, 2019, 136:837–845.
[77] Chen C, Qu S, Guo M, *et al*. Waste limescale derived recyclable catalyst and soybean dregs oil for biodiesel production: analysis and optimization. *Process Safety Environ Prot*, 2021, 149:465–475.
[78] Elangovan T, Anbarasu G. Analysis of biodiesel properties from various oil resources and develop relationships among the properties. *Asian J Sci Technol*, 2016, 7:2658–2664.
[79] Dharma S, Ong HC, Masjuki HH, *et al*. An overview of engine durability and compatibility using biodiesel–bioethanol–diesel blends in compression-ignition engines. *Energy Convers Manage*, 2016, 128:66–81.
[80] Gouveia L, Oliveira AC, Congestri R *et al*. Biodiesel from microalgae. In: Gonzalez-Fernandez C, Munoz R (eds). *Microalgae-Based Biofuels and Bioproducts*. Amsterdam: Elsevier, 2018, 235–258.
[81] Lin CY, Ma L. Effects of water removal from palm oil reactant by electrolysis on the fuel properties of biodiesel. *Processes*, 2022, 10:115.
[82] Noushabadi AS, Dashti A, Raji M, *et al*. Estimation of cetane numbers of biodiesel and diesel oils using regression and PSO-ANFIS models. *Renew Energy*, 2020, 158:465–473.
[83] Lin CY, Wu XE. Determination of cetane number from fatty acid compositions and structures of biodiesel. *Processes*, 2022, 10:1502.
[84] Ozcanli M, Gungor C, Aydin K. Biodiesel fuel specifications: a review. *Energy Sources Part A*, 2013, 35:635–647.
[85] Van Gerpen J, Shanks B, Pruszko R, *et al*. *Biodiesel Analytical Methods*. Technical Report NREL/SR-510-36240. Golden, CO, USA: National Renewable Energy Laboratory, 2004.
[86] Gorky Reyes G, Rivera Rubio AR, Morales Morales A. Efecto del poder calorífico en la relación de combustión del motor con distintos tipos de biodiesel. *Revista Nexos Científicos*, 2018, 2:20–24.
[87] Abed KA, Gad MS, El Morsi AK, *et al*. Effect of biodiesel fuels on diesel engine emissions. *Egypt J Pet*, 2019, 28:183–188.
[88] Prasetiyo DHT, Ilminnafik N, Junus S. The flame characteristics of diesel fuel blend with Kepuh (Sterculia Foetida) biodiesel. *J Mech Eng Sci Technol*, 2019, 3:70–80.
[89] Gautam R, Kumar S. Performance and combustion analysis of diesel and tallow biodiesel in CI engine. *Energy Rep*, 2020, 6:2785–2793.

[90] Budiman Y, Putra ZA. Biodiesel production from waste cooking oil: a review. In: Gurner K (ed). *Recycled Cooking Oil: Processing and Uses*. New York: Nova Science, 2018, 89–109.
[91] Tesfa B, Mishra R, Gu F, *et al*. Prediction models for density and viscosity of biodiesel and their effects on fuel supply system in CI engines. *Renew Energy*, 2010, 35:2752–2760.
[92] Arifin MM, Ilminnafik N, Kustanto MN, *et al*. Spray characteristics at preheating temperature of diesel-biodiesel-gasoline fuel blend. *J Mech Eng Sci Technol*, 2021, 5:135–144.
[93] Wahyuni S, Ramli, Mahrizal. Pengaruh Suhu Proses Dan Lama Pengendapan Terhadap Kualitas Biodiesel Dari Minyak Jelantah. *Pillar Phys*, 2015, 6:33–40.
[94] Hamid A, Jakfar A, Romaniyah SB, *et al*. Transesterification of waste cooking oil using CaO catalyst derived from madura limestone for biodiesel production and its application in diesel engine. *Automot Exp*, 2023, 6:80–93.
[95] Rosset M, Perez-Lopez OW. FTIR spectroscopy analysis for monitoring biodiesel production by heterogeneous catalyst. *Vib Spectrosc*, 2019, 105:102990.
[96] Emma AF, Alangar S, Yadav AK. Extraction and characterization of coffee husk biodiesel and investigation of its effect on performance, combustion, and emission characteristics in a diesel engine. *Energy Convers Manage: X*, 2022, 14:100214.
[97] Samanta S, Sahoo RR. Waste cooking (palm) oil as an economical source of biodiesel production for alternative green fuel and efficient lubricant. *Bioenergy Res*, 2020, 14:163–174.
[98] Zayed MA, Abd El-Kareem MSM, Zaky NHS. Gas chromatography-mass spectrometry studies of waste vegetable mixed and pure used oils and its biodiesel products. *J Pharm Appl Chem*, 2017, 3:109–116.
[99] EL-Seesy AI, He Z, Kosaka H. Combustion and emission characteristics of a common rail diesel engine run with n-heptanol-methyl oleate mixtures. *Energy*, 2021, 214:118972.
[100] Hoang MH, Ha NC, Thom LT, *et al*. Extraction of squalene as value-added product from the residual biomass of Schizochytrium mangrovei PQ6 during biodiesel producing process. *J Biosci Bioeng*, 2014, 118:632–639.
[101] Barabas I, Todoru I-A. Biodiesel quality, standards and properties. In: Montero G, Stoytcheva M (eds). *Biodiesel-Quality, Emissions and By-Products*. London: IntechOpen, 2011, 4–28.
[102] Barabás I, Todoru A, Bldean D. Performance and emission characteristics of an CI engine fueled with diesel-biodiesel-bioethanol blends. *Fuel*, 2010, 89:3827–3832.
[103] Solikhah MD. *Pedoman Penanganan dan Penyimpanan Biodiesel dan Campuran Biodiesel (B30)*. Tangerang Selatan: Balai Teknologi bahan Bakar dan Rekayasa Disain, 2020.
[104] Isioma N, Muhammad Y, Sylvester O, *et al*. Cold flow properties and kinematic viscosity of biodiesel. *Univers J Chem*, 2013, 1:135–141.
[105] Hardi J, Ruslan, Prismawiryanti. Utilizing of CaO catalyst from chicken eggshells at several concentrations to produce biodiesel based on moringa seed oil. *J Phys Conf Ser*, 2021, 1763:012053.
[106] Parekh PP, Khwaja HA, Khan AR, *et al*. Lead content of petrol and diesel and its assessment in an Urban environment. *Environ Monit Assess*, 2002, 103:255–262.
[107] Sirviö K, Niemi S, Heikkilä S, *et al*. The effect of sulphur content on B20 fuel stability. *Agron Res*, 2016, 14:244–250.
[108] Fayad MA, Chaichan MT, Dhahad HA, *et al*. Reducing the effect of high sulfur content in diesel fuel on NOx emissions and PM characteristics using a PPCI mode engine and gasoline-diesel blends. *ACS Omega*, 2022, 7:37328–37339.
[109] Kalghatgi GT. *Fuel/Engine Interactions*. Warrendale, PA: SAE International, 2014.
[110] Heywood JB. *Internal Combustion Engine Fundamentals*. New York: McGraw-Hill, 1988.
[111] Verma TN, Shrivastava P, Rajak U, *et al*. A comprehensive review of the influence of physicochemical properties of biodiesel on combustion characteristics, engine performance and emissions. *J Traffic Transp Eng*, 2021, 8:510–533.
[112] El-Adawy M. Effects of diesel-biodiesel fuel blends doped with zinc oxide nanoparticles on performance and combustion attributes of a diesel engine. *Alex Eng J*, 2023, 80:269–281.
[113] Habibullah M, Masjuki HH, Kalam MA, *et al*. Biodiesel production and performance evaluation of coconut, palm and their combined blend with diesel in a single-cylinder diesel engine. *Energy Convers Manage*, 2014, 87:250–257.
[114] Tan P, Hu Z, Lou D, *et al*. Exhaust emissions from a light-duty diesel engine with Jatropha biodiesel fuel. *Energy*, 2012, 39:356–362.
[115] Suardi S, Ikhwani RJ, Aulia APR. Effect of temperature variations of corn (maize) oil biodiesel on torque values and thermal efficiency of diesel engines. *J Mech Eng Sci Technol*, 2023, 7:87–95.
[116] Song J, Yao J, Lv J, *et al*. Experimental study on a diesel engine fueled with soybean biodiesel. *Res J Appl Sci Eng Technol*, 2013, 6:3060–3064.
[117] Dwivedi G, Jain S, Sharma MP. Impact analysis of biodiesel on engine performance: a review. *Renew Sustain Energy Rev*, 2011, 15:4633–4641.
[118] Ryu K. The characteristics of performance and exhaust emissions of a diesel engine using a biodiesel with antioxidants. *Bioresour Technol*, 2010, 101:S78–S82.
[119] Ghuge NC. Performance analysis of diesel engine using biodiesel for variable compressible ratio. *Int Eng Res J*, 2019, 5:563–571.
[120] Boudy F, Seers P. Impact of physical properties of biodiesel on the injection process in a common-rail direct injection system. *Energy Convers Manage*, 2009, 50:2905–2912.
[121] Rizwanul Fattah IM, Kalam MA, Masjuki HH, *et al*. Biodiesel production, characterization, engine performance, and emission characteristics of Malaysian Alexandrian laurel oil. *RSC Adv*, 2014, 4:17787–17796.

ARTICLES FOR FACULTY MEMBERS

ELUCIDATING THE CALCIUM OXIDE DERIVED FROM THE WASTE SHELLS OF MUD CLAM (GELOINA EXPANSA) AS A CATALYST FOR BIODIESEL PRODUCTION

Calcium oxide waste-based catalysts for biodiesel production and depollution: A review / Teo, C. K., Chia, P. W., Nordin, N., Kan, S. Y., Ismail, N. M., Zakaria, Z., Liew, R. K., Wu, L., & Yong, F. S. J.

Environmental Chemistry Letters
Volume 22 Issue 4 (2024) Pages 1741–1758
https://doi.org/10.1007/s10311-024-01740-4
(Database: Springer Nature Link)

Environmental Chemistry Letters (2024) 22:1741–1758
https://doi.org/10.1007/s10311-024-01740-4

REVIEW ARTICLE

Calcium oxide waste-based catalysts for biodiesel production and depollution: a review

Chook Kiong Teo[1] · Poh Wai Chia[2,6] · Nurhamizah Nordin[2] · Su-Yin Kan[3] · Noor Maizura Ismail[1] · Zainal Zakaria[1] · Rock Keey Liew[4] · Lei Wu[5] · Fu Siong Julius Yong[6]

Received: 14 November 2023 / Accepted: 15 April 2024 / Published online: 2 May 2024

Abstract

Pollution, climate change and waste accumulation are critical societal issues calling for advanced methods to recycle matter and clean polluted ecosystems. Here, we review the use of calcium oxide waste-based catalysts for industrial and environmental applications such as biodiesel production, and pollutant degradation and removal. Catalysts can be produced from mud clam shell, eggshell, spent coffee ground, fish bones waste, marble waste, face mask waste, and snail shell. The preparation of composite catalysts, adsorbents, nanoparticles, and photocatalysts is presented.

Keywords Calcium oxide · Waste-based catalysts · Municipal · Agricultural · Green chemistry · Environment

Abbreviations

FESEM Field emission scanning electron microscopy
MWAC Mask waste ash catalyst

Introduction

The excessive utilization of certain metals for industrial purposes presents substantial social challenges, notably with regard to the contamination of heavy metals (Waqas et al. 2024). This overexploitation has caused element depletion and resource deficits (Hunt et al. 2015). Human and industrial activities have resulted in significant contamination of heavy metals, which has raised considerable alarm in the society (Shi et al. 2022). Pollution which originates from modern economies and extensive transportation networks has caused ecological ramifications and impacts the worldwide distribution of species (Boivin et al. 2016). The discharge of toxic metals from many sectors, along with the generation of substantial amounts of agricultural and food

✉ Poh Wai Chia
pohwai@umt.edu.my

Chook Kiong Teo
tchookkiong@gmail.com

Nurhamizah Nordin
nurhamizah316@gmail.com

Su-Yin Kan
suyinkan@unisza.edu.my

Noor Maizura Ismail
maizura@ums.edu.my

Zainal Zakaria
zainalz@ums.edu.my

Rock Keey Liew
lrklrk1991@gmail.com

Lei Wu
wulei@xauat.edu.cn

Fu Siong Julius Yong
yongjulius@umt.edu.my

[1] Faculty of Engineering, Universiti Malaysia Sabah, Jalan UMS, 88400 Kota Kinabalu, Sabah, Malaysia

[2] Faculty of Science and Marine Environment, 21030 Kuala Nerus, Terengganu, Malaysia

[3] Faculty of Health Sciences, Universiti Sultan Zainal Abidin, 21300 Kuala Nerus, Terengganu, Malaysia

[4] Center for Global Health Research (CGHR), Saveetha Medical College, Saveetha Institute of Medical and Technical Sciences (SIMATS), Saveetha University, Chennai, India

[5] School of Chemistry and Chemical Engineering, Xi'an University of Architecture and Technology, Xi'an 710055, China

[6] Institute of Climate Adaption and Marine Biotechnology, Universiti Malaysia Terengganu, Kuala Nerus, Terengganu, Malaysia

residues, presents significant challenges for both society and the environment (Ahmad and Zaidi 2021). The process of industrialization has significantly amplified the environmental burden of heavy metal toxicity, resulting in civilizations relying on these metals for their operations (Gaur et al. 2017). The issue of heavy metal pollution is urgent because of the emissions resulting from industrial operations such as waste gas, wastewater, and residue, as well as other sources such automotive exhaust, pesticides, and mining activities (Liu et al. 2024). Metal smelting generates industrial effluent that contains a multitude of heavy metals, which have adverse effects on aquatic species, crops, and soil (Chen and Yan 2022). In addition, the rapid exhaustion of natural resources caused by a high demand for raw materials has resulted in the use of waste materials as substitutes (Tezyapar Kara et al. 2023). This highlights the difficulties that modern civilization is currently facing (Egerić et al. 2018). The sustainable growth of human society is highly dependent on metals, necessitating the proper utilization and oversight of these resources (Osman et al. 2024). Industrial operations and urbanization have caused the overuse of natural resources, such as metals, leading to the deterioration of groundwater and soil resources (Morin-Crini et al. 2022). This has worsened environmental issues (Diamantis et al. 2016).

Toxic elements can be replaced by alternative metal oxides, especially metal oxides derived from sustainable sources (Akash et al. 2024). Over the years, many green catalysts have been reported in the literature, notably in terms of their resource availability, efficacy, stability, and scaling up of the production of catalysts, which have been noted in several studies (Balakrishnan et al. 2022; Anaya-Rodríguez et al. 2023; Tran et al. 2023). Today, scientists are interested in researching affordable, effective, and renewable sources for preparing green catalysts for industrial use and environmental remediation (Wu et al. 2023a, b). Waste refers to organic or inorganic wastes produced by forestry, agriculture, food processing, and municipal waste (Fang et al. 2023). The employment of these waste as resources for production of calcium oxide waste-derived catalysts has attracted the attention of scientists in recent years owing to its ability to effectively tackle environmental and economic issues simultaneously. The production of calcium oxide waste-derived catalysts can be cost-effective, as the raw materials are often readily available and inexpensive. Calcium oxide has drawn the attention of researchers among the heterogeneous catalysts as they are available ubiquitous in nature or from waste. Calcium is not an endangered element and lately it is used to replace other deficit elements in the preparation of commercial products in large scale (Kouzu et al. 2008). Here, we review the use of calcium oxide waste-based catalysts derived from mud clam shell, eggshell, spent coffee ground, fish bones waste, marble waste, face mask waste, and snail shell focus on the several potential applications including biodiesel production, degradation of organic pollutants, and effective removal of methylene blue dye. These calcium-based catalysts have been researched extensively for sustainable development goals, with advantages over traditional catalysts. Examples include mud clam shell and eggshell catalysts for dye breakdown, recycled coffee and eggshell waste for dye removal, hydroxyapatite from vertebrates' skeletal structures for wastewater treatment, marble waste-derived catalyst for biodiesel production, mask waste ash catalyst for bisindolylmethanes synthesis, and snail shell-based perovskite as a substitute for titanium dioxide and zinc oxide in photocatalysis. In view of the usefulness of calcium-based waste catalyst, the current trend of research utilizing calcium oxide waste-derived catalysts for preparation of composite catalysts, adsorbents, nanoparticles and photocatalysts and their applications at industry and in environmental remediation is reviewed. Figure 1 shows the various applications of mud clam shell photocatalysts at industrial and environmental aspects.

Mud clam shell

The photocatalyst derived from the mud clam shell have been widely researched and synthesized by calcining the mud clam shell and characterized under various spectroscopic methods (Ismail et al. 2016). The catalyst performance of mud clam shell photocatalyst was investigated in the transesterification of castor oil as biodiesel, and the highest biodiesel yield of 96.7% was obtained. A high reusability with minimal loss of catalytic activity was reported using this catalyst. Moreover, the calcium oxide photocatalyst derived from mud clam shell was found to have better stability compared to the commercially available calcium oxide (Ismail et al. 2016). Overall, the calcium oxide-based photocatalyst derived from mud-class shell exhibited excellent performance in biodiesel preparation (Wang et al. 2021). In future, the mud clam shell can be a potential source of photocatalyst which can be prepared by environmental-friendly method, cheap, recyclable material, which lacking in today's heterogeneous catalyst preparation. Moreover, studies have shown that the utilization of abandoned mud clam shells could reduce the environmental burden exerted by this waste to the environment (Rachmawati et al. 2020). Therefore, mud clam shells are cost-effective and sustainable resources in the design of sustainable technology for combating environmental pollution. Moreover, calcium oxide nanoparticles are treated as a photocatalyst by using mangrove oyster shell as a precursor for degradation of procaine penicillin in an aqueous solution (Eddy et al. 2023).

In addition, it was revealed that mud clam shell photocatalysts were efficient at degrading organic pollutants, namely

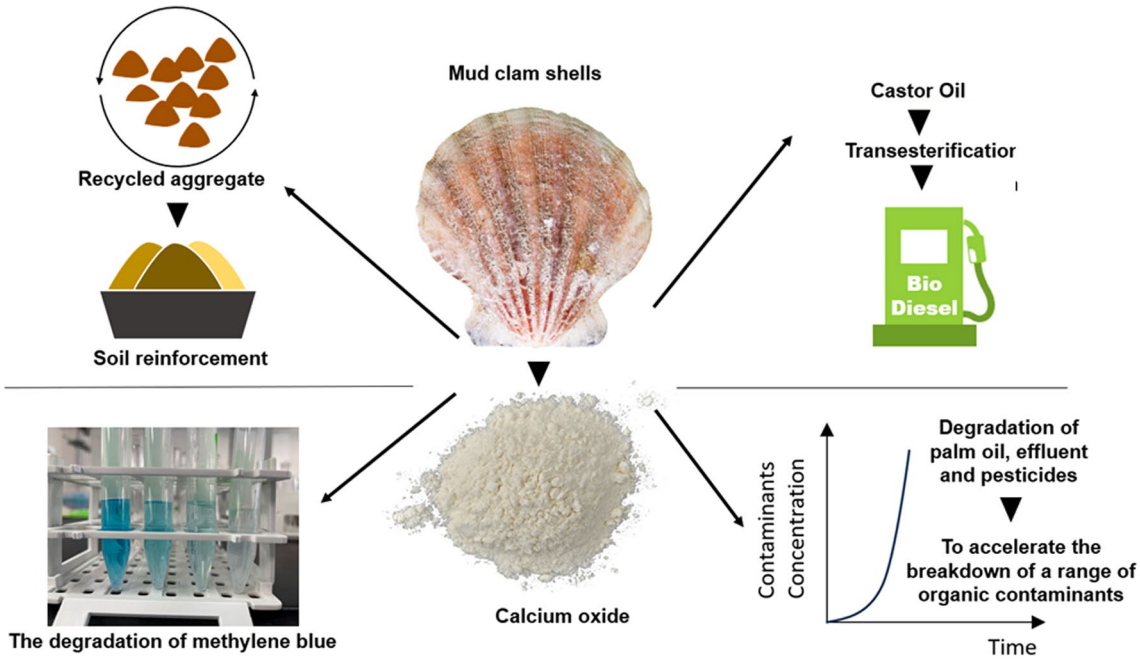

Fig. 1 A calcium oxide-based photocatalyst obtained from mud clam shells for industrial and environmental sustainability. The mud clam shell photocatalysts are a promising material for environmental applications such as in the biodiesel production, soil reinforcement, and degradation of dye and organic pollutants

the methylene blue dye (Wang et al. 2020). The research revealed that the mud clam shell photocatalyst could efficiently breakdown the dye and had a high level of photocatalytic activity. The composites have a maximal degradation capacity of 2265 mg/g and show excellent methylene blue degradation activity over a broad pH range (Wang et al. 2020). The high photocatalytic activity of the photocatalyst derived from mud clam shell is the result of its significant surface area, which gives the dye molecules plenty of room to adsorb and interact with reactive oxygen species. The high degree of crystallinity of the mud clam shell photocatalyst also contributes to improved photocatalytic activity and more effective electron transfer. In addition, the photocatalytic properties of the mud clam shell can be enhanced by adding certain impurities or dopants such as strontium or magnesium. The mud mussel photocatalyst has significant potential as a viable option for various applications in wastewater treatment and water purification processes as it is an effective and affordable material for the photocatalytic degradation of dyes.

Likewise, it was reported that an efficient catalytic activity in the degradation of the palm oil mill effluent utilizing calcium oxide-based mud clam shell photocatalyst (Ismail et al. 2016). According to their research, calcium-based mud clam shell photocatalysts could be utilized to accelerate the breakdown of a range of organic contaminants, such as colors, medications, and insecticides. The Brunauer–Emmett–Teller analysis revealed the mud clam shell photocatalyst possesses a large surface area and high level of contact with the targeted pollutants. The mesoporosity and a large surface area of photocatalysts is the main reason in the increase in photocatalysis effectiveness (Ovodok et al. 2017). The utilization of mud clam shell photocatalysts has several advantages over earlier techniques or research, including affordability, high efficiency, reusability, and adaptability. Overall, mud clam shell photocatalysts are a promising material for environmental applications. It was found as an effective catalyst in the biodiesel production and the degradation of organic pollutants. The employment of mud clam shells as a photocatalyst could be a sustainable and environmentally friendly catalyst. Overall, we found that calcium oxide from mud clam shell is an efficient catalyst for biodiesel production, and optimum parameters for transesterification of castor oil were determined.

Eggshell

Eggshells are a common household waste that has limited uses, such as in arts and crafts. However, because of their high calcium content, they are also a valuable source of photocatalytic materials, and their accessibility and affordability make them desirable substitutes for more expensive photocatalytic materials. The high calcium content of eggshells can be converted into a calcium oxide catalyst through a 2-h calcination process at 800 °C (Wei et al.

2009), with the reaction proceeding as an exothermic reaction. Calcium oxide is well known as a commonly used basic catalyst, and it is well-established that basic catalysts exhibit superior catalytic activity compared to acidic catalysts (Zabeti et al. 2009). Therefore, alkaline catalysts are the preferred choice. Moreover, calcium oxide is used as a catalyst in a variety of industries such as a toxic waste disposal agent, binder in paints, adsorbent, and bactericide (Tangboriboon et al. 2012; Niju et al. 2014).

Calcium oxide nanoparticles obtained from eggshells are utilized as a photocatalyst to effectively degrade dyes, demonstrating the sustainable repurposing of kitchen waste (eggshells). The biological calcium oxide was found as a booster nanopriming agent for both monocot and dicot plants (Ganesan and Paramathevar 2024). The larger porosity of calcium oxide nanoparticles resulted in a better adsorption capacity. The calcium oxide produced from eggshells was employed for both adsorption and photodegradation in the congo red dye. The process of adsorption reached equilibrium with a 93.4% reduction in just 6 min. However, the process of photocatalysis took 120 min to break down 95.0% of congo red. This time was decreased to 45 min when sono-photocatalysis was employed (Ganesan and Paramathevar 2024). In addition, the calcium–magnesium oxide composite was successfully synthesized by the ball milling process, using a cheap eggshell as a calcium oxide source for photodegradation of methylene blue in 20 min with the sample annealed at 750 °C (Reyes-Vallejo et al. 2023).

Calcium oxide is used as a photocatalyst for the degradation of organic dyes, including malachite green (Bathla et al. 2019), violet GL2B (Madhusudhana et al. 2012), indigo carmine (Veeranna et al. 2014), crystal violet (Sawant et al. 2015), congo red (Anantharaman et al. 2016; Ganesan and Paramathevar 2024), and methylene blue (Ameta et al. 2014; Reyes-Vallejo et al. 2023). The photocatalytic efficacy of calcium oxide was also examined for the dyes, including toluidine blue, rhodamine B, and methylene blue. The reaction mixture of catalyst and dye solution were subjected to sonication and afterward placed in a light-free environment for the adsorption test. Following a duration of one hour, the samples underwent centrifugation, and subsequently, the ultraviolet spectral data were analyzed. Upon 15 min light exposure, toluidine blue and methylene blue decomposed into a colorless solution, suggesting that calcium oxide photodegradation has taken place efficiently in toluidine blue and methylene blue (Sree et al. 2020). The experiments were expanded to a solar environment and spectral analysis was performed on each sample at 5 min intervals. The spectral data show a gradual reduction in absorbance during a duration of 10 min for toluidine blue and 15 min for methylene blue. The rapid degradation was possible due to the smaller size of the calcium oxide nanoparticles, which offer a greater surface area for photon absorption, larger free radical production, and faster dye degradation.

Besides, the reuse of eggshells for the purpose of synthesizing the photocatalysis in dye removal has been studied lately. When calcined eggshell powder is used instead of raw eggshell powder in the degradation of the lanasyn F5B which is an industrial dye, the dye degradation efficiency is observed to be more effective using calcined eggshell powder, with an equilibrium dye adsorption capacity of 1.2 mg/g. In addition, calcined eggshell powder has demonstrated an almost 50.0% increase in degradation of dye in the dark compared to the raw eggshell powder and the results show that it removes dye under pseudo-second-order kinetics. As a result, calcined eggshell powder exhibits superior dye degradation performance compared to raw eggshell powder, underscoring the possibility of employing it as a state-of-the-art in the field of environmental remediation (Amarasinghe and Wanniarachchi 2019). Furthermore, the utilization of calcium oxide obtained from eggshells and applied on the surface of activated carbon made from palm kernel shells shown a very effective removal of hydrogen sulfide (Omar et al. 2017).

According to previous studies, calcium oxide obtained from eggshells has been often used as a promising catalyst in the transesterification process of converting oil or fat into biodiesel. Calcination has been the predominant method used to produce calcium oxide catalysts. In this process, temperatures over 800.0 °C are used to activate the catalysts, resulting in high yields ranging from 91.0 to 99.0%. It is noteworthy that, in general, a reaction temperature over 60.0 °C and a reaction period of at least 2 h were necessary to achieve a biodiesel yield above 90.0%. In terms of feedstock, palm oil and soybean oil are the most used raw materials. The eggshell with a greater calcium amount produced a higher conversion rate of biodiesel with 98.0%, compared to the 83.0% conversion rate achieved by the crab shell using sunflower oil as the feedstock. The fundamental characteristic feature of calcium oxide species is a crucial factor that determines the conversion of feedstock into biodiesel. The study revealed the possible use of chicken eggshells as heterogeneous basic catalysts using waste cooking oil as the raw material (Tan et al. 2015). According to reports, using waste cooking oil as a raw material cuts the total cost of producing biodiesel by 60.0–90.0% (Talebian-Kiakalaieh et al. 2013).

In another study, chicken eggshell combined with transition metal oxides including zinc oxide, manganese dioxide, ferric oxide, and aluminum oxide was found to enhance the efficiency for biodiesel production. The effectiveness of different calcium-based mixed metal oxides in the methanolysis process of Jatropha and Karanja oils was studied. The catalysts exhibited higher surface areas during calcination at 900 °C, which therefore resulted in enhanced catalytic activity. Catalysts coated with metal oxides have shown

superior activity as compared to neat calcium oxide and zinc oxide–calcium oxide catalyst was found to exhibit superior performance compared to other catalysts, resulting in a biodiesel yield of 98.2% (Jatropha) and 96.0% (Karanja). The increase in optimal catalyst loading, methanol/oil molar ratio, and reaction temperature did not have a significant impact on the biodiesel production. The reusability of zinc oxide–calcium oxide catalyst was also observed by performing the transesterification of Jatropha and Karanja oils with methanol under optimized reaction condition (Joshi et al. 2015). The reused catalyst gave more than 95.0% gas chromatography conversions of Jatropha biodiesel and more than 92.0% gas chromatography conversions for Karanja biodiesel after four successive cycles. The result of this finding showed that calcium oxide derived from the chicken egg combined with zinc oxide capable to yield excellent biodiesel from Jatropha and Karanja oils, and the result was found to be comparable to the use of other efficient catalyst (Sahoo and Das 2009).

Furthermore, the lithium-doped calcium oxide derived from eggshell was investigated for the transesterification process of *Mesua Ferrea Linn* (nahor oil), a non-edible feedstock often used in the biodiesel production (Boro et al. 2014). In this study, maximum biodiesel conversion was achieved under the optimum reaction conditions, which included a 2.0% lithium loading, 5.0% per weight catalyst amounts, a 10:1 methanol to oil ratio, a 4 h reaction time, and a temperature of 65 °C. Besides, it was observed that the catalyst exhibited reusability and the decrease in its activity was ascribed to the coverage of the catalyst surface by the product formed during the reaction. The initial catalytic activity was associated with the formation of mixed lithium–calcium phase along with the presence of lithium oxide and calcium oxide. When calcium oxide was loaded with 2.0% of lithium salt in the preparation of calcium oxide derived eggshell photocatalysts in the preparation of biodiesel from nahor oil, a biodiesel conversion rate of 94.0% was achieved under the optimal reaction condition. Though the catalyst was found non-recyclable, its catalytic activity may be enhanced by the process of activation at a suitable temperature and subsequent reloading with lithium. As a conclusion, calcined eggshell powder has higher dye degradation capability compared to raw eggshell powder and can be used as an eco-friendly photocatalyst for dye degradation. Figure 2 shows the various applications of eggshell photocatalysts at industrial and environmental aspects.

Spent coffee ground

Coffee is often regarded as one of the most extensively consumed beverages on a worldwide basis and is typically made from roasted coffee beans due to its refreshing properties. Due to its far-reaching impact on various aspects of society, its consumption has a significant economic, social, and cultural impact, which contributes to its global appeal (Goya et al. 2007). The annual production of coffee grounds was estimated at about 6,600,000 tons (Lee et al. 2015) and is mainly driven by high demand in society. These coffee grounds are made up of various organic compounds such as

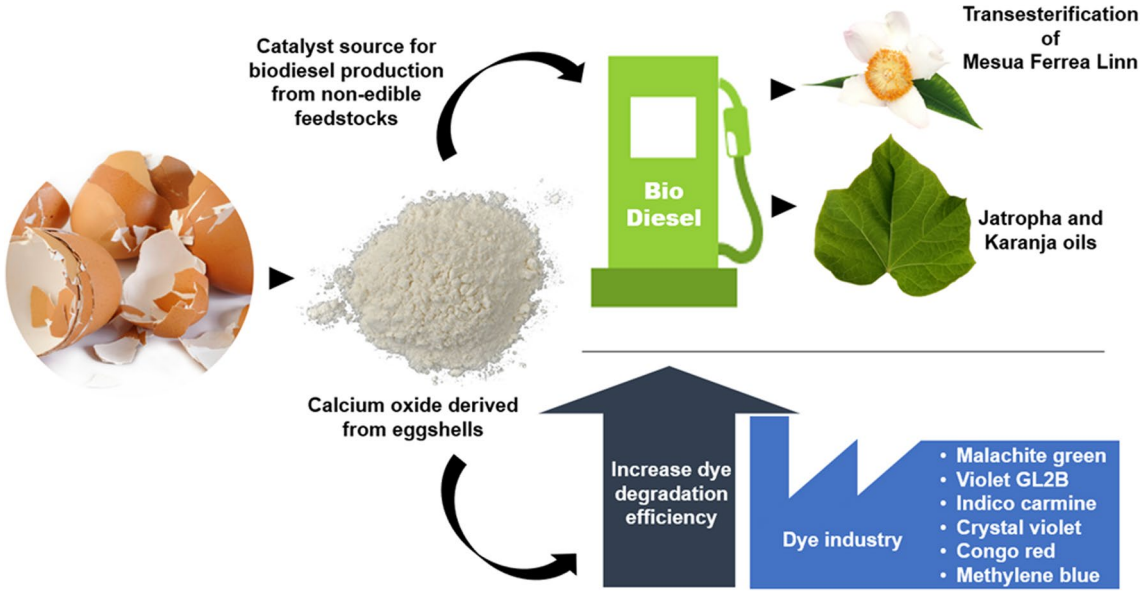

Fig. 2 A calcium-based photocatalyst obtained from eggshells for industrial and environmental sustainability. Calcium oxide nanoparticles obtained from eggshells are utilized as a photocatalyst to effectively degrade dyes. It has been often used as a promising catalyst in the transesterification process of converting oil or fat into biodiesel

lignin, fatty acids, cellulose, and hemicellulose. However, most of these coffee grounds are discarded as waste after use for coffee consumption, forming a final byproduct (Safarik et al. 2012). The study has shown that spent coffee grounds, which contain approximately 25.0% mannan, 15.0% cellulose, and 5.0% arabinogalactan, serve as a significant carbon source (Mohamed et al. 2021). When these soils are burned, carbon dioxide is released to the air and cause pollution in environment. Therefore, alternative methods to valorize coffee grounds for beneficial applications are needed. Although there are some methods of reusing coffee waste, such as fertilizer, animal feed production, sugar source, as well as its potential as a metal ion sorbent and biodiesel feedstock. Yet, there is still a significant obstacle in the form of developing more effective strategies and ways to convert coffee waste into a novel resource material (Chitra et al. 2014).

The calcium oxide/carbon photocatalyst can be synthesized from recycled coffee and eggshell waste for effective removal of methylene blue dye (Mohamed et al. 2021). It sees the use of spent coffee grounds as the main material in the synthesis of photocatalyst. The synthesis of calcium oxide/carbon was achieved through the process of thermal cracking. A mixture was prepared by combining spent coffee grounds with eggshells, maintaining a weight ratio of 1:1. The composites were calcined in a furnace at a temperature of 900 °C for 4 h under atmospheric air conditions. Photodegradation experiments of methylene blue dye and calcium oxide and calcium oxide/carbon photocatalysts were carried out in the presence of sunlight for 35 min.

Based on the result, the percentage of photocatalytic degradation was recorded as 88.0% for calcium oxide to 99.0% for calcium oxide/carbon. More dye was removed when the pH of the solution was increased from 2 to 10 h or when the catalyst loading was increased from 10.0 mg to 75.0 mg. The calcium oxide/carbon was also a photo-catalytically stable substance that can be used for at least ten times. Moreover, the addition of carbon to the surface of the resulting calcium oxide increases the crystallite size while decreasing the bandgap value. With increasing crystallinity, the diffraction peaks of the calcium oxide/carbon photocatalyst became stronger than the calcium oxide peaks. High photocatalytic performance requires a superior crystal structure (Zhu et al. 2018). The high defect density in calcium oxide/carbon has a positive effect on the photocatalytic activity as it increases the active surface and leads to the formation of a high density of active sites (Parmar et al. 2019). The generation of static charge fields along the dislocation lines could be the cause of these active centers (Lawrence and Van 1989). The photocatalytic efficiency of the calcium oxide/carbon catalyst was found to be enhanced by the increase in surface area and dye adsorption, which effectively eliminates methylene blue. Figure 3 shows the degradation of methylene blue by using calcium oxide/carbon photocatalyst.

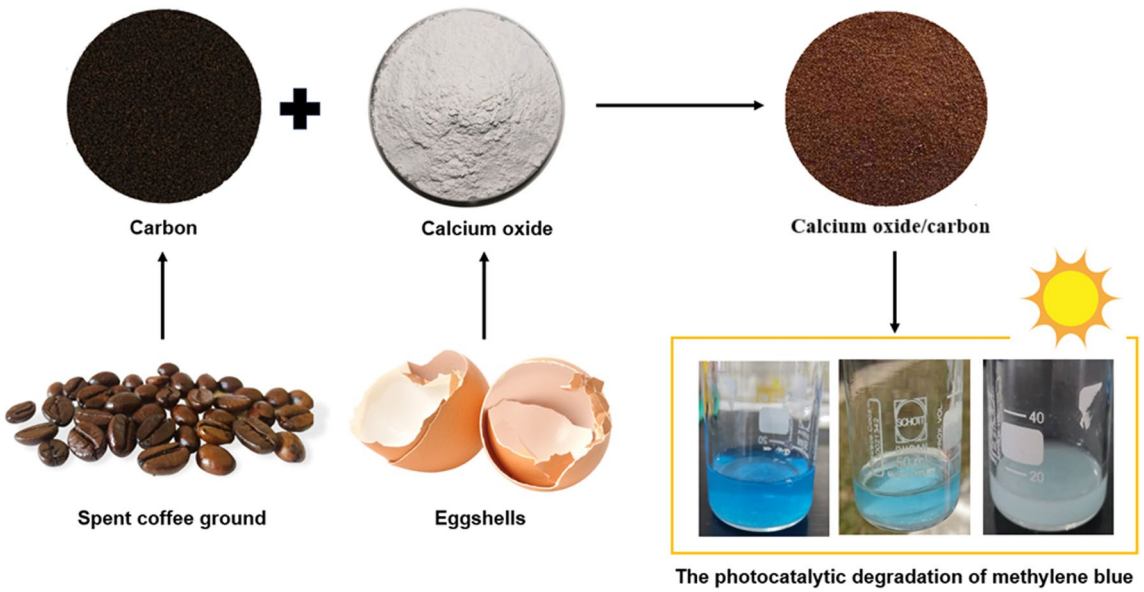

Fig. 3 A calcium oxide photocatalyst derived from eggshells mixed with carbon derived from spent coffee ground. The calcium oxide/carbon was also a photo-catalytically stable substance. The calcium oxide/carbon photocatalyst can be synthesized from recycled coffee and eggshell waste for effective removal of methylene blue dye

Fish bones waste

Hydroxyapatite is a major inorganic substance found ubiquitously in the skeletal structures of all vertebrates. The composition of the substance consists mostly of around 70.0% apatite calcium phosphate or often referred to as hydroxyapatite. It is ideal for bone tissue applications including artificial bone grafting, orthopedic therapy, and drug delivery systems due to its biocompatibility, biodegradability, and ion exchange ability (Pal et al. 2017). In a previous study (Hong et al. 2012), the fish bone-hydroxyapatite was used to catalyze the degradation of congo red and crystal violet in the present of direct sunlight. In the laboratory test, it was found that almost 87.0% of congo red and 77.0% crystal violet were degraded by fish bone-hydroxyapatite, respectively (Sathiyavimal et al. 2020). As reported, the photocatalytic performances of hydroxyapatite prepared with biological substances were time dependent (Hong et al. 2012; Liu et al. 2016). It is possible that the porous nature of the fish bone-hydroxyapatite contributed to the colors being degraded quickly and easily. The degradation of congo red and crystal violet was caused by the conversion of the valence bond into the conductive band, resulting in the formation of electron–hole pairs. The high area specificity of the fish bone-hydroxyapatite mesoporous structure would be responsible for its strong adsorption capacity (Hong et al. 2012). Oxygen and water molecules were converted into superoxide anion radicals and hydroxyl radicals due to the interactions between the positively charge mesoporous holes and the negatively charge electrons.

These active fish bone-hydroxyapatite species have formed strong bonds with the positive holes, which play a crucial role in the decomposition of the adsorbed congo red and crystal violet molecules into carbon dioxide and water. The enhanced adsorption capacity of the mesoporous fish bone-hydroxyapatite enabled the accelerated degradation of congo red and crystal violet. Therefore, fish bone-hydroxyapatite would provide a solid basis for its use in wastewater treatment and toxic dye removal. A non-toxic and environmentally friendly method of bioremediation for future generations would be to create a fine mesoporous structure of fish bone-hydroxyapatite utilizing biological substrates such as fish bones. Furthermore, comparable studies found that hydroxyapatite has high photocatalytic activity for removing azo dyes from wastewater pollution (Corami et al. 2007; Stötzel et al. 2009). Overall, we found that fish bone-hydroxyapatite is a potential catalyst for dye degradation fish bone-hydroxyapatite that showed rapid degradation of crystal violet and congo red dyes. Figure 4 shows the photocatalytic degradation of industrial dyes by the fish bone-hydroxyapatite.

Marble waste

Marble is a common, naturally occurring substance composed of calcium carbonate and magnesium carbonate arranged in alternating layers. Marble wastes have been used

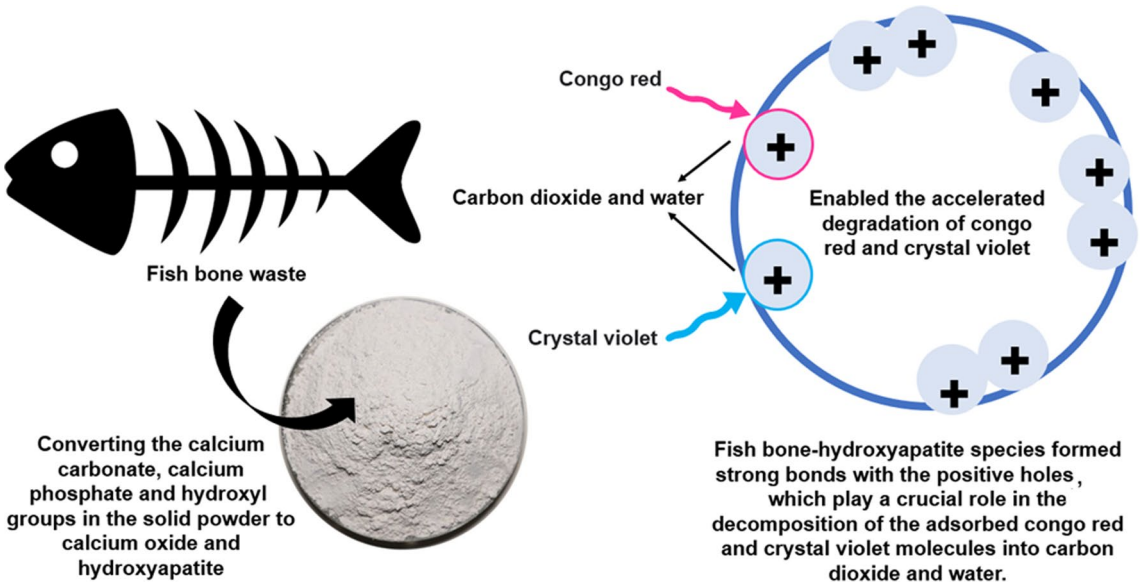

Fig. 4 Hydroxyapatite is a major inorganic substance found in fish bone. The fish bone-hydroxyapatite was used to catalyze the degradation of congo red and crystal violet in the present of direct sunlight. Fish bone-hydroxyapatite would provide a solid basis for its use in wastewater treatment and toxic dye removal

extensively in building construction, iron and steel works (Khan et al. 2022). Interestingly, waste marble can be used directly as a catalyst using two simple processes: purification and calcination. In recent years, the use of marble detritus as a solid base catalyst has increased, mostly attributed to its low cost and non-toxicity. The use of marble powder as an abundant and accessible mineral resource for the development of an environmentally friendly and sustainable calcium-based photocatalyst. This research project focuses on the use of calcium as a fundamental element for the treatment of wastewater. The article reports that marble powder finds widespread use primarily in the building industry and as an adsorbent for wastewater treatment purposes. Hence, the development of a photocatalyst for the remediation of bio-refractory substances would provide an environmentally friendly and sustainable methodology. Marble is composed of many minerals, including calcium and magnesium, which have the potential to serve as reactants in the creation of photocatalysts (Khan et al. 2022).

According to literature, the calcium oxide-based catalyst derived from marble waste facilitated the transesterification process of triglycerides in the presence of methanol (Tahvildari et al. 2015). Waste cooking oil was also transesterified with methanol in the presence of a calcium oxide catalyst derived from marble waste. It was reported that during calcination, the calcium carbonate of the marble is converted to calcium oxide, releasing carbon dioxide in the process (Adams et al. 2017). The calcium oxide was then employed as a catalyst for the synthesis of biodiesel from waste cooking oil. Calcium oxide derived from marble waste offers improved efficiency, reaction time, repeatability, weight percentage of catalyst used, methanol volume, and mass yield in biodiesel production because of its inherent nature. Due to its surface structure, when used with calcium oxide derived from marble waste, the basic properties of the material improve, and it becomes a suitable base for the catalyst, thereby increasing the calcium oxide contact surface area and the yield of the transesterification reaction.

In addition to biodiesel, the calcium oxide catalyst derived from marble waste was employed to convert 1,4-butanediol to tetrahydrofuran in the vapor phase. 1,4-butanediol is one of the biomass-derived chemicals that has the capability to be used in the synthesis of various chemicals including solvents and polymers. Of all the other compounds, tetrahydrofuran is the most important due to its wide range of uses as high-performance solvents, precursors to polyurethanes, elastic fibers, and molded elastomeric co-polymers. In addition, it is utilized as a precursor for the synthesis of organic compounds (Sivaramakrishnan and Ravikumar 2012; Atadashi 2015; Lourinho and Brito 2015). The dehydration of 1,4-butanediol has been achieved with a variety of acidic and basic supported catalysts, including lanthanum/zirconium dioxide (Fu et al. 2009), ytterbium (III) oxide (Ayoub et al. 2016), and silicotungstic acids (Predojević 2008). The use of the catalysts listed above releases significant quantities of environmentally hazardous chlorides, nitrates, and radioactive elements, which is the main problem with their use.

In addition, the use of a calcium oxide catalyst derived from marble waste was employed to enhance the catalytic efficiency of the polyethersulfone membrane in the context of biodiesel production and purification. The calcium oxide catalyst produced by activating marble particles at 900 °C in 4 h appeared to have an average particle diameter between 0.3 µm and 1.0 µm, with numerous openings serving as a barrier between the particles, which revealed by scanning electron microscopy experiment. As a result, these tiny catalyst particles have a large surface area and an abundance of active centers. In addition, the Fourier transform infrared analysis showed the existence of the important functional groups inside the membrane (Alhanif et al. 2018). The diameter of the calcium oxide particles decreases upon thermal activation, while the size and number of their openings increase (Ljupković et al. 2014). It was found marble powder can be used as a sustainable calcium-based photocatalyst with effective in wastewater treatment. Figure 5 shows the various applications of calcium oxide from marble waste at industrial and environmental dimensions.

Face mask waste

The face mask is composed of non-biodegradable polymers including polycarbonate, polypropylene, polystyrene, polyethylene, polyurethane, and polyacrylonitrile. Plastic components from improperly disposed face masks not only endanger the ecosystem and environment, but also to aquatic animals (Facciolà et al. 2021; Selvaranjan et al. 2021). It was reported the conversion of discarded masks into a catalyst known as mask waste ash catalyst through direct combustion in an oven for use in bisindolylmethanes synthesis, where the calcium-containing catalyst found in mask waste ash catalyst could facilitate the synthesis of bisindolylmethanes (Kiong et al. 2022). Bisindolylmethanes are alkaloids that exhibit diverse biological characteristics, including antibacterial, antiviral, and antioxidant activities (Praveen et al. 2015). Numerous catalysts have been produced for

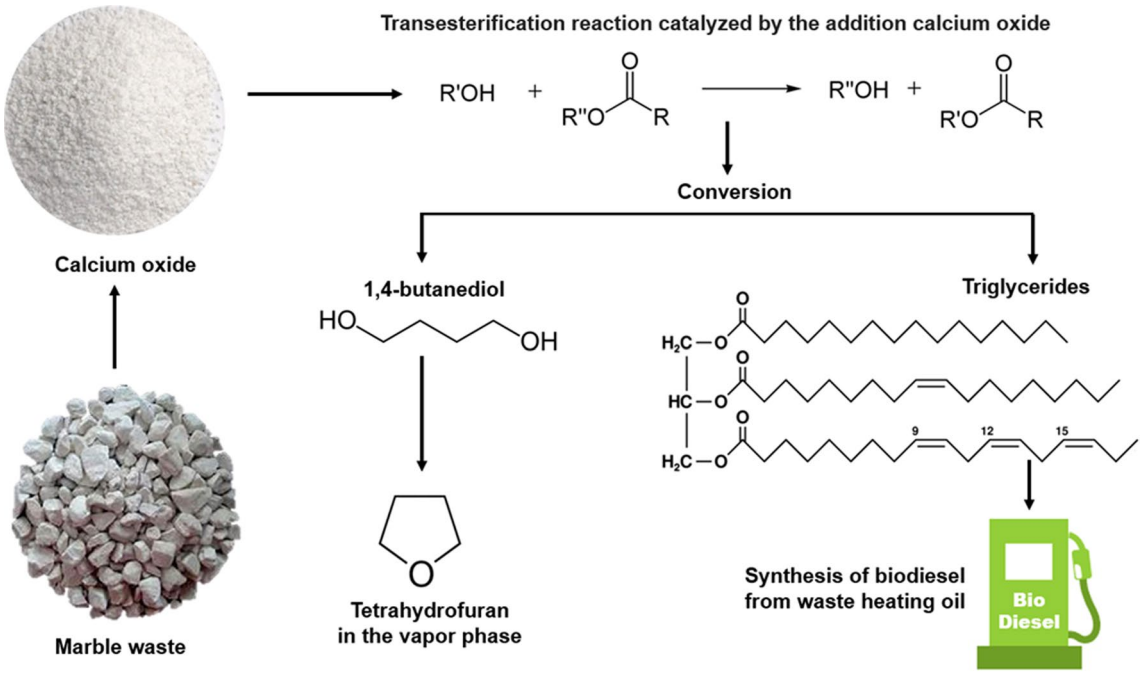

Fig. 5 Synthesis of marble waste sustainable catalyst for industrial and environmental remediation application. Calcium oxide-based photocatalyst derived from marble waste facilitated the transesterification process of triglycerides in the presence of methanol. It is also used to convert 1.4-butanediol to tetrahydrofuran and improve the catalytic activity of the polyethersulfone membrane. (R′ and R″ = Aliphatic groups)

bisindolylmethanes syntheses; nonetheless, some catalysts have used perilous and costly reagents, hence impeding their pragmatic application.

For the synthesis of bisindolylmethanes, a selection of commercially available aldehydes was selected to perform the control experiment. A diverse range of substituted bisindolylmethanes was obtained with yields between 60.0% and 94.0% (Kiong et al. 2022). Bisindolylmethanes were synthesized in high yields by replacing benzaldehydes with electron-withdrawing groups under optimal reaction conditions. The experimental findings indicated that benzaldehydes with electron-donating substituents gave lower product yield compared to benzaldehydes with electron-withdrawing substituents when the reaction time was increased. The observed phenomenon may be ascribed to the electron-donating effect of the substituted benzaldehydes, which leads to a decrease in the electro positivity of the carbon atoms in the carbonyl groups.

To demonstrate its versatility, the photodegradation of experiments were investigated by exposing aqueous solutions of methylene blue, orange 16, green 19, and red 120 in the presence of mask waste ash catalyst. According to previous research (Stewart et al. 2022), the presence of long fibers connected into a network with free areas of 100.0–500.0 microns can be visualized under the scanning electron microscopy experiment. The scanning electron microscopy image of mask waste ash catalyst, on the other hand, shows a porous, fiber-like shape with many grain boundaries. The mask waste ash catalyst has pore sites which were shown to facilitate the bisindolylmethanes syntheses and degradation of dyes that occur at a higher temperature after calcination of waste mask (Loo et al. 2018). Overall, we found mask waste ash catalyst is effective in photodegradation of dye and efficient synthesis of bioactive compounds. Figure 6 shows the current applications of mask waste ash catalyst.

Snail shell

Calcium oxide from snail shells has been discovered to be a possible alternative source for making photocatalysts. In the synthesis of photocatalysts, the utilization of snail shell materials lowers prices and has favorable ecological and economic effects. A different source of calcium oxide, the snail shell is rich in the element calcium and has a distinctive microstructure. Additionally, using shell resources wisely to

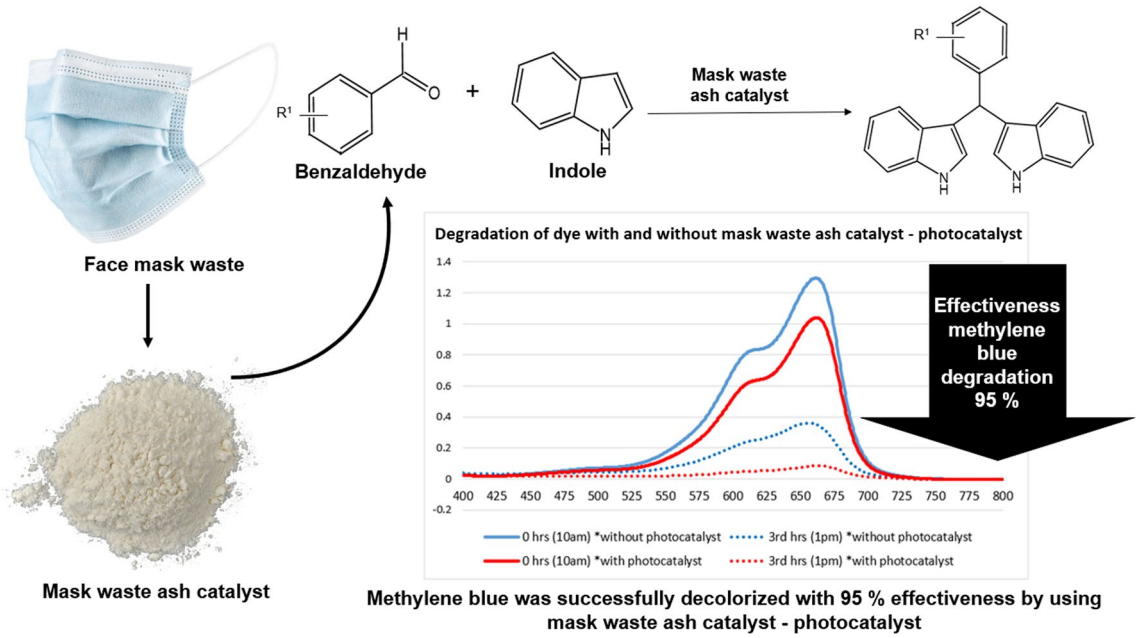

Fig. 6 Calcium-containing catalyst found in mask waste ash catalyst could facilitate the synthesis of bisindolylmethanes. The degradation of dye with and without using mask waste ash catalyst photocatalyst were analyzed and showed methylene blue was successfully decolorized with 95.0% effectiveness. (R′ = Electron-withdrawing and electron-donating groups)

make photocatalysts may not only lower manufacturing costs but also be utilized to minimize pollution, which is advantageous for both the environment and the economy (Roschat et al. 2016; Laskar et al. 2018; Pooladi and Bazargan-Lari 2020). Calcium carbonate, which is present in the snail shell, was changed into calcium oxide during the calcination process (Nopriansyah et al. 2016). It was employed as a source of calcium oxide to create aluminum oxide/calcium oxide nanoparticles for use as a photocatalyst in the degradation of the harmful pesticide diazinon, after being calcined at 800 °C, contain 62.0% calcium oxide (Rodiah et al. 2020). The catalytic activity of this photocatalyst was found to be improved after the inclusion of aluminum and reduced by using natural plant extract (Rodiah et al. 2020).

In some earlier publications, the employment of semiconductor materials as potential substitutes to titanium dioxide and zinc oxide, which have been of interest for photocatalysis applications, is explored. The substance perovskite is one of them and perovskite itself is found as mineral perovskite materials (Heydari et al. 2012). Typical piezoelectric materials are lead zirconate, barium titanate, and lead titanate (Seo et al. 2005; Liotta et al. 2009). With a perovskite structure and a high dielectric loss for a variety of applications such as photocatalysis, calcium titanate is one of a significant class of chemicals. In the past, calcium oxide made from snail shell was used in the calcium titanate synthesis process. Perovskite made from snail shells was examined for its physicochemical properties and compared to calcium oxide and calcium carbonate as calcium sources (Fatimah et al. 2018). Perovskite created utilizing calcium oxide from snail shells has a similar X-ray diffraction pattern to perovskites made using commercial chemicals. According to the laboratory results, calcium titanate prepared from snail shell exhibited photodegradation activity of methylene blue that is comparable to that of prepared from commercial chemicals. The methylene blue photodegradation was discovered to follow a second-order process based on the results of the kinetic simulation.

Another work examined the creation and characteristics of a calcium oxide/zinc oxide nanocomposite generated from the snail shell *Achatina fulica*. According to the research, the snail shell is a possible alternative source of calcium oxide for producing photocatalysts since it has a distinctive microstructure and a high calcium content (Jiang et al. 2021). In addition to lowering manufacturing costs, the wise use of snail shell materials for photocatalyst synthesis has positive effects on the environment and the economy (Jiang et al. 2021). The process of oxidation leads to the degradation of calcium carbonate into calcium oxide, accompanied by the breakdown of organic materials. This results in the

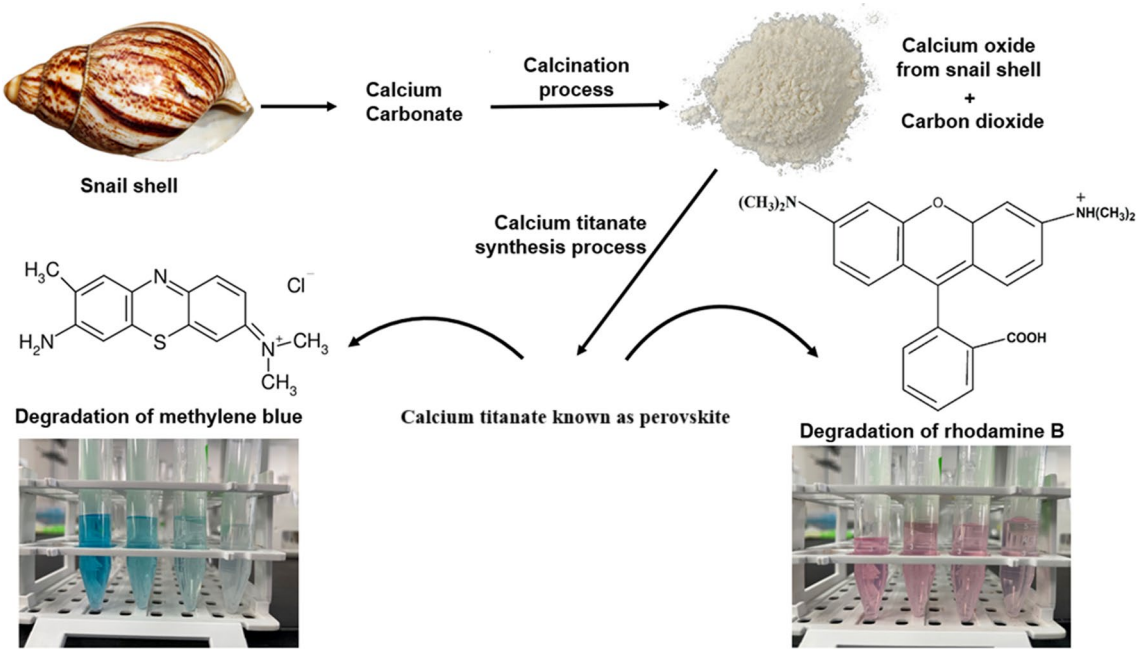

Fig. 7 Applications of sustainable calcium-based derived from snail shell as photocatalyst for methylene blue and rhodamine B degradation. In the synthesis of photocatalysts, the utilization of snail shell materials lowers prices and has favorable ecological and economic effects. The catalyst was used for the process of photocatalytic degradation of rhodamine B in the presence of visible light irradiation

development of a pore structure that is evenly distributed throughout the material. The nanocomposite demonstrates the presence of nanoflowers characterized by spindle-shaped petals, with lengths ranging from 500 nm to 1,000 nm. These nanoflowers are shown to develop on a spherical calcium oxide substrate, which serves as the supporting material. In the absence of a calcium oxide carrier, zinc oxide nanoparticles tend to aggregate into rod-shaped structures with sizes ranging from 50 nm to 1,000 nm. The catalyst that was synthesized was used for the process of photocatalytic degradation of rhodamine B in the presence of visible light irradiation. The composite material exhibited a significant degrading efficiency of 91.0%, may be attributed to the proliferation of zinc oxide on the calcium oxide template. Unfortunately, the recyclability test showed there was a minor drop in the degradation efficiency. However, the structural integrity of the calcium oxide/zinc oxide composite photocatalyst remained intact as shown by scanning electron microscopy analysis. The inclusion of ethylenediaminetetraacetic acid disodium salt and isopropyl alcohol resulted in a decrease in rhodamine B degradation rates to 54.0% and 67.0%, respectively. This suggests that the contribution of electrons is more significant than hydroxyl radicals in the photocatalytic process of calcium oxide/zinc oxide. The calcium oxide/zinc oxide nanocomposite generated from the snail shell *Achatina fulica* has significant potential for use in the field of photocatalytic destruction of water contaminants, owing to the presence of calcium oxide/zinc oxide nanoflowers. This work presents a novel approach for valorizing snail shell waste and the fabrication of biomass composites, resulting in improved performance. It was found calcium titanate synthesized from snail shell shows similar

Table 1 Literature reviews on calcium waste-based catalysts

Title	Summarized Abstract	Methods Used	Results	Conclusions	Contributions	References
Biodiesel production from castor oil by using calcium oxide derived from mud clam shell	Calcium oxide from mud clam shell used as catalyst Highest biodiesel yield of 97.0% achieved	Synthesis of calcium oxide from mud clam shell Transesterification of castor oil using calcium oxide	Biodiesel yield of 97.0% obtained with optimal parameters Catalyst reusable up to five times	Calcium oxide from mud clam shell is an efficient catalyst for biodiesel production Optimum parameters for transesterification of castor oil were determined	Calcium oxide from mud clam shell used as catalyst Physical and chemical properties of catalyst studied	Ismail et al. (2016)
Eco-friendly photocatalyst derived from eggshell waste for dye degradation	Study on using eggshell waste for dye degradation Calcined eggshell powder shows higher dye degradation capability	Calcined eggshell powder and raw eggshell powder comparison Langmuir and Freundlich isotherms for dye adsorption	Calcined eggshell powder has significantly higher dye degradation capability (80.0%) Calcined eggshell powder shows nearly 50.0% increase in dye degradation under light conditions compared to dark conditions	Calcined eggshell powder has higher dye degradation capability compared to raw eggshell powder Calcined eggshell powder can be used as an eco-friendly photocatalyst for dye degradation	Evaluation of dye removal efficiency of calcined eggshell powder Study of dye adsorption processes and kinetics	Amarasinghe and Wanniarachchi (2019)
Synthesis of novel eco-friendly calcium oxide/carbon photocatalyst from coffee and eggshell wastes for dye degradation	Calcium oxide/carbon photocatalyst prepared from coffee and eggshell wastes Efficient removal of methylene blue dye under solar energy irradiation	X-ray diffraction analysis scanning electron microscope with energy Dispersive x-ray spectroscopy Fourier transform infrared spectroscopy analysis Ultraviolet visible-near infrared spectrophotometer with integrating sphere attachment	Calcium oxide/carbon showed significant improvement in methylene blue dye removal (99.0%) Calcium oxide/carbon has a bandgap value of 1.5 electron-volt	Calcium oxide/carbon photocatalyst efficiently removes methylene blue dye Increase in photocatalytic efficiency due to increased surface area and dye adsorption	Design of novel calcium oxide/carbon photocatalyst from waste materials High efficiency for dye removal applications	Mohamed et al. (2021)
Sustainable calcium-based photocatalyst derived from waste marble powder for environmental sustainability: A review on synthesis and application in photocatalysis	Review on calcium-based catalysts for wastewater treatment Utilization of waste marble powder as a sustainable approach	Co-precipitation and sol–gel method Ultrasonically assisted synthesis	The potential reactant reviewed for obtaining the best photocatalyst has been identified as calcium-based reactants such as calcium chloride and calcium carbonate derived from waste marble particles	Marble powder can be used as a sustainable calcium-based photocatalyst Calcium-based reactants derived from marble powder are effective in wastewater treatment	Waste marble particle is an eco-friendly economic adsorbent Waste marble particle must be studied for various applications	Khan et al. (2022)

Table 1 (continued)

Title	Summarized Abstract	Methods Used	Results	Conclusions	Contributions	References
Facile synthesis and characterization of hydroxyapatite from fish bones: Photocatalytic degradation of industrial dyes (crystal violet and congo red)	Fish bone-hydroxyapatite synthesized from natural biowaste has showed high degradation of industrial dyes	X-ray diffraction Fourier transform infrared spectroscopy Field emission scanning electron microscopy Transmission electron microscopy Thermogravimetric analysis	Fish bone-hydroxyapatite showed 77.0% degradation of crystal violet Fish bone-hydroxyapatite showed 87.0% degradation of congo red	Fish bone-hydroxyapatite synthesized from fish bones showed rapid degradation of crystal violet and congo red dyes Fish bone-hydroxyapatite is a potential candidate for dye degradation	Synthesis and characterization of hydroxyapatite from fish bones Application of hydroxyapatite for photocatalytic degradation of dyes	Sathiyavimal (2020)
Valorization of discarded face mask for bioactive compound synthesis and photodegradation of dye	Discarded face masks transformed into catalyst for bioactive compound synthesis Catalyst facilitates photodegradation of dye compounds	Condensation of indole and benzaldehyde with catalysts Transformation of discarded face mask into catalyst	Discarded face masks can be transformed into a catalyst for bioactive compound synthesis The catalyst derived from face masks can efficiently degrade dye compounds	Efficient synthesis of bioactive compounds using mask waste ash catalyst Mask waste ash catalyst is effective in photodegradation of dye compounds	Transformation of discarded masks into mask waste ash catalyst Sustainable strategy for resolving discarded face masks	Kiong et al. (2022)
Photocatalyst of perovskite calcium titanate nanopowder synthesized from calcium oxide derived from snail shell in comparison with the use of calcium oxide and calcium carbonate	Calcium titanate synthesized from snail shell shows similar properties to calcium oxide and calcium carbonate sources Photocatalytic activity of calcium titanate is comparable to other sources	Solid reaction of calcium sources with titanium dioxide Photocatalytic reactor equipped with ultraviolet lamp	Calcium titanate synthesized from snail shell shows similar X-ray diffraction pattern and photocatalytic activity compared to calcium oxide and calcium carbonate sources Impurities such as silica and magnesium oxide are present in the synthesized materials	Calcium titanate synthesized from snail shell shows similar properties to those prepared from calcium oxide and calcium carbonate Photocatalytic activity of calcium titanate is comparable to calcium oxide and calcium carbonate	Photocatalysis in wastewater treatment- reusability and efficiency of the process	Fatimah (2018)

Table 2 Potential applications of eggshell nanocatalysts with performance

Application	Performance	Authors
Ball mill assisted preparation of nanocalcium carbonate as a novel and sustainable catalyst	1. It was found that the nanoeggshell generated the nanocrystalline calcium carbonate with a crystallite size less than 100 nm 2. Scanning electron microscope images study showed an increase in porosity of nanocalcium carbonate due to the downsizing of the powder during ball mill treatment	Mosaddegh et al. (2013)
Reinforce in ceramic composite	1. Porous structure of implant is one of the major aspects that need to be concerned before practicing it for bone application 2. Biomedical porous glass ceramic orbital implants from eggshell-based calcium-silicate glasses being prepared 3. Close pore accompanied with rough surface were developed in the glass ceramic samples when the temperature increased from 900 °C to 1100 °C	Razak et al. (2022)
Green adsorbents for removal of hydrogen sulfide from wastewaters	1. It is concluded that the chickens' eggshell are very useful green and economic adsorbents due to their availability and absence of any toxic and hazardous constituent's elements from all adsorbents 2. The calcinate modified been the most suitable followed by the activate carbon modified adsorbent	Habeeb and Danhassan (2014)
Eggshell coated gray cast iron for corrosion applications	1. Zeta potential is the voltage value occurring between the surface of a solid particle immersed in a conducting liquid 2. Calcium oxide has shown up to 70.0% of the overall chemical composition of eggshell powder before coating process	Teknologi et al. (2017)
Synthesis of glycerol carbonate from biowaste glycerol using calcium oxide-titanium dioxide nanocatalysts	1. The mass loss of the catalyst occurred at different temperature ranges at different three zones like first, second and third zones 2. The first phase of mass loss occurred at 60–300 °C which might be due to dehydration of crystals of water molecules 3. The synthetic strategy opens avenues for obtaining one of the value-added product glycerol carbonates by use of sustainable and environmental benign routes 4. The basic strength of calcium oxide/titanium dioxide mixed oxide is highly favorable for total conversion of glycerol	Pradhan and Sharma (2021)

properties and its photocatalytic activity is comparable to calcium oxide and calcium carbonate. Figure 7 shows the degradation of photocatalytic degradation of industrial dyes methylene blue and rhodamine B by using snail shell as photocatalyst. Comparison on the published review references is listed in Table 1 and potential applications of eggshell nanocatalysts with performance in Table 2.

Conclusion

In the past, many successful and viable environmentally sustainable catalysts have been reported to remediate environmental pollutants, yet the preparation of these catalysts required the use of hazardous reagents and uses endangered metals, which led to resource deficit in the future. Considering these, where resource deficit and pollution have been a major issue faced by mankind, much greener, sustainable, and economical environmental catalysts are highly sought after by scientists. In the last decades, waste-based catalysts have emerged as potential replacements for toxic and expensive catalysts that might contribute to sustainable issues in the future. In addition, the use of waste-based resources can reduce the reliance on current expensive and endangered metals that will lead to elemental deficit on day in future. This review highlights the importance of using sustainable resources in synthesizing environmental catalysts. In this regard, waste-based

resources exhibit clear viability and the potential utilization of waste-based catalysts for environmental remediation, as a substitute for regular used metals, warrants significant consideration within the future trajectory of environmental protection.

Author contributions TCK, PWC, NN, S-YK, NMI involved in critical thinking, figure editing and writing. TCK, RKL, LW, FSJY involved in conceptualization, original draft writing, review and editing. PWC and ZZ were involved in supervision and project administration. All authors read and approved the final draft.

Funding This research was supported by MOHE (FRGS/1/2022/STG01/UMT/02/2). The authors would like to thank Saveetha Institute of Medical and Technical Sciences for the research facilities provided.

Data availability All data is available.

Code availability Not applicable.

Declarations

Conflict of interest The authors would like to declare non-financial competing interest in this manuscript. Rock Keey Liew declares that he is a member of editorial board in Environmental Chemistry Letters.

Ethical approval Not applicable.

Consent to participate Not applicable.

Consent for publication Not applicable.

References

Adams IU, Nnamonu L, Itodo AU et al (2017) Calcination analysis, characterization and dyestuff adsorption potential of Nigerian limestones comparative analysis of mineralogical characteristics of clay-rich soil samples obtained from Gbajimba, Angbaaye and Makurdi areas of Benue State view project calcination analysis, characterization and dyestuff adsorption potential of Nigerian limestones. Am J Chem Appl 4:6–20

Ahmad F, Zaidi S (2021) Potential use of agro/food wastes as biosorbents in the removal of heavy metals. https://doi.org/10.5772/intechopen.94175

Akash S, Rameshwar SS, Rajamohan N et al (2024) Metal oxide nanobiochar materials to remediate heavy metal and dye pollution: a review. Environ Chem Lett. https://doi.org/10.1007/s10311-024-01724-4

Alhanif M, Purnomo A, Zuhra UA et al (2018) Preparation and characterization of calcium oxide (CaO) catalyst - Polyethersulfone (PES) membrane for biodiesel production and purification. AIP Conf Proc 2026:1–7. https://doi.org/10.1063/1.5065045

Amarasinghe A, Wanniarachchi D (2019) Eco-Friendly photocatalyst derived from eggshell waste for dye degradation. J Chem 2019:1–13. https://doi.org/10.1155/2019/8184732

Ameta R, Kumar D, Jhalora P (2014) ACPI photocatalytic degradation of Methylene blue using Calcium oxide (CaO). In Acta Chim Pharm Indica 4(1):20–28

Anantharaman A, Ramalakshmi S, George M (2016) Green synthesis of Calcium oxide (CaO) nanoparticles and its applications. J Eng Res Appl 6(10):27–31

Anaya-Rodríguez F, Durán-Álvarez JC, Drisya KT et al (2023) The challenges of integrating the principles of green chemistry and green engineering to heterogeneous photocatalysis to treat water and produce green H_2. Catalysts 13:1–32. https://doi.org/10.3390/catal13010154

Atadashi IM (2015) Purification of congo redude biodiesel using dry washing and membrane technologies. Alex Eng J 54:1265–1272. https://doi.org/10.1016/j.aej.2015.08.005

Ayoub M, Ullah S, Inayat A et al (2016) Process optimization for biodiesel production from waste frying oil over montmorillonite clay K-30. Proc Eng 148:742–749. https://doi.org/10.1016/j.proeng.2016.06.606

Balakrishnan A, Appunni S, Chinthala M et al (2022) Biopolymer-supported TiO_2 as a sustainable photocatalyst for wastewater treatment: a review. Environ Chem Lett 20:3071–3098. https://doi.org/10.1007/s10311-022-01443-8

Bathla A, Singla D, Pal B (2019) Highly efficient $CaCO_3$-Calcium oxide (CaO) extracted from tap water distillation for effective adsorption and photocatalytic degradation of Malachite green dye. Mater Res Bull 116:1–7. https://doi.org/10.1016/j.materresbull.2019.04.010

Boivin N, Zeder M, Fuller D et al (2016) Ecological consequences of human niche construction: examining long-term anthropogenic shaping of global species distributions. Proc Natl Acad Sci 113:6388–6396. https://doi.org/10.1073/pnas.1525200113

Boro J, Konwar LJ, Deka D (2014) Transesterification of nonedible feedstock with lithium incorporated eggshell derived Calcium oxide (CaO) for biodiesel production. Fuel Process Technol 122:72–78. https://doi.org/10.1016/j.fuproc.2014.01.022

Chen W, Yan W (2022) The impact of metal waste imports on industrial wastewater discharge in China. Front Environ Sci. https://doi.org/10.3389/fenvs.2022.911497

Chitra NJ, Vasanthakumari R, Amanulla S (2014) Preliminary studies of the effect of coupling agent on the properties of spent coffee grounds polypropylene bio-composites. Int J Eng Res Technol 7:9–16

Corami A, Mignardi S, Ferrini V (2007) Copper and zinc decontamination from single- and binary-metal solutions using hydroxyapatite. J Hazard Mater 146:164–170. https://doi.org/10.1016/j.jhazmat.2006.12.003

Diamantis K, Stamatis G, Champidi P (2016) Determination of heavy metals concentrations in water and soil resources in the mesogeia valley (athens). Eph - Int J Agric Environ Res 2:25–35

Eddy NO, Odiongenyi AO, Garg R et al (2023) Quantum and experimental investigation of the application of Crassostrea gasar (mangrove oyster) shell–based CaO nanoparticles as adsorbent and photocatalyst for the removal of procaine penicillin from aqueous solution. Environ Sci Pollut Res 30:64036–64057. https://doi.org/10.1007/s11356-023-26868-8

Egerić M, Smičiklas I, Mraković A et al (2018) Experimental and theoretical consideration of the factors influencing cationic pollutants retention by seashell waste. J Chem Technol Biotechnol 93:1477–1487. https://doi.org/10.1002/jctb.5516

Facciolà A, Laganà P, Caruso G (2021) The COVID-19 pandemic and its implications on the environment. Environ Res 201:1–14. https://doi.org/10.1016/j.envres.2021.111648

Fang B, Yu J, Chen Z et al (2023) Artificial intelligence for waste management in smart cities: a review. Environ Chem Lett 21:1959–1989. https://doi.org/10.1007/s10311-023-01604-3

Fatimah I, Rahmadianti Y, Pudiasari RA (2018) Photocatalyst of perovskite $CaTiO_3$ nanopowder synthesized from CaO derived from snail shell in comparison with the use of CaO and $CaCO_3$. IOP Conf Ser: Mater Sci Eng 349:012026. https://doi.org/10.1088/1757-899X/349/1/012026

Fu B, Gao L, Niu L et al (2009) Biodiesel from waste cooking oil via heterogeneous superacid catalyst SO42-/ZrO2. Energ Fuel 23:569–572. https://doi.org/10.1021/ef800751z

Ganesan VS, Paramathevar N (2024) Utilising calcined eggshell waste as a multifunctional sustainable agent as a nano-adsorbent, photocatalyst and priming elicitor. Environ Sci Pollut Res 31:12112–12130. https://doi.org/10.1007/s11356-023-31777-x

Gaur S, Singh N, Singh A et al (2017) Biological influences of mercury on living organisms. Int J Med Biomed Stud 1:16–25

Goya L, Delgado-Andrade C, Rufián-Henares JA et al (2007) Effect of coffee Melanoidin on human hepatoma HepG2 cells. Protection against oxidative stress induced by terf-butylhydroperoxide. Mol Nutr Food Res 51:536–545. https://doi.org/10.1002/mnfr.200600228

Habeeb OA, Danhassan UA (2014) Characterization and application of chicken eggshell as green adsorbents for removal of H_2S from wastewaters. IOSR J Environ Sci 8:7–12

Heydari M, Fazaeli R, Yousefi M (2012) Preparation of perovskite nanocomposites and photochemical degradation kinetics of acid yellow 199. J Appl Chem Res 6:7–15

Hong X, Wu X, Zhang Q et al (2012) Hydroxyapatite supported Ag3 PO4 nanoparticles with higher visible light photocatalytic activity. Appl Surf Sci 258:4801–4805. https://doi.org/10.1016/j.apsusc.2012.01.102

Hunt AJ, Matharu AS, King AH et al (2015) The importance of elemental sustainability and congo reditical element recovery. Green Chem 17:1949–1950. https://doi.org/10.1039/c5gc90019k

Ismail S, Ahmed AS, Anr R et al (2016) Biodiesel production from castor oil by using Calcium oxide (CaO) derived from mud clam shell. J Renew Energy 2016:1–8. https://doi.org/10.1155/2016/5274917

Jiang Q, Han Z, Yuan Y et al (2021) Preparation and properties of floral Calcium oxide (CaO)/ZnO composite from Achatina fulica snail shell. Environ Sci Pollut Res 28:61841–61847. https://doi.org/10.1007/s11356-021-16260-9

Joshi G, Rawat DS, Lamba BY et al (2015) Transesterification of Jatropha and Karanja oils by using waste eggshell derived calcium based mixed metal oxides. Energy Convers Manag 96:258–267. https://doi.org/10.1016/j.enconman.2015.02.061

Khan A, Bhoi RG, Saharan VK et al (2022) Green calcium-based photocatalyst derived from waste marble powder for environmental sustainability: a review on synthesis and application in photocatalysis. Environ Sci Pollut Res 29:86439–86467. https://doi.org/10.1007/s11356-022-20941-4

Kiong TC, Nordin N, Ahmad Ruslan NAA et al (2022) Valorization of discarded face mask for bioactive compound synthesis and photodegradation of dye. Environ Res 213:1–7. https://doi.org/10.1016/j.envres.2022.113737

Kouzu M, Kasuno T, Tajika M et al (2008) Calcium oxide (CaO) as a solid base catalyst for transesterification of soybean oil and its application to biodiesel production. Fuel 87:2798–2806. https://doi.org/10.1016/j.fuel.2007.10.019

Laskar IB, Rajkumari K, Gupta R et al (2018) Waste snail shell derived heterogeneous catalyst for biodiesel production by the transesterification of soybean oil. RSC Adv 8:20131–20142. https://doi.org/10.1039/c8ra02397b

Lawrence H, Van V (1989) Elements of materials science and engineering, 6th edn. Addison-Wesley Reading, Mass., USA

Lee HK, Park YG, Jeong T et al (2015) Green nanocomposites filled with spent coffee grounds. J Appl Polym Sci 132:2–7. https://doi.org/10.1002/app.42043

Liotta LF, Gruttadauria M, Di Carlo G et al (2009) Heterogeneous catalytic degradation of phenolic substrates: catalysts activity. J Hazard Mater 162:588–606. https://doi.org/10.1016/j.jhazmat.2008.05.115

Liu W, Qian G, Zhang B et al (2016) Facile synthesis of spherical nano hydroxyapatite and its application in photocatalytic degradation of methyl orange dye under UV irradiation. Mater Lett 178:15–17. https://doi.org/10.1016/j.matlet.2016.04.175

Liu T, Ni SY, Wang Z (2024) Contamination and health risk assessment of heavy metals in soil surrounding an automobile industry factory in Jiaxing, China. Front Environ Sci 12:1362366. https://doi.org/10.3389/fenvs.2024.1362366

Ljupković RB, Radulović NS, Bojić AL et al (2014) Significance of the structural properties of Calcium oxide (CaO) catalyst in the production of biodiesel: an effect on the reduction of greenhouse gas emissions. Hem Ind 68:399–412. https://doi.org/10.2298/HEMIND130612063L

Loo WW, Pang YL, Wong KH et al (2018) Adsorption-photocatalysis of organic dyes using empty fruit bunch activated carbon-metal oxide photocatalyst. IOP Conf Ser Mater Sci Eng 458:1–9. https://doi.org/10.1088/1757-899X/458/1/012042

Lourinho G, Brito P (2015) Advanced biodiesel production technologies: novel developments. Rev Environ Sci Biotechnol 14:287–316. https://doi.org/10.1007/s11157-014-9359-x

Madhusudhana N, Yogendra K, Mahadevan KM (2012) A comparative study on photocatalytic degradation of Violet GL2B azo dye using Calcium oxide (CaO) and TiO_2 nanoparticles. Int J Sci Res 1:91–95

Mohamed F, Shaban M, Aljohani G et al (2021) Synthesis of novel eco-friendly Calcium oxide (CaO)/C photocatalyst from coffee and eggshell wastes for dye degradation. J Mater Res Technol 14:3140–3149. https://doi.org/10.1016/j.jmrt.2021.08.055

Morin-Crini N, Lichtfouse E, Liu G et al (2022) Worldwide cases of water pollution by emerging contaminants: a review. Environ Chem Lett 20:2311–2338. https://doi.org/10.1007/s10311-022-01447-4

Mosaddegh E, Hassankhani A, Pourahmadi S et al (2013) Ball mill–assisted preparation of nano-$CaCO_3$ as a novel and green catalyst–based eggshell waste. Int J Green Nanotechnol 1:1–15. https://doi.org/10.1177/1943089213507160

Niju S, Begum MMMS, Anantharaman N (2014) Modification of eggshell and its application in biodiesel production. J Saudi Chem Soc 18:702–706. https://doi.org/10.1016/j.jscs.2014.02.010

Nopriansyah E, Baehaki A, Nopianti R (2016) Pembuatan serbuk cangkang keong mas (*Pomacea canaliculata* L.) serta aplikasinya sebagai penjernih air sungai dan pengikat logam berat kadmium. Fishtech J Teknol Has Perikan 5:1–10

Omar AH, Ramesh K, Gomaa AMA et al (2017) Experimental design technique on removal of hydrogen sulfide using CaO-eggshells dispersed onto palm kernel shell activated carbon: experiment, optimization, equilibrium and kinetic studies. J Wuhan Univ Technol-Mat Sci Edit 32:305–320. https://doi.org/10.1007/s11595-017-1597-7

Osman AI, Nasr M, Farghali M et al (2024) Optimizing biodiesel production from waste with computational chemistry, machine learning and policy insights: a review. Environ Chem Lett. https://doi.org/10.1007/s10311-024-01700-y

Ovodok E, Ivanovskaya M, Poznyak S et al (2017) Characterization of surface species on mesoporous TiO_2 prepared by TiC oxidation.

Phys Chem Appl Nanostruct 2017:311–314. https://doi.org/10.1142/9789813224537_0072
Pal A, Paul S, Choudhury AR et al (2017) Synthesis of hydroxyapatite from lates calcarifer fish bone for biomedical applications. Mater Lett 203:89–92. https://doi.org/10.1016/j.matlet.2017.05.103
Parmar V, Changela K, Srinivas B et al (2019) Relationship between dislocation density and antibacterial activity of congo redyo-rolled and cold-rolled copper. Materials (basel) 12:1–11. https://doi.org/10.3390/ma12020200
Pooladi A, Bazargan-Lari R (2020) Simultaneous removal of copper and zinc ions by chitosan/hydroxyapatite/nano-magnetite composite. J Mater Res Technol 9:14841–14852. https://doi.org/10.1016/j.jmrt.2020.10.057
Pradhan G, Sharma YC (2021) A greener and cheaper approach towards synthesis of glycerol carbonate from bio waste glycerol using CaO–TiO_2 nanocatalysts. J Clean Prod 315:127860. https://doi.org/10.1016/j.jclepro.2021.127860
Praveen PJ, Parameswaran PS, Majik MS (2015) Bis(indolyl)methane Alkaloids: isolation, bioactivity, and syntheses. Synth 47:1827–1837. https://doi.org/10.1055/s-0034-1380415
Predojević ZJ (2008) The production of biodiesel from waste frying oils: a comparison of different purification steps. Fuel 87:3522–3528. https://doi.org/10.1016/j.fuel.2008.07.003
Rachmawati SH, Hossain Z, Shiau J (2020) Shear strength of soil by using clam shell waste as recycle aggregate. J Agric Eng 51:155–160. https://doi.org/10.4081/jae.2020.1043
Razak A, Najah MI, Munirah et al (2022) Review on eggshell waste in tissue engineering application. Int J Integr Eng 14:64–80
Reyes-Vallejo O, Sánchez-Albores R, Maldonado-Álvarez A et al (2023) Calcium-Magnesium oxide by the ball-milling method using eggshell as calcium source: its study for photodegradation of methylene blue. J Mater Sci: Mater Electron 34:770. https://doi.org/10.1007/s10854-023-10163-w
Rodiah S, Erviana D, Rahman F et al (2020) Modified Calcium oxide (CaO) catalyst from golden snail shell (Pomacea canaliculata) for transesterification reaction of used cooking oil. Al-Kimia 8:83–92
Roschat W, Siritanon T, Kaewpuang T et al (2016) Economical and green biodiesel production process using river snail shells-derived heterogeneous catalyst and co-solvent method. Bioresour Technol 209:343–350. https://doi.org/10.1016/j.biortech.2016.03.038
Safarik I, Horska K, Svobodova B et al (2012) Magnetically modified spent coffee grounds for dyes removal. Eur Food Res Technol 234:345–350. https://doi.org/10.1007/s00217-011-1641-3
Sahoo PK, Das LM (2009) Combustion analysis of Jatropha, Karanja and Polanga based biodiesel as fuel in a diesel engine. Fuel 88:994–999. https://doi.org/10.1016/j.fuel.2008.11.012
Sathiyavimal S, Vasantharaj S, Shanmugavel M et al (2020) Facile synthesis and characterization of hydroxyapatite from fish bones: photocatalytic degradation of industrial dyes (Crystal violet and Congo red). Prog Org Coat. https://doi.org/10.1016/j.porgcoat.2020.105890
Sawant S, Somani S, Omanwar SK et al (2015) Chemical and photocatalytic degradation of Congo redystal violet dye by Indian Edible Chuna (Calcium oxide (CaO)/Hydroxide). J Green Sci Technol 2:45–48. https://doi.org/10.1166/jgst.2015.1038
Selvaranjan K, Navaratnam S, Rajeev P et al (2021) Environmental challenges induced by extensive use of face masks during COVID-19: a review and potential solutions. Environ Challenges 3:1–11. https://doi.org/10.1016/j.envc.2021.100039
Seo SSA, Lee HN, Noh TW (2005) Infrared spectroscopy of $CaTiO_3$, $SrTiO_3$, $BaTiO_3$, $Ba_{0.5}Sr_{0.5}TiO_3$ thin films, and $(BaTiO_3)_5$/$(SrTiO_3)_5$ superlattice grown on $SrRuO_3$/$SrTiO_3$(001) substrates. Thin Solid Films 486:94–97. https://doi.org/10.1016/j.tsf.2004.10.061
Shi D, Wu W, Li X (2022) Ultrasensitive detection of mercury(ii) ions on a hybrid film of a graphene and gold nanoparticle-modified electrode. Anal Methods 14:2161–2167. https://doi.org/10.1039/d2ay00413e
Sivaramakrishnan K, Ravikumar P (2012) Determination of cetane number of biodiesel and it's influence on physical properties. ARPN J Eng Appl Sci 7:205–211
Sree GV, Nagaraaj P, Kalanidhi K et al (2020) Calcium oxide (CaO) a sustainable photocatalyst derived from eggshell for efficient photo-degradation of organic pollutants. J Clean Prod 270:1–80. https://doi.org/10.1016/j.jclepro.2020.122294
Stewart DJC, Fisher LV, Warwick MEA et al (2022) Facemasks and ferrous metallurgy: improving gasification reactivity of low-volatile coals using waste COVID-19 facemasks for iron-making application. Sci Rep 12:1–13. https://doi.org/10.1038/s41598-022-06691-w
Stötzel C, Müller FA, Reinert F et al (2009) Ion adsorption behaviour of hydroxyapatite with different congo redystallinities. Colloids Surf B: Biointerfaces 74:91–95. https://doi.org/10.1016/j.colsurfb.2009.06.031
Tahvildari K, Anaraki YN, Fazaeli R et al (2015) The study of Calcium oxide (CaO) and MgO heterogenic nano-catalyst coupling on transesterification reaction efficacy in the production of biodiesel from recycled cooking oil. J Environ Heal Sci Eng 13:1–10. https://doi.org/10.1186/s40201-015-0226-7
Talebian-Kiakalaieh A, Amin NAS, Mazaheri H (2013) A review on novel processes of biodiesel production from waste cooking oil. Appl Energy 104:683–710. https://doi.org/10.1016/j.apenergy.2012.11.061
Tan YH, Abdullah MO, Nolasco-Hipolito C et al (2015) Waste ostrich- and chicken-eggshells as heterogeneous base catalyst for biodiesel production from used cooking oil: catalyst characterization and biodiesel yield performance. Appl Energy 160:58–70. https://doi.org/10.1016/j.apenergy.2015.09.023
Tangboriboon N, Kunanuruksapong R, Sirivat A et al (2012) Preparation and properties of calcium oxide (CaO) from eggshells via calcination. Mater Sci Pol 30:313–322. https://doi.org/10.2478/s13536-012-0055-7
Teknologi J, Asma T, Bakar A et al (2017) Eggshell coated grey cast iron for corrosion application. J Teknol 79:1–6
Tezyapar Kara I, Kremser K, Wagland ST et al (2023) Bioleaching metal-bearing wastes and by-products for resource recovery: a review. Environ Chem Lett 21:3329–3350. https://doi.org/10.1007/s10311-023-01611-4
Tran GT, Nguyen NTH, Nguyen NTT et al (2023) Plant extract-mediated synthesis of aluminum oxide nanoparticles for water treatment and biomedical applications: a review. Environ Chem Lett 21:2417–2439. https://doi.org/10.1007/s10311-023-01607-0
Veeranna DK, Lakshamaiah MT, Narayan RT (2014) Photocatalytic degradation of Indigo carmine dye using Calcium oxide (CaO). Int J Photochem 2014:1–6. https://doi.org/10.1155/2014/530570
Wang G, Xiang J, Lin J et al (2020) Sustainable advanced fenton-like catalysts based on mussel-inspired magnetic cellulose nanocomposites to effectively remove organic dyes and antibiotics. ACS

Appl Mater Interfaces 12:51952–51959. https://doi.org/10.1021/acsami.0c14820

Wang J, Tao S, Zhao Y et al (2021) Utilization of waste clam shell as cost-effective catalyst for heterogeneous biodiesel production. Am Sci Publ 15:296–301. https://doi.org/10.1166/jbmb.2021.2074

Waqas W, Yuan Y, Ali S et al (2024) Toxic effects of heavy metals on crustaceans and associated health risks in humans: a review. Environ Chem Lett. https://doi.org/10.1007/s10311-024-01717-3

Wei Z, Xu C, Li B (2009) Application of waste eggshell as low-cost solid catalyst for biodiesel production. Bioresour Technol 100:2883–2885. https://doi.org/10.1016/j.biortech.2008.12.039

Wu L, Guan Y, Li C et al (2023a) Free-radical behaviors of co-pyrolysis of low-rank coal and different solid hydrogen-rich donors: a critical review. Chem Eng J 474:145900. https://doi.org/10.1016/j.cej.2023.145900

Wu L, Wu H, Wen Q et al (2023b) Gas stripping coupled with in-situ oxidation assisted microwave remediation of contaminated soil for efficient removal of polycyclic aromatic hydrocarbons (PAHs). Chem Eng J 473:145411. https://doi.org/10.1016/j.cej.2023.145411

Zabeti M, Wan Daud WMA, Aroua MK (2009) Activity of solid catalysts for biodiesel production: a review. Fuel Process Technol 90:770–777. https://doi.org/10.1016/j.fuproc.2009.03.010

Zhu Q, Liu N, Zhang N et al (2018) Efficient photocatalytic removal of RhB, MO and MB dyes by optimized Ni/NiO/TiO_2 composite thin films under solar light irradiation. J Environ Chem Eng 6:2724–2732. https://doi.org/10.1016/j.jece.2018.04.017

ARTICLES FOR FACULTY MEMBERS

ELUCIDATING THE CALCIUM OXIDE DERIVED FROM THE WASTE SHELLS OF MUD CLAM (GELOINA EXPANSA) AS A CATALYST FOR BIODIESEL PRODUCTION

Efficient conversion of leather tanning waste to biodiesel using crab shell-based catalyst: Waste-to-energy approach / Yuliana, M., Santoso, S. P., Soetaredjo, F. E., Ismadji, S., Ayucitra, A., Gunarto, C., Angkawijaya, A. E., Ju, Y. H., & Truong, C. T.

Biomass and Bioenergy
Volume 151 (2021) 106155 Pages 1-9
https://doi.org/10.1016/J.BIOMBIOE.2021.106155
(Database: ScienceDirect)

Biomass and Bioenergy 151 (2021) 106155

Contents lists available at ScienceDirect

Biomass and Bioenergy

journal homepage: www.elsevier.com/locate/biombioe

Efficient conversion of leather tanning waste to biodiesel using crab shell-based catalyst: WASTE-TO-ENERGY approach

Maria Yuliana [a,*], Shella Permatasari Santoso [a,b], Felycia Edi Soetaredjo [a,b], Suryadi Ismadji [a,b], Aning Ayucitra [a], Chintya Gunarto [b], Artik Elisa Angkawijaya [c], Yi-Hsu Ju [b,c,d], Chi-Thanh Truong [e]

[a] Department of Chemical Engineering, Widya Mandala Catholic University Surabaya, Kalijudan 37, Surabaya, 60114, Indonesia
[b] Department of Chemical Engineering, National Taiwan University of Science and Technology, 43, Keelung Rd. Sec. 4, Taipei, 10607, Taiwan
[c] Graduate Institute of Applied Science and Technology, National Taiwan University of Science and Technology, 43 Keelung Road, Sec 4, Taipei, 10607, Taiwan
[d] Taiwan Building Technology Center, National Taiwan University of Science and Technology, 43 Keelung Road, Sec 4, Taipei, 10607, Taiwan
[e] Department of Chemical Engineering, Can Tho University, 3-2 Street, Can Tho City, Viet Nam

ARTICLE INFO

Keywords:
Leather tannery waste
Crab shell
Biodiesel
Waste-derived fuel
Reusability
Optimization study

ABSTRACT

To promote the use of waste-originated resources in biodiesel production, this study proposes the utilization of leather tanning waste (LTW) and crab-shell (CS) waste as the respective lipid source and catalyst material. The obtained CS-based calcium oxide (CaO) has comparable textural properties with those of existing waste-based catalysts and shows high catalytic activity for the conversion of LTW to biodiesel. The optimum yield of fatty acid ethyl esters (FAEE) is predicted at 97.9 wt%, while it is experimentally observed at 98.7 ± 0.4 wt% (purity of 98.6 ± 0.4 wt%) using the following operating condition: reaction time $t = 3.58$ h, catalyst amount $m_c = 3.87$ wt%, and a molar ratio of ethanol to LTW $m_{eo} = 12{:}1$. The CS-based CaO shows good reusability with FAEE yield staying above 90 wt% for four cycles. The fuel properties of LTW-based biodiesel meet ASTM D6751 and ASTM D975-08 standards, with the ethyl ester ranging from C14 to C20.

1. Introduction

Worldwide interest in the use of waste to fulfill the energy demand is currently growing in a very rapid manner. Many types of research related to waste-to-energy have been conducted to improve the trans-esterification yield, find the simplest and low-cost technique as well as fabricate waste-based catalysts. Known as an archipelago country, the aquaculture industries are one of the biggest and most important sectors in Indonesia. Approximately 30,000 tons of crab are produced annually, where its meat only accounts for only around 35 wt% of the total crab mass. This leaves almost 20,000 tons of solid waste discharged each year [1]. While in the developed countries, waste disposal is costly, crab shells (CS) in Indonesia are often directly discharged to the environment.

CS exhibits potential value due to its valuable chemical contents, namely protein (20–40 wt%), calcium carbonate (20–50 wt%), and chitin (15–40 wt%) [2]. Being the largest component in CS, calcium carbonate finds extensive applications in pharmaceutical, agricultural, material development, and catalysis. Many studies have been conducted to develop calcium-based solid catalyst, with calcium oxide (CaO) as the main focus due to its advantages of substantial catalytic activity, high basicity, non-toxicity [3,4], good availability, and low cost [5]. In addition, the conversion of calcium carbonate to CaO can be achieved using a relatively simple method, that is, by thermal decomposition via calcination at high temperatures to liberate carbon dioxide from the raw materials [6].

Currently, transesterification of lipid to biodiesel is employed mainly using a homogenous catalyst, due to its phase homogeneity and shorter reaction time [5,7]. However, this type of catalyst cannot be reused and requires additional washing and separation steps, hence inducing attention in the use of the heterogeneous solid catalyst for the biodiesel preparation process. Despite its comparable catalytic activity and

Abbreviations: ANOVA, Analysis of variance; CaO, Calcium oxideCS Crab shell; DOE, Design of experiment; FA, Fatty acid; FAEE, Fatty acid ethyl esters; FFA, Free fatty acid; FID, Flame ionized detection; LTW, Leather tanning waste; MLFD, Multilevel factorial design; RSM, Response surface methodology; SEE, Standard error of estimate; TGA, Thermogravimetric analysis.

* Corresponding author.
E-mail addresses: maria_yuliana_liauw@yahoo.com, mariayuliana@ukwms.ac.id (M. Yuliana).

https://doi.org/10.1016/j.biombioe.2021.106155
Received 8 January 2021; Received in revised form 16 May 2021; Accepted 6 June 2021
Available online 15 June 2021

simpler use in the transesterification process, many heterogeneous catalysts are not viable for industrial usage since most of the catalysts are expensive and require complicated preparation efforts [8,9]. Therefore, synthesizing simple yet highly active catalysts for biodiesel preparation is important. Due to this very reason, an increasing number of studies on the neat, supported, loaded, and mixed CaO has been widely investigated [3,6]. The high catalytic activity of CaO might be attributed to the presence of oxygen attached to its surface, which acts as a strong basic conjugate [10]. These basic sites abstract a proton from the organic compounds and initiate the basic catalysis reaction [6]. The catalytic activity of CaO-based catalyst in the transesterification has been conducted using various natural-based raw materials as follows: mussel shells [11,12], eggshells [13], waste capiz shells [8,9], cockle shells [12], Pomacea sp. shells [14] and river snail shells [15]. Extensive utilization of waste-based catalysts is expected to reduce the material cost as well as to conduct a good waste management practice.

To date, the development of waste-based solid catalyst mainly focuses on the conversion of refined oils, rather than waste lipid materials, to biodiesel. The selection of refined oils as the raw materials is generally due to its low free fatty acid (FFA) and moisture content; therefore, it is easier to process and gives a more stable yield. However, the mass utilization of this type of lipid will disrupt the food supply chain. Yuliana et al. [16] mentioned that non-edible oils, specifically fat, oil, and grease (FOG) and animal fats, are currently the best options for biodiesel feedstock compared to edible ones due to their low price. Moreover, the valorization of the waste-based lipid will significantly lessen the amount of the waste, and at the same time, turn them into a valuable asset. Therefore, this study combines the use of CS-based catalysts and leather tanning waste (LTW) as a lipid source to produce biodiesel.

With 80 wt% of the rawhide is discharged as waste during the commercial tanning process of leather [17,18], the annual production of LTW in Indonesia reaches 100,000 tons [19,20]. LTW contains a substantial amount of crude fat (>60 wt%) [18] that can be converted to biodiesel; which renders it an abundant raw material to prepare biodiesel. A number of valorization approaches have been previously conducted to prepare biodiesel from LTW, namely using supercritical methanol [20], Cs_2O-loaded Fe_3O_4 nanoparticles [21], solid-state fermentation using silica-immobilized micro bacteria soaked in inorganic nutrients (e.g., $MgSO_4$, $FeSO_4$, $CoCl_2$, $MnCl_2$, $CaCl_2$, and $(NH_4)_6Mo_7O_{24}$) [22], and conventional basic catalyst (e.g., potassium methoxide [23], sodium and potassium hydroxide [24,25], and methanolic tetramethylammonium hydroxide [26]). While the first three techniques require a high amount of energy and complicated processing steps, the last technique using basic catalysts often faces many challenges due to the presence of high water and FFA content. These two components promote the hydrolysis and saponification reactions during the traditional conversion [16], which leads to a difficult separation and lower yield. Therefore, with the above-mentioned advantages of simple preparation, low cost, and insensitivity to contaminants during use, CS-based CaO can be considered highly potential to prepare biodiesel with commercial yield and specification from LTW in one-pot transesterification. Besides, due to the nature of the two waste materials, a waste-to-energy approach can be achieved via the utilization of CS and LTW as the starting catalyst and biodiesel feedstocks, respectively.

The influence of three independent processing variables (catalyst loading m_c, reaction time t, and the molar ratio of ethanol to LTW m_{eo}) on the yield of fatty acid ethyl esters (FAEE) is studied. The optimization approach is conducted using a combination of response surface methodology (RSM) and multilevel factorial design (MLFD) to obtain the optimized reaction parameters, which can be implemented in industrial practice. Among many statistical and mathematical approaches, MLFD is selected because it (1) incorporates all interactions of the three variables at all levels, and (2) offers more flexibility in assessing these interactions when the number of degrees of freedom is sufficient [27]. Moreover, the use of the factorial design also increases the statistical sensitivity and generalizability without decreasing precision [28]; therefore, it is superior compared to the other methods. This study also uses ethanol as the alcohol source to maintain the phase homogeneity in the reaction system which leads to an increase in reaction rate [29,30]. The reusability of the CS-based CaO is also monitored at the optimum operating condition.

2. Materials and methods

2.1. Materials

Both raw waste materials, CS and LTW, were collected from a local supplier in Surabaya, Indonesia. While CS was obtained from a local fish market, LTW was provided by a leather tannery in Indonesia. The pretreatment of CS was conducted using the following procedures [8]: CS was first rinsed to remove the impurities. The cleansed CS was pulverized to a powder and subjected to the calcination process at 900 °C for 2 h. The calcined CS was further ground to a powder with a particle size of smaller than 25 μm. The obtained powder was then stored in a vacuum container before use. At the same time, LTW was washed with water to remove unwanted dirt and impurities, followed by heating at 120 °C to remove retaining moisture. LTW was then purified using a membrane filter.

All solvents and chemicals used for biodiesel preparation and analysis were purchased from Merck (Germany) and of analytical grade; therefore, does not require any further purification. The gases required for gas chromatography analysis, namely nitrogen and helium (>99.9%) were procured from Aneka Gas Industry Pty. Ltd., Surabaya. The composition of the biodiesel product was identified using the FAEE certified reference (10008188) obtained from Cayman Chemicals (MI, USA), while methyl heptadecanoate, which acts as the internal standard to calculate the purity of FAEE, was purchased from Sigma-Aldrich (Germany).

2.2. The properties determination of CS-based CaO and LTW

The surface topography and morphology images of CS-based CaO were captured by FESEM JEOL JSM-6500F (Jeol Ltd., Japan), with the respective voltage and working distance of 10 kV and 8.0 mm. Meanwhile, the textural properties of CS-based CaO, such as its specific surface area and pore volume, were obtained using Micromeritics ASAP 2010 Sorption Analyzer at 77 K. The XRD diffractogram of the catalyst was acquired in $2\theta = 15°–90°$ using an X'PERT Panalytical Pro X-Ray diffractometer (Philips-FEI, Netherlands). The wavelength of monochromatic Cu $K\alpha_1$ radiation (λ) is set at 0.154 nm. The voltage and tube current is adjusted at 40 kV and 30 mA, respectively. To measure its thermal stability, 6 mg of CS-based CaO powder were placed in a platinum pan and subjected to a PerkinElmer TG/DTA Diamond (PerkinElmer, Japan). The oven temperature was then increased from 30 °C to 900 °C at a rate of 10 °C/min under a continuous nitrogen purge (velocity of nitrogen purge = 20 ml/min) to monitor the degradation profile of the CS-based CaO.

Meanwhile, the crude fat, FFA, and moisture content in LTW were determined following AOAC 991.36, ASTM D5555-95, and AOCS Ca 2e-84, respectively. LTW is also further analyzed for its fatty acid (FA) profile using GC-2014 (Shimadzu Ltd., Japan), following the method of ISO 12966. Restek Rtx-65TG (30 m × 0.25 mm ID x 0.10 μm film

Table 1
The encoded reaction parameters and their corresponding values.

Variables	Encoded factor	Factor level				
		1	2	3	4	5
Catalyst loading (mc, wt%)	A	1	2	3	4	5
		1		**2**		**3**
Reaction time (t, h)	B	2		3		4
Molar ratio of ethanol to LTW (m_{eo})	C	6:1		9:1		12:1

thickness, Restek, USA) was selected as the separation column to identify the FA profile in LTW.

2.3. Biodiesel preparation using LTW and CS-based CaO

Ethanol as the alcohol source and LTW at m_{eo} = 6:1, 9:1, and 12:1 was added into a three-neck flask, fully installed along with a condenser, magnetic stirrer, and heater. A specified amount of CS-based CaO (m_c = 1, 2, 3, 4, 5 wt%) was introduced into the system. The reaction system was then heated to 60 °C and maintained isothermally throughout the process with constant agitation at 700 rpm for various t (2, 3, 4 h). After the reaction was completed, the catalyst was separated from the liquid product mixture by centrifugation and regenerated through a cycle of repeated washing and calcination at 900 °C. The product mixture was settled to obtain two layers, the top layer consisting FAEE and other minor components, and the bottom layer which is the mixture of glycerol, excess ethanol, and other undesirable by-products. The separated FAEE-rich phase was then subjected to vacuum evaporation to obtain the biodiesel product.

Using the optimized reaction condition obtained in section 2.5, a repetition of transesterification using the same catalyst was performed until the yield of FAEE reached below 90 wt% to measure the reusability of the CS-based CaO. All runs were conducted in triplicates.

2.4. Compositional analysis of LTW-based biodiesel using GC-FID

The FAEEs composition in the LTW-based biodiesel was identified by Shimadzu GC-2014, with the split/splitless injection and the flame ionized detection (FID) mode. The stationary silica phase used in the chromatography separation is the narrow bore type of DB-WAX capillary column (30 m × 0.25 mm ID x 0.25 μm film thickness, Agilent Technology, CA). Before analysis, 100 mg of biodiesel product was dissolved in 2 ml of methyl heptadecanoate solution (10 μg/ml) which acts as an internal standard. The mixture was then injected at a split ratio of 1:50 into the GC column which temperature has been initially adjusted at 50 °C before injection. The temperature profile of the instrument and the carrier gas (helium, > 99.9%) purge flowrate for the compositional analysis follows the study performed by Santosa et al. [31].

The chromatogram of the FAEE certified reference (10008188) was used against that of the biodiesel product to identify the FAEE peaks. The FAEE purity and yield were computed using equations (1) and (2).

$$FAEE\ Purity\ (F_p,\ wt\%) = \left(\frac{\sum A_{FAEE} - A_{IS}}{A_{IS}} \times \frac{V_{IS} C_{IS}}{m_{FAEE}}\right) \times 100\% \quad (1)$$

where $\sum A_{FAEE}$ is the area sum of FAEE peaks, A_{IS} is the area of methyl heptadecanoate peak, V_{IS} is the volume of methyl heptadecanoate solution (ml), C_{IS} is the concentration of methyl heptadecanoate solution (g/ml), m is the actual mass of the FAEE sample used in the GC-FID analysis (g).

Table 2
The DOE matrix based on MLFD.

Run	Input variables			Response (FAEE yield, wt%)		
	A	B	C	Experimental[a]	Predicted (Y_{FAEE})[a]	Standard deviation[b]
1	4	3	3	95.8	97.4	1.11
2	1	3	1	63.8	66.9	2.20
3	3	1	2	85.1	87.1	1.44
4	5	1	3	92.2	90.2	1.42
5	4	1	3	91.4	92.8	0.96
6	4	2	2	93.5	96.1	1.86
7	2	3	1	83.1	82.9	0.14
8	2	3	3	91.2	86.7	3.16
9	5	2	3	93.3	93.5	0.16
10	1	2	2	63.9	65.9	1.42
11	3	2	2	93.4	92.8	0.45
12	1	1	2	59.1	58.1	0.72
13	4	1	2	90.2	91.6	0.98
14	3	3	1	94.6	92.2	1.70
15	3	3	3	95.6	95.4	0.14
16	1	3	3	68.2	71.3	2.22
17	1	3	2	67.6	69.5	1.32
18	3	3	2	94.3	94.2	0.11
19	1	2	3	65.9	67.9	1.40
20	1	2	1	63.6	63.2	0.26
21	1	1	3	57.6	60.2	1.81
22	4	3	1	92.3	94.8	1.75
23	5	3	2	92.3	92.0	0.24
24	5	1	2	92.2	89.3	2.03
25	3	2	1	92.9	90.7	1.55
26	2	1	1	71.2	73.5	1.62
27	4	3	2	95.3	96.4	0.79
28	3	1	1	82.5	85.0	1.75
29	2	1	3	80.2	77.7	1.74
30	5	2	2	92.0	92.8	0.55
31	3	1	3	87.9	88.6	0.50
32	2	3	2	88.6	85.2	2.43
33	2	1	2	75.6	76.0	0.26
34	2	2	3	89.2	84.4	3.42
35	2	2	1	82.8	80.3	1.75
36	3	2	3	94.8	94.1	0.47
37	5	1	1	91.2	87.8	2.42
38	5	2	1	91.6	91.3	0.19
39	2	2	2	86.3	82.7	2.55
40	4	1	1	87.4	89.7	1.65
41	4	2	1	89.5	94.4	3.45
42	5	3	3	92.1	92.6	0.36
43	4	2	3	94.5	97.2	1.90
44	1	1	1	58.9	55.3	2.54
45	5	3	1	93.1	90.6	1.75

[a] The average standard error of estimate (SEE) between the two corresponding responses is 1.24%.

[b] The deviation between the two corresponding responses for each run.

$$FAEE\ Yield\ (wt\%) = \left(\frac{m_{FAEE}}{m_{LTW}} x\ F_p\right) \times 100\% \quad (2)$$

where m_{FAEE} is the final FAEE mass obtained (g), m_{LTW} is the initial mass of LTW (g) and F_p is the FAEE purity obtained from equation (1).

2.5. Design of experiment and determination of optimum point using RSM

The statistical analysis using the combination of RSM and MLFD as the design of experiment (DOE) was performed for the determination of the optimum transesterification parameters to obtain the maximum

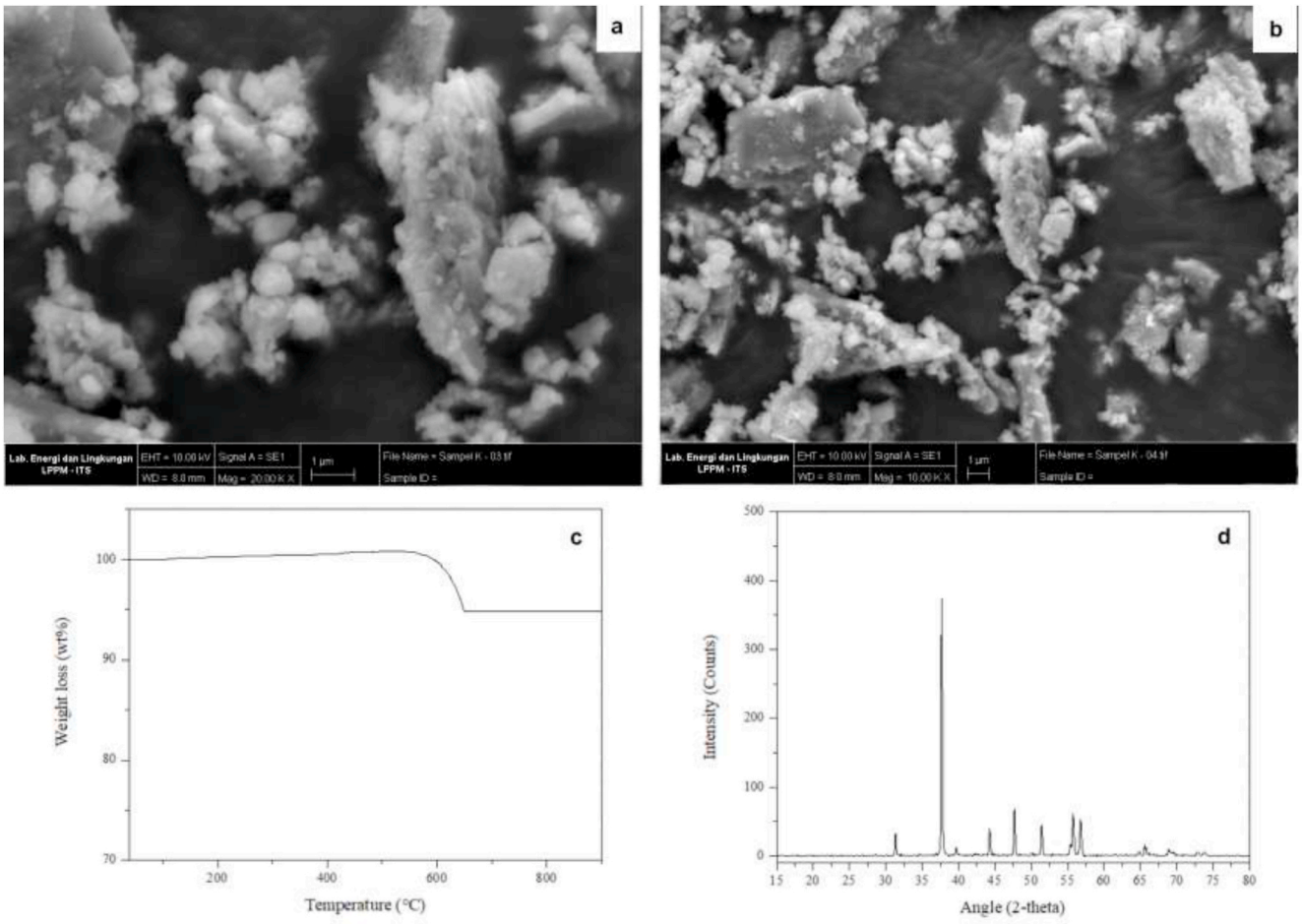

Fig. 1. (a)–(b) FESEM images, (c) TGA analysis, (d) XRD pattern of CS-based CaO.

Table 3
The textural properties of CS and CS-based CaO.

Materials	Specific surface area (S_{BET}, m^2/g)	Pore volume (V_p, cm^3/g)
CS	0.91	0.022
CS-based CaO	12.47	0.081

yield of FAEE as the response. The input variables, namely m_c (wt%), t (h), and m_{eo} (mol/mol) were chosen as the critical parameters due to their relevance to the industrial applicability since these parameters greatly affect the processing efficiency and operational cost. While both t and m_{eo} are separated into three levels: low (1), middle (2), and high (3), m_c is classified into five levels with an ascending order to accurately observe the influence of the parameter on the yield of FAEE (wt%). Table 1 presents the encoded parameters and their actual values.

The DOE matrix, shown in Table 2, lists the correlation between the reaction parameters for each run with their corresponding experimental and predicted responses (FAEE yield, wt%). To attain good data reproducibility and accuracy, the experimental runs were carried out in triplicates and randomized order. Analysis of variance (ANOVA) is employed by using Minitab (ver. 18.1) with a confidence level of 95% to generate the fitted equation, to describe the behavior of the three operating variables on the yield of FAEE. The goodness-of-fit analysis on the generated mathematical model is also evaluated using the R-squared value.

The following equation (3) shows the correlation between the predicted response (FAEE yield, wt%) and the input variables, where Y_{FAEE} is the predicted FAEE yield (wt%); k_0, k_i, k_{ii}, k_{ij} are the coefficients for the intercept, linear, quadratic, and two-way interactions of the input variables, respectively; X_i and X_j are the encoded reaction variables (A, B, C). While the value of i lies between 1 and 3 for t and m_{eo}, it ranges from 1 to 5 for m_c.

$$Y_{FAEE} = k_0 + \sum_{i=1}^{3} k_i X_i + \sum_{i=1}^{3} k_{ii} X_i^2 + \sum_{i=1}^{3} \sum_{j=1}^{3} k_{ij} X_i X_j \quad (3)$$

3. Results and discussions

3.1. Characterization of CS-based CaO

Fig. 1 (a) and (b) present the surface topographies of CS-based CaO. It is notable that the catalyst particle is irregular in shape and has a rough surface with a honeycomb-like structure (Fig. 1 (a)). The calcination reaction at 900 °C removes a substantial amount of bound water from the catalyst pores, hence creating high porosity [11]. However, it is also evident from the FESEM images that catalyst particles are aggregated, resulting in non-uniform particle size. Valverde et al. [32] stated that the presence of carbon in the CS-based CaO will induce the formation of CO_2 during the calcination. This CO_2 gas will then react with the CaO product to produce calcium carbonate, the primary cause of particle aggregation.

The textural properties of CS and CS-based CaO analyzed by nitrogen sorption are provided in Table 3. The CS-based CaO has superior properties than those of raw CS. Yoosuk et al. [33] stated that the removal of impurities and moisture during the high-temperature calcination plays a critical role in improving the porosity and textural properties of the CS-based CaO. As the surface area and pore volume of catalyst have a

Table 4
The chemical properties of LTW.

Parameters	Result
Moisture, wt%	11.45
FFA, wt%	18.89
Total crude fat, wt%	69.66
Molecular mass, g/mol	798.5
FA composition, wt%	
C14:0	4.30
C16:0	28.70
C16:1	2.60
C17:0	0.70
C18:0	13.40
C18:1	43.50
C18:2	4.90
C18:3	1.80
C20:0	0.10

proportional influence on its catalytic activity, it is expected that CS-based CaO has a comparable, if not superior, catalytic activity compared to the existing CaO catalyst.

To demonstrate the thermal stability of the CS-based CaO, a thermogravimetric analysis (TGA) was carried out, and its profile is presented in Fig. 1 (c). The figure shows a 5 wt% decrease when the temperature is elevated from 595 °C to 650 °C which corresponds to the evaporation of chemically-bound moisture [34], decomposition, and transition of calcite ($CaCO_3$) to CaO [11]. As the complete decomposition of $CaCO_3$ can be achieved at the temperature of around 700 °C; the selection of calcination temperature at 900 °C is deemed suitable to ensure the complete phase transition of calcite and its derivatives to CaO [34,35], which leads to the formation of a porous structure. Hu et al. [11] also reported that the catalytic activity of a catalyst escalates along with the activation [11]. The XRD image (Fig. 1 (d)) shows that the diffraction pattern of CS-based CaO follows the characteristic fingerprint of CaO (JCPDS file no. 82–1691) as the primary component and calcite (JCPDS file no. 47–1743) as the minor substance.

3.2. Transesterification parameter study

The chemical properties of LTW are presented in Table 4, with palmitic acid (C16:0), stearic acid (C18:0), and oleic acid (C18:1) as the three principal fatty acids constituting LTW. As homogenous catalysts are sensitive to FFA and impurities, the conventional conversion of LTW to FAEE requires at least a two-stage process: (1) acid-catalyzed esterification to generate FAEE from the FFA content in LTW, and (2) base-

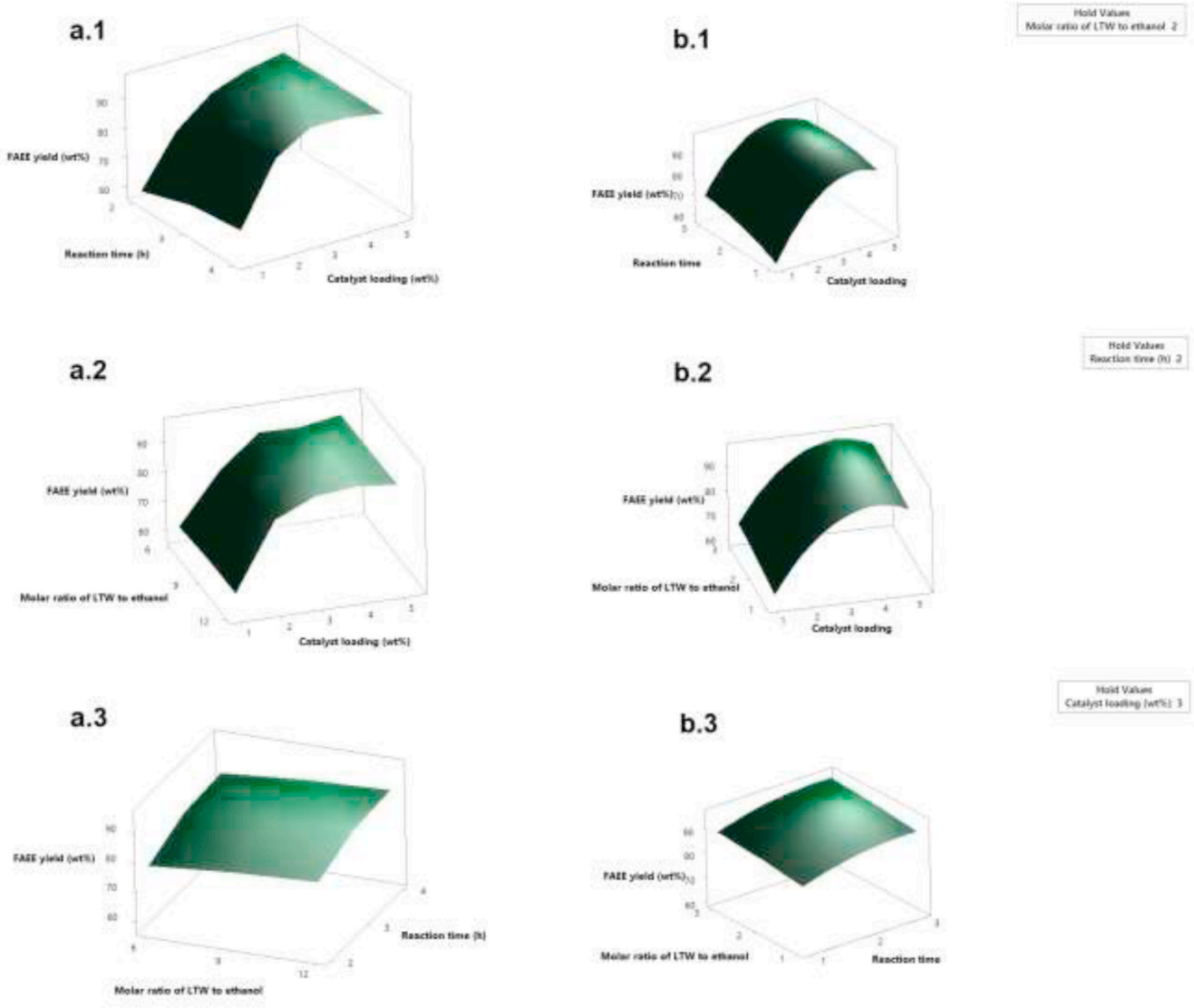

Fig. 2. (a) The experimental and (b) the predicted FAEE yield (wt%), based on their interaction between (1) catalyst loading m_c (wt%) and reaction time t (h), (2) catalyst loading m_c (wt%) and molar ratio of ethanol to LTW m_{eo}, (3) reaction time t (h) and the molar ratio of ethanol to LTW m_{eo}.

Table 5
The three-way ANOVA study of the tested variables.

Term	Coef	SE Coef	T-Value	P-Value
Constant	92.76	1.01	92.25	0.000
A	13.433	0.561	23.95	0.000
B	3.507	0.486	7.22	0.000
C	1.713	0.486	3.53	0.001
A^2	−13.432	0.948	−14.17	0.000
B^2	−2.127	0.841	−2.53	0.016
C^2	−0.347	0.841	−0.41	Non-significant
(*A*)(*B*)	−2.190	0.687	−3.19	0.003
(*A*)(*C*)	−0.613	0.687	−0.89	Non-significant
(*B*)(*C*)	−0.105	0.595	−0.18	Non-significant
R-squared (R^2)			0.9607	
Adjusted R-squared (Adj-R^2)			0.9506	
Predicted R-squared (Pred-R^2)			0.9317	

catalyzed transesterification to convert the acyl glycerides into FAEE. However, heterogeneous catalysts show good tolerance towards the FFA and water content in the lipid materials, therefore efficient conversion from LTW to FAEE can be achieved in a single step.

Fig. 2 presents the yield of FAEE obtained at various m_c, t, and m_{eo}. The experimental results indicate that the catalyst amount, specifically the number of active sites offered by CS-based CaO, is proportional to the yield of FAEE (Fig. 2 (a.1) - (a.2)). Its value increases with m_c when m_c is within 3 wt%. A stagnant FAEE yield at $m_c > 3$ wt% is monitored, which is probably contributed by (1) the aggregation and inconsistent dispersity of the catalyst in the reaction system [36], and (2) the enhanced viscosity of the LTW, ethanol, and catalyst mixture [37]. Wei et al. [38] also reported that the reaction rate governing step is the sorption of reactants from the catalyst; therefore, while the number of active sites is important, further addition of catalyst higher than a certain extent does not give a significant increase of the yield of FAEE.

Fig. 2 (a.1) and (a.3) show a mild increase of the FAEE yield by extending the duration of reaction from $t = 2$ h to $t = 4$ h. Prolonged t provides sufficient opportunities for the catalyst to be dispersed and come into proper contact with the reactants, and ensures the reaction to reach the equilibrium [21]; therefore, increasing the conversion of acyl glycerides and FFA into FAEE. From another viewpoint, lengthening the duration of the reaction also gives the catalyst enough time to adsorb the reactants and desorb the resulting product [39].

The influence of m_{eo} is depicted in Fig. 2 (a.2) – (a.3). As seen from the figure, having excess ethanol from m_{eo} = 6:1 to m_{eo} = 12:1 contributes to a slightly higher FAEE yield, and its prominence is incomparable to the effect of m_c. It is known that excess alcohol in the reaction system triggers intensive contact between reactants and catalysts, hence, accelerating the reaction rate. However, this is only beneficial to a certain degree because the excess alcohol hinders the phase separation and decreases the apparent FAEE yield [40].

3.3. Process optimization

To determine the optimum operating condition, RSM combined with MLFD is statistically employed by simultaneously integrating three critical parameters (m_c, t, m_{eo}). Table 2 presents the relation between the responses and their corresponding input variables. Using the least square analysis, the experimental responses are found to fit into a second-order polynomial model as follows:

$$Y_{FAEE}(FAEE\ yield,\ wt\%) = 13.23 + 29.67(A) + 15.51(B) + 4.23(C) - 3.358(A^2) - 2.127(B^2) - 0.347(C^2) - 1.095(A)(B) - 0.307(A)(C) - 0.105(B)(C) \quad (4)$$

where Y_{FAEE} is the predicted FAEE yield (wt%) which is presented in Table 2; *A*, *B*, *C* are the coded level of reaction variables (1, 2, 3, 4, 5 for *A* and 1, 2, 3 for *B* and *C*). The mathematical equation indicates that all linear variables (*A*, *B*, *C*) give a favorable effect on the yield of biodiesel, and conversely, the other variables (A^2, B^2, C^2, (*A*)(*B*), (*A*)(*C*), (*B*)(*C*)) reduce the response. The statistical ANOVA results presented in Table 5 shows that all terms, except that of C^2, (*A*)(*C*), and (*B*)(*C*), are prominent to the reaction (p-value < 0.05), with the significance order of $A > A^2 >$

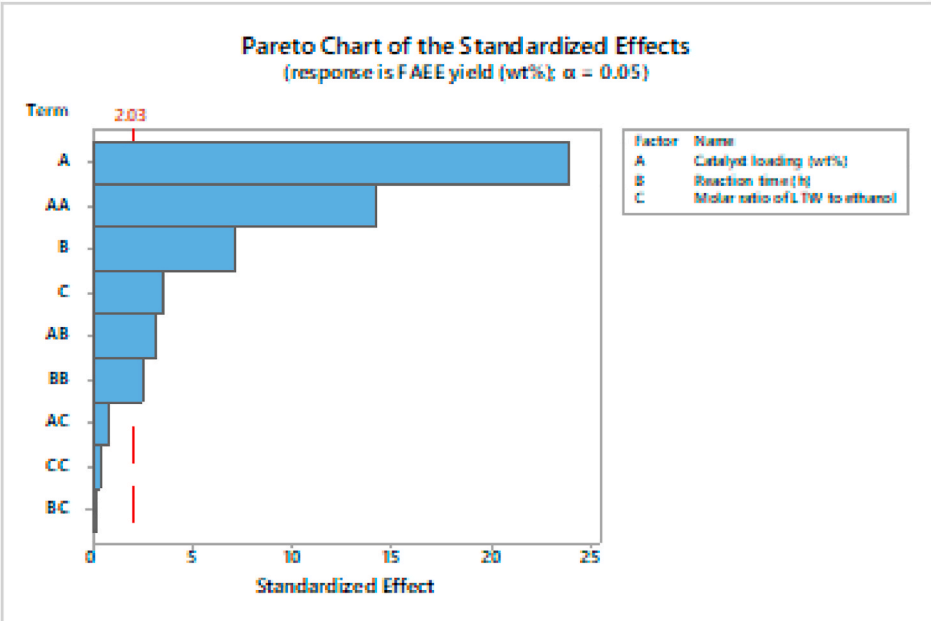

Fig. 3. The Pareto chart of the standardized effect showing the significance order of various reaction variables.

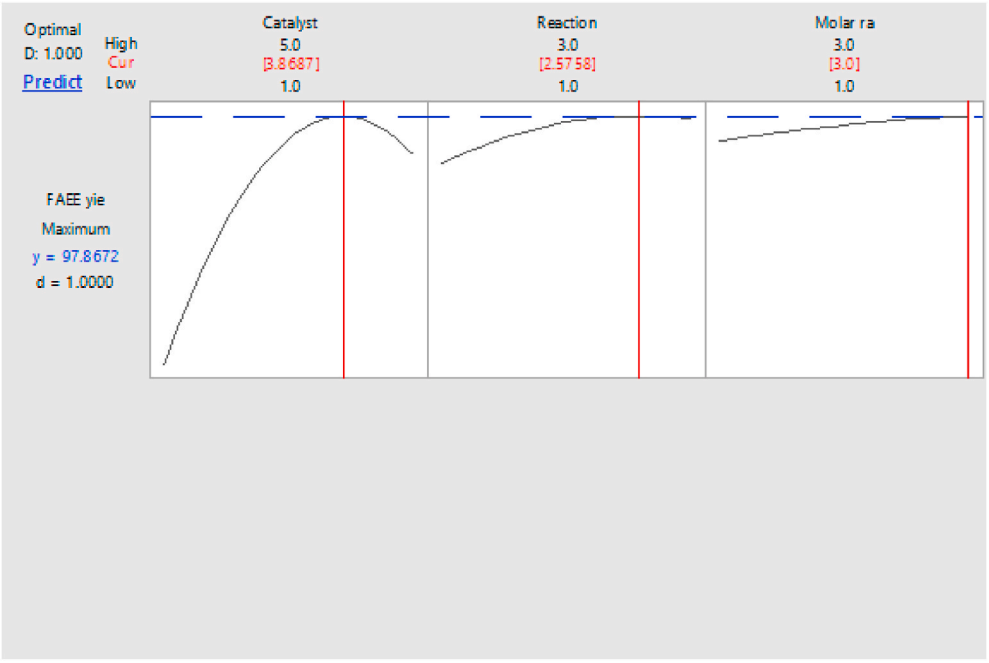

Fig. 4. The optimization plot of the reaction variables.

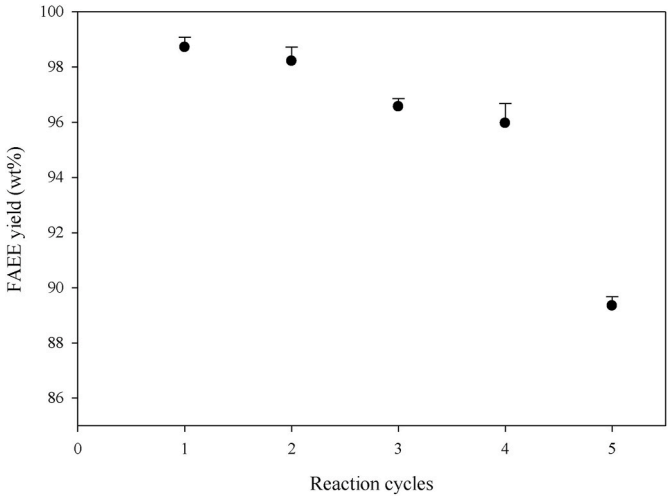

Fig. 5. The catalytic activity of reused CS-based CaO.

$B > C > (A)(B) > B^2$ as shown in Fig. 3.

The goodness-of-fit analysis for the fitted equation (equation (4)) is measured by using the R-squared (R^2), where the R^2 value for the model is obtained at 0.9607, pointing that 96.07% of the actual experimental data can be interpreted by equation (4). The values of the adjusted and predicted R^2 are also respectively monitored at 0.9506 and 0.9317, indicating that the predicted and experimental FAEE yields are in good agreement. Table 2 shows that the average standard error of estimate (SEE) between the two corresponding responses is observed at 1.24% (n = 45), indicating sufficient data accuracy. Fig. 2 (b.1) – (b.3) further prove that both experimental and predicted plots share a similar response profile. Therefore, the mathematical model is considered adequate to predict the response for all input variables within the tested range.

The optimized reaction condition is generated using Minitab (ver. 18.1) and predicted at m_c = 3.87 wt%, t = 3.58 h, and m_{eo} = 12:1. The computed response at this condition is obtained at 97.9 wt%, with desirability = 1.0 (Fig. 4). To confirm the plausibility of the mathematical model, triplicate experiments are carried out at the optimum condition. The average FAEE yield is found at 98.7 ± 0.4 wt%, with the purity of 98.6 ± 0.4 wt%. The established model is deemed reliable and accurate for all operating conditions within the tested range, as the error between the predicted and experimental results is only 0.85%. A

Table 6
The performance of various techniques for the production of biodiesel from waste-originated materials.

Lipid material	Catalyst type	Operating condition	Biodiesel yield (wt %)	Catalyst reusability	Reference
Vegetable oil wastewater sludge	N/A *(Subcritical methanol)*	T = 215 °C, P = 6.5 MPa, m_{mo}[b] = 5:1, t = 12 h	92.7	-	[41]
Waste cooking oil	Zn-doped waste-egg shells CaO	T = 65 °C, m_c = 5 wt%, m_{mo}[b] = 20:1, t = 4 h	96.7	2	[42]
Tallow fats	KOH	T = 60 °C, m_c = 0.8 wt%, m_{mo}[b] = 6:1, t = 2 h	90.8	-	[43]
LTW	N/A[a] *(Supercritical ethanol)*	T = 374.6 °C, P = 15 MPa, m_{eo} = 40.02:1, t = 47.4 min	98.9	-	[16]
LTW	CS-based CaO	T = 60 °C, m_c = 3.87 wt%, m_{eo} = 12:1, t = 3.58 h	98.7	4	This work

[a] Not available.

[b] m_{mo} stands for molar ratio of methanol to oil.

Table 7
The properties of LTW-based biodiesel.

Properties	Methods	LTW-based biodiesel	ASTM D6751	Diesel fuel (ASTM D975-08)
Kinematic viscosity (at 40 °C), mm^2/s	ASTM D445	2.1	1.9–6.0	1D: 1.3–2.4 2D: 1.9–4.1
Density (at 15 °C, kg/m^3)	ASTM D1298	865	-	-
Flash point, °C	ASTM D93	167	93 min	1D: 38 min 2D: 52 min
Cloud point	ASTM D2500	10.2	-	-
Cetane number	ASTM D613	53	47 min	46 min
Water and sediment, vol%	ASTM D2709	0.01	0.05 max	0.05 max
Acid value, mg KOH/g	ASTM D664	0.22	0.50 max	-
Iodine value, g I_2/100 g	AOCS Cd 1-25	52.9	-	-
Ester content, wt%	EN 14103	98.7	-	-
Linolenic acid ethyl ester content, wt%	EN 14103	1.2	-	-
Polyunsaturated ethyl ester content, wt%	EN 15779	6.1	-	-
Total glycerine, wt%	ASTM D6584	0.16	0.24 max	-
Free glycerine, wt%	ASTM D6584	0.01	0.02 max	-
Sulfur, ppm	ASTM D5453	3.67	15 max (S15) 500 max (S500)	1D and 2D: 15 max (S15) 500 max (S500)
Phosphorus, ppm	ASTM D4951	0.21	10 max	-
Carbon residue, wt%	ASTM D4530	0.002	0.05 max	1D: 0.15 max 2D: 0.35 max
Oxidation stability, h	EN 14112	12.7	3 min	-
Calorific value, MJ/kg	ASTM D240	44.67	-	-

relatively short reaction time ($t = 3.58$ h) and low catalyst amount ($m_c =$ 3.87 wt%) is highly beneficial in practice, as these variables directly influence the production efficiency.

The reusability of CS-based CaO is presented in Fig. 5, where the results show that the regenerated CS-based CaO can maintain a high yield of FAEE (>90 wt%) until the fourth run before significantly decline to 89.4 wt% in the fifth cycle. The FAEE yields for the first four cycles are 98.7 wt%, 98.2 wt%, 96.6 wt%, 96.0 wt%, with the respective purity of 98.6 wt%, 98.9 wt%, 97.3 wt, 98.2 wt%. The deactivation of CS-based CaO is probably due to the clogged pores, caused by the deposition of deactivation-induced molecules, e.g., free glycerol, acyl glycerides, and biodiesel. The FFA content may as well deactivate the basic sites of CS-based CaO through neutralization [5] to form calcium carboxylate. A comparative study of the biodiesel production from waste-originated materials using various methods is presented in Table 6. In general, the conversion of LTW to biodiesel using CS-based CaO shows comparable performance with the other preparation processes, indicated by its high product yield (higher than 90 wt%) and reusability number.

3.4. Characteristics of LTW-based biodiesel

Table 7 presents the fuel properties of LTW-based biodiesel generated using CS-based CaO as a catalyst. The measurements indicate that the properties of the resulting biodiesel product are in accordance with the standard of ASTM D6751 and ASTM D975-08. A high flash point, which is the result of the sufficient post-separation step, shows that the product can be treated, stored, and transported safely. Its calorific value, 44.67 MJ/kg, is within the range of that of petroleum diesel fuel (42–46 MJ/kg) [44]. The chemical compositional analysis of the LTW-based FAEE using GC-FID shows that there are ten distinguished peaks in the chromatogram: myristic acid ethyl ester (C14:0), myristoleic acid ethyl ester (C14:1), palmitic acid ethyl ester (C16:0), palmitoleic acid ethyl ester (C16:1), heptadecanoic ethyl ester (C17:0), stearic acid ethyl ester (C18:0), oleic acid ethyl ester (C18:1), linoleic acid ethyl ester (C18:2), α-linolenic acid ethyl ester (C18:3), arachidic acid ethyl ester (C20:0).

4. Conclusions

Successful conversion of LTW to biodiesel is achieved using a CS-based CaO, with the highest FAEE yield of 98.7 ± 0.4 wt% (purity of 98.6 ± 0.4 wt%) obtained at the following reaction condition: $m_c = 3.87$ wt%, $t = 3.58$ h, and $m_{eo} = 12{:}1$. The CS-based CaO shows good reusability; the FAEE yield stays above 90 wt% for four reaction cycles. The fuel properties of LTW-based FAEE comply with ASTM D6751 and ASTM D975-08. The valorization of CS and LTW will prominently allow better environmental destination for these wastes and meanwhile offers an environmentally benign route to produce high value-added renewable energy.

Acknowledgment

This research did not receive any specific grant from funding agencies in the public, commercial, or not-for-profit sectors.

References

[1] Y. Widria, Prospek Pasar Ekspor Rajungan Dan Kepiting Indonesia Ke China [The Prospect of Indonesian Crab and Crab Export Market to China], Balai Besar Penguji, Penerapan Prod. Kelaut. Dan Perikan., 2019 accessed, https://kkp.go.id/djpdspkp/bbp2hp/artikel/15122-prospek-pasar-ekspor-rajungan-dan-kepiting-indonesia-ke-china. (Accessed 15 September 2020).
[2] N. Yan, X. Chen, Don't waste seafood waste: turning cast-off shells into nitrogen-rich chemicals would benefit economies and the environment, Nature 524 (2015) 155–157.
[3] P.L. Boey, G.P. Maniam, S.A. Hamid, Performance of calcium oxide as a heterogeneous catalyst in biodiesel production: a review, Chem. Eng. J. 168 (2011) 15–22, https://doi.org/10.1016/j.cej.2011.01.009.
[4] W. Roschat, T. Siritanon, B. Yoosuk, V. Promarak, Biodiesel production from palm oil using hydrated lime-derived CaO as a low-cost basic heterogeneous catalyst, Energy Convers. Manag. 108 (2016) 459–467, https://doi.org/10.1016/j.enconman.2015.11.036.
[5] M. Kouzu, J.S. Hidaka, Transesterification of vegetable oil into biodiesel catalyzed by CaO: a review, Fuel 93 (2012) 1–12, https://doi.org/10.1016/j.fuel.2011.09.015.
[6] D.M. Marinković, M.V. Stanković, A.V. Veličković, J.M. Avramović, M. R. Miladinović, O.O. Stamenković, V.B. Veljković, D.M. Jovanović, Calcium oxide as a promising heterogeneous catalyst for biodiesel production: current state and perspectives, Renew. Sustain. Energy Rev. 56 (2016) 1387–1408, https://doi.org/10.1016/j.rser.2015.12.007.
[7] I.M. Rizwanul Fattah, H.C. Ong, T.M.I. Mahlia, M. Mofijur, A.S. Silitonga, S. M. Ashrafur Rahman, A. Ahmad, State of the art of catalysts for biodiesel production, Front. Energy Res. 8 (2020) 1–17, https://doi.org/10.3389/fenrg.2020.00101.
[8] W. Suryaputra, I. Winata, N. Indraswati, S. Ismadji, Waste capiz (Amusium cristatum) shell as a new heterogeneous catalyst for biodiesel production, Renew. Energy 50 (2013) 795–799, https://doi.org/10.1016/j.renene.2012.08.060.
[9] M. Yuliana, S.P. Santoso, F.E. Soetaredjo, S. Ismadji, A.E. Angkawijaya, W. Irawaty, Y.-H. Ju, P.L. Tran-Nguyen, S.B. Hartono, Utilization of waste capiz shell – based catalyst for the conversion of leather tanning waste into biodiesel, Int. J. Chem. Environ. Eng. 8 (2020) 104012, https://doi.org/10.1016/j.jece.2020.104012.
[10] C. Chambers, A. Holliday, Acids and bases: oxidation and reduction. Mod. Inorg. Chem., Butterworth & Co., Chichester, 1975, pp. 84–111.
[11] S. Hu, Y. Wang, H. Han, Utilization of waste freshwater mussel shell as an economic catalyst for biodiesel production, Biomass Bioenergy 35 (2011) 3627–3635, https://doi.org/10.1016/j.biombioe.2011.05.009.
[12] A. Buasri, N. Chaiyut, V. Loryuenyong, P. Worawanitchaphong, S. Trongyong, Calcium oxide derived from waste shells of mussel, cockle, and scallop as the heterogeneous catalyst for biodiesel production, Sci. World J. 2013 (2013), https://doi.org/10.1155/2013/460923.
[13] S. Niju, M.M.M.S. Begum, N. Anantharaman, Modification of egg shell and its application in biodiesel production, J. Saudi Chem. Soc. 18 (2014) 702–706, https://doi.org/10.1016/j.jscs.2014.02.010.
[14] Y.Y. Margaretha, H.S. Prastyo, A. Ayucitra, S. Ismadji, Calcium oxide from pomacea sp. shell as a catalyst for biodiesel production, Int. J. Energy Environ. Eng. 3 (2012) 1–9, https://doi.org/10.1186/2251-6832-3-33.

[15] S. Kaewdaeng, P. Sintuya, R. Nirunsin, Biodiesel production using calcium oxide from river snail shell ash as catalyst, Energy Procedia 138 (2017) 937–942, https://doi.org/10.1016/j.egypro.2017.10.057.
[16] M. Yuliana, S.P. Santoso, F.E. Soetaredjo, S. Ismadji, A. Ayucitra, A. E. Angkawijaya, Y.-H. Ju, P.L. Tran-Nguyen, A One-Pot Synthesis of Biodiesel from Leather Tanning Waste Using Supercritical Ethanol: Process Optimization, Biomass Bioenergy vol. 142 (2020), https://doi.org/10.1016/j.biombioe.2020.105761.
[17] J. Kanagaraj, K.C. Velappan, N.K. Chandra Babu, S. Sadulla, Solid wastes generation in the leather industry and its utilization for cleaner environment - a review, J. Sci. Ind. Res. (India) 65 (2006) 541–548, https://doi.org/10.1002/chin.200649273.
[18] S. Zafar, Wastes generation in tanneries, Bioenergy Consult (2019). https://www.bioenergyconsult.com/waste-from-tanneries/.
[19] F. Alihniar, Di Industri Penyamakan Kulit Leather Tanning Industry, 2011.
[20] L.K. Ong, A. Kurniawan, A.C. Suwandi, C.X. Lin, X.S. Zhao, S. Ismadji, Transesterification of leather tanning waste to biodiesel at supercritical condition: kinetics and thermodynamics studies, J. Supercrit. Fluids 75 (2013) 11–20, https://doi.org/10.1016/j.supflu.2012.12.018.
[21] V.K. Booramurthy, R. Kasimani, D. Subramanian, S. Pandian, Production of biodiesel from tannery waste using a stable and recyclable nano-catalyst: an optimization and kinetic study, Fuel 260 (2020) 116373, https://doi.org/10.1016/j.fuel.2019.116373.
[22] S. Krishnan, Z.A. Wahid, L. Singh, M. Sakinah, Production of biodiesel using tannery fleshing as a feedstock: an investigation of feedstock pre-treatment via solid-state fermentation, ARPN J. Eng. Appl. Sci. 11 (2016) 7354–7357.
[23] S. Çolak, G. Zengin, H. Özgünay, Ö. Sari, H. Sarikahya, L. Yüceer, Utilization of leather industry pre-fleshings in biodiesel production, J. Am. Leather Chem. Assoc. 100 (2005) 137–141.
[24] H. Dagne, R. Karthikeyan, S. Feleke, Waste to energy: response surface methodology for optimization of biodiesel production from leather fleshing waste, J. Energy (2019) 1–19, https://doi.org/10.1155/2019/7329269.
[25] Ş. Altun, F. Yaşar, Biodiesel production from leather industry wastes as an alternative feedstock and its use in diesel engines, Energy Explor. Exploit. 31 (2013) 759–770, https://doi.org/10.1260/0144-5987.31.5.759.
[26] J. Pecha, K. Kolomaznik, M. Barinova, L. Sanek, High quality biodiesel and glycerin from fleshings, J. Am. Leather Chem. Assoc. 107 (2012) 312–322.
[27] B. Panneton, H. Philion, P. Dutilleul, R. Thériault, M. Khelifi, Full factorial design versus centra composite design: statistical comparison and implications for spray droplet deposition, experiments 42 (1999) 877–883.
[28] J. Cutting, Research methods in psychology (Lectures Week 7), (n.d.), https://psychology.illinoisstate.edu/jccutti/psych231/SP01/wk7/week7.htm. (Accessed 5 May 2021). accessed.
[29] P. Verma, M.P. Sharma, Comparative analysis of effect of methanol and ethanol on Karanja biodiesel production and its optimisation, Fuel 180 (2016) 164–174, https://doi.org/10.1016/j.fuel.2016.04.035.
[30] Basque Research, Ethanol and Heterogeneous Catalysts for Biodiesel Production, Sciencedaily, 2014. www.sciencedaily.com/releases/2014/11/141112084246.htm.
[31] F.H. Santosa, L. Laysandra, F.E. Soetaredjo, S.P. Santoso, S. Ismadji, M. Yuliana, A facile noncatalytic methyl ester production from waste chicken tallow using single step subcritical methanol: optimization study, Int. J. Energy Res. 43 (2019) 8852–8863, https://doi.org/10.1002/er.4844.
[32] J.M. Valverde, P.E. Sanchez-Jimenez, L.A. Perez-Maqueda, Limestone calcination nearby equilibrium: kinetics, CaO crystal structure, sintering and reactivity, J. Phys. Chem. C 119 (2015) 1623–1641, https://doi.org/10.1021/jp508745u.
[33] B. Yoosuk, P. Udomsap, B. Puttasawat, P. Krasae, Improving transesterification acitvity of CaO with hydration technique, Bioresour. Technol. 101 (2010) 3784–3786, https://doi.org/10.1016/j.biortech.2009.12.114.
[34] Z.X. Tang, Z. Yu, Z.L. Zhang, X.Y. Zhang, Q.Q. Pan, L.E. Shi, Sonication-assisted preparation of CaO nanoparticles for antibacterial agents, Quim. Nova 36 (2013) 933–936, https://doi.org/10.1590/S0100-40422013000700002.
[35] Y. Zhu, S. Wu, X. Wang, Nano CaO grain characteristics and growth model under calcination, Chem. Eng. J. 175 (2011) 512–518, https://doi.org/10.1016/j.cej.2011.09.084.
[36] C. Samart, C. Chaiya, P. Reubroycharoen, Biodiesel production by methanolysis of soybean oil using calcium supported on mesoporous silica catalyst, Energy Convers. Manag. 51 (2010) 1428–1431, https://doi.org/10.1016/j.enconman.2010.01.017.
[37] B. Gurunathan, A. Ravi, Biodiesel production from waste cooking oil using copper doped zinc oxide nanocomposite as heterogeneous catalyst, Bioresour. Technol. 188 (2015) 124–127, https://doi.org/10.1016/j.biortech.2015.01.012.
[38] Z. Wei, C. Xu, B. Li, Application of waste eggshell as low-cost solid catalyst for biodiesel production, Bioresour. Technol. 100 (2009) 2883–2885, https://doi.org/10.1016/j.biortech.2008.12.039.
[39] T. Pangestu, Y. Kurniawan, F.E. Soetaredjo, S.P. Santoso, W. Irawaty, M. Yuliana, S. B. Hartono, S. Ismadji, The synthesis of biodiesel using copper based metal-organic framework as a catalyst, J. Environ. Chem. Eng. 7 (2019) 103277, https://doi.org/10.1016/j.jece.2019.103277.
[40] G. Anastopoulos, Y. Zannikou, S. Stournas, S. Kalligeros, Transesterification of vegetable oils with ethanol and characterization of the key fuel properties of ethyl esters, Energies 2 (2009) 362–376, https://doi.org/10.3390/en20200362.
[41] F. Gunawan, A. Kurniawan, I. Gunawan, Y.H. Ju, A. Ayucitra, F.E. Soetaredjo, S. Ismadji, Synthesis of biodiesel from vegetable oils wastewater sludge by in-situ subcritical methanol transesterification: process evaluation and optimization, Biomass Bioenergy 69 (2014) 28–38, https://doi.org/10.1016/j.biombioe.2014.07.005.
[42] M.J. Borah, A. Das, V. Das, N. Bhuyan, D. Deka, Transesterification of waste cooking oil for biodiesel production catalyzed by Zn substituted waste egg shell derived CaO nanocatalyst, Fuel 242 (2019) 345–354, https://doi.org/10.1016/j.fuel.2019.01.060.
[43] T.M. Mata, N. Cardoso, M. Ornelas, S. Neves, N.S. Caetano, Sustainable production of biodiesel from tallow, lard and poultry fat and its quality evaluation, Chem. Eng. Trans. 19 (2010) 13–18, https://doi.org/10.3303/CET1019003.
[44] W.N. Association, Heat values of various fuels. http://www.world-nuclear.org/information-library/facts-and-figures/heat-values-of-various-fuels.aspx, 2018.

ARTICLES FOR FACULTY MEMBERS

ELUCIDATING THE CALCIUM OXIDE DERIVED FROM THE WASTE SHELLS OF MUD CLAM (GELOINA EXPANSA) AS A CATALYST FOR BIODIESEL PRODUCTION

Exploration of efficiency of nano calcium oxide (CaO) as catalyst for enhancement of biodiesel production / Malek, M. N. F. A., Pushparaja, L., Hussin, N. M., Embong, N. H., Bhuyar, P., Rahim, M. H. A., & Maniam, G. P.

Journal of Microbiology, Biotechnology and Food Sciences
Volume 11 Issue 1 (2021) e3935 Pages 1-4
https://doi.org/10.15414/JMBFS.3935
(Database: Faculty of Biotechnology and Food Sciences, Universiti Malaysia Pahang)

JMBFS

Journal of Microbiology, Biotechnology and Food Sciences

International peer-reviewed scientific online journal

Published by Faculty of Biotechnology and Food Sciences

EXPLORATION OF EFFICIENCY OF NANO CALCIUM OXIDE (CaO) AS CATALYST FOR ENHANCEMENT OF BIODIESEL PRODUCTION

*Muhammad Nor Fazli Abd Malek, Livitra Pushparaja, Noraini Mat Hussin, Nurul Hajar Embong, Prakash Bhuyar, Mohd Hasbi Ab. Rahim, Gaanty Pragas Maniam**

Address(es): Dr. Gaanty Pragas Maniam,
Faculty of Industrial Sciences & Technology, Universiti Malaysia Pahang, Lebuhraya Tun Razak, 26300 Gambang, Kuantan, Pahang, Malaysia.

*Corresponding author: gaanty@ump.edu.my

https://doi.org/10.15414/jmbfs.3935

ARTICLE INFO

Received 6. 11. 2020
Revised 6. 2. 2021
Accepted 10. 2. 2021
Published xx.xx.201x

Regular article

OPEN ACCESS

ABSTRACT

Present work proposes on the synthesis of nano calcium oxide derived from waste cockle shell (Anadara granosa) and applied as heterogenous catalyst in biodiesel production via transesterification reaction under reaction parameter 15:1 methanol to oil ratio, 5 wt.% catalyst and 3 hour reation time and constant temperature at 65 ± 2 °C. The waste cockle shell was prepared in nano size via ball mill technique which was run for 36 hours at 350 rpm speed and then calcined at 900 °C for 2 hours to decompose calcium carbonate, $CaCO_3$ into nano calcium oxide, n-CaO. The catalyst was characterized by particle size analyzer, Transmission Electron Microscopy, Field Emission Scanning Electron Microscope, Surface Area Analyser, X-Ray Diffractometer, Fourier transform infrared, Hammet indicator and benzoic acid titration. Particle size of n-CaO catalyst was found within the range of 29 nm to 67.5 nm. Specific surface area of synthesised n-CaO is 8.41 m^2/g with basicity strength of 0.055 mmol/g. Methyl ester conversion of palm oil with n-CaO as a catalyst was 88.87 wt.%.

Keywords: cockle shell, nano CaO as heterogeneous catalyst, particle size, specific surface area, basicity strength, methyl ester yield

INTRODUCTION

Massive consumption of fossil fuel for numerous purposes cause the deficiency of natural resources available nowadays. At the same time fully relying on renewable energy sources such as solar, wind energy and biomass as an alternative energy source makes life of people even more devastating as this type of energy source not always available at any time anywhere and expensive. This cause biodiesel becoming better and cheaper alternative than any other sources (**Banković-Ilić *et al.*, 2017; Bhuyar *et al.*, 2020; Saengsawang *et al.*, 2020**).
Generally, biodiesel is biodegradable, nontoxic, and has lower carbon dioxide and sulfur emissions when utilised in internal combustion engines. Biodiesel can be produced via several processing method. It can be produced via supercritical process, catalyst-free mehod at high temperature and pressure (**Bunyakiat et al., 2006**), ultrasonic reactor method (**Malek *et al.*, 2020**) and enzyme-catalysed method (**Du *et al.*, 2004).** Common way of producing biodiesel is through transesterification process of oils or fats with methanol (**Ahmad *et al.*, 2020**). Biodiesel feedstock can be derived from various sources such as plant oils (**Ge, Yoon, and Choi 2017; Ishola *et al.*, 2020**), animal (**Toldrá-Reig, Mora, and Toldrá 2020**), microalgae (**Khammee *et al.*, 2020**) and microbial (**Bhuyar *et al.*, 2020; Boock *et al.*, 2019**). Transesterification reaction of biodiesel can be accelerated with the aid of inorganic (heterogeneous or homogeneous) or organic catalysts (enzymes). Inorganic heterogeneous catalysts offer abundant benefits relative to either inorganic homogenous or organic catalyst including ease of separation, recovery of catalyst, reusability of catalyst, cheap and minimized corrosion (**Mazaheri *et al.*, 2018; Bhuyar *et al.*, 2019**).
Among the heterogeneous catalyst that was used in transesterification reaction, calcium oxide, CaO proven to be highly effective catalyst in biodiesel production by many literature studies. CaO is inexpensive, easily available, noncorrosive, environmentally friendly, easy to handle material with low solubility and high basicity which can be reused (**Borah *et al.*, 2019**). These benefits triggered interest of many researchers for further investigations of CaO for the purpose of improvement of its properties. There are abundant sources of CaO around the world, but the cockle shell (*Anadara granosa*) is known to be rich in CaO. The generation of waste cockle shells which are easily available make it feasible for the shell to be used as a catalyst in the biodiesel industry which lead to production of biodiesel in an inexpensive way as the catalyst used is derived from waste shell as well.
However, according to (**Banković-Ilić *et al.*, 2017**), the role of nanoparticles in catalytic processes affect conversion rate of methyl ester due to their catalytic properties, which are very high surface reactivity, large pore size and large surface area compared to macroscopic catalysts. It makes the nano size particle to be more attractive as catalysts for higher conversion rate of methyl ester in biodiesel production.
Hence, the main purpose of this study is to prepare nano calcium oxide, nCaO catalyst from cockle shells (*Anadara granosa*) and evaluate the performance of the synthesized n-CaO compared to commercial calcium oxide c-CaO as a catalyst in the transesterification of palm oil into biodiesel. The properties of both catalysts were studied via characterization by particle size analyzer, Transmission Electron Microscopy, Field Emission Scanning Electron Microscope, Surface Area Analyser, X-Ray Diffractometer, Fourier transform infrared, Hammet indicator and Benzoic acid titration. The reaction parameters which are methanol to oil ratio, reaction time, and catalyst amount are optimized to 15:1, 3 hours, and 5% respectively. Finally, the comparison of methyl ester conversion at each 30minutes interval for both n-CaO and c-CaO catalyzed reaction was determined through analysis of thin layer chromatography and gas chromatography-flame ionization detector.

MATERIAL AND METHODS

Materials

Refined bleached deodorized palm oil (RBDPO) was purchased from local groceries. Waste cockle shells were collected from local restaurants. Internal standard (methyl heptadecanoate) and calcium oxide were obtained from Sigma-Aldrich. Potassium hydroxide, methanol, acetone, and n-hexane were obtained from Merck. Chloroform was provided by Surechem product Ltd. (Soffolk,England) and phenolphthalein (H+=8.2) , 2,4-dinitroanilline (H+=15.0), 4-nitroanilline (H+=18.4) were purchased from Sigma (Deisenhofen,Germany). Both anhydrous sodium sulphate and petroleum ether (60 °C-80 °C) were obtained from BDH Chemical Ltd.(Poole,England). All the chemicals mentioned above were analytical reagent grade. Thin Layer Chromatography (TLC) aluminum sheets were purchased from Merck (Darmstadt, Germany).

Preparation of catalyst

The waste cockle shells were washed thoroughly with warm water and then dried under daylight for 48 hours before crushed in a pestle and mortar. Then, the crushed shells were grinded using a dry mill grinder to obtain gross powder and sieved using 100 µm sieve tray and micron sized powder obtained. After that, ball milling process for 36 hours with 350 rpm speed was conducted using Planetary Ball Mill (Retsch, PM100) to get further finest powder in nano size. After been ball milled, half amount of the ball milled powder was calcined in furnace at 900 °C for 2 hours. The calcined CaO powder (labeled as n-CaO) was stored in an air-tight glass container and then placed inside a desiccator to avoid any moisture content. The c-CaO powder was also calcined at 900 °C for 2 hours to be used as reference to compare its efficiency with the synthesized n-CaO in biodiesel yield.

Catalyst Characterization

The surface morphology of the synthesized uncalcined and calcined n-CaO catalyst were studied through scanning electron microscopy with electron dispersive x-ray (SEMEDEX) that was obtained using Field Emission SEM (FESEM). Malvern Zeta sizer model Nano-S90 particle size analyzer measured average particle size distribution of catalyst. photomicrographs were obtained using FEI/Technai G2 20 TWIN model Transmission Electron Microscope. The surface area of the catalyst was determined using Micromeritics ASAP 2020 by using Brunauer, Emmet and Teller (BET) analysis from the corresponding nitrogen adsorption–desorption isotherms at liquid nitrogen temperature (-196 °C). The x-ray diffraction analysis (XRD) was used to study the crystallography of calcium carbonate, $CaCO_3$ and CaO presence in the synthesized uncalcined and calcined nano catalysts using an X-ray Diffractometer (Bruker, model D8 Advance). FTIR Perkin Elmer System 2000 instrument used to determine the surface functional group of the solid catalyst compound in the range of 400 to 4000 cm^{-1}. The Hammett indicators such as phenolphthalein (H_ = 9.3), 2,4-dinitroaniline (H_ = 15.0) and 4-nitroniline (H_=18.4) were used to determine the catalyst basicity strength. Solid catalyst basicity was analyzed by benzoic acid titration method (**Bampidis and Robinson 2006**) where the solid catalyst was suspended in benzene and was titrated with 0.01N benzoic acid. The endpoint of titration was determined when all the green color disappeared.

Transesterification

Biodiesel was produced from palm oil through base-catalyzed transesterification process with presence of methanol and potassium hydroxide as catalyst. The reaction was done at condition of 15:1 methanol to oil ratio, 5 % catalyst and 3 hours reaction time at constant temperature of 68 ± 2 °C was carried out. The contents were refluxed under magnetic stirring. Tap water was allowed to flow inside the condenser to prevent methanol from evaporating which might ruin the reaction. At each 30 min interval, small amount of sample from the product mixture in the flask reactor were taken. The samples were centrifuged at 5000 rpm for 20 minutes to reach complete phase separation. After that, fatty acid methyl ester (the top layer) was analyzed to determine the percentage content of methyl ester.

Analysis and characterization of methyl ester

In thin layer chromatography (TLC) technique, sample and standard (methyl heptadecanoate) were dotted on the plate and left inside the flask containing the mixture of petroleum ether and chloroform (3:2 volume ratio). Once the solvent has reached the upper line drawn at the top as indicator, TLC plate was taken out and shaken with small amount of solid iodine to enable separation to be seen very well. Besides, standard and sample was analyzed through gas chromatography (Agilent 7890A-GC) using flame ionization detector (FID) with a polar capillary column (HP-INNOWax 30 m x 0.25 mm, i.d x 0.25 µm) was used to determine conversion of methyl ester. As for characterization of methyl ester was carried out in terms of acid value (ASTM D664).

RESULTS AND DISCUSSION

Catalyst characterization

Field emission scanning electron microscope (FESEM)

FESEM analysis proved that calcination process at 900 °C for 2 hours on n-CaO catalyst prepared from cockle shell changed the morphology of the CaO from irregular shapes to a smooth cluster of well- developed cubic crystal. Besides, more pores with smooth surface was shown by calcined CaO nano catalyst as shown in figure 1(a) compared to uncalcined CaO nano catalyst where a rough surface with no pores observed as shown in figure 1(b).

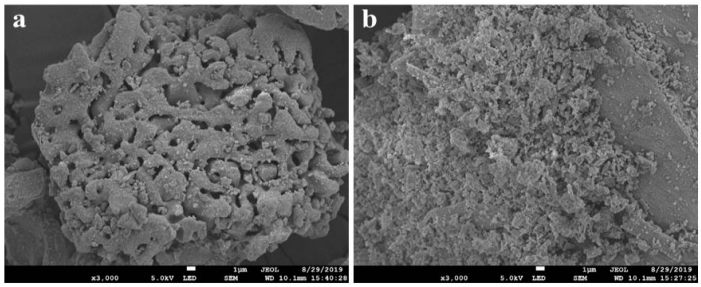

Figure 1 FESEM micrographs of (a) calcined nano CaO and (b) uncalcined nano CaO

Particle size analysis

Particle size distribution of the uncalcined CaO were mostly in the range between 1000 to 10000 nm but after calcined at 900 °C for 2 hours, its size reduced to below 1000 nm. This proved that calcination process leads to reduction of particle size of the CaO catalyst. Whereas, the synthesized CaO catalyst before ball milled was 969.3 nm in size but after ball milled for 36 hours at 350 rpm speed the particle size obtained was 104 nm and the frequency distribution curve for this was shown in figure 2 (a). This proved that ball milling process is an efficient way that able to reduce the micron size particles to nano scale particles (**Wong *et al.*, 2014**).

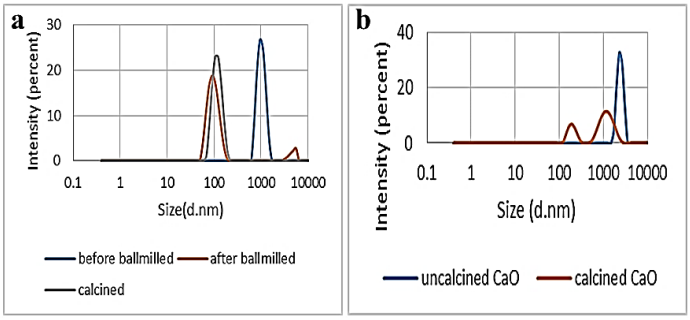

Figure 2 Zone Graph of size distribution by intensity of (a) synthesised n-CaO and (b) c-CaO catalyst

Transmission electron microscopy (TEM)

Based on the TEM result, the size of the synthesized CaO is in the range from 29 nm to 67.5 nm and the average particle size of the synthesized nano calcined CaO is approximately 43.16 nm. Hence, it is proven that through ball milling process for 36 hours at 350 rpm speed the shell derived CaO catalyst can be made into nano size catalyst powder.

Surface area analysis (BET)

Surface area of n-CaO and c-CaO was determined by Brunauer-Emmett-Teller analysis and gave a BET value of 8.41 m2/g and 3.0 m2/g, respectively. n-CaO and c-CaO. The smaller particle size of nano CaO catalyst cause its surface area to be larger. According to the International Union of Pure and Applied Chemistry classification, calcined commercial CaO figure 3(a) catalyst exhibit type V isotherm which explained non-porous form of catalyst. Whereas, CaO catalyst exhibit the type-IV isotherm based on figure 3(b) with type H4 hysteresis loop, which means that the synthesized catalysts having mesoporous structure.

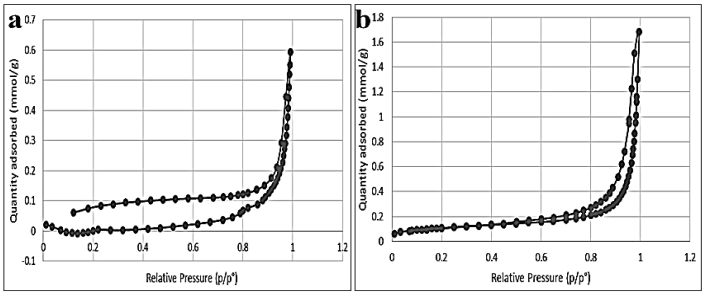

Figure 3 N_2 adsorption-desorption isotherm of (a) calcined commercial CaO and (b) calcined nano CaO

X-ray diffraction (XRD) analysis

Figure 4(a) shows the XRD pattern of the synthesized nano $CaCO_3$ powder before calcination treatment at 900 °C for 2 hours the peaks at 2θ27.42θ, 33.29θ,

38.69θ, 46.03θ 48.57θ, and 52.56θ with higher intensity indicated the presence of carbonate (CO_3^{2-}) in that sample. The main peaks of $CaCO_3$ observed on the uncalcined nano $CaCO_3$ catalyst were very similar with data from Joint Committee on Powder Diffraction Standard (JCPDS) file. Presence of CaO peaks at 2θ 32.25θ, 37.3θ, 53.96θ, 64.24θ and 67.46θ were observed for the synthesized calcined nano CaO catalyst as shown in figure 4 (b).

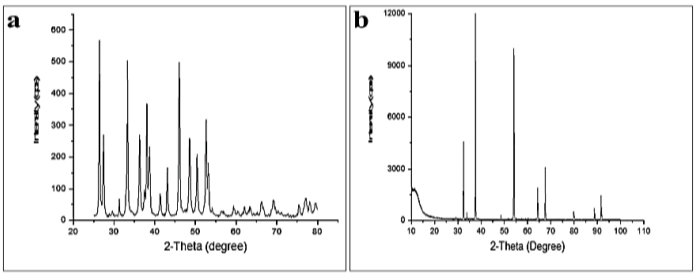

Figure 4 XRD pattern of the synthesized n-CaO (a) before and (b) after calcined.

Fourier Transform Infrared Spectroscopy (FTIR)

As shown in figure 5(b), the appearance of a small peak at 2922.45cm-1 absorption band depicted that there is still some carbonate, CO_32- compound at very low intensity available in the commercial calcined CaO catalyst. This might be due to the incomplete decomposition of the $CaCO_3$ into CaO. Whereas, the disappearance of moderate to weak signals and the shifting of absorption bands corresponding to CO_32- after calcination of the synthesized nano CaO as shown in figure 5 (a) verified the decomposition of CaCO3 to CaO. IR absorption bands in the uncalcined and calcined cockle shell derived CaO catalyst spectra completely matched with FTIR spectrum of the reported literature (**Laskar *et al.*, 2018**).

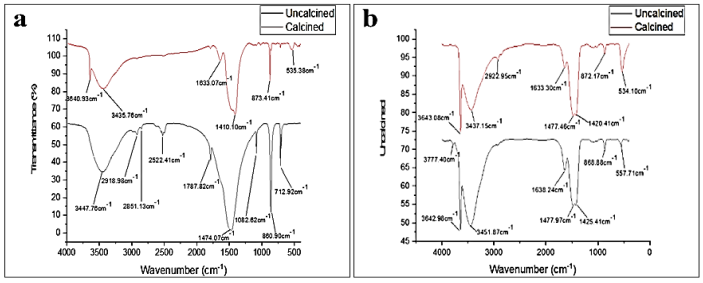

Figure 5 FTIR spectrum of the (a) synthesized nano CaO catalyst before and after calcined and (b) commercial CaO catalyst before and after calcined.

Hammett Indicator

The color of 2,4-dinitroaniline and 4-nitroaniline remain unchanged whereas color of phenolphthalein indicator changes to pink after 2 hours for both calcined commercial and n-CaO catalyst indicating H value for both the catalyst falls within the range of 8.2 to 15.

Benzoic acid titration method

The basicity value of the synthesized nano calcined CaO was 0.055 mmol/g which is higher than commercial calcined CaO which is 0.025 mmol/g. The result obtained was supported by research findings (**Syazwani *et al.*, 2017**), where natural derived waste shell contains higher amount of total basicity than commercial CaO catalyst which responsible for its higher catalytic activity.

Analysis of methyl ester

Based on Thin Layer Chromatography (TLC) result, the conversion rate of oil to methyl ester for calcined n-CaO catalyzed transesterification was found to be faster at each 30 minutes interval compared to calcined c-CaO catalyzed transesterification reaction. According to GC-FID result as shown in figure 3.6, it was shown that the overall rate of conversion of palm oil to methyl ester when using synthesized calcined n-CaO catalyst was much greater compared to that of calcined c-CaO catalyst. For the synthesized n-CaO catalyst, the nano size of the catalyst particle possess a large BET surface area which increase the availability of the basic sites on the catalyst surface for reaction compared to the c-CaO catalyst (**Maniam *et al.*, 2015**). This accelerates the rate of transesterification contributing to higher conversion of oil to methyl ester (**Bharti, Singh, and Dey 2019**).

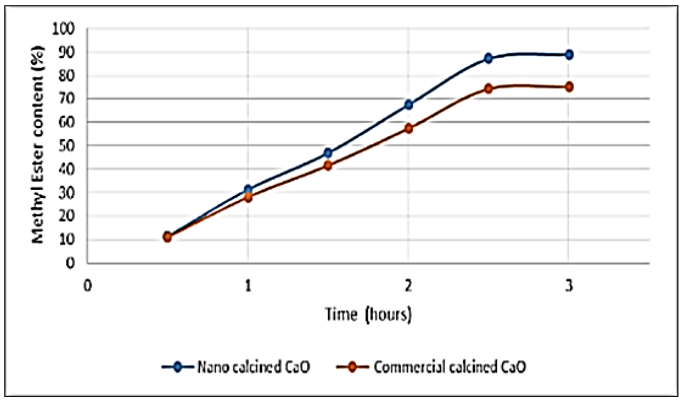

Figure 6 Graph of methyl ester yield (%) against time for both commercial and nano calcined CaO catalyst.

Characterization of methyl ester

The acid value of methyl ester obtained using commercial CaO catalyst were much higher than that of using the synthesized nano CaO catalyst which were confirmed with the ASTM standard.

CONCLUSION

CaO nanostructure derived from *Anadara granosa* cockle shell was prepared by calcination process at 900 °C for 2 hours. n-CaO exhibit better catalyst performance compared to c-CaO with higher methyl ester conversion of (88.87%). According to the obtained results, nanostructure of CaO catalyst provides a better characteristic of catalyst. Higher BET surface area (8.41 m2/g), smaller particle size (~100 nm) and higher basicity (0.055 mmol/g) contribute to the higher catalytic activity in transesterification reaction compared to c-CaO. Smaller particles increase the number of available active sites for the transesterification reaction to occur effectively and with higher rate, that are evident from the higher methyl esters conversion as well as higher basicity.

Acknowledgments: The authors gratefully acknowledged Universiti Malaysia Pahang (UMP) for the financial assistance through the Fundamental Research Grant Scheme (FRGS) FRGS/1/2019/STG01/UMP/02/2. Authors are thankful to UMP and Central Laboratory for providing research facilities.

REFERENCES

Ahmad, M.S., Cheng, C.K., Bhuyar, P., Atabani, A.E., Pugazhendhi, A., Chi, N.T.L., Witoon, T., Lim, J.W., Juan, J.C. (2021). Effect of reaction conditions on the lifetime of SAPO-34 catalysts in methanol to olefins process–A review. Fuel, 283, p.118851. https://doi.org/10.1016/j.fuel.2020.118851

Bampidis, V. A., & Robinson, P. H. (2006). Citrus by-products as ruminant feeds: A review. Animal Feed Science and Technology, 128(3-4), 175-217. https://doi.org/10.1016/j.anifeedsci.2005.12.002

Banković–Ilić, I. B., Miladinović, M. R., Stamenković, O. S., & Veljković, V. B. (2017). Application of nano CaO–based catalysts in biodiesel synthesis. Renewable and Sustainable Energy Reviews, 72, 746-760. https://doi.org/10.1016/j.rser.2017.01.076

Bharti, P., Singh, B., & Dey, R. K. (2019). Process optimization of biodiesel production catalyzed by CaO nanocatalyst using response surface methodology. Journal of Nanostructure in Chemistry, 9(4), 269-280. https://doi.org/10.1007/s40097-019-00317-w

Bhuyar, P., Rahim, M. H. A., Sundararaju, S., Ramaraj, R., Maniam, G. P., & Govindan, N. (2020). Synthesis of silver nanoparticles using marine macroalgae Padina sp. and its antibacterial activity towards pathogenic bacteria. Beni-Suef Univ J Basic Appl Sci, 9(1), 1-15. https://doi.org/10.1186/s43088-019-0031-y

Bhuyar, P., Sundararaju, S., Math, K. R., Maniam, G. P., Govindan, N. (2020). Production of bioethanol from starchy tuber (Amorphophallus commutatus) and antimicrobial activity study of its extracts. Afr. J. of Bio. Sci., 2(2), 70-76. https://doi.org/10.33472/AFJBS.2.2.2020.70-76

Bhuyar, P., Sundararaju, S., Rahim, M. H. A., Ramaraj, R., Maniam, G. P., & Govindan, N. (2019). Microalgae cultivation using palm oil mill effluent as growth medium for lipid production with the effect of CO2 supply and light intensity. Biomass Conv. Bioref.1-9. https://doi.org/10.1007/s13399-019-00548-5

Bhuyar, P., Yusoff, M. M., Rahim, M. H. A., Sundararaju, S., Maniam, G. P., Govindan, N. (2020). Effect of plant hormones on the production of biomass and lipid extraction for biodiesel production from microalgae chlorella sp." The J. of Micro. Biotech. and Food Sci. 9, no. 4 (2020): 671. https://doi.org/10.15414/jmbfs.2020.9.4.671-674

Bhuyar, P., Rahim, M. H. A., Yusoff, M. M., Maniam, G. P., Govindan, N. (2019). A selective microalgae strain for biodiesel production in relation to higher lipid profile. Maejo Int J Energy Environ Commun, 1(1), 8–14.

Boock, J.T., Freedman, A.J., Tompsett, G.A., Muse, S.K., Allen, A.J., Jackson, L.A., Castro-Dominguez, B., Timko, M.T., Prather, K.L. and Thompson, J.R., 2019. Engineered microbial biofuel production and recovery under supercritical carbon dioxide. Nature communications, 10(1), pp.1-12. 587 | https://doi.org/10.1038/s41467-019-08486

Borah, M. J., Das, A., Das, V., Bhuyan, N., & Deka, D. (2019). Transesterification of waste cooking oil for biodiesel production catalyzed by Zn substituted waste eggshell derived CaO nanocatalyst. Fuel, 242, 345-354. https://doi.org/10.1016/j.fuel.2019.01.060

Bunyakiat, K., Makmee, S., Sawangkeaw, R., & Ngamprasertsith, S. (2006). Continuous production of biodiesel via transesterification from vegetable oils in supercritical methanol. Energy & Fuels, 20(2), 812-817. https://doi.org/10.1021/ef050329b

Du, W., Xu, Y., Liu, D., & Zeng, J. (2004). Comparative study on lipase-catalyzed transformation of soybean oil for biodiesel production with different acyl acceptors. Journal of Molecular Catalysis B: Enzymatic, 30(3-4), 125-129. https://doi.org/10.1016/j.molcatb.2004.04.004

Ge, J. C., Yoon, S. K., & Choi, N. J. (2017). Using canola oil biodiesel as an alternative fuel in diesel engines: A review. Applied Sciences, 7(9), 881. https://doi.org/10.3390/app7090881

Ishola, F., Adelekan, D., Mamudu, A., Abodunrin, T., Aworinde, A., Olatunji, O., & Akinlabi, S. (2020). Biodiesel production from palm olein: A sustainable bioresource for Nigeria. Heliyon, 6(4), e03725. https://doi.org/10.1016/j.heliyon.2020.e03725

Khammee, P., Ramaraj, R., Whangchai, N., Bhuyar, P., Unpaprom, Y. (2020). The immobilization of yeast for fermentation of macroalgae Rhizoclonium sp. for efficient conversion into bioethanol. Biomass Conv. Bioref.53:2. https://doi.org/10.1007/s13399-020-00786-y

Laskar, I. B., Rajkumari, K., Gupta, R., Chatterjee, S., Paul, B., & Rokhum, L. (2018). Waste snail shell derived heterogeneous catalyst for biodiesel production by the transesterification of soybean oil. RSC advances, 8(36), 20131-20142. https://doi.org/10.1039/C8RA02397B

Malek, M.N.F.A., Hussin, N.M., Embong, N.H., Bhuyar, P., Rahim, M. H. A., Govindan, N., Maniam, G. P. (2020). Ultrasonication: a process intensification tool for methyl ester synthesis: a mini review. Biomass Conv. Bioref. https://doi.org/10.1007/s13399-020-01100-6

Maniam, G. P., Hindryawati, N., Nurfitri, I., Manaf, I. S. A., Ramachandran, N., & Rahim, M. H. A. (2015). Utilization of waste fat from catfish (Pangasius) in methyl esters preparation using CaO derived from waste marine barnacle and bivalve clam as solid catalysts. Journal of the Taiwan Institute of Chemical Engineers, 49, 58-66. https://doi.org/10.1016/j.jtice.2014.11.010

Mazaheri, H., Ong, H. C., Masjuki, H. H., Amini, Z., Harrison, M. D., Wang, C. T., ... & Alwi, A. (2018). Rice bran oil-based biodiesel production using calcium oxide catalyst derived from Chicoreus brunneus shell. Energy, 144, 10-19. https://doi.org/10.1016/j.energy.2017.11.073

Saengsawang, B., Bhuyar, P., Manmai, N., Ponnusamy, V. K., Ramaraj, R., Unpaprom, Y. (2020). The optimization of oil extraction from macroalgae, Rhizoclonium sp. by chemical methods for efficient conversion into biodiesel. Fuel, 274, 117841. https://doi.org/10.1016/j.fuel.2020.117841

Syazwani, O. N., Teo, S. H., Islam, A., & Taufiq-Yap, Y. H. (2017). Transesterification activity and characterization of natural CaO derived from waste venus clam (Tapes belcheri S.) material for enhancement of biodiesel production. Process Safety and Environmental Protection, 105, 303-315. https://doi.org/10.1016/j.psep.2016.11.011

Toldrá-Reig, F., Mora, L., & Toldrá, F. (2020). Trends in Biodiesel Production from Animal Fat Waste. Applied Sciences, 10(10), 3644. https://doi.org/10.3390/app10103644

Wong, Y. C., Y. P. Tan, Y. H. Taufiq-Yap, and I. Ramli. 2014. “Effect of Calcination Temperatures of CaO/Nb2O5 Mixed Oxides Catalysts on Biodiesel Production.” Sains Malaysiana 43(5):783–90.

ARTICLES FOR FACULTY MEMBERS

ELUCIDATING THE CALCIUM OXIDE DERIVED FROM THE WASTE SHELLS OF MUD CLAM (GELOINA EXPANSA) AS A CATALYST FOR BIODIESEL PRODUCTION

From waste to catalyst: Transforming mussel shells into a green solution for biodiesel production from jatropha curcas oil / Alsabi, H. A., Shafi, M. E., Almasoudi, S. H., Mufti, F. A. M., Alowaidi, S. A., Sharawi, S. E., & Alaswad, A. A.

Catalysts
Volume 14 Issue 1 (2024) 59 Pages 1-18
https://doi.org/10.3390/catal14010059
(Database: MDPI)

catalysts

MDPI

Article

From Waste to Catalyst: Transforming Mussel Shells into a Green Solution for Biodiesel Production from *Jatropha curcas* Oil

Halimah A. Alsabi [1], Manal E. Shafi [2,*], Suad H. Almasoudi [3], Faten A. M. Mufti [3], Safaa A. Alowaidi [1], Somia E. Sharawi [1] and Alaa A. Alaswad [4]

[1] Department of Biology, Faculty of Sciences, King Abdulaziz University, Jeddah 21589, Saudi Arabia; halsabee@stu.kau.edu.sa (H.A.A.)
[2] Sustainable Agriculture Production Research Group, Department of Biological Sciences, Zoology, King Abdulaziz University, Jeddah 21589, Saudi Arabia
[3] Department of Biology, Faculty of Sciences, Umm Al-Qura University, Makkah 96612, Saudi Arabia
[4] Department of Biological Sciences, Faculty of Sciences, University of Jeddah, Jeddah 21589, Saudi Arabia
* Correspondence: meshafi@kau.edu.sa

Abstract: This study introduces an innovative approach to sustainable biodiesel production using mussel shell-derived calcium oxide (CaO) as a catalyst for converting *Jatropha curcas* oil into biodiesel. By repurposing waste mussel shells, the research aims to provide an eco-friendly and cost-effective solution for environmentally responsible biodiesel production, aligning with global standards. The study involves characterizing the catalyst, optimizing reaction conditions, and achieving a remarkable 99.36% Fatty Acid Methyl Ester (FAME) yield, marking a significant step toward cleaner and more economically viable energy sources. Biodiesel, recognized for its lower emissions, is produced through transesterification using mussel shell-derived CaO as a sustainable catalyst. This research contributes to cleaner and economically viable energy sources, emphasizing the importance of sustainable energy solutions and responsible catalytic processes. This research bridges the gap between waste management, catalyst development, and sustainable energy production, contributing to the ongoing global shift towards cleaner and more economically viable energy sources.

Keywords: biodiesel production; mussel shell-derived CaO catalyst; sustainable catalyst; transesterification; *Jatropha curcas* oil; renewable energy

Citation: Alsabi, H.A.; Shafi, M.E.; Almasoudi, S.H.; Mufti, F.A.M.; Alowaidi, S.A.; Sharawi, S.E.; Alaswad, A.A. From Waste to Catalyst: Transforming Mussel Shells into a Green Solution for Biodiesel Production from *Jatropha curcas* Oil. *Catalysts* **2024**, *14*, 59. https://doi.org/10.3390/catal14010059

Academic Editor: Claudia Carlucci

Received: 14 December 2023
Revised: 3 January 2024
Accepted: 6 January 2024
Published: 12 January 2024

1. Introduction

The global energy landscape is currently characterized by increased greenhouse gas emissions, including CO_2, and how combusting fossil fuels affect the environment. In response, there is a pressing need to transition towards sustainable alternative fuels, including biodiesel, bioethanol, and biomass, which align with the sustainability goals outlined in Saudi Arabia's Vision 2030 strategy [1,2]. This transition is essential to mitigate the environmental challenges posed by the current energy paradigm [3].

Biodiesel, as a sustainable energy source, offers a compelling alternative to traditional petroleum diesel. Its green credentials include renewability, biodegradability, non-toxicity, reduced CO and CO_2 emissions, sulfur-free composition, and straightforward production [4]. Moreover, biodiesel is environmentally friendly because it minimizes hazardous exhaust emissions [5,6].

Mussel shell formation is a vital natural process in marine ecosystems, where mussels actively produce calcium carbonate for their protective shells. These shells contribute significantly to marine habitats, providing shelter and influencing local biodiversity. Beyond its ecological importance, researchers explore mussel shell production for potential applications in materials science and environmental remediation [7]. The annual production of mussel shells thus stands as a crucial element in the intricate balance of marine ecosystems, influencing biodiversity and contributing to the overall health of coastal environments [7].

Catalysts are essential in biodiesel production, with three primary types: homogeneous, heterogeneous (basic or acidic), and biocatalysts [8]. Heterogeneous catalysts are gaining popularity due to their environmental and economic advantages [9]. Biodiesel production is shifting towards non-edible oils like *J. curcas*, which offer high oil content and can grow in adverse conditions without competing with food sources [10]. Hence, *J. curcas* oil is a promising candidate for biodiesel transesterification [11,12].

Catalysts are crucial in facilitating the dominant technique to produce biodiesel, the transesterification process [13]. Homogeneous catalysts, heterogeneous catalysts, and biocatalysts constitute the three primary categories, each further classified into acid and base catalysts [14]. Homogeneous catalysts, such as KOH and NaOH, are commonly used as base catalysts. However, their retrieval and the substantial volume of wastewater from catalyst separation present significant drawbacks [15]. In contrast, heterogeneous catalysts offer several advantages, notably in mitigating environmental and economic drawbacks related to homogeneous catalysts [16]. Heterogeneous catalysts can be separated and reused more efficiently, minimizing the environmental footprint. This streamlined separation process reduces wastewater generation and simplifies biodiesel synthesis, eliminating the need for certain process steps [17].

The transesterification process, a key step in biodiesel synthesis, is influenced by various factors, such as the catalyst type, reaction conditions (like temperature, time, and reactant ratios), and the ability to reuse the catalyst [18,19]. Understanding how these factors impact biodiesel production is crucial for optimizing the process and ensuring high-quality biofuels. Additionally, exploring the use of natural waste products like chicken eggshells, crab shells, mussel shells, and clamshells, all rich in calcium carbonate ($CaCO_3$), presents an interesting opportunity. These discarded shells could create CaO-based catalysts, especially suitable for biodiesel synthesis at high temperatures [20–22].

Transesterification using mussel shells as a heterogeneous catalyst offers several advantages [23]. Firstly, they show potential for high catalyst yields. Secondly, waste materials promote environmental sustainability. Thirdly, they are cost-effective, lowering biofuel production costs and supporting the shift to sustainable energy sources. Lastly, their ready availability in substantial quantities locally adds to their appeal as a catalyst source [24,25].

This study introduces a fresh perspective to the field of biodiesel production. Its primary objective is to investigate the use of discarded mussel shells as a renewable source for a solid base catalyst, which represents a departure from traditional catalyst materials. This novel application addresses environmental concerns and taps into the abundance of cost-effective waste materials. The choice of mussel shell-derived CaO as a catalyst is motivated by its potential advantages over commercially available CaO. Additionally, the research aims to identify the optimal operating conditions that balance the quantity and quality of biodiesel, addressing efficiency challenges. This study underscores the research's dedication to addressing modern energy and environmental issues through inventive, environmentally conscious methods.

2. Results

2.1. Transesterification Reaction

The study examined the process parameters for trans-esterifying *J. curcas* oil into biodiesel using the mussel shell waste catalyst. It investigated the influence of reaction temperature, time, methanol-to-oil ratio, calcination temperature, and catalyst amount.

2.1.1. Impact of Reaction Time

The reaction time is a crucial factor in optimizing biodiesel yield. Batch experiments were conducted with consistent conditions: 50 g of oil, 110°C, methanol-to-oil ratio of 1:12, 6 wt.% catalyst calcined at 900°C, and varying reaction times of 3, 4, 5, and 6 h. Figure 1a indicates that the conversion percentage rose from 40.90% to 46.54% as the

transesterification time extended from 3 to 6 h. However, at 5 h, there was a slight drop to 44.79%, but the highest conversion of 62.51% was achieved after 6 h.

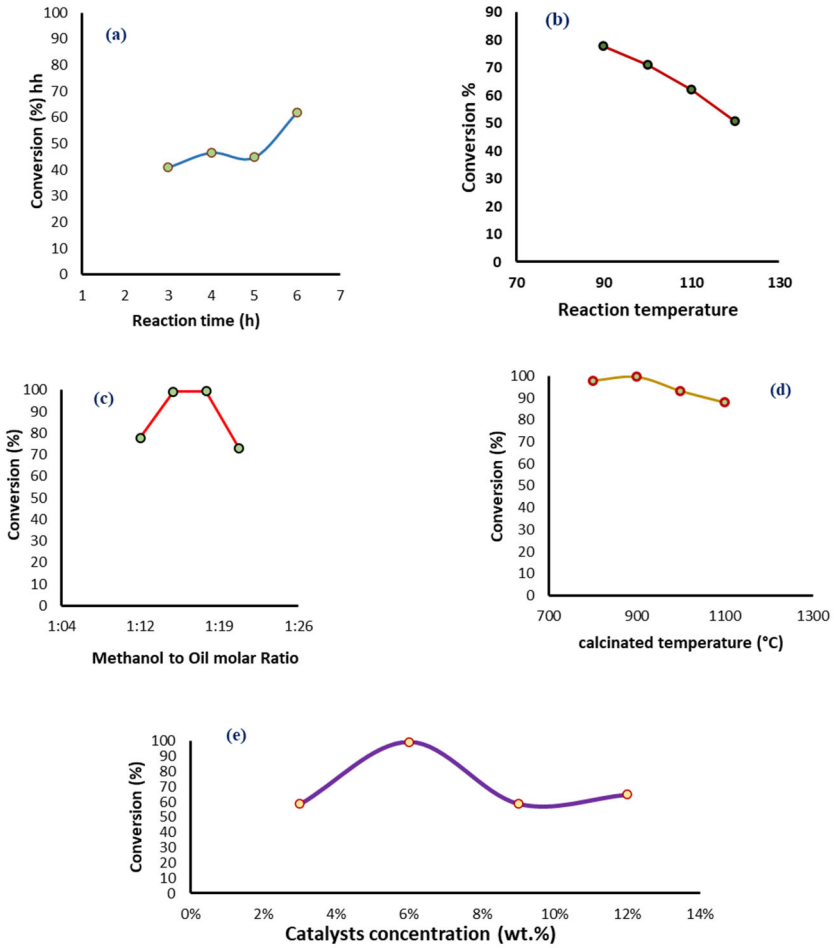

Figure 1. (**a**) Effect of reaction time on biodiesel yield. (**b**) Effect of reaction temperature on biodiesel yield. (**c**) Effect of molar ratio on biodiesel yield. (**d**) Effect of catalyst calcination temperature on biodiesel yield. (**e**) Effect of catalyst concentration.

2.1.2. Effects of Different Reaction Temperatures

Temperature significantly affects the biodiesel reaction and its yield. This study conducted transesterification for 6 h with a 12:1 molar ratio, using 6 wt.% of mussel waste shell catalyst calcined at 900°C. Different temperature ranges (90, 100, 110, and 120°C) were investigated. As shown in Figure 1b, the reaction rate decreased with increasing temperature, resulting in reduced yield, especially at 120°C. The maximum methyl ester yield, approximately 77.78%, was achieved at 90 °C, while it dropped to 71.03% at 100 °C, 62.01% at 110 °C, and 50.53% at 120 °C.

2.1.3. Impact of Various Methanol to Oil Ratios

The molar ratio between methanol and oil is a crucial factor in manufacturing biodiesel. While the stoichiometric molar ratio for transesterification is 3:1, higher ratios are often used to expedite the reaction and increase product yield. In this study, *J. curcas* oil was subjected to transesterification with varying methanol to oil molar ratios (12:1, 14:1, 18:1, and 21:1) using 6 wt.% of calcined mussel shell catalyst for 6 h at 90 °C. Figure 1c shows how the molar ratio affects the amount of biodiesel produced. Initially, increasing the molar ratio led to a higher yield. The highest yield of 99.36% was achieved at a 1 molar ratio of 18:1, but it started to decline when the ratio was further increased to 21:1.

2.1.4. Effect of the Calcined Catalyst Temperatures

Mussel shell catalysts were subjected to different calcination temperatures (800, 900, 1000, and 1100 °C) and then used in transesterification processes with a methanol-to-oil molar ratio of 18:1 for 6 h at 90 °C. The influence of calcination temperature on the oil yield percentage is depicted in Figure 1d. It is evident that the percentage yield increased as the calcination temperature rose. The highest yield was 99.36% at 900°C, which is consistent with SEM results. However, when the calcination temperature exceeded 900 °C, the yield percentages dropped to 87.73% at 1100 °C.

2.1.5. Impact of Catalyst Concentration

To assess the impact of catalyst quantity on the maximum conversion of *J. curcas*, methyl ester catalysts calcined at 900 °C were used in amounts of 3, 6, 9, and 12 wt.% at a temperature of 90 °C for 6 h, and with a molar ratio of 18:1. As depicted in Figure 1e, the quantity of catalyst added significantly influences the conversion of *J. curcas* oil to biodiesel.

Increasing the catalyst amount from 3 to 6 wt.% resulted in a significant increase in the methyl ester content of *J. curcas* oil, rising from approximately 58.66% to 99.36%. However, as the catalyst quantity increased to 9%, the conversion efficiency dropped to 65.89%. The yield increased to 63.88% when the catalyst quantity was raised to 12%.

2.2. Catalyst Characterization

2.2.1. Thermogravimetric Analysis

To find the optimal calcination temperature for CaO production, we conducted a DSC/TGA analysis on the mussel shell sample, and the results are depicted in Figure 2. Initially, between 50 and 400 °C, a decrease in mass occurred due to the removal of surface-adsorbed water. The most significant mass loss, observed from 400 to 600 °C, was attributed to eliminating mineral or volatile components in the mussel shell. Notably, between 600 and 800 °C, there was a maximum weight reduction, indicating complete decomposition at 800 °C with the simultaneous release of CO_2, as shown in reaction 1. Beyond 800 °C, the sample's weight remained constant at 53.31 wt.%.

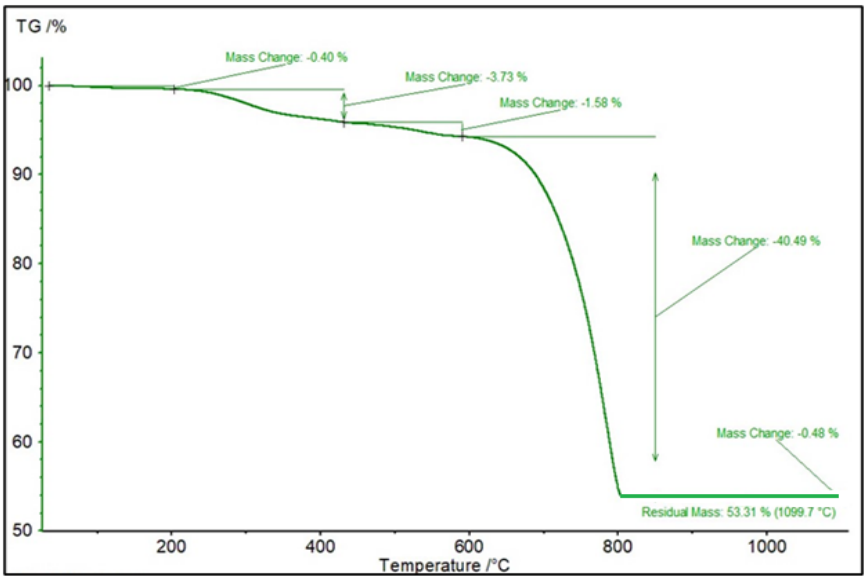

Figure 2. DSC/TGA analysis of mussel shells.

2.2.2. Thermogravimetric Analysis

The Fourier transform infrared spectra of non-calcined and calcined mussel shell catalysts at temperatures of 800, 900, 1000, and 1100 °C are depicted in Figure 3. Initially, absorption bands in the non-calcined mussel shell are observed at 705 cm^{-1}, 858 cm^{-1},

1099 cm^{-1}, and 1457 cm^{-1}. During calcination, as $CaCO_3$ in the mussel shell decomposes into CaO, releasing CO_2, the strength of these absorption bands at 3693 cm^{-1}, 1436 cm^{-1}, and 865 cm^{-1} decreases. Additionally, the production of basic OH groups attached to the calcium atoms produces a distinct sharp band at 3639 cm^{-1}.

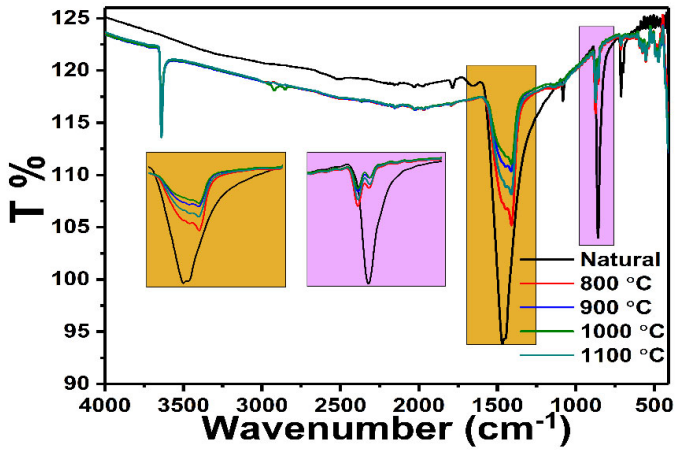

Figure 3. FTIR spectra of mussel shell catalyst non-calcined and calcined at 800, 900, 1000, and 1100 °C.

2.2.3. Thermogravimetric Analysis

Figure 4 displays the chemical constitution of waste mussel shells upon being calcined for 4 h at temperatures of 800, 900, 1000, and 1100 °C. The primary mineral component, as revealed by XRF analysis, is CaO. The waste mussel shell catalysts contain high CaO concentrations, ranging from 98.67 to 98.85 wt.%. This substantial presence of calcium suggests that the initial material was composed of $CaCO_3$, which becomes CaO after calcination.

The methyl ester composition in biodiesel was analyzed at different calcined catalyst temperatures using gas chromatography–mass spectrometry (GC–MS). The components of methyl ester examined included Palmitoleic ME ($C_{17}H_{32}O_2$, C16:1), Palmitic Acid ME ($C_{17}H_{34}O_2$, C16:0), Linoleic Acid ME ($C_{19}H_{34}O_2$, C18:2), Oleic Acid ME ($C_{19}H_{36}O_2$, C18:1), Stearic Acid ME ($C_{19}H_{38}O_2$, C18:0), and Crotonic Acid ME ($C_5H_8O_2$, C4:0). All the above components were found at 900°C, as shown in Figure S1.

2.2.4. Sample Structures

Figure 5 presents the XRD patterns of natural and calcined mussel shells. The natural mussel shells show a predominant composition of $CaCO_3$, as indicated by the XRD results, with no discernible CaO peak. However, with increased calcination temperature, $CaCO_3$ completely transforms into CaO, accompanied by the release of (CO_2). The main component of calcined catalysts at or above 800 °C is the active ingredient (CaO). The XRD pattern exhibits sharp, high-intensity peaks, signifying the well-defined crystalline structure of the CaO catalyst. The catalyst peak is observed at 2θ values of 32.28°, 37.45°, 54°, 64.33°, 67.56°, and 79.89°, indicating reflections from planes with (1 1 1), (2 0 0), (2 2 0), (3 1 1), (2 2 2), and (4 0 0) orientations, respectively (JCPDS card 01-075-0264). These peaks align with the CaO standard pattern and the XRF investigation, which revealed a substantial concentration of CaO.

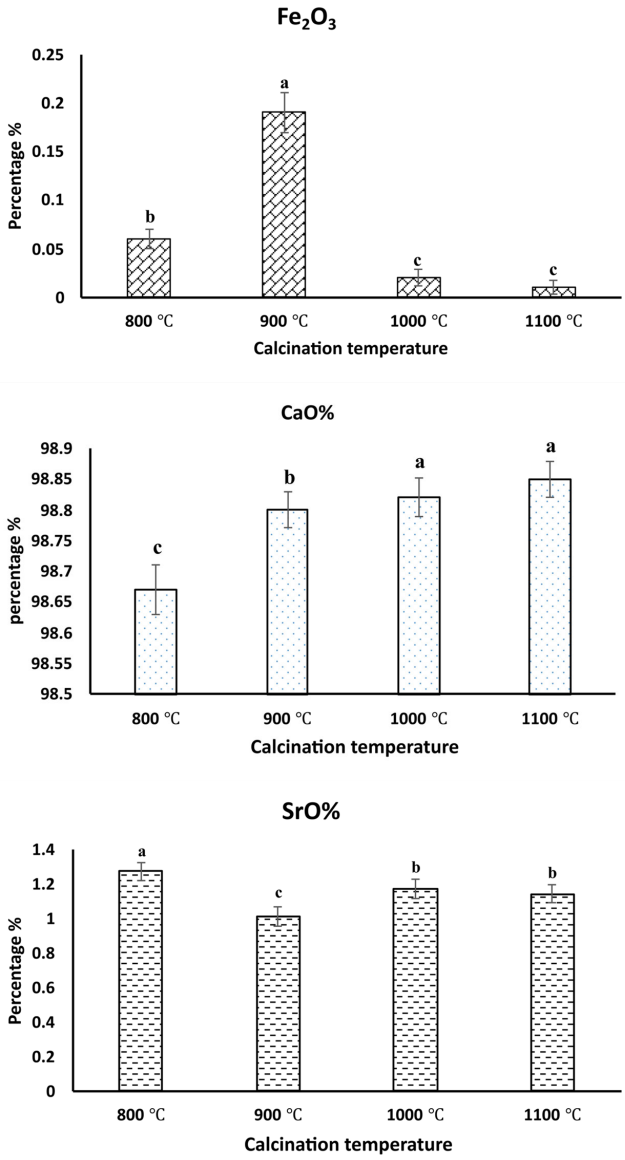

Figure 4. The average weight % of elements by XRF. (**a–c**) different letters means significant differences.

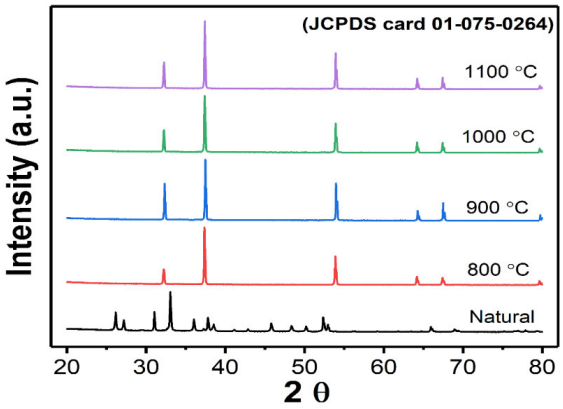

Figure 5. XRD patterns of natural and calcined mussel shells.

2.2.5. Morphological Properties

Scanning electron microscopy images at various magnifications are presented for mussel shells calcined at 800 °C (Figure 6), 900 °C (Figure 7), 1000 °C (Figure 8), and

1100 °C (Figure 9). In the SEM image of the sample calcined at 800 °C, the particles exhibit a relatively smooth and slightly cracked surface. However, in the sample calcined at 900 °C, the surface becomes rougher and more cracked; suggesting increased surface area and enhanced contact between reactants and the catalyst surface. Furthermore, the samples calcined at 1000 °C and 1100 °C display a similar morphology with a roughly textured surface, albeit less cracked than those calcined at 900 °C.

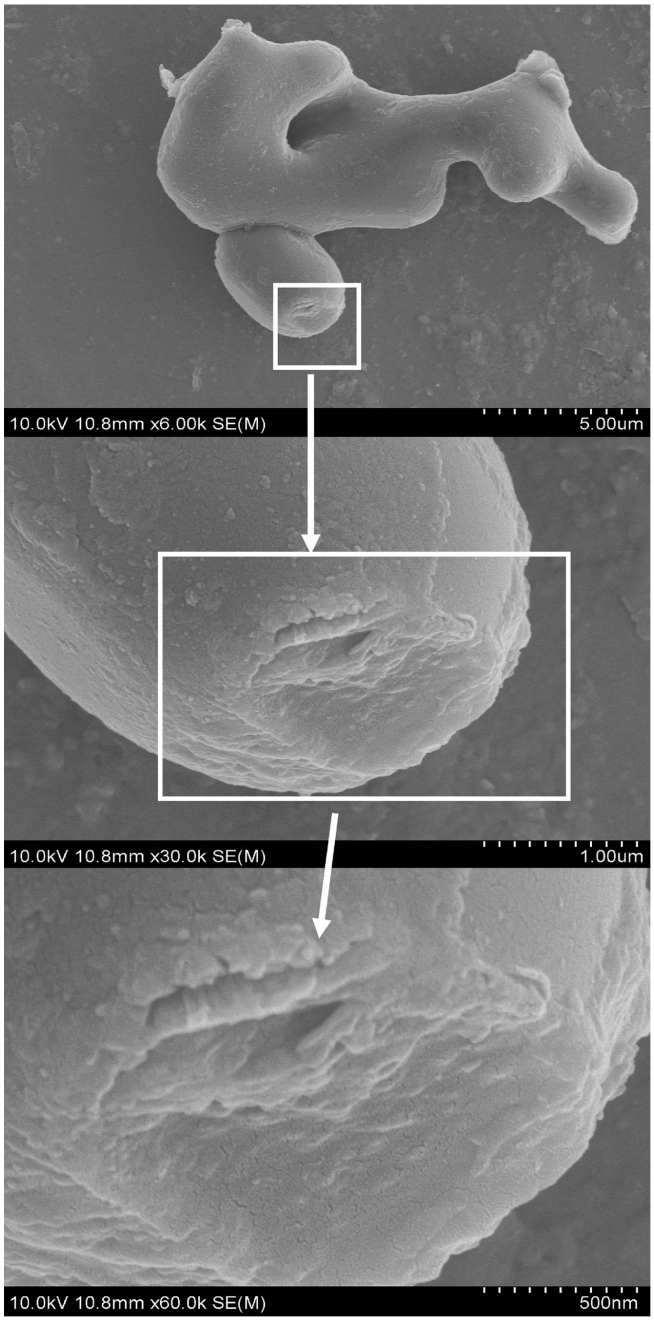

Figure 6. SEM image of a mussel shell subjected to a temperature of 800 °C for 4 h.

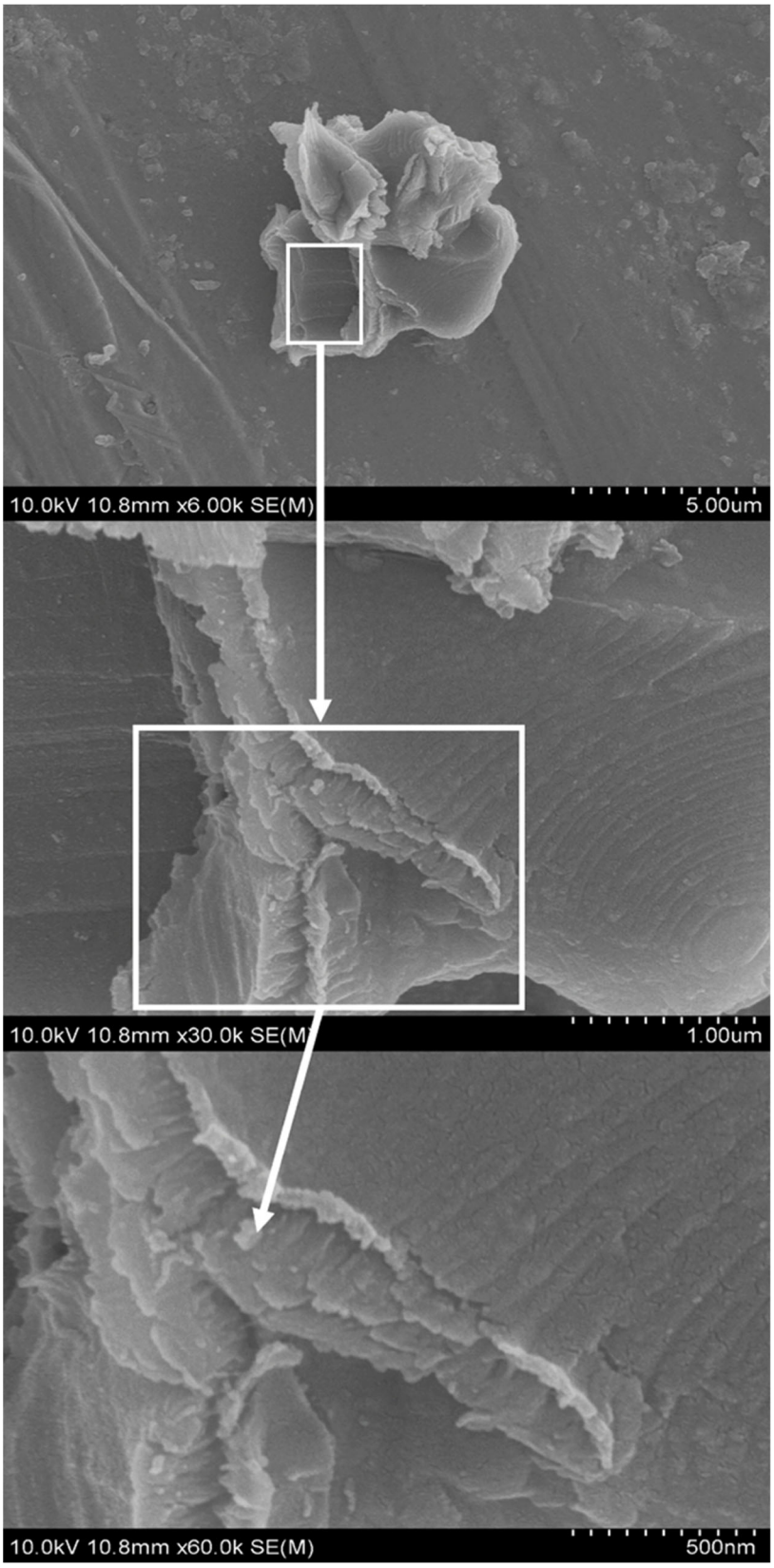

Figure 7. SEM image of a mussel shell subjected to a temperature of 900 °C for 4 h.

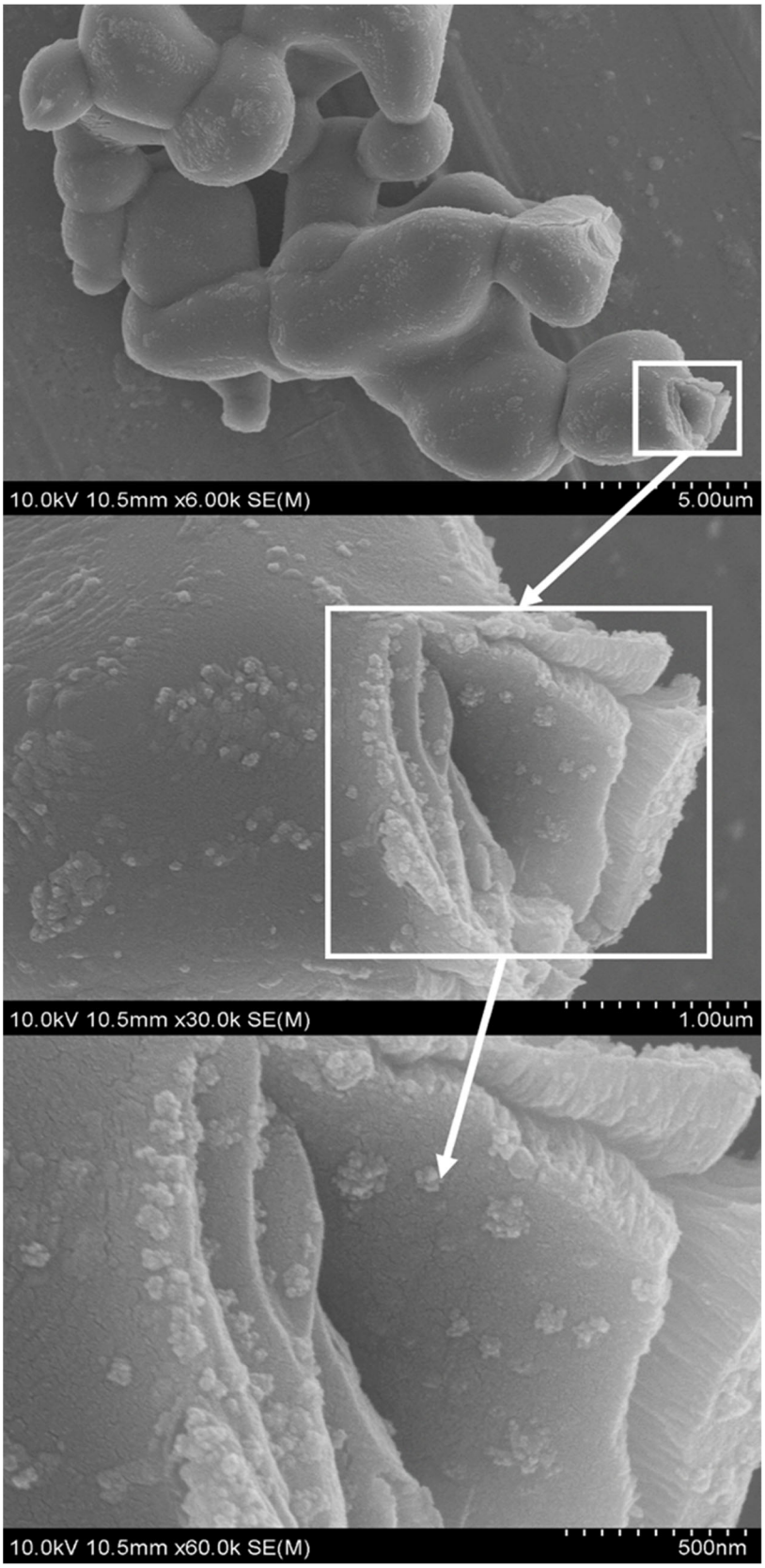

Figure 8. SEM image of a mussel shell subjected to a temperature of 1000 °C for 4 h.

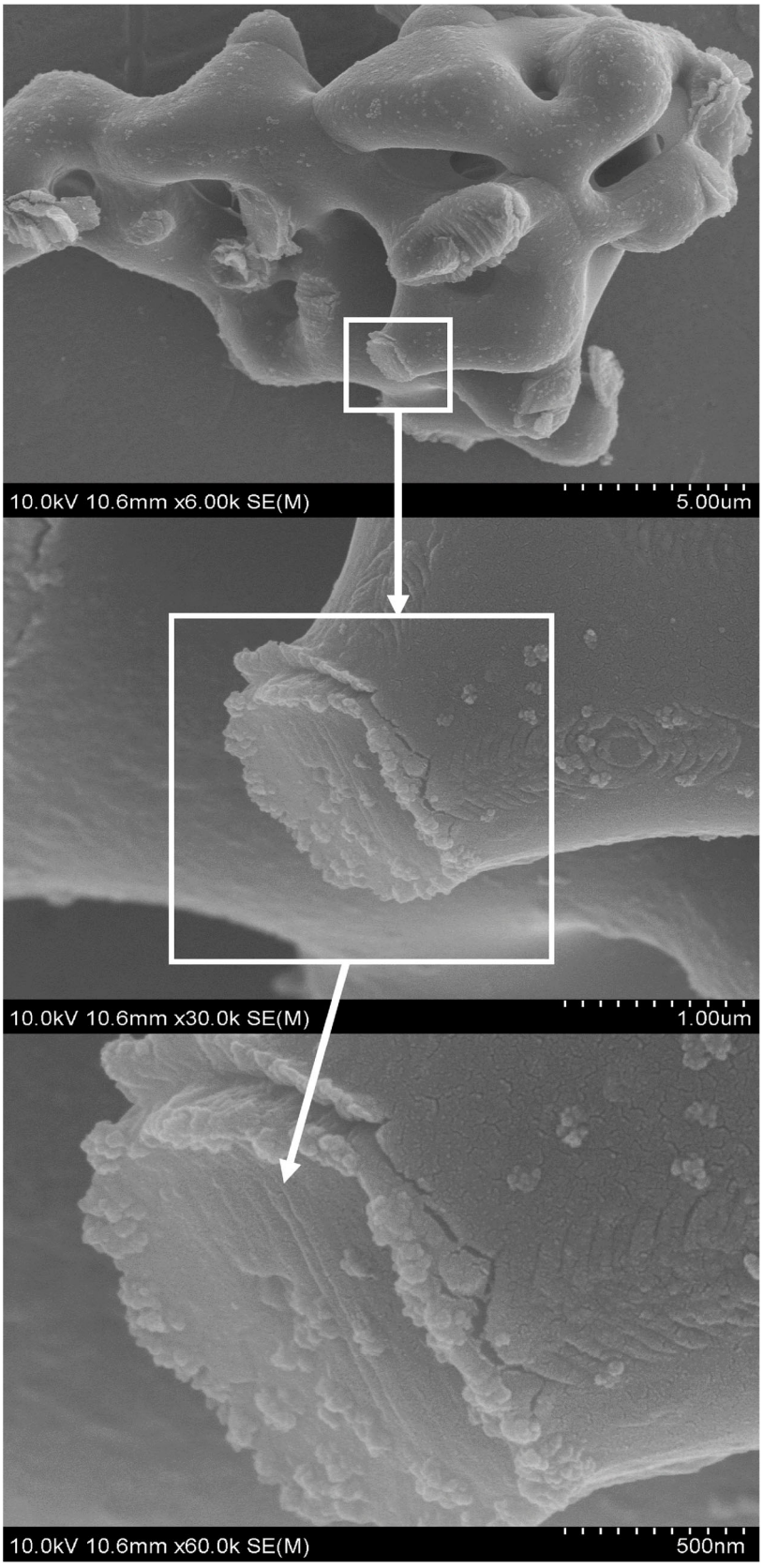

Figure 9. SEM image of a mussel shell subjected to a temperature of 1100 °C for 4 h.

2.2.6. Chemical and Physical Properties of J. curcas Methyl Ester and Number of Reusability

The results in Table 1 indicate that the prepared biodiesel meets most standards for diesel fuels, although it slightly exceeds the cloud point limit. However, its density (0.856 g/cm^3) and calorific value (38.140 MJ/kg) are within acceptable limits. The distillation profile (98–309 °C) suggests suitability for diesel engines. The flash point (110°C) exceeds the minimum requirement, and viscosity (4.89 mm^2/s) falls within specified ranges for both standards.

Table 1. Chemical and Physical Properties of *J. curcas* Methyl Ester.

Contents	ASTM D-6751	Prepared Biodiesel	EN 14214
Cloud point	−3 to 15 °C	0	--------
Pour point	−5 to 10 pp	−3 pp	--------
Calorific value	---	38.140 MJ/kg	32.9
Viscosity	1.9–6 mm^2/s	4.89 mm^2/s	3.5–5 mm^2/s
Cetane number	47–65	50.5	51 to 120
Density at 15 °C	0.82–0.9 g/cm^3	0.856 g/cm^3	0.86–0.9 g/cm^3
Flash point	>120 °C	110 °C	>120 °C
Oxidation stability	Max. 3 h	4.5 h	Min. 6 h
Sulfur content	≤15 ppm	8 ppm	≤10 ppm
Free glycerol content	≤0.020% wt.%	0.011% wt.%	≤0.020% wt.%
Total glycerol content	---	0.032%	Max. 0.25%
Iodine value	≤120 I_2/100 g	99.2 I_2/100 g	≤120 I_2/100 g
Phosphorus content	Max. 10 ppm	5 ppm	Max. 10 ppm
Water content	Max. 500 ppm	350 ppm	Max. 500 ppm
Ash content	Max. 0.01%	0.005%	Max. 0.02%
Carbon residue	Max. 0.050%	0.035%	Max. 0.20%
Acid value	≤0.050 mg KOH/g	0.030 mg KOH/g	≤0.050 mg KOH/g
	Vol.	Temp. °C	
Distillation profile Initial	50 mL	191	
boiling point	80 mL	296	
	90 mL	309	

The catalyst, prepared with 6% by weight, calcined at 900°C, and a methanol-to-oil ratio of 18:1 at 90 °C for 6 h, was tested through multiple cycles. Results demonstrate that the calcined mussel shell can be reused up to five times, with FAME yields of 99.2%, 94.13%, 81.53%, 76.56%, and 66.41% for each cycle, as illustrated in Figure 10.

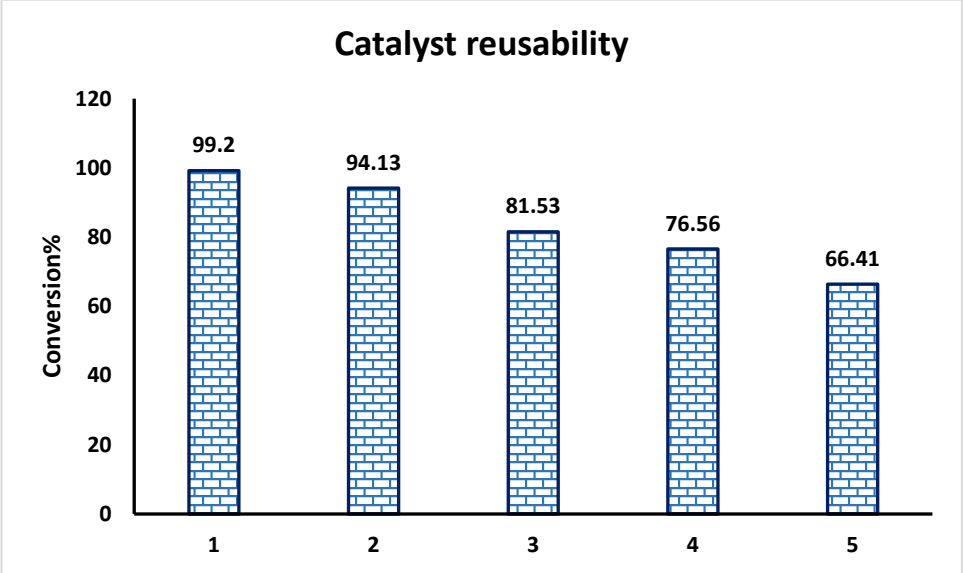

Figure 10. Number of reusability for the *Jatropha curcas* catalyst.

3. Discussion

Over the past decade, the world's energy demand has seen a significant increase, driven by rapid industrialization. Traditional energy sources not only lack sustainability but also pose environmental challenges. The expanding global industries have hastened the depletion of conventional resources [26]. Projections indicate a 40% increase in worldwide energy demand from 2010 to 2030. Biodiesel, a biofuel capable of substituting petroleum-based diesel, comprises a chemically intricate mixture of fatty acid mono-alkyl esters, primarily derived from plant oils or animal fats. Non-edible sources are favored for biodiesel production due to their cost-effectiveness and lack of competition with food supplies [27].

Jatropha curcas, an agricultural plant with abundant oil content, can thrive in marginal soils in tropical and subtropical climates. This plant offers various economic benefits while aiding soil improvement and erosion prevention. Its latex leaves and fruit can be used to make medicine, manure, and insect repellent. Additionally, press cake from Jatropha can be used to generate biogas. Over the last decade, numerous Jatropha projects worldwide have capitalized on the potential value chain it offers [28].

Catalysts play a crucial role in the transesterification process [29]. When transforming vegetable oils into biodiesel, heterogeneous catalysts show potential. Unlike homogeneous catalysts, heterogeneous ones can be reused, regenerated, and employed continuously [30]. Our study aimed to create biodiesel from crude *J. curcas* oil using mussel waste shells as a sustainable source for a heterogeneous catalyst. We conducted various tests to comprehend the catalyst's properties, including TGA, XRD, XRF, SEM, and FTIR.

Various factors impact the transesterification process, and their optimization is crucial to achieving high-quality biodiesel meeting regulatory standards. Each of these factors plays an equally vital role in the process.

Thermal stability (TGA) is a common method to determine the calcination temperature of biomass precursors, assessing compound loss at different temperatures [31]. Previous studies have reported the conversion of $CaCO_3$ into CaO at different calcination temperatures. Research by Rahman et al. [32] investigated the influence of calcination temperature (ranging from 800°C to 1100°C) on the transesterification process. It was found that calcining oyster shells at 800 °C significantly enhances catalyst performance. TG/DTA research by Lin et al. [33] indicated that full conversion of $CaCO_3$ to CaO can be achieved by calcination at temperatures between 800 °C and 1000 °C. All calculations in our study were performed between 800 °C and 1100 °C for four hours. As a result, the sample's weight remained constant at 53.31 wt.% at 800 °C, consistent with the expected weight change (44 wt.%) during the $CaCO_3$ to CaO conversion [34].

The fundamental properties of the CaO catalyst in both mussel shells and calcined mussel shells were evaluated through FTIR spectra conducted at temperatures of 800, 900, 1000, and 1100 °C. $CaCO_3$ displays well-defined infrared bands at 705, 858, 1099, and 1457 cm^{-1}, corresponding to C–O's bending and stretching modes [35]. These bands show variations in intensity and characteristics during the calcination process at temperatures ranging from 800 to 1100 °C, attributed to the thermal breakdown of $CaCO_3$ and the formation of $Ca(OH)_2$ and CaO. An additional distinctive band at 3639 cm^{-1} arises from creating basic OH groups associated with Ca atoms [32]. Previous research studies [36] have reported similar findings, reinforcing the results of the DSC/TGA, XRD, and XRF tests.

X-ray fluorescence (XRF) results confirmed that the mussel shell catalysts contained over 98.60% CaO, consistent with DSC/TGA and FTIR data findings. The high calcium content indicates that the waste material was primarily composed of $CaCO_3$, successfully transformed into CaO through calcination [37,38].

In this study, waste mussel shells underwent X-ray diffraction (XRD) examination to determine their chemical composition before and after calcination. Initially, the mussel shells had a $CaCO_3$ concentration ranging from 95% to 99%. After calcination, the shells appeared entirely white, indicating a complete conversion of $CaCO_3$ to CaO [37]. These

results align with the CaO signals observed in previous research [33,39]. It can be inferred that samples calcined at 800, 900, 1000, and 1100 °C for 4 h predominantly contained CaO, with no detectable $CaCO_3$ remaining, consistent with TGA and XRF analyses indicating a high CaO content.

The SEM images of CaO derived from mussel shells reveal surface morphology and area variations among different catalysts. When calcined at 900 °C, the particles exhibited rough surfaces with significant porosity due to the thermal modification of organic components within the mussel shell catalysts [37]. This phenomenon is in line with research trends exemplified in [38], which contribute valuable insights into the nuanced relationship between surface characteristics and overall catalyst efficiency since the diversity of catalysts and reaction systems discussed in these references broadens the context of our findings, reinforcing the significance of surface modifications in enhancing catalytic properties.

Regarding the impact of reaction time on biodiesel conversion, the data indicates that extending the transesterification time from 3 to 4 h increased the conversion percentage (from 40.90% to 46.54%). However, at 5 h, there was a decrease in yield (44.79%), possibly because the liquid product that had been deoxygenated broke down into lighter portions. Similarly, selectivity increased with a reaction time of 6 h (yielding 62.51%). This suggests that an extended reaction duration is required to improve the effectiveness of the interaction between the reactant's molecules and the catalyst's surface, promoting a more extensive reaction [40]. This is in line with the results of Nurdin et al. [41] and Mohammed et al. [42], which indicated that Jatropha oil achieved the highest conversion rate in 6 h. It is worth noting that Kamel et al. [43] also observed the effects of reaction duration on the transesterification process using *J. curcas* oil.

Temperature is another crucial factor that must be controlled to enhance biodiesel production. It has been observed that as the temperature increases, the reaction rate decreases, leading to lower yields, especially beyond 120°C. The highest methyl ester yield, 77.78%, was achieved at 90°C, but this yield decreased to 71.03%, 62.51%, and 50.53% at 100 °C, 110 °C, and 120 °C, respectively. This decrease is primarily due to higher temperatures causing methanol to evaporate, resulting in reduced yields [44]. Additionally, when the reaction temperature surpasses the optimal range, biodiesel yields drop due to triglycerides undergoing saponification [45–47]. The highest methyl ester production reached 86% under operational conditions after 6 h, highlighting the substantial impact of temperature on oil transesterification [48]. The initial increase in conversion from 3 to 6 h signifies the importance of extended transesterification time for biodiesel yield. This can be attributed to the completion of the transesterification reaction, allowing for a more thorough conversion of triglycerides to (FAMEs). However, the slight dip in conversion at 5 h may indicate a transitional phase where certain reactants are in the process of depletion or by-products start to influence the overall conversion rate. The subsequent rise to the highest conversion at 6 h suggests a continued positive effect of prolonged reaction time, allowing for further reaction completion and FAME formation.

One important aspect affecting the generation of biodiesel is the molar ratio of methanol to oil. The stoichiometric molar ratio for methanol to oil in transesterification is 3:1 [30,49]. A higher molar ratio is preferred to expedite the reaction and increase product generation [50,51]. The biodiesel output rose with an increase in the methanol-to-oil molar ratio, peaking at 99.36% at 18:1. However, as the ratio was further elevated to 21:1, the proportion of biodiesel output began to decline. A larger alcohol-to-oil molar ratio enhances glycerol solubility in biodiesel, with free glycerol forming droplets or dissolving in biodiesel. This occurs because alcohols can serve as co-solvents, enhancing the solubility of glycerol in biodiesel [52]. Several other studies also support the optimal molar ratio of 18:1 for achieving the highest biodiesel yield [53]. Concerning the methanol-to-oil molar ratio, the initial increase in yield up to a 1:18 molar ratio aligns with the conventional understanding that higher methanol concentrations facilitate faster reaction kinetics and enhance overall biodiesel production. The peak yield at this ratio could be attributed to

an optimal balance between reactants, ensuring sufficient methanol for transesterification without an excess that may lead to undesirable side reactions or hinder the reaction equilibrium. The subsequent decline in yield at a 1:21 molar ratio may be attributed to an excess of methanol, leading to diminishing returns as an excessively high concentration may disrupt the equilibrium of the transesterification reaction or promote unwanted side reactions, ultimately reducing overall biodiesel yield.

As scientists emphasize, optimizing the calcination temperature in catalyst production is crucial for achieving effective catalytic performance. The calcination process influences the structural and catalytic characteristics of catalysts, leading researchers to explore various calcination temperatures [54]. The XRD analysis confirmed that the high CaO concentration in the samples resulted in high yields across all tests. The maximum conversion rate of 98.52% was observed at 900 °C, aligning with SEM data showing a rougher, more fractured surface that increases the reaction's surface area. Due to less surface cracking, the yields for samples calcined at 1000 °C and 1100 °C were 92.93% and 87.73%, respectively. The temperature of 900 °C for the mussel shell catalyst, as per the existing literature [55], was selected as the optimal choice.

The catalyst's concentration plays a pivotal role in improving the yield of methyl ester synthesis [29]. The highest yield of 92.78% was achieved at a catalyst loading of 6 wt.%, indicating increased active catalytic sites with a higher quantity [48,56]. However, as the catalyst quantity was increased to 9–12%, the conversion efficiency dropped to 65.89% and 64.88%. This decrease can be attributed to excessive surface-active sites on the catalyst for reactant adsorption, leading to no improvement [40]. Several studies have reported that increasing the catalyst amount adversely affects yield [46,57].

4. Materials and Methods

4.1. Seed Material

We obtained local *Jatropha curcas* seeds from Ahmad Qashash farm in Al-Baha, KSA, and procured mussel shells from a local community market in Jeddah, KSA. We used high-purity methanol (99.9%) for the experiments. The *J. curcas* seeds were carefully sorted, with damaged seeds discarded. The selected, undamaged seeds were cleaned, de-shelled, and dried at 100–105 °C for 35 min.

4.2. Oil Extraction

We extracted oil from the seeds using a mechanical press technique [43,58]. Following extraction, the obtained oil was filtered, resulting in an approximate oil yield of 50% (as shown in Figure S1).

4.3. Catalyst Preparation

Mussel shells were collected from a local community market in Jeddah, KSA. The mussel shell waste underwent thorough cleaning with warm water, followed by drying at 100 °C in an oven for 4 h. Subsequently, the dried shell waste was crushed and sieved to achieve a particle size of 250 µm using a laboratory sieve shaker [56].

4.4. Catalyst Calcination

The cleaned and crushed mussel shell particles were divided into four groups and then calcined in a muffle furnace for 4 h at temperatures 800, 900, 1000, and 1100 °C. This calcination process transformed the mussel shells from $CaCO_3$ to CaO, resulting in a white powder that was stored in a silica gel desiccator [56].

4.5. Transesterification

J. curcas oil was converted into biodiesel in 3-neck flasks (250 mL) utilizing CaO obtained from mussel shells as a heterogeneous catalyst. This reaction occurred in a paraffin oil bath with magnetic stirring and a water-cooled condenser. Various conditions were explored, including catalyst loadings (3, 6, 9, 12 wt.%), catalyst calcination temperatures

(800, 900, 1000, 1100 °C), conversion time intervals (3, 4, 5, 6 h), transesterification temperatures (90, 100, 110, 120 °C), and oil/methanol ratios (12:1, 15:1, 18:1, 21:1). After each test, the solid catalyst was separated through centrifugation for 20 min at 4000 rpm, allowing for the isolation of methyl ester, glycerol, and the catalyst. Excess methanol was evaporated under a vacuum, and the filtrate liquid was collected in a glass-separating funnel [47,59–63].

Notably, to minimize methanol evaporation, a water-cooled condenser was used to control the vaporization of methanol and ensure a closed system. Additionally, efficient stirring techniques were employed to reduce the likelihood of methanol escaping further. Moreover, we preferred not to use transesterification temperatures exceeding 120 °C since beyond 120 °C, we anticipated potential complications such as increased energy consumption and undesired side reactions, which could affect the overall efficiency of the process. By limiting the temperature range, we aimed to balance maximizing biodiesel production and avoiding potential drawbacks associated with higher temperatures.

4.6. Catalyst Characterization

The resulting catalyst's physicochemical properties were assessed through several techniques:

- DSC/TGA Analysis: Thermal stability was assessed using differential scanning calorimetry thermogravimetric analysis in a compressed air flow, ramping from 35 to 1100 °C at 10 °C per minute.
- FTIR Analysis: Fourier-transform infrared spectroscopy with attenuated total reflection (ATR-FTIR) was employed to investigate surface structure properties and identify functional groups. This analysis covered a wave number range of 400–4000 cm^{-1} at a resolution of 4 cm^{-1}. The related data were recorded using Spectrum 10TM software (version 142) with a $LiTaO_3$ detector (New York, NY, USA), which was included with the device.
- XRF Analysis: The elemental compositions of both mussel shells and the resulting catalysts were determined using an X-ray fluorescence spectrophotometer (Horiba 7000 model, Montpellier, France).
- XRD Analysis: X-ray diffraction (XRD) was employed to determine the materials' crystalline phases. Using a Shimadzu Model XRD 6000 (Kyoto, Tapan), diffraction patterns were detected with 1.5406 of Cu-K generated at 40 kV and 40 mA tube voltage, radiating in a range of 20°–80°. The crystallographic phases of catalysts were determined using the Powder Diffraction File (PDF) database maintained by the Joint Committee on Powder Diffraction Standards (JCPDS).
- SEM Analysis: Scanning electron microscopy (SEM), facilitated by an SEM TM3030 instrument from Hitachi, Tokyo, Japan, was employed to examine the surface morphology of the CaO catalyst within the mussel shell.

4.7. Statistical Analysis

The statistical analysis was conducted using the least significant difference (LSD) test, and the interpretation of significant differences among the calcined catalyst temperatures was determined using letters from Duncan's multiple range test.

5. Conclusions

This study highlights the promising potential of mussel shell-derived CaO as a sustainable catalyst for converting *J. curcas* oil into biodiesel. Our eco-friendly and cost-effective approach aligns seamlessly with global initiatives for cleaner and economically viable energy sources. We have delved into the surface properties of the mussel shell-derived CaO catalyst using advanced characterization techniques such as X-ray photoelectron spectroscopy (XPS), Fourier-transform infrared spectroscopy (FTIR), and scanning electron microscopy (SEM). The catalyst exhibits outstanding performance in transesterification, yielding an impressive 99.36% FAME, and demonstrates exceptional reusability, surpassing traditional homogeneous catalysts in five cycles. The resulting biodiesel meets stringent

global standards, emphasizing its status as a cleaner and economically viable energy source. This research addresses environmental concerns and offers a compelling and cost-effective solution, marking a significant advancement toward a greener energy landscape. Repurposing waste mussel shells for CaO catalysts aligns with the global pursuit of sustainability in biodiesel production, contributing substantially to a more responsible and efficient energy future, bridging the gap between waste management, catalyst development, and sustainable energy production.

Supplementary Materials: The following supporting information can be downloaded at: https://www.mdpi.com/article/10.3390/catal14010059/s1: Figure S1: Composition of methyl ester in biodiesel at different calcined catalyst temperature by GC–MS.

Author Contributions: Conceptualization, M.E.S.; methodology, H.A.A.; software, S.H.A.; validation, F.A.M.M., S.E.S. and S.A.A.; investigation, H.A.A.; resources, F.A.M.M., A.A.A., S.E.S. and S.A.A.; data curation, M.E.S. and S.H.A.; writing—original draft preparation, M.E.S. and A.A.A.; writing—review and editing, S.E.S. and S.H.A.; visualization, F.A.M.M., A.A.A. and S.A.A.; supervision, M.E.S. All authors have read and agreed to the published version of the manuscript.

Funding: This research received no external funding.

Data Availability Statement: Data are contained within the article and Supplementary Materials.

Acknowledgments: The authors acknowledge their respective universities and institutes for the support provided.

Conflicts of Interest: The authors declare no conflicts of interest.

References

1. Hassan, M.H.; Kalam, M.A. An Overview of Biofuel as a Renewable Energy Source: Development and Challenges. *Procedia Eng.* **2013**, *56*, 39–53. [CrossRef]
2. Keera, S.T.; El Sabagh, S.M.; Taman, A.R. Castor oil biodiesel production and optimization. *Egypt. J. Pet.* **2018**, *27*, 979–984. [CrossRef]
3. Mosly, I.; Makki, A.A. Current status and willingness to adopt renewable energy technologies in Saudi Arabia. *Sustainability* **2018**, *10*, 4269. [CrossRef]
4. Onoji, S.E.; Iyuke, S.E.; Igbafe, A.I.; Nkazi, D.B. Rubber seed oil: A potential renewable source of biodiesel for sustainable development in sub-Saharan Africa. *Energy Convers. Manag.* **2016**, *110*, 125–134. [CrossRef]
5. Elumalai, P.; Parthasarathy, M.; Lalvani, J.S.C.I.J.; Mehboob, H.; Samuel, O.D.; Enweremadu, C.C.; Saleel, C.A.; Afzal, A. Effect of injection timing in reducing the harmful pollutants emitted from CI engine using N-butanol antioxidant blended eco-friendly Mahua biodiesel. *Energy Rep.* **2021**, *7*, 6205–6221. [CrossRef]
6. Živković, S.; Veljković, M. Environmental impacts the of production and use of biodiesel. *Environ. Sci. Pollut. Res.* **2018**, *25*, 191–199. [CrossRef]
7. Zhang, X.; Huang, Q.; Deng, F.; Huang, H.; Wan, Q.; Liu, M.; Wei, Y. Mussel-inspired fabrication of functional materials and their environmental applications: Progress and prospects. *Appl. Mater. Today* **2017**, *7*, 222–238. [CrossRef]
8. Basumatary, B.; Nath, B.; Basumatary, S. Homogeneous Catalysts Used in Biodiesel Production. In *Biodiesel Production: Feedstocks, Catalysts, and Technologies*; Wiley: Hoboken, NJ, USA, 2022; pp. 83–101.
9. Avhad, M.; Marchetti, J. Innovation in solid heterogeneous catalysis for the generation of economically viable and ecofriendly biodiesel: A review. *Catal. Rev.* **2016**, *58*, 157–208. [CrossRef]
10. Ewunie, G.A.; Morken, J.; Lekang, O.I.; Yigezu, Z.D. Factors affecting the potential of *Jatropha curcas* for sustainable biodiesel production: A critical review. *Renew. Sustain. Energy Rev.* **2021**, *137*, 110500. [CrossRef]
11. Abd El-Hack, M.E.; Alagawany, M.; El-Sayed, S.A.A.; Fowler, J. Influence of dietary inclusion of untreated or heat-treated Jatropha meal on productive and reproductive performances and biochemical blood parameters of laying Japanese quail. *Poult. Sci.* **2017**, *96*, 2761–2767. [CrossRef]
12. Saeed, M.; Arain, M.A.; Arif, M.; Lagawany, M.; Abd El-Hack, M.E.; Kakar, M.U.; Chao, S. Jatropha (*Jatropha curcas*) meal is an alternative protein source in poultry nutrition. *World's Poult. Sci. J.* **2017**, *73*, 783–790. [CrossRef]
13. Bin Rashid, A. Utilization of nanotechnology and nanomaterials in biodiesel production and property enhancement. *J. Nanomater.* **2023**, *2023*, 102894. [CrossRef]
14. Ruhul, A.; Kalam, M.; Masjuki, H.; Fattah, I.R.; Reham, S.; Rashed, M. State of the art of biodiesel production processes: A review of the heterogeneous catalyst. *RSC Adv.* **2015**, *5*, 101023–101044. [CrossRef]
15. Rashid, U.; Akinfalabi, S.I.; Ibrahim, N.A.; Ngamcharussrivichai, C. Bio-Based Catalysts in Biodiesel Production. In *Nano-and Biocatalysts for Biodiesel Production*; John Wiley & Sons, Inc.: Hoboken, NJ, USA, 2021; pp. 201–248.

16. De, S.; Zhang, J.; Luque, R.; Yan, N. Ni-based bimetallic heterogeneous catalysts for energy and environmental applications. *Energy Environ. Sci.* **2016**, *9*, 3314–3347. [CrossRef]
17. Faruque, M.O.; Razzak, S.A.; Hossain, M.M. Application of heterogeneous catalysts for biodiesel production from microalgal oil—A review. *Catalysts* **2020**, *10*, 1025. [CrossRef]
18. Eldiehy, K.S.; Daimary, N.; Borah, D.; Sarmah, D.; Bora, U.; Mandal, M.; Deka, D. Towards biodiesel sustainability: Waste sweet potato leaves as a green heterogeneous catalyst for biodiesel production using microalgal oil and waste cooking oil. *Ind. Crops Prod.* **2022**, *187*, 115467. [CrossRef]
19. Teng, W.K.; Ngoh, G.C.; Yusoff, R.; Aroua, M.K. A review on the performance of glycerol carbonate production via catalytic transesterification: Effects of influencing parameters. *Energy Convers. Manag.* **2014**, *88*, 484–497. [CrossRef]
20. Ling, J.S.J.; Tan, Y.H.; Mubarak, N.M.; Kansedo, J.; Saptoro, A.; Nolasco-Hipolito, C. A review of heterogeneous calcium oxide based catalyst from waste for biodiesel synthesis. *SN Appl. Sci.* **2019**, *1*, 1–8. [CrossRef]
21. Jayakumar, M.; Karmegam, N.; Gundupalli, M.P.; Gebeyehu, K.B.; Asfaw, B.T.; Chang, S.W.; Ravindran, B.; Awasthi, M.K. Heterogeneous base catalysts: Synthesis and application for biodiesel production–A review. *Bioresour. Technol.* **2021**, *331*, 125054. [CrossRef]
22. Basumatary, S.F.; Brahma, S.; Hoque, M.; Das, B.K.; Selvaraj, M.; Brahma, S.; Basumatary, S. Advances in CaO-Based Catalysts for Sustainable Biodiesel Synthesis. *Green Energy Resour.* **2023**, *2023*, 100032. [CrossRef]
23. Khan, S.G.; Hassan, M.; Anwar, M.; Khan, U.M.; Zhao, C. Mussel shell based CaO nano-catalyst doped with praseodymium to enhance biodiesel production from castor oil. *Fuel* **2022**, *330*, 125480. [CrossRef]
24. Shan, R.; Lu, L.; Shi, Y.; Yuan, H.; Shi, J. Catalysts from renewable resources for biodiesel production. *Energy Convers. Manag.* **2018**, *178*, 277–289. [CrossRef]
25. Athar, M.; Zaidi, S. A review of the feedstocks, catalysts, and intensification techniques for sustainable biodiesel production. *J. Environ. Chem. Eng.* **2020**, *8*, 104523. [CrossRef]
26. Shobana, R.; Vijayalakshmi, S.; Deepanraj, B.; Ranjitha, J. Biodiesel production from Capparis spinosa L seed oil using calcium oxide as a heterogeneous catalyst derived from oyster shell. *Mater. Today Proc.* **2023**, *80*, 3216–3220. [CrossRef]
27. Boey, P.-L.; Maniam, G.P.; Hamid, S.A. Biodiesel production via transesterification of palm olein using waste mud crab (*Scylla serrata*) shell as a heterogeneous catalyst. *Bioresour. Technol.* **2009**, *100*, 6362–6368. [CrossRef]
28. Naeem, A.; Wali Khan, I.; Farooq, M.; Mahmood, T.; Ud Din, I.; Ali Ghazi, Z.; Saeed, T. Kinetic and optimization study of sustainable biodiesel production from waste cooking oil using novel heterogeneous solid base catalyst. *Bioresour. Technol.* **2021**, *328*, 124831. [CrossRef]
29. Kasim, F.H.; Harvey, A.P. Influence of various parameters on reactive extraction of *Jatropha curcas* L. for biodiesel production. *Chem. Eng. J.* **2011**, *171*, 1373–1378. [CrossRef]
30. Meher, L.; Vidyasagar, D.; Naik, S. Technical aspects of biodiesel production by transesterification—A review. *Renew. Sustain. Energy Rev.* **2006**, *10*, 248–268. [CrossRef]
31. Chua, S.Y.; Periasamy, L.A.P.; Goh, C.M.H.; Tan, Y.H.; Mubarak, N.M.; Kansedo, J.; Khalid, M.; Walvekar, R.; Abdullah, E.C. Biodiesel synthesis using natural solid catalyst derived from biomass waste—A review. *J. Ind. Eng. Chem.* **2020**, *81*, 41–60. [CrossRef]
32. Rahman, S.M.A.; Fattah, I.M.R.; Maitra, S.; Mahlia, T.M.I. A ranking scheme for biodiesel underpinned by critical physicochemical properties. *Energy Convers. Manag.* **2021**, *229*, 113742. [CrossRef]
33. Lin, Y.-C.; Amesho, K.T.T.; Chen, C.-E.; Cheng, P.-C.; Chou, F.-C. A cleaner process for green biodiesel synthesis from waste cooking oil using recycled waste oyster shells as a sustainable base heterogeneous catalyst under the microwave heating system. *Sustain. Chem. Pharm.* **2020**, *17*, 100310. [CrossRef]
34. Muciño, G.G.; Romero, R.; Ramírez, A.; Martínez, S.L.; Baeza-Jiménez, R.; Natividad, R. Biodiesel production from used cooking oil and sea sand as heterogeneous catalyst. *Fuel* **2014**, *138*, 143–148. [CrossRef]
35. Suryaputra, W.; Winata, I.; Indraswati, N.; Ismadji, S. Waste capiz (*Amusium cristatum*) shell as a new heterogeneous catalyst for biodiesel production. *Renew. Energy* **2013**, *50*, 795–799. [CrossRef]
36. Singh, D.; Sharma, D.; Soni, S.L.; Inda, C.S.; Sharma, S.; Sharma, P.K.; Jhalani, A. A comprehensive review of biodiesel production from waste cooking oil and its use as fuel in compression ignition engines: 3rd generation cleaner feedstock. *J. Clean. Prod.* **2021**, *307*, 127299. [CrossRef]
37. Kaewdaeng, S.; Sintuya, P.; Nirunsin, R. Biodiesel production using calcium oxide from river snail shell ash as catalyst. *Energy Procedia* **2017**, *138*, 937–942. [CrossRef]
38. Chen, J.; Yan, W.; Townsend, E.J.; Feng, J.; Pan, L.; Del Angel Hernandez, V.; Faul, C.F. Tunable surface area, porosity, and function in conjugated microporous polymers. *Angew. Chem. Int. Ed.* **2019**, *58*, 11715–11719. [CrossRef]
39. Tang, D.; Yin, M.; Du, X.; Duan, Y.; Chen, J.; Qiu, T. Wettability tunable conjugated microporous poly (aniline) s for long-term, rapid and ppb level sequestration of Hg (II). *Chem. Eng. J.* **2023**, *474*, 145527. [CrossRef]
40. Lou, X.; Tang, D.; Ye, C.; Chen, J.; Qiu, T. Conjugated micro-mesoporous poly (aniline) s for ultrafast Hg (II) capture. *Sep. Purif. Technol.* **2023**, *325*, 124616. [CrossRef]
41. Tang, D.; Lyu, X.; Huang, Z.; Xu, R.; Chen, J.; Qiu, T. Nitrogen-doped microporous carbons as highly efficient adsorbents for CO_2 and Hg (II) capture. *Powder Technol.* **2023**, *427*, 118769. [CrossRef]

42. Buasri, A.; Chaiyut, N.; Loryuenyong, V.; Worawanitchaphong, P.; Trongyong, S. Calcium oxide derived from waste shells of mussel, cockle, and scallop as the heterogeneous catalyst for biodiesel production. *Sci. World J.* **2013**, *2013*, 460923. [CrossRef]
43. Gollakota, A.R.K.; Volli, V.; Shu, C.-M. Transesterification of waste cooking oil using pyrolysis residue supported eggshell catalyst. *Sci. Total Environ.* **2019**, *661*, 316–325. [CrossRef] [PubMed]
44. Asikin-Mijan, N.; Lee, H.V.; Abdulkareem-Alsultan, G.; Afandi, A.; Taufiq-Yap, Y.H. Production of green diesel via cleaner catalytic deoxygenation of *Jatropha curcas* oil. *J. Clean. Prod.* **2017**, *167*, 1048–1059. [CrossRef]
45. Nurdin, S.; Rosnan, N.A.; Ghazali, N.S.; Gimbun, J.; Nour, A.H.; Haron, S.F. Economical Biodiesel Fuel Synthesis from Castor Oil Using Mussel Shell-Base Catalyst (MS-BC). *Energy Procedia* **2015**, *79*, 576–583. [CrossRef]
46. Mohammed, N.I.; Kabbashi, N.A.; Alam, M.Z.; Mirghani, M.E.S. Esterification of *Jatropha curcas* hydrolysate using powdered niobic acid catalyst. *J. Taiwan Inst. Chem. Eng.* **2016**, *63*, 243–249. [CrossRef]
47. Kamel, D.A.; Farag, H.A.; Amin, N.K.; Zatout, A.A.; Ali, R.M. Smart utilization of jatropha (*Jatropha curcas* L.) seeds for biodiesel production: Optimization and mechanism. *Ind. Crops Prod.* **2018**, *111*, 407–413. [CrossRef]
48. Kidan, T.G.; Habtu, N.G. Activated carbon supported CaO for conversion of palm oil to biodiesel: Kinetic experiment. *Ethiop. J. Sci. Technol.* **2017**, *10*, 193. [CrossRef]
49. Chozhavendhan, S.; Vijay Pradhap Singh, M.; Fransila, B.; Praveen Kumar, R.; Karthiga Devi, G. A review on influencing parameters of biodiesel production and purification processes. *Curr. Res. Green Sustain. Chem.* **2020**, *1–2*, 1–6. [CrossRef]
50. Komintarachat, C.; Chuepeng, S. Catalytic enhancement of calcium oxide from green mussel shell by potassium chloride impregnation for waste cooking oil-based biodiesel production. *Bioresour. Technol. Rep.* **2020**, *12*, 100589. [CrossRef]
51. Lee, S.L.; Wong, Y.C.; Tan, Y.P.; Yew, S.Y. Transesterification of palm oil to biodiesel by using waste obtuse horn shell-derived CaO catalyst. *Energy Convers. Manag.* **2015**, *93*, 282–288. [CrossRef]
52. Roschat, W.; Siritanon, T.; Kaewpuang, T.; Yoosuk, B.; Promarak, V. Economical and green biodiesel production process using river snail shells-derived heterogeneous catalyst and co-solvent method. *Bioresour. Technol.* **2016**, *209*, 343–350. [CrossRef]
53. Sahoo, P.K.; Das, L.M. Process optimization for biodiesel production from Jatropha, Karanja and Polanga oils. *Fuel* **2009**, *88*, 1588–1594. [CrossRef]
54. Verma, P.; Sharma, M.P. Review of process parameters for biodiesel production from different feedstocks. *Renew. Sustain. Energy Rev.* **2016**, *62*, 1063–1071. [CrossRef]
55. Sitepu, E.K.; Heimann, K.; Raston, C.L.; Zhang, W. Critical evaluation of process parameters for direct biodiesel production from diverse feedstock. *Renew. Sustain. Energy Rev.* **2020**, *123*, 109762. [CrossRef]
56. Tabatabaei, M.; Aghbashlo, M.; Dehhaghi, M.; Panahi, H.K.S.; Mollahosseini, A.; Hosseini, M.; Soufiyan, M.M. Reactor technologies for biodiesel production and processing: A review. *Prog. Energy Combust. Sci.* **2019**, *74*, 239–303. [CrossRef]
57. Buasri, A.; Worawanitchaphong, P.; Trongyong, S.; Loryuenyong, V. Utilization of Scallop Waste Shell for Biodiesel Production from Palm Oil—Optimization Using Taguchi Method. *APCBEE Procedia* **2014**, *8*, 216–221. [CrossRef]
58. Islam, A.; Taufiq-Yap, Y.H.; Chu, C.-M.; Chan, E.-S.; Ravindra, P. Studies on design of heterogeneous catalysts for biodiesel production. *Process Saf. Environ. Prot.* **2013**, *91*, 131–144. [CrossRef]
59. Hu, S.; Wang, Y.; Han, H. Utilization of waste freshwater mussel shell as an economic catalyst for biodiesel production. *Biomass Bioenergy* **2011**, *35*, 3627–3635. [CrossRef]
60. Hadiyanto, H.; Afianti, A.H.; Navi'a, U.I.; Adetya, N.P.; Widayat, W.; Sutanto, H. The development of heterogeneous catalyst C/CaO/NaOH from waste of green mussel shell (*Perna viridis*) for biodiesel synthesis. *J. Environ. Chem. Eng.* **2017**, *5*, 4559–4563. [CrossRef]
61. Irwan, M.; Saidi, H.; Rachman, M.A.; Ramli, R.; Marlinda, M. Rapid Alcoholysis of *Jatropha curcas* oil for biodiesel production using ultrasound irradiation. *Bull. Chem. React. Eng. Catal.* **2017**, *12*, 306–311. [CrossRef]
62. Abd El-Hack, M.E.; Alagawany, M.; Patra, A.; Abdel-Latef, M.; Ashour, E.A.; Arif, M.; Dhama, K. Use of brewers dried grains as an unconventional feed ingredient in the diets of broiler chickens: A review. *Adv. Anim. Vet. Sci.* **2019**, *7*, 218–224. [CrossRef]
63. Mohamad, M.; Ngadi, N.; Lani, N.S. Production of Biodiesel from Cooking Oil Using CaO Catalyst. *Adv. Mater. Res.* **2015**, *1113*, 518–522. [CrossRef]

ARTICLES FOR FACULTY MEMBERS

ELUCIDATING THE CALCIUM OXIDE DERIVED FROM THE WASTE SHELLS OF MUD CLAM (GELOINA EXPANSA) AS A CATALYST FOR BIODIESEL PRODUCTION

Preparation and characterization of shell-based CaO catalysts for ultrasonication-assisted production of biodiesel to reduce toxicants in diesel generator emissions / Chong, N. S., Nwobodo, I., Strait, M., Cook, D., Abdulramoni, S., & Ooi, B. G.

Energies
Volume 16 Issue 14 (2023) 5408 Pages 1-20
https://doi.org/10.3390/en16145408
(Database: MDPI)

energies

IMPACT FACTOR 3.2

CITESCORE 5.5

Article

Preparation and Characterization of Shell-Based CaO Catalysts for Ultrasonication-Assisted Production of Biodiesel to Reduce Toxicants in Diesel Generator Emissions

Ngee S. Chong, Ifeanyi Nwobodo, Madison Strait, Dakota Cook, Saidi Abdulramoni and Beng G. Ooi

Special Issue

Advancements in Catalytic Conversion of Biomass into Biofuels and Chemicals II

Edited by

Prof. Dr. Tae Hyun Kim and Dr. A.V.S.L. Sai Bharadwaj

MDPI

https://doi.org/10.3390/en16145408

energies

MDPI

Article

Preparation and Characterization of Shell-Based CaO Catalysts for Ultrasonication-Assisted Production of Biodiesel to Reduce Toxicants in Diesel Generator Emissions

Ngee S. Chong [1,*], Ifeanyi Nwobodo [2], Madison Strait [3], Dakota Cook [4], Saidi Abdulramoni [5] and Beng G. Ooi [1,*]

[1] Department of Chemistry, Middle Tennessee State University, Murfreesboro, TN 37132, USA
[2] Jacam Catalyst, Gardendale, TX 79758, USA; ifeanyi.nwobodo@jacamcatalyst.com
[3] Department of Chemistry, Iowa State University, Ames, IA 50011, USA; mastrait@iastate.edu
[4] Department of Food, Nutrition and Culinary Sciences, Clemson University, Clemson, SC 29634, USA; dakotadcook98@gmail.com
[5] Catalent Pharma Solutions, Bloomington, IN 08873, USA; saidi.abdulramoni@catalent.com
* Correspondence: ngee.chong@mtsu.edu (N.S.C.); beng.ooi@mtsu.edu (B.G.O.)

Abstract: The environmentally sustainable production of biodiesel is important for providing both a renewable alternative transportation fuel as well as a fuel for power generation using diesel engines. This research evaluates the use of inexpensive catalysts derived from waste materials for converting triglycerides in seed oils into biodiesel composed of fatty acid methyl esters. The performance of CaO catalysts derived from the shells of oysters, mussels, lobsters, and chicken eggs was investigated. The shell-derived powders were calcined with and without the addition of zinc nitrate at 700–1000 °C for 4 h to yield CaO whereas the CaO-ZnO mixed catalyst were prepared by wet impregnation followed by calcination at 700 °C. The catalysts were characterized by XRF, XRD, TGA, SEM, FTIR and GC-MS. The CaO-ZnO catalysts showed slightly better conversion efficiency compared to CaO catalysts for the transesterification of canola oil. The mixed CaO-ZnO catalysts derived mainly from oyster shells showed the highest catalytic activity with >90% biodiesel yield at a 9:1 methanol-to-oil mole ratio within 10 min of ultrasonication. The reduction of toxicant emission from the generator is 43% and 60% for SO_2, 11% and 26% for CO, were observed for the biodiesel blending levels of B20 and B40, respectively.

Keywords: biodiesel production; ultrasonication-assisted synthesis; transesterification catalysts; shell-derived CaO and CaO/ZnO; calcination of oyster, mussel, lobster, and egg shells; B20 and B40 biodiesel emission profiles; CO and SO_2 emission; generator emissions of toxicants

Citation: Chong, N.S.; Nwobodo, I.; Strait, M.; Cook, D.; Abdulramoni, S.; Ooi, B.G. Preparation and Characterization of Shell-Based CaO Catalysts for Ultrasonication-Assisted Production of Biodiesel to Reduce Toxicants in Diesel Generator Emissions. *Energies* **2023**, *16*, 5408. https://doi.org/10.3390/en16145408

Academic Editors: Tae Hyun Kim and A.V.S.L. Sai Bharadwaj

Received: 16 June 2023
Revised: 30 June 2023
Accepted: 5 July 2023
Published: 16 July 2023

1. Introduction

Biodiesel has become one of the major alternative energy sources to replace fossil fuel, due to its advantages including reduced emissions, low toxicity, and environmental sustainability. Besides, biodiesel is produced from renewable sources such as oilseeds from edible and non-edible crops, animal fat, and microorganisms which makes it a viable fuel from a sustainability viewpoint [1]. The increased interest in biodiesel fuel as an alternative source of energy is due to its beneficial aspects in the reduction of greenhouse gases, improvement in energy security, and as a means of generating revenue [2]. The current global climate change and depletion of natural resources are partly related to the excessive dependence on fossil fuels to meet energy needs. Scientists have anticipated that fossil fuels might run out in 2050 due to the enormous demand and utilization of fossil resources [3]. Petroleum-based fuels are derived from the finite oil reserves in certain regions of the world. Consequently, those countries with limited oil production and refining capacity are confronted with a foreign exchange crisis, basically due to the importation of petroleum products. Therefore, it is imperative to look for alternative fuels that can be produced from renewable materials [4].

Biofuels such as bioethanol and biodiesel have been proposed for use in internal combustion engines. Biodiesel could reduce the emission of hydrocarbons and CO by up to 70% and 50%, respectively, compared to petroleum diesel. Furthermore, biofuels can be blended with petroleum-based fuels with little or no engine modification [5]. Biodiesel has higher density and kinematic viscosity values compared to petroleum diesel, which infers that biodiesel has greater energy density output and better lubricity than petroleum diesel. The high cetane number is an indication of the diesel ignition quality and completeness of fuel combustion whereas its high flash point ensures safer storage and handling [6]. Biodiesel is composed of fatty acid alkyl esters obtained by the transesterification of vegetable oil or animal fat [7]. Biodiesel is a non-petroleum-based fuel, or an alternative fuel produced by the transesterification reaction between a vegetable oil or animal fat and methanol or ethanol in the presence of an appropriate catalyst (homogenous, heterogeneous, or enzyme-based catalyst) [8].

Biodiesel is a promising alternative to fossil fuel and is comprised of mono-alkyl esters of long-chain fatty acids derived from renewable feedstocks designated B100. A mono-alkyl ester is the reaction product of straight-chain alcohol like methanol or ethanol, with triglyceride (fat or oil), which also produces glycerin or glycerol. Biodiesel can be used as B100 (neat) or in a blend with petroleum diesel. There are different blends of biodiesel with ultralow sulfur petroleum diesel (ULSPD) ranging from 1% to 50% [9]. A blend of 20% biodiesel with 80% petroleum diesel, by volume, is termed B20 and a blend of 40% biodiesel with 60% petroleum diesel is referred to as B40 [9].

Transesterification

Transesterification refers to the reaction of triglyceride (oil or fat) with an alcohol in the presence of a catalyst to form esters and glycerol [10]. Biodiesel produced via transesterification have comparable properties with diesel fuel. Transesterification is also called alcoholysis, because of the reaction of free fatty acid with alcohol. After the transesterification process, the end products (biodiesel or mixture of alkyl esters and glycerol), are separated into two immiscible layers with biodiesel on the top and glycerol settling at the bottom due to their different densities. Methanol and ethanol are common alcohols used in transesterification. If methanol is used to react with triglyceride, the transesterification process is commonly known as methanolysis. During the methanolysis process, heat is applied to the reaction mixture of oil (80–90%) and methanol (10–20%) and 0.5–1.5% (w/w) catalyst. The most commonly used catalyst is NaOH or KOH but other types of homogeneous catalysts based on strong acids and enzymes have also been reported. Heterogeneous catalysts based on Group IIA oxides such as CaO prepared from eggshells have been studied based on the ease of biodiesel product separation and their reusability [11,12]. Statistical analysis has been used to determine the optimum reaction conditions for biodiesel production yield of 93.16% at a temperature of 60.5 °C, methanol to oil ratio of 6.7:1, and catalyst loading of 0.79% (w/w) [13]. Methanol solubility in oil is limited and hence proper mixing is vital. Biodiesel produced from this process is fatty acid methyl ester (FAME). Methanol is preferred for transesterification because it has higher reactivity and is less expensive than other alcohols. When ethanol is reacted with triglyceride, the transesterification process is referred to as ethanolysis. Biodiesel produced using the ethanolysis process contains fatty acid ethyl ester (FAEE). Biodiesel can be used to substitute petroleum-based diesel in engines with minimal changes to the diesel engine because their characteristics are nearly similar [10]. Although most biodiesel production facilities use mechanical stirring, the ultrasonication process has been shown to dissipate energy more efficiently and can improve the transesterification reaction rate constant by 7–9 times relative to mechanical stirring [14].

As shown in Figure 1, the transesterification reaction or alcoholysis of triglycerides from canola, soya bean, and palm oils in the presence of alcohol and catalyst will lead to the formation of alkyl esters or biodiesel and the glycerol by-product. The first step involves the conversion of triglycerides to diglycerides; in the second step, diglycerides

are converted to monoglycerides, and in the final step, monoglycerides are converted to glycerol. Each of the three sequential steps generates biodiesel esters. This process requires 3 moles of alcohol for 1 mole of triglyceride to produce 1 mole of glycerol and 3 moles of fatty acid alkyl esters or biodiesel [15]. Most commercial production processes use 6 moles of methanol for each mole of triglyceride. This excess methanol ensures that the reaction is favorably driven toward the direction of biodiesel production [16].

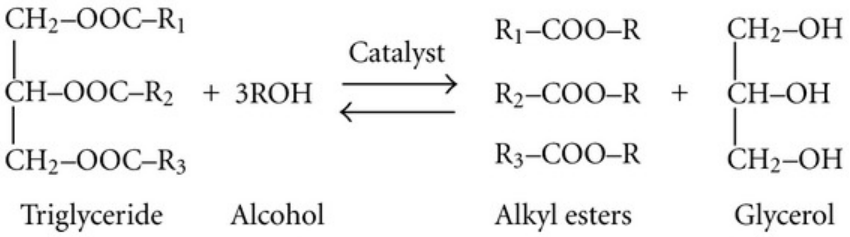

Figure 1. Transesterification reaction in biodiesel production.

The two main objectives of this study are to evaluate the suitability of four commonly available shell materials for preparing the CaO catalysts used in biodiesel production and assess the degree of reduction of toxicant emissions for biodiesel-blended fuels for powering diesel generators. Most current research publications are aimed at the study of single shell materials including those of chicken egg [11,12,17], abalone [18], snail [19,20], crab [21], scallop [22], lobster [23], oyster [24,25], and mussel [26]. Due to the varying experimental conditions that influence the biodiesel yields, it is difficult to compare the suitability of shell-derived CaO catalysts unless they are evaluated under the same conditions of catalyst loading, methanol-to-oil ratio, reaction time, temperature, stirring rate, and reaction mode (e.g., conventional heating, microwave, or ultrasonication power). This study evaluated the performance of CaO catalysts prepared from the shells of chicken eggs, mussels, oysters, and lobster under the reaction conditions of 1.00 wt.% loading of shell-derived CaO or 5% Zn/CaO catalysts, and 9:1 mole ratio of methanol to canola oil. Furthermore, the environmental benefits of reducing toxicant emissions from power generators using B20 and B40 fuels were compared to the ULSPD diesel fuel. Since power generators are sometimes used indoors and may not be equipped with pollutant reduction devices such as catalytic converters used in cars and trucks, it is necessary to compare the emission profiles of the fuels for the power generators.

2. Materials and Methods

2.1. Materials and Reagents

The seafood waste of shells from mussels, lobsters, oysters and chicken eggs were obtained from local restaurants. The spectroscopic grade methanol from Burdick and Jackson (Muskegon, MI, USA) was used for the transesterification reaction with the canola oil purchased from the local Kroger grocery store. The zinc nitrate hexahydrate from Thermo Fischer Scientific (Waltham, MA, USA). was used for the preparation of the CaO catalyst with zinc. Deuterated chloroform for NMR determination of biodiesel yield was purchased from Cambridge Isotope Laboratories Incorporated (Andover, MA, USA). The ultra-low sulfur petroleum diesel (ULSPD) used for generator emission testing of B20, B40, and ULSPD was purchased from a Shell gas station (Murfreesboro, TN, USA).

2.2. Preliminary Preparation of Shells

The waste shells (mussel, oyster, lobster, and eggshell) were first washed with water to get rid of dirt, other tough impurities, and organic matter on the surface of the shells were scrapped off and rewashed with deionized water before drying the shells in the oven at 115 °C for 15 h.

2.2.1. Preparation of CaO Catalyst via Calcination

The dried shells were pulverized using Corona® Mill grinder purchased from Amazon (Seattle, WA, USA). The shell powder was calcined in a KSL-1100MX muffle furnace from MTI Corporation (Richmond, CA, USA) at 800 °C and 1000 °C, respectively, at a heating rate of 10 °C per minute for 4 h. The CaO catalyst obtained was transferred into an airtight container kept in the desiccator to prevent the adsorption of atmospheric moisture.

2.2.2. Preparation of CaO-ZnO Mixed Catalyst

The CaO-ZnO mixed catalyst was prepared by a modified wet impregnation method reported by Kumar and Ali [27]. In this preparation, 10.0 g of CaO obtained from the calcined mussel, oyster, lobster, and eggshell were separately suspended in 18 mΩ high purity deionized water before adding dissolved zinc nitrate to the suspension. The zinc nitrate concentration was varied to obtain Zn^{2+} concentration in CaO ranging from 5% (w/w) to 25% (w/w). The slurry was stirred for 4 h with a magnetic stirrer at room temperature before being dried in the oven at 120 °C for 24 h. The dried mixture was calcined at 700 °C for 4 h in the muffle furnace.

2.3. Catalyst Characterization

A Thermo Scientific™ Niton XL3t Ultra X-ray fluorescence analyzer (Billerica, MA, USA) was used to determine the elemental composition of the uncalcined and calcined shell samples using the Test All Geo Method with a spectral acquisition time of 4 min.

The Rigaku Miniflex 600 X-ray powder diffractometer (Tokyo, Japan) was used to analyze the crystalline phases and diffraction pattern of the shell-derived catalysts and CaO-ZnO mixed catalyst. The Rigaku Miniflex was operated at 40 kV tube voltage and 15 mA tube current using Cu(Kα) radiation at the speed of 1°/min over a 2θ range from 10° to 70° with a step size of 0.010°.

The Varian 7000 Fourier transform infrared spectrometer (Varian Inc., Walnut Creek, CA, USA) was used to confirm the presence of characteristic absorption bands and to distinguish among the calcium forms of carbonate, oxide, and hydroxide present in the uncalcined shell, calcined shell (CaO) and CaO-ZnO mixed catalyst. FTIR spectral measurements were obtained in the wavenumber range of 400–4000 cm^{-1} at a resolution of 4 cm^{-1} with 32 co-added scans and Happ-Genzel apodization using a HgCdTe detector cooled with liquid nitrogen. The concentrations of carbon monoxide, formaldehyde, methane, and ethylene were determined using the Varian FTIR spectrometer with a 10-m pathlength gas cell.

The Hitachi (Schaumburg, IL, USA) S-3400N scanning electron microscope (SEM) was used to determine the morphological characteristics and surface structure of the shell derived catalysts. The elemental composition of samples was analyzed by Oxford Instruments (High Wycombe, UK) energy-dispersive X-ray detector (EDX). The SEM-EDX analysis was carried out with and without the use of the gold-palladium sputter coater to get optimal results with SEM imaging and elemental analysis.

The Q500 thermogravimetric analyzer (TA Instruments, New Castle, DE, USA) was used to characterize the profile of mass loss in uncalcined shell powders as a function of temperature from 20 °C to 1000 °C. The decomposition patterns of shell samples from chicken eggs, oysters, mussels, and lobsters were determined.

2.4. Ultrasonication-Assisted Biodiesel Synthesis and Yield Measurement

The catalytic efficiency for the transesterification of canola oil and methanol was carried out using the Hielscher model UP200St ultrasonication equipment (Teltow, Germany). The ultrasonic processor is equipped with an ultrasonic transducer, sonotrode, generator, temperature sensor, power supply and other attachments.

The loading of 1% (w/v) catalyst (e.g., mussel-CaO, oyster-CaO, egg-CaO, lobster-CaO, mussel-CaO-ZnO, oyster-CaO-ZnO, egg-CaO-ZnO, lobster-CaO-ZnO) was prepared by mixing 0.25 g of each catalyst with 9.75 mL of methanol and stirred for about 15 min before

adding 25 mL canola oil. The mixture was preheated to 60 °C and the ultrasonication was carried out for 10 min with 9:1 methanol to canola oil mole ratio. The reaction was performed in a 100-mL container with ultrasonication operating conditions of 100% amplitude, 100% pulse, 180 W power, and an operating frequency of 26 kHz. The biodiesel upper layer was separated from the glycerol bottom layer by centrifugation. The percentage conversion of triglyceride into FAME was determined using the JEOL 500 MHz ^{1}H-NMR (Peabody, MA, USA). The biodiesel yields were calculated by comparing the integrated signals of the methoxy hydrogen and the α-methylene hydrogen as described earlier [28].

2.5. GC-MS Analysis of Diesel Generator Emissions

A Yanmar 4000-watt diesel power generator was used to evaluate the emissions of B20, B40, and ULSPD fuels by directing the generator exhausts through a 5-foot copper tubing of 0.25-inch outer diameter for cooling the diesel engine emissions before collecting the gas samples in 3-L Tedlar bags that were subsequently attached to the Nutech autosampler for GC-MS analysis.

An Agilent 6890 gas chromatograph interfaced with an Agilent 5973 quadrupole mass spectrometer (GC-MS) (Agilent Technologies, Santa Clara, CA, USA) were used for the analysis of emission samples from the generator fueled with biodiesel-blended fuels. A 16-position Nutech autosampler for automated sequential analysis was used to introduce 20.0 mL of gas samples into the Agilent GC-MS via the Nutech 8900DS preconcentrator (GD Environmental Supplies, Inc., Richardson, TX, USA). The preconcentrator has three cryogenic traps including the glass bead trap, Tenax TA trap and the cryofocuser for the selective enrichment of the volatile organic compounds (VOCs) in the samples by controlling the trap temperatures and desorption time settings to achieve low detection limits. The detailed preconcentrator and GC-MS conditions were described in a previous publication [29]. Agilent ChemStation and Markes TargetView V2.0 software were used to process the GC-MS data via the use of the mass spectral database from the National Institute of Standards and Technology.

3. Results

3.1. Catalyst Characterization

3.1.1. Thermogravimetric Analysis (TGA)

TGA was used to measure the change in weight of various shell materials as a function of temperature and hence reveal the decomposition patterns of the shells at the temperature range of 20 °C to 1000 °C. As shown in Figure 2a,b for the mussel and lobster shell samples, the shells are composed mainly of calcium carbonate which decomposes into calcium oxide and carbon dioxide at approximately 800 °C and above. The variation seen in the thermal curve of the oyster, mussel, lobster, and eggshell is due to the different structural compositions of the individual shells. These shells may also contain other forms of carbonates together with $CaCO_3$. Figure 1a shows the decomposition pattern of the mussel shell with the weight loss occurring in two stages. The weight loss between 100 °C–440 °C is due to the organic impurities breaking down in the mussel shell powder. About 3.42% sample weight loss is shown at this temperature range. A significant weight loss was measured at 560 °C–810 °C which is displayed in the derivative weight loss curve of the shell in blue color (Figure 2a). This weight loss measured is due to the CO_2 released from the decomposition of $CaCO_3$.

$$CaCO_3\ (s) \longrightarrow CaO\ (s) + CO_2\ (g)$$

The observed weight loss of 41.75% from the mussel shell sample is close to the actual weight percent of CO_2 in $CaCO_3$ at 44%. This indicates that CO_2 was lost during thermal decomposition and the mussel sample was converted to CaO at 810 °C. Above 810 °C, there is no further change in the weight of the mussel shell because the sample has been completely converted to CaO.

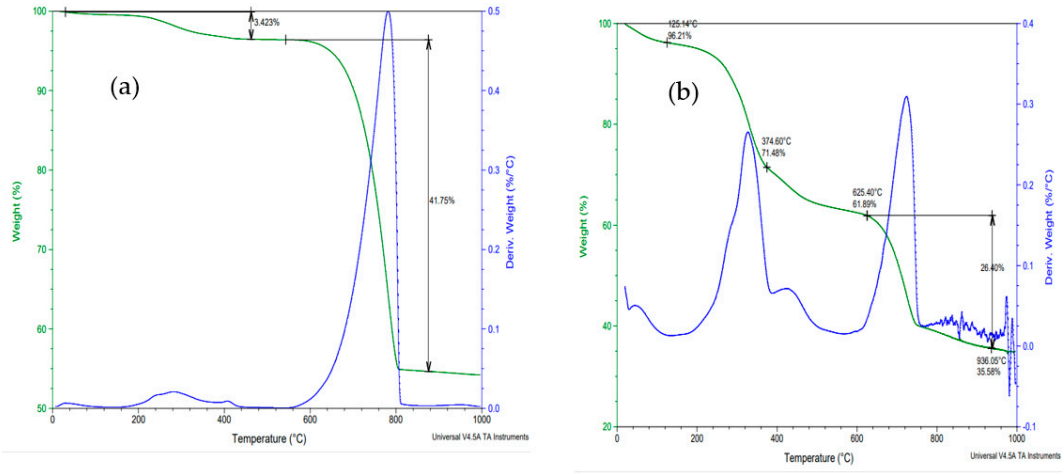

Figure 2. TGA plots for calcination of (**a**) mussel shell and (**b**) lobster shell. Note that the Y-axes correspond to the weight % and change in weight % per degree Celsius for the regular TGA plot (green) and first derivative TGA plot (blue), respectively.

The chicken eggshell decomposition pattern also occurred in two stages as shown in Figure 3. The weight loss seen between 200 °C–480 °C is associated with the different organic impurities in the eggshell powder. This accounts for about 6.92% of the sample weight loss. A substantial weight loss of 41.74% can be seen from the thermal curve of the second stage at a temperature range of 600 °C–825 °C due to the CO_2 evolved from the decomposed $CaCO_3$. Unlike the mussel and the eggshell, the oyster shell decomposition pattern occurred in a single step. A weight loss of 44.05% from the oyster shell is attributed to the actual weight percent of CO_2 lost during the thermal decomposition of calcium carbonate of the shell into calcium oxide. This is an indication that the crystalline structure of the oyster shell is composed almost exclusively of $CaCO_3$ with no organic constituents found in either chicken eggshell or lobster shell. The thermal decomposition curve shows a significant weight loss between the temperature range of 560 °C–785 °C. At a temperature of 785 °C and above, the oyster shell is completely converted to CaO, and the sample weight remained constant at this point.

The lobster shell decomposition pattern occurred in three distinct stages. From Figure 2b shown above, it could be seen that the decomposition of the lobster shell started very early at a lower temperature range between 20–125 °C due to the loss of water (3.79%) present in its structure. Unlike oyster shell which is composed mainly of $CaCO_3$, the lobster shell contains water, proteins and chitins which account for 38.11% of the weight loss at the temperature range of 20–625 °C. This was followed by the gradual decomposition of its $CaCO_3$ after 625 °C to CaO with loss of CO_2. Romano et al. 2007 reported similar findings for TGA of lobster cuticles that chitin degradation occurred between 270 °C to about 600 °C followed by decarboxylation of $CaCO_3$ after 650 °C [30].

The major component of the four types of shells is calcium carbonate which decomposes into calcium oxide and carbon dioxide. The weight loss of about 44% in the shell sample is attributed to the actual weight percent of CO_2 (in $CaCO_3$), released during the decomposition process. There is a variation in temperature at which each of these shell samples attain complete conversion into CaO. A temperature of 800 °C and above is required for the complete conversion of mussel, egg, and lobster shells into CaO whereas at a temperature below 800 °C, around 785 °C, the oyster shell is completely converted into CaO. This is due to the different structural compositions of the shells and the varying levels of organic impurities present in some of the shell samples.

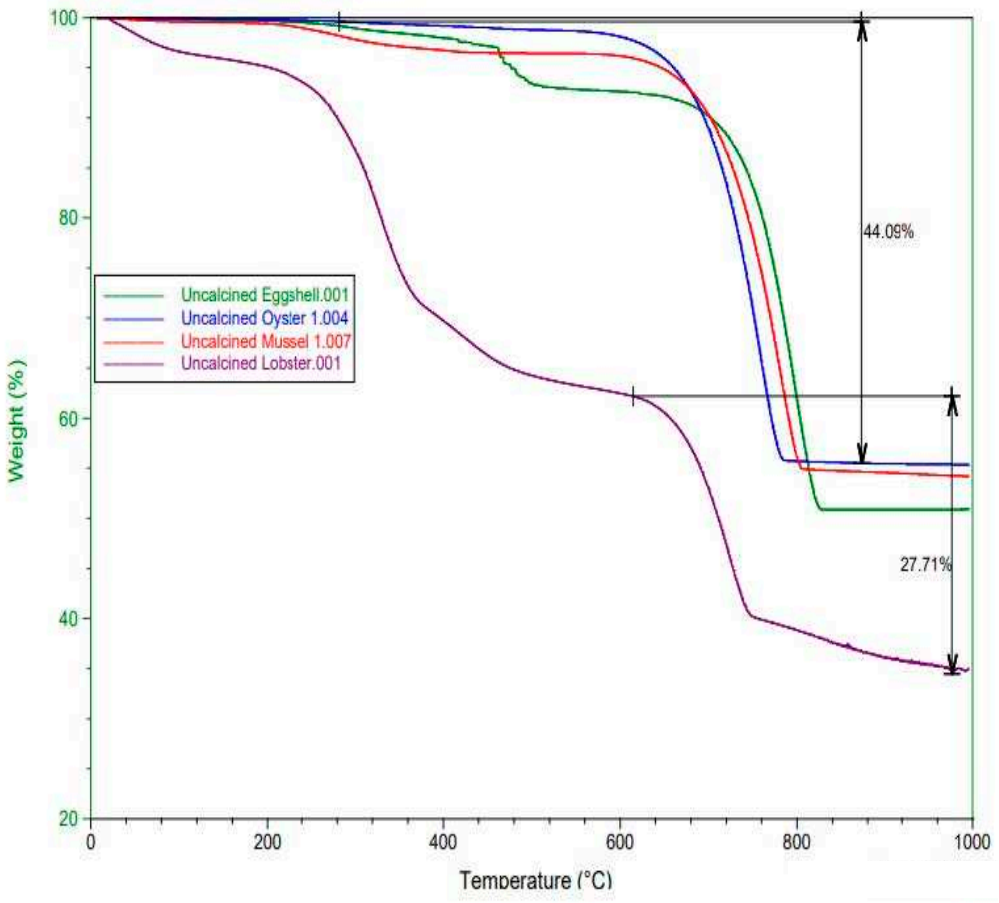

Figure 3. Comparative TGA plots for calcination of shell-derived powders from chicken egg (green), oyster (blue), mussel (red), and lobster (purple).

3.1.2. Characterization of Catalysts by SEM/EDX and XRF Methods

The shell-derived CaO catalysts prepared from four different sources of seafood or chicken egg wastes were characterized by SEM/EDX and the SEM images are shown in Figure 4. The comparison of calcined oyster shell and lobster shell are shown in Figure 4a,b, respectively, at the same magnification of 1000-fold with the micron scale bar shown. The oyster-derived CaO particles are larger and more crystalline than the particles of lobster shell which are composed of 7.8% phosphate in addition to 92.2% carbonate as the primary anions. There is also a direct correlation between calcium and phosphorus levels for lobster shells from different body parts including cephalon, thorax, abdomen, uropod, legs, and chela [31]. The EDX elemental data shows that the calcined lobster shell contains 3.2% magnesium, 0.34% strontium, and 0.28% sodium in comparison to the calcined oyster shell crystallites which show only 0.2% magnesium. The chicken eggshell sample shows the smallest particle size. The calcination of the shell samples at 1000 °C changed the composition and the structure of the shell with a resultant increase in the surface area and better catalytic activity. After calcination, some particles show the features of holes (Figure 4c) associated with the loss of CO_2 or collapse of the mesoporous structure during the initial transformation of $CaCO_3$ to CaO. The sintering process at 1000 °C allows the aggregation of nanoparticles to form faceted crystallites along with the reduction in surface area and porosity [32].

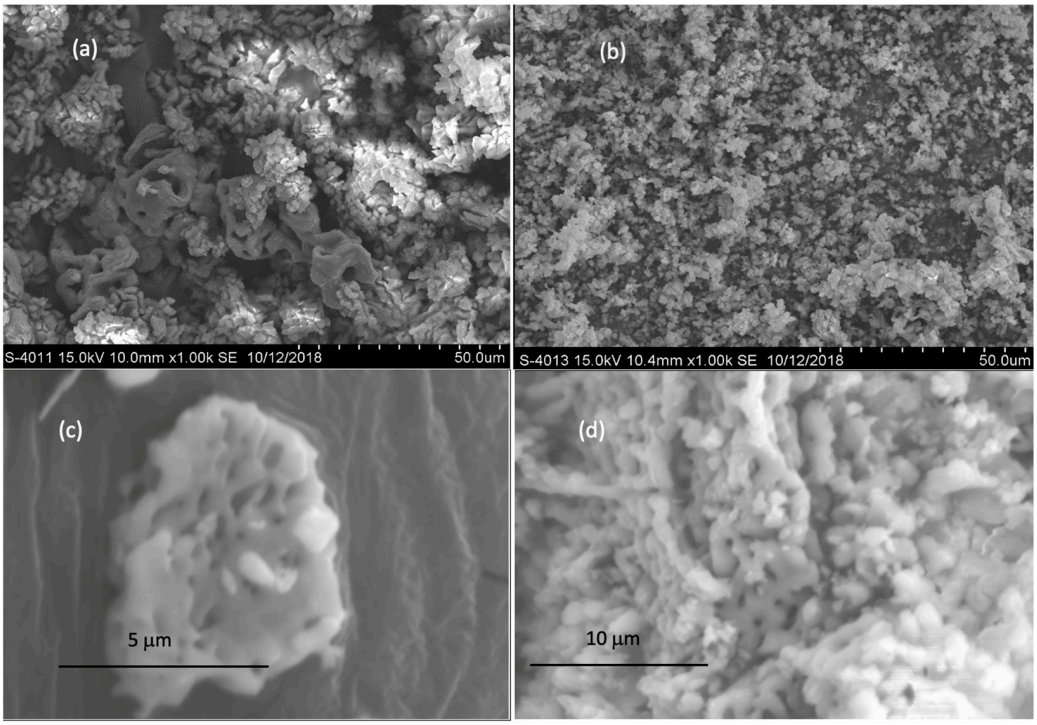

Figure 4. SEM images of (**a**) a calcined sample of oyster shell, (**b**) a calcined sample of lobster shell, (**c**) a calcined sample of mussel shell with 0.29% Zn, and (**d**) a calcined sample of lobster shell with 0.35% Zn.

The calcined lobster shell powders in Figure 4d show the presence of long fibrils of chitin with high carbon content interspersed with CaO particles. The EDX data of calcined shell materials show that the calcium content is the lowest in the lobster samples at 40.4% by weight compared to 45–50 wt.% for the samples of oyster, mussel, and chicken egg. This is due to the presence of other elements including phosphorus, magnesium, and strontium that are either absent or found at lower levels in the other types of shell samples. Phosphorus and magnesium were measured at 1.08 wt.% and 1.86 wt.%, respectively, which are consistent with previously reported values of 0.52–2.41 wt.% phosphorus and 0.33–1.46 wt.% magnesium for various parts of the lobster shell [31]. The 1.08 wt.% phosphorus as phosphate and the 6.95 wt.% carbon in the form of carbonate and organic carbon residue of chitin possess minimal catalytic activity compared to CaO. The Ca:C elemental ratio expressed in atomic or mole percent is also a useful parameter for estimating the degree of calcination, i.e., the higher Ca:O mole ratio of 4.27 for calcined mussel shell and 3.09 for calcined oyster shell implies that they have higher conversion efficiency for forming CaO relative to calcined lobster shell and eggshell. The organic matter in the lobster exoskeleton, mostly chitin, accounts for the 19.7–38.2 wt.% range [33]

The uncalcined and calcined shell powders were also analyzed by XRF and their results were shown in Figure 5. The sums of the seven elements plotted for the four types of shells are given as "SM" values and decreases in the order of mussel (0.86%), lobster (0.57%), oyster (0.37%), and chicken egg (0.14%). The calcium contents of calcined samples $[Ca]_c$ measured in the range of 69.78% to 71.99% agree with the theoretical value of pure CaO at 71.43%. However, the uncalcined samples give XRF values of $[Ca]_{uc}$ in the range of 31.57% to 48.98% following the trend of oyster > mussel, chicken egg > lobster. Uncalcined lobster shell shows the lowest $[Ca]_{uc}$ value of 31.57% and hence gives the smallest yield of CaO for the transesterification reaction.

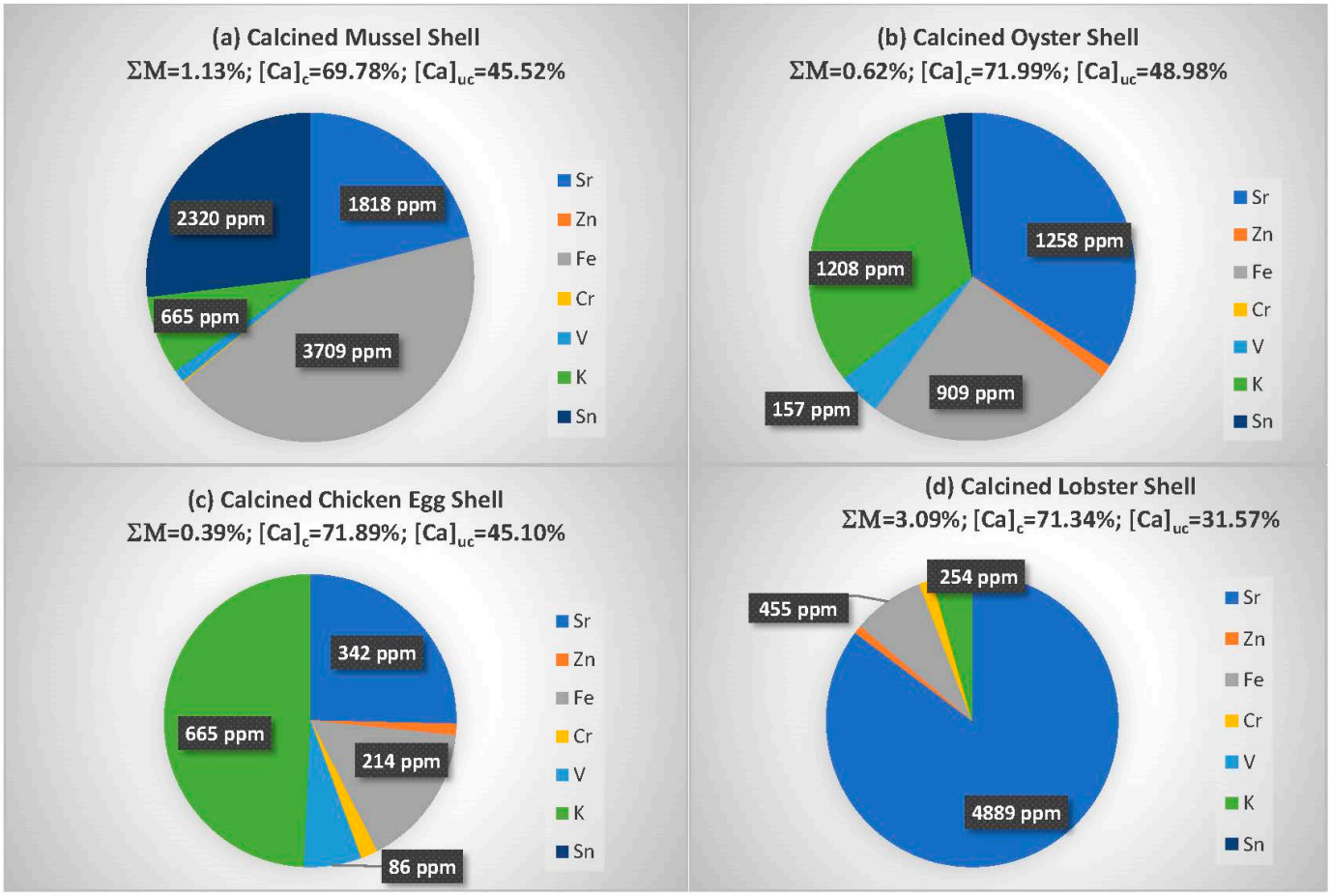

Figure 5. Elemental composition of calcined shell samples of (**a**) mussel (**b**) oyster (**c**) chicken egg, and (**d**) lobster. The notations of ΣM, $[Ca]_c$, and $[Ca]_{uc}$ stand for sum of metals excluding calcium in percent, percent of calcined calcium, and percent of uncalcined calcium, respectively.

Potassium (1208 ± 2 ppm) and strontium (1257.6 ± 0.6 ppm) in the form of oxides for oyster shells are important constituents that can also exhibit strong basicity for producing biodiesel esters. The values of tin at 2320 ± 0.4 ppm and iron at 3709 ± 1.4 ppm are observed for calcined mussel shell. Besides calcium, potassium (665 ± 3.1 ppm) and strontium (4888 ± 0.6 ppm) are the most abundant trace elements for chicken eggshell and lobster shell, respectively. Among the trace elements measured by XRF, strontium and potassium are potentially important due to the increase in the basicity of K_2O and SrO relative to CaO that may contribute to enhanced reactivity for biodiesel production. The concentrations of strontium are 342 ppm, 1258 ppm, 1818 ppm, and 4889 ppm in calcined shells of chicken egg, oyster, mussel, and lobster, respectively. The values of potassium concentration for calcined shells are 254 ppm for lobster shells, 665 ppm for both mussel and chicken eggshells, and 1208 ppm for oyster shells. The substitution of Ca^{2+} by Sr^{2+} in the crystalline lattice is likely because the cation radius of strontium (Sr^{2+}) is 132 pm compared to 114 pm for calcium (Ca^{2+}) whereas Mg^{2+} and K^+ have significantly different ionic radii of 86 pm and 152 pm, respectively. In general, lattice substitution for ions of the same charge but with a difference in ion radii of less than 15% is highly probable and the ionic radii difference of 15–30% will be less probable [34]. Additional XRF data for the elemental composition of uncalcined and calcined shells are given in Table S1 in the Supplementary Materials.

3.1.3. FTIR Analysis of CaO and CaO-ZnO Mixed Catalysts Derived from Shell Samples

Figure 6a,b shows the overlaid IR spectrum of the uncalcined and calcined oyster shell, the fundamental absorption bands of 712 cm^{-1}, 875 cm^{-1}, and 1450 cm^{-1} are indications of asymmetric stretch, out-of-plane bend, and in-plane vibration of C-O bonds of $CaCO_3$, respectively. There is a noticeable reduction in the intensity of these absorption bands for the calcined shells due to the calcination at high temperatures resulting in the decomposition of the $CaCO_3$ into CaO and CO_2. The sharp peak at 3640 cm^{-1} is attributed to OH group stretching in $Ca(OH)_2$, which is formed upon the exposure of CaO to atmospheric moisture [35]. Similar spectral signals were observed for the mussel shell powder with absorption bands of 716 cm^{-1}, 863 cm^{-1}, and 1458 cm^{-1} attributed to the asymmetric stretching, out-of-plane bending, and in-plane vibration of the O-C-O bond of $CaCO_3$. The $Ca(OH)_2$ peak due to moisture absorption of CaO appears at 3647 cm^{-1}.

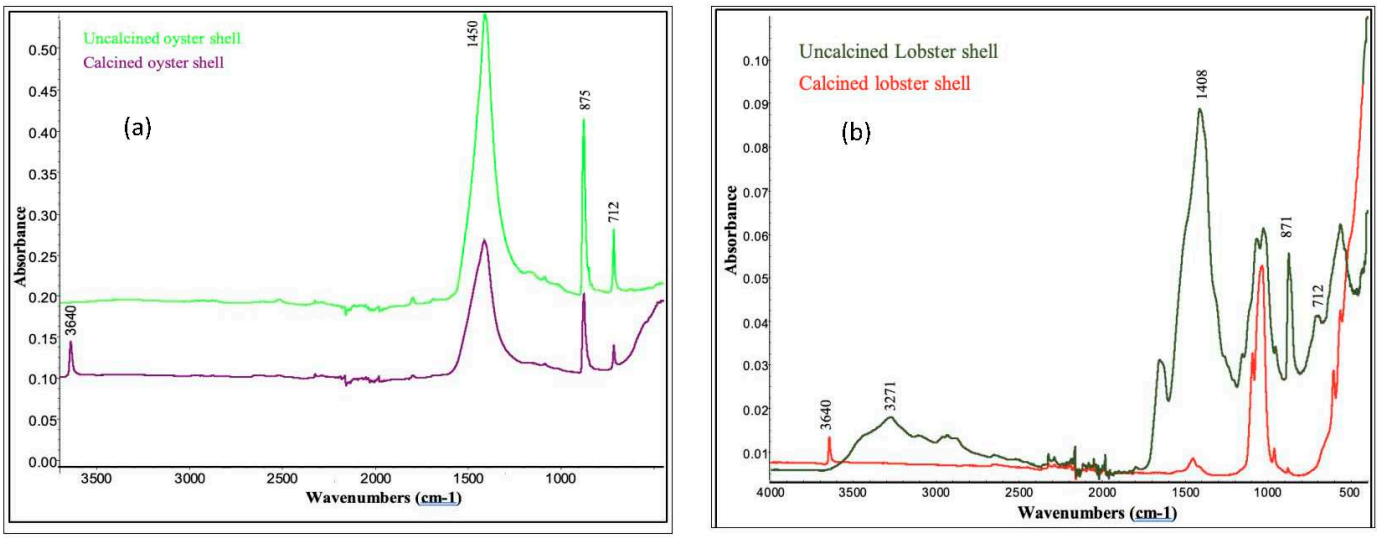

Figure 6. Infrared spectra of uncalcined and calcined samples of (**a**) oyster shell; the absorption bands of 712 cm^{-1}, 875 cm^{-1}, 1450 cm^{-1} are related to the C-O bonds of $CaCO_3$. The peak at 3640 cm^{-1} is due to the O-H stretching in $Ca(OH)_2$ and (**b**) lobster shell; the absorption bands at 712 cm^{-1}, 871 cm^{-1} and 1408 cm^{-1} are related to the C-O bonds of $CaCO_3$. The peak at 3640 cm^{-1} is due to the O-H stretching in $Ca(OH)_2$. The intense peak around 1100 cm^{-1} is due to the phosphate group in hydroxyapatite [36] whereas the peak at 3271 cm^{-1} is due to the chitin OH group [37].

The chicken eggshell has characteristic CO_3^{2-} absorption bands at 710 cm^{-1}, 872 cm^{-1}, and 1410 cm^{-1}. The peak at 3644 cm^{-1} is associated with OH^- stretching of $Ca(OH)_2$ formed from the absorption of moisture by the eggshell-derived CaO. For the lobster shell, the absorption peak indicative of the asymmetric stretch of the C-O bond of $CaCO_3$ could be seen at 746 cm^{-1}, 872 cm^{-1}, and 1413 cm^{-1}. The sharp peak at 3640 cm^{-1} is attributed to the OH-stretching of $Ca(OH)_2$, which was formed when CaO absorbs atmospheric moisture. The broad peak at 3271 cm^{-1} is due to the presence of an OH group of chitin in the lobster shell. The calcination of the shell lead to a decrease in the absorption bands at 1408 cm^{-1}, 871 cm^{-1} and 712 cm^{-1} which are associated with $CaCO_3$. Due to the analytical sampling depth of the attenuated total reflectance accessory for the FTIR spectrometer at about 0.5–2.0 microns, the ratio of the 3640 cm^{-1} to 1450 cm^{-1} peaks gives the estimate of the size of the particles with a surface layer of CaO and the underlying $CaCO_3$ substrate. The heat treatment of shell powders at 5–10 g quantities in the furnace resulted in calcined catalysts with only partial conversion to CaO compared to the complete conversion of 1–2 mg of shell powders in TGA analysis. In reusing the calcined catalysts after multiple batches of catalytic cycles, it is important to monitor the 3640 cm^{-1} peak and the biodiesel yield to determine when the activity of the catalyst needs to be regenerated via calcination.

3.1.4. X-ray Diffraction Patterns of the Shell-Derived CaO and CaO-ZnO Mixed Catalysts

The diffractograms obtained from the uncalcined shells in general showed the predominance of $CaCO_3$ in shell composition. After calcination at 800 °C and 1000 °C, the $CaCO_3$ originally present in the shells were converted to CaO which could be seen in the diffraction patterns of the calcined shells of mussels and oyster in Figure 6a,b. However, the calcination of lobster shell and chicken eggshell to form CaO is not complete at 800 °C as seen in Figure 6a. The calcined shells showed diffraction peaks characteristic of pure CaO at 2θ values of 32.0°, 37.7°, 53.7°, 64.0° and 67.2°; these peaks correspond to the cubic crystal structure associated with the reflections from (111), (200), (220), (311) and (222) planes, respectively [38,39]. For the calcined shell materials produced at 1000 °C for 4 h, the following sets of diffraction peaks with a slight variation of 2θ values corresponding to (111), (200), (220), (311) and (222) planes, respectively, were identified as follows:

- Lobster CaO: → 32.1°, 37.0°, 53.5°, 63.8° and 67.0°
- Eggshell CaO: → 32.3°, 37.5°, 54.0°, 64.5° and 67.5°
- Mussel CaO: → 32.8°, 38.0°, 54.5°, 64.8° and 68.1°
- Oyster CaO: → 32.8°, 38.0°, 54.5°, 64.8° and 68.1°

These XRD results are similar to those reported by Samantaray et al. [38]. After calcination at 1000 °C for 4 h, all the shell samples were able to attain a similar degree of crystallinity to that of pure CaO. The slightly larger 2θ values of mussel CaO and oyster CaO compared to CaO obtained from chicken eggs are likely due to the higher levels of strontium and iron substitution of calcium in the crystalline structures. In Figure 7a, the calcination conditions of 800 °C for 4 h yield XRD diffraction patterns obtained for lobster and eggshell still show the presence of $CaCO_3$ and other organic constituents besides CaO. For lobster shell that was subjected to heat treatment at 800 °C, the XRD pattern reveals the presence of CaO, MgO and hydroxyapatite that are consistent with the results of previous studies [33,40]. The chitin XRD peaks at 2θ values of 9.4, 13.6, 19.7, 21.2, 23.9, 26.8, 28.6, 39.7, 43.0, 78.0 degrees are not observed since chitin would have been degraded after 600/625 °C based on TGA plots shown in Figure 2b and published results of Romano et al. [30,37]. Purer shell materials without phosphate-based constituents like hydroxyapatite will show the decomposition of $CaCO_3$ into CaO at calcination temperatures of 800 °C [41]. The TGA analyses of the shell samples confirmed that the lobster and eggshell contain more organic impurities in their structures thereby requiring a higher calcination temperature above 800 °C, preferably 1000 °C, to attain the crystalline phase of CaO.

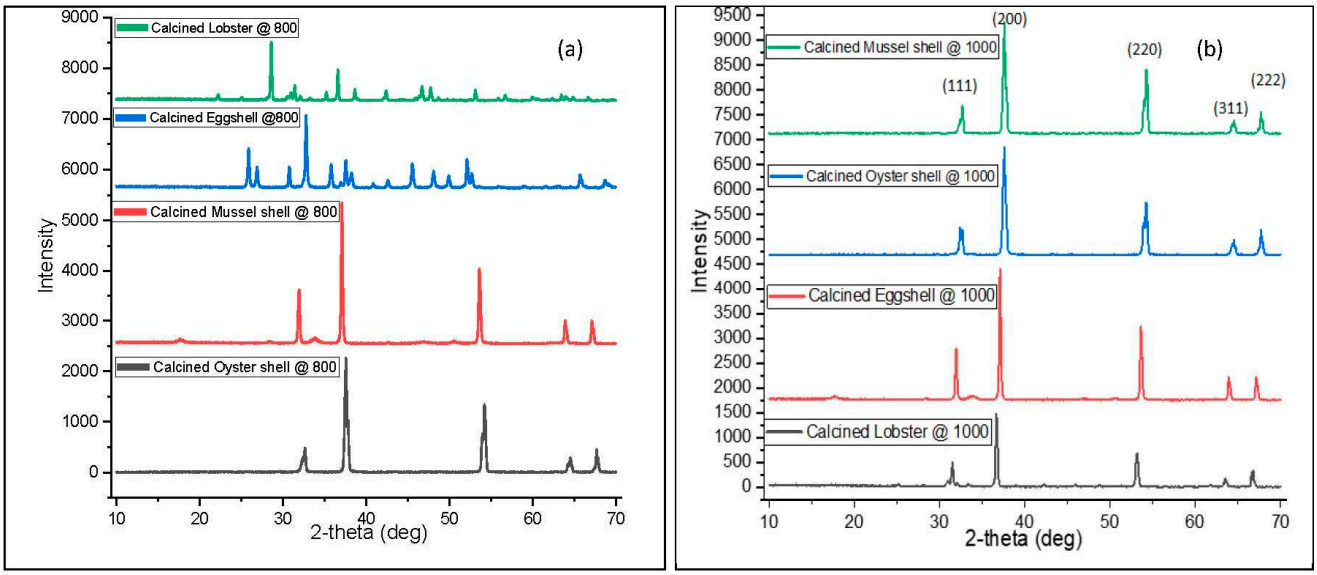

Figure 7. Powder X-ray diffraction patterns of CaO catalysts derived from various shell materials calcined at (**a**) 800 °C and (**b**) 1000 °C.

Figure 8a compares XRD patterns of CaO-ZnO mixed metal oxide catalysts prepared with 5 wt.% zinc concentration at 700 °C calcination temperature. The XRD diffraction patterns of 5% Zn-oyster-CaO, 5% Zn-mussel-CaO, 5% Zn-lobster-CaO and 5% Zn-eggshell-CaO show the exclusive presence of CaO in cubic crystalline phase in all the calcined materials except the 5% Zn-lobster-CaO material that shows tiny XRD peaks belonging to hydroxyapatite in addition to the Zn. When the Zn levels were studied at 5%, 7%, 10%, and 25% wt.% in the calcined oyster samples, the distinct peaks corresponding to the ZnO phase were only observed when calcined samples with Zn^{2+} concentrations of 10 wt.%, 25 wt.%, and the reference ZnO samples were prepared from Zn nitrate at 700 °C as shown in Figure 8b. Nevertheless, a further increase in the Zn^{2+} concentration (≥7 wt.%) in the shell-derived CaO leads to formation of ZnO in the hexagonal phase which is seen in the low-intensity peaks at 2θ (10% Zn-oyster-CaO) = 34.45°, 56.62°, and 62.89° and 2θ (25% Zn-oyster-CaO) = 34.0°, 56.18°, and 62.18°. This result is similar to the work reported by Kumar and Ali [27]. The diffraction peak obtained for Zn nitrate calcined at the same temperature of 700 °C for 4 h matches some of the characteristic peaks of ZnO at 2θ (Calcined $Zn(NO_3)_2$ at 700 °C) = 34.04°, 47.22°, 56.37° and 62.7°. The increase of Zn^{2+} concentration from 5 wt.% to above 7 wt.% (i.e., 10 wt.% and 25 wt.%) leads to the formation of two distinct phases of CaO-ZnO. The American Mineralogist Crystallography Database information for the XRD patterns of oxides in the calcined materials is provided in the Table S2 of the Supplementary Materials.

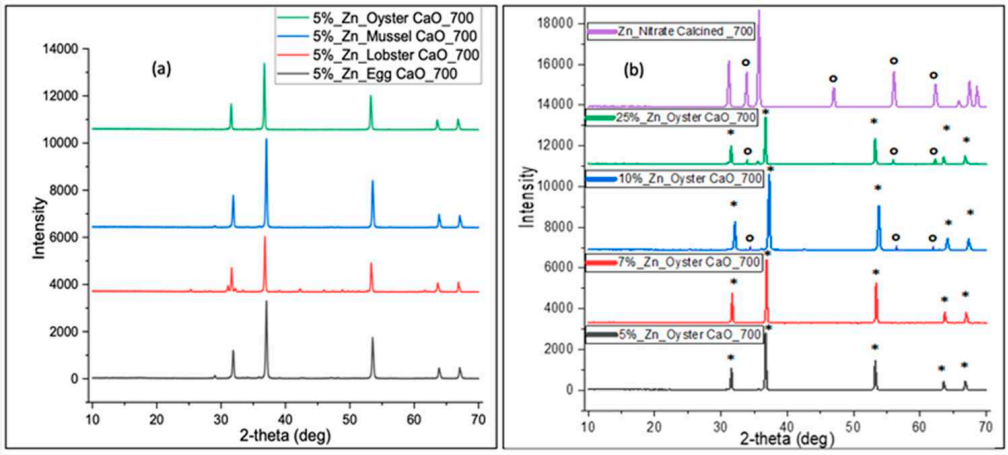

Figure 8. (**a**) XRD patterns of 5% Zn-Oyster-CaO, 5% Zn-Mussel-CaO, 5% Zn-Eggshell-CaO and 5% Zn-Lobster-CaO calcined at 700 °C for 4 h. (**b**) XRD patterns of 5% Zn-Oyster-CaO, 7% Zn-Oyster-CaO, 10% Zn-Oyster-CaO, 25% Zn-Oyster-CaO, and $Zn(NO_3)_2$ calcined at 700 °C for 4 h (*: CaO phase; o: ZnO phase).

3.2. Comparison of Biodiesel Yields Using Different Calcined Catalysts

The experimental biodiesel yields for various catalysts are summarized in Table 1. The calculation of yields is based on the NMR measurements of the ratios of the a-methylene protons to methoxy protons in reaction products as explained in a prior study [28]. The catalytic activity of the individual shell-derived CaO including oyster CaO, mussel CaO, lobster CaO and eggshell CaO have been investigated and compared to the activities of Zn-spiked CaO mixed metal oxide catalysts of 5% Zn-oyster-CaO, 5% Zn-mussel-CaO, 5% Zn-lobster-CaO, 5% Zn-eggshell-CaO. The ultrasonication-assisted transesterification reaction conditions are 1 wt.% catalyst loading, 9:1 methanol to oil mole ratio, reaction temperature of 60 °C and ultrasonication time of 10 min. The percentage conversion of triglycerides in the canola oil into biodiesel by CaO catalysts derived from the shells of oysters, mussels, chicken eggs, and lobsters were 92.9%, 89.0%, 90.3% and 50.6%, respectively. The oyster-derived CaO catalyst showed the best biodiesel yield due to the highest level of calcium content in the chemical composition of both uncalcined and calcined materials as revealed by XRF analysis, crystallite size and morphology that provide a large surface area for

transesterification, and concentrations of trace transition metals in the crystalline structure to augment the catalyst activity of the shell-derived CaO. There is not much loss of yield when using waste-shell-based CaO in comparison to pure CaO [42].

The spiking of the shell-derived CaO with Zn^{2+} (i.e., 5 wt.% Zn^{2+} concentration in CaO), resulted in increased biodiesel yields of fatty acid methyl esters (FAME) for all the shell-based catalysts used in this study. As shown in Table 1, the CaO-ZnO mixed metal oxide catalysts showed higher biodiesel yields than the CaO counterparts under the same reaction conditions. The 5% Zn-oyster-CaO, 5% Zn-mussel-CaO, 5% Zn-eggshell-CaO, and 5% Zn-lobster-CaO recorded biodiesel percentage yields of 93.9%, 92.8%, 92.5% and 59.5%, respectively. The highest observed FAME yield for oyster-CaO-ZnO (with 5% of Zn^{2+} concentration) can be related to its basic properties, as biodiesel yield increases with the increasing number of basic sites [27,43]. Kumar and Ali reported that the catalytic activity of the ZnO-CaO catalyst toward the transesterification reaction of biodiesel production was found to be a function of their basic strength and in the case of Zn/CaO weight ratio, the maximum basic strength was observed for CaO-ZnO at 1.5–7% Zn^{2+} concentration [27]. The EDX measurements of zinc showed that the actual Zn levels in the Zn/CaO mixed catalyst were only 1.78–3.41 wt.% instead of the targeted 5 wt.% Zn-spiked CaO catalyst. Further increase in Zn^{2+} levels in the CaO-ZnO mixed metal oxide catalyst beyond 1.5% resulted in a decrease in biodiesel yield as can be seen in the comparative study of Zn^{2+} concentrations in 5% Zn-oyster-CaO, 7% Zn-oyster-CaO, and 10% Zn-oyster-CaO mixed catalyst, which produced biodiesel yields of 93.9%, 67.2%, and 62.3%, respectively.

It is inconclusive from the results of Table 1 that the biodiesel yields in this study are improved by the preparation of mixed oxide catalysts that contain ZnO. Although there are slight increases of 1.0% for oyster-based catalysts and 2.3% for catalysts prepared from chicken eggshells, they are smaller than the pooled standard deviation of 2.35%. In the case of mussel-based catalysts, there is a decrease in the biodiesel yield of 3.8%. For comparison in the case of lobster, there is a statistically significant increase in its yield of 9.9% when a mixed oxide catalyst containing ZnO was used. In a study conducted using CaO prepared from snail shells, the waste palm cooking oil showed a biodiesel yield of 80% for CaO and 90% for CaO modified with ZnO [20]. A remarkable aspect of the present study is the reaction time of 10 min for ultrasonication-assisted reaction compared to 45–360 min for the cited studies describing biodiesel synthesis using a hotplate.

Table 1. Comparison of biodiesel yields for different CaO catalysts and reaction conditions. The current study is based on the use of 1.00 wt.% shell-derived CaO or 5% Zn/CaO catalysts, and 9:1 mole ratio of methanol to canola oil.

Catalyst (Weight %)	Method	Time (min)	Yield (%)
Oyster CaO (1%)	Present ultrasonication study	10	92.9
Mussel CaO (1%)	Present ultrasonication study	10	89.0
Eggshell CaO (1%)	Present ultrasonication study	10	90.3
Lobster CaO (1%)	Present ultrasonication study	10	50.6
5%Zn-Mussel-CaO (1%)	Present ultrasonication study	10	92.8
5%Zn-Eggshell-CaO (1%)	Present ultrasonication study	10	92.5
5%Zn-Lobster-CaO (1%)	Present ultrasonication study	10	59.5
5%Zn-Oyster-CaO (1%)	Present ultrasonication study	10	93.9
7%Zn-Oyster-CaO (1%)	Present ultrasonication study	10	67.2
10%Zn-Oyster-CaO (1%)	Present ultrasonication study	10	62.3
CaO (3%)	Hotplate with stirring, 25:1 CH_3OH-jatropha oil, [44]	180	91

Table 1. *Cont.*

Catalyst (Weight %)	Method	Time (min)	Yield (%)
CaO-ZnO (3%)	Hotplate with stirring, 25:1 CH_3OH-jatropha oil, [44]	180	94
$CaZn_2(OH)_6.2H_2O$ (2%)	Hotplate with stirring, 10:1 CH_3OH-sunflower oil, [45]	120	92
1.5-Zn/CaO-550 (5%)	Hotplate with stirring, 9:1 CH_3OH-cottonseed oil, 1.5 wt.% Zn-CaO calcined at 550 °C [27]	45	>99
CaO-ZnO (10%)	Hotplate with stirring, 40:1 CH_3OH-soybean oil, [46]	360	73
Eggshell CaO (6.04%)	Ultrasonication 299.7 W; 8.3:1 CH_3OH-waste cooking oil, 55 °C [12]	39.8	98.6
Crab shell CaO (3%)	250 rpm stirring rate; 9:1 CH_3OH-fishmeal plant oil, 60 °C [21]	60	88.2
Snail shell CaO (3%)	Heating mantle, 65 °C; 6:1 CH_3OH-waste palm cooking oil [20]	180	80

3.3. Emissions of Biodiesel Fuel Blends in Diesel Generators

Diesel generators are commonly used in countries where electric power grid infrastructures are very minimal or sparse in rural areas or even cities due to budgetary constraints. Diesel generators are easy to install and are frequently used in developing countries in agricultural, residential, and industrial sectors. In Nigeria, the public electricity grid only meets at most 30% of consumer power usage, and most homes have access to public electricity supply for only 6 h daily [47]. The shortfalls in electricity supply account for the installation of 15 million diesel-powered generators in over 90% of businesses and 30% of homes in Nigeria. Due to concerns about the toxicity of carbon monoxide released, inhalable exhaust particulate matter, carcinogens including formaldehyde, 1,3-butadiene, and benzene, and the potential fire risks of diesel fuel, it is important to evaluate the safety of biodiesel fuel blends for use in diesel generators. The California Air Resources Board has developed screening risk assessment tables for diesel engine owners to estimate their overall exposure risk from diesel engine exhaust particulate matter [48]. Since diesel generators are frequently used indoors among businesses and homes, toxicant concentrations will be increased due to the lack of ventilation.

3.3.1. FTIR Analysis of Emissions from Diesel Power Generators

FTIR spectroscopy was used to analyze the small molecular weight compounds in the emissions from diesel power generators. Figure 9 shows the concentrations of carbon monoxide (CO), ethylene (C_2H_4), methane (CH_4), formaldehyde (H_2CO), and sulfur dioxide (SO_2) as the oxygen content of the fuel blends is increased by the fatty acid methyl esters in 20% (B20) and 40% (B40) biodiesel blended with ultralow sulfur petroleum diesel (ULSPD). The 100% ULSPD has significantly higher levels of CO, C_2H_4, CH_4, H_2CO, and SO_2 relative to the B20 and B40. The emission of highly toxic CO was reduced from 258 ppm in ULSPD emission to 229 ppm and 192 ppm in B20 and B40 emissions, respectively, in the infrared spectral region of 2134–2138 cm^{-1}. The corresponding relative standard deviation is 16.9%, 11.5%, and 3.5% for the CO levels in ULSPD, B20, and B40. The FTIR signals for formaldehyde are in the spectral region of 2683–2949 cm^{-1}. The formaldehyde concentrations of B20 and B40 were reduced by 58% and 59%, respectively, relative to ULSPD. At above 50 ppm, formaldehyde can cause severe pulmonary reactions including pulmonary edema, pneumonia, and bronchial irritation which can result in death. Methane, which is much less toxic than CO and formaldehyde, was measured in the spectral region of

2874–3188 cm^{-1}. The methane concentrations of B20 and B40 were reduced by 39% and 54%, relative to the ULSPD emission.

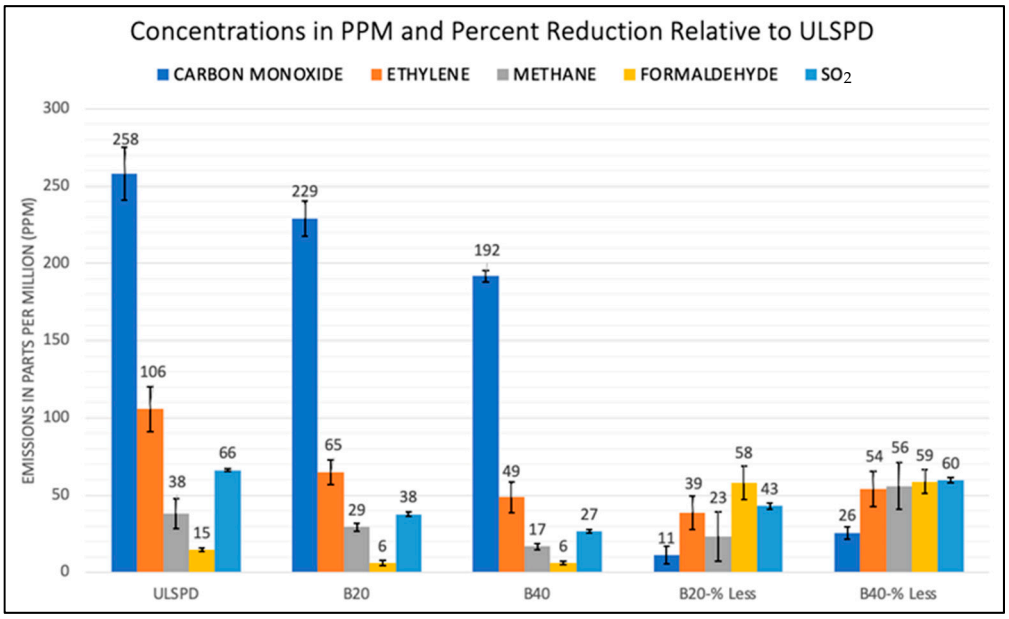

Figure 9. Generator emissions of air pollutants measured by infrared spectroscopy in parts per million units and their percent reduction in B20 and B40 biodiesel fuels relative to ultralow sulfur petroleum diesel (ULSPD).

Due to the adverse human health effects associated with inhalation exposure to diesel emissions, CO is regulated by both the United States Environmental Protection Agency (USEPA) and the Occupational Safety and Health Administration (OSHA). The National Ambient Air Quality Standards of USEPA for CO is 9 ppm for a 24-h period and 35 ppm standard for a 1-h period. The OSHA permissible exposure limit (PEL) for CO is 50 ppm for worker exposure during an 8-h period. Without proper ventilation, CO emissions can exceed both the USEPA and OSHA standards for protecting human health. Ethylene and methane play key roles in forming larger VOCs including aromatics such as benzene, toluene, ethylbenzene, and xylene isomers. Sulfur dioxide has many adverse human health effects and could contribute to acid rain. As seen in Figure 9, B40 can clearly provide a greater reduction in the emission of toxicants compared to B20 except for formaldehyde, which shows similar reduction efficiency for B20 and B40 when compared to USLPD. The emission test results supported previous studies showing the reduction of VOCs but there are other studies that reported an increase in hydrocarbon emissions for biodiesel-blended fuels compared to petroleum-based diesel [49].

3.3.2. GC-MS Analysis of VOCs

GC-MS results indicate that there are about 180–200 VOCs detected in the generator emissions. About half of these compounds were detected with a high degree of confidence based on their match indices of greater than 800 out of 1000. There were about 27 target compounds specified in USEPA's Compendium of Air Toxics TO-15 Method that were detected and quantified. Out of the 27 compounds, 11 were quantified with a high degree of confidence for the comparison of generator emissions from ULSPD, B20, and B40. The percent reduction (PR%) values of diesel generator fuel emissions from B20 and B40 relative to ULSPD for these 11 compounds are given in Table S3 in Supplementary Materials. Five of these including benzene, 2-butanone, propene, ethyl benzene and propyl benzene were plotted in Figure 10a,b show a significant reduction of their generator emission concentrations due to the blending of ULSPD with biodiesel. All 11 compounds show lower emissions compared to the ULSPD. Except for two compounds, propene and isopropyl

alcohol, B40 has higher reduction efficiencies relative to ULSLPD when compared to the B20 emissions.

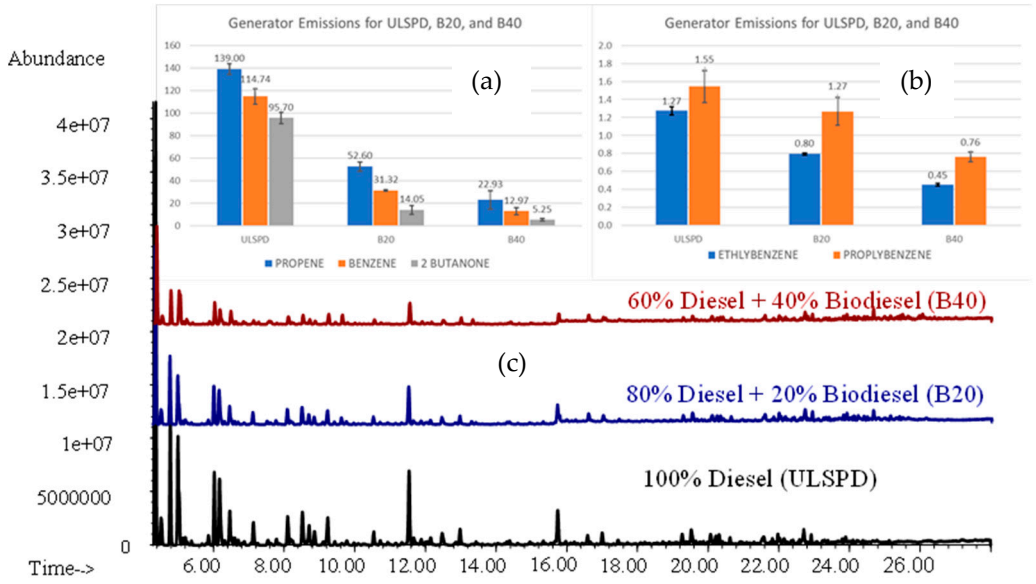

Figure 10. Comparison of GC-MS data for generator emissions from ULSPD, B20, and B40 fuel blends with (**a**) concentration plots of propene, benzene, and 2-butanone in the range of 0–140 parts per billion (**b**) concentration plots of ethylbenzene and n-propylbenzene in in the range of 0–2.0 parts per billion, and (**c**) chromatograms showing significant reduction of volatile organic compounds for B20 and B40 fuel emissions relative to the ULSPD; the X-axis represents the GC retention time window of 4–28 min and the Y-axis denotes the MS ion abundance from 0 to 4 × 10^7 counts per second with the three plots offset on the common scale.

Three compounds, namely benzene, 1,3-butadiene, and formaldehyde, are classified as Group 1 human carcinogens by the International Agency for Research on Cancer (IARC). At low levels, benzene can cause dizziness, headache, and respiratory tract irritation. However, long-term exposure to higher levels of benzene may cause anemia, alterations to the immune system, and leukemia. OSHA has regulatory standards for PELs and STELs for these three carcinogens and USEPA has detailed information on their toxicological properties in the Integrated Risk Information System (IRIS) database [50]. The Inhalation Unit Risk values of cancer incidence for benzene, 1,3-butadiene, and formaldehyde are 2.2 × 10^{-6} per μg/m^3, 3 × 10^{-5} per μg/m^3, and 1.3 × 10^{-5} per μg/m^3, respectively. At the concentrations indicated in Figure 10c and the conversion factor of 1 μg/m^3 being equal to 0.313 ppbv, 0.452 ppbv, and 0.814 ppbv for the three carcinogens at the standard conditions of 1 atm and 25 °C, respectively, the cancer risks are deemed to be significant for inhalation exposure to diesel generator emissions, especially those from ULSPD. The GC-MS chromatogram in Figure 10c shows an overall decrease in the levels of almost 200 VOCs as the oxygen content of fuel blends increases in the order of ULSPD < B20 < B40, thereby lowering inhalation exposure.

4. Discussion

The results presented in this study are promising for CaO-based heterogeneous catalysts to replace homogeneous catalysts such as NaOH or KOH that are currently used in most commercial biodiesel production facilities. CaO-based catalysts can reduce the need for washing the biodiesel product to remove the residual NaOH that is corrosive to diesel engines. The lower volume of wastewater generation from biodiesel washing is particularly desirable in countries where the use of water for fuel production instead of human consumption is not viewed favorably. This study shows data from multiple instrumentation techniques that the production of CaO catalysts is easy, inexpensive, and

does not generate toxicants harmful to human health. The TGA, FTIR, XRD, and XRF results show that after the calcination of shell materials at 1000 °C for 4 h, all the shell samples containing calcite or $CaCO_3$ are converted to almost pure CaO powders that give biodiesel yields of greater than 90%.

Although the TGA data show complete conversion of predominantly $CaCO_3$ into CaO, the FTIR and EDX data show residual $CaCO_3$ signals which could be interpreted as calcined particles having an outer layer of CaO and an inner core of $CaCO_3$. Since the sample penetration or signal excitation depths are 1.0–1.5 microns for FTIR and 2.0–2.5 microns for SEM-EDX whereas the CaO crystallites have larger dimensions as revealed by the SEM images, it can be inferred that the particle size distribution and the loading weight in the furnace of uncalcined shell powders in the furnace may influence the degree of calcination or completion CaO formation, and consequently the biodiesel yield and/or the catalyst loading necessary to achieve a high yield. The published studies on the use of CaO catalysts generally do not address their particle size distribution or their correlation with biodiesel yields as well as the durability or reusability of the catalysts. The durability of the CaO catalysts is affected by the dissolution of the surface layer containing $Ca(OH)_2$ as well as the loss of catalyst active sites through the adsorption or accumulation of oil or biodiesel by-products.

The evaluation of mixed catalysts containing CaO/ZnO seems to suggest that there is no appreciable improvement in biodiesel yields for shell-derived catalysts compared to CaO catalysis except for the case of lobster. It is noteworthy that the SEM-EDX analysis shows the presence of zinc in all the Zn-spiked CaO catalyst samples, but the XRD data only show the presence of distinct ZnO phases at the 10% Zn and 25% Zn mixed oxide samples but not for the 5% Zn and 7% Zn mixed oxide samples. These observations imply that the zinc ion substitution of calcium ions occurred up to a certain point before the distinctive ZnO phases started to form. To confirm this, a future study should rely on the use of elemental mapping by EDX to fully characterize the presence of CaO or ZnO particles and their size distribution.

5. Conclusions

This study demonstrates the feasibility of preparing inexpensive and yet effective heterogeneous CaO catalysts derived from the waste shells of oysters, mussels, lobsters, and chicken eggs. Furthermore, very high biodiesel yields of 90–94% are achieved in 10 min by the ultrasonication-assisted transesterification of canola oil using the CaO catalysts. The incorporation of Zn^{2+} at varying concentrations into the shell-derived CaO structure gives a more efficient CaO-ZnO mixed metal oxide catalyst prepared by the wet impregnation method. The use of CaO-based solid heterogenous catalysts in biodiesel production minimizes wastewater generation for removing residual catalysts in the biodiesel and high energy consumption associated with acid or base homogenous catalysts. The use of shell-based CaO catalysts can also reduce the level of the corrosive base in the biodiesel compared to the commonly used NaOH or KOH catalysts. The use of biodiesel in diesel power generation potentially reduces human exposure to toxicants including CO, SO_2, benzene, and formaldehyde.

Since the shell materials from food waste and furnaces for calcination of shells to yield CaO catalyst are easily available in most countries, the small-scale production of biodiesel is viable in rural areas or developing countries where there is minimal refining capacity to produce diesel fuel for use in vehicles, farm equipment, and power generation. Together with the initiatives to collect used cooking oil and cultivate indigenous crops producing non-edible oils as biodiesel feedstocks, there could be strong incentives to implement a circular economy of producing biodiesel using waste materials and non-edible crops like Jatropha curcas that grow well naturally in many locations.

Supplementary Materials: The following supporting information can be downloaded at: https://www.mdpi.com/article/10.3390/en16145408/s1, Table S1: XRF elemental data for uncalcined and calcined shell samples; Table S2: The American Mineralogist Crystallography Database information for the XRD patterns of oxides in the calcined materials; Table S3: The percent reduction (PR%) values of diesel generator fuel emissions from B20 and B40 relative to ULSPD.

Author Contributions: This manuscript has been prepared using the data and results of the Masters' theses of I.N. and S.A. with additional summer research contribution by D.C. and M.S. The specific contribution of authors is noted as follows. Conceptualization, N.S.C. and B.G.O.; methodology and experimentation, I.N.; formal analysis, I.N., S.A. and N.S.C.; validation, D.C. and M.S.; investigation, N.S.C. and B.G.O.; data curation, M.S.; writing—original draft preparation, I.N. and S.A.; writing—review and editing, N.S.C., B.G.O. and M.S.; visualization, I.N., S.A. and N.S.C.; supervision, N.S.C. and B.G.O.; project administration, N.S.C. and B.G.O.; resources, N.S.C. and B.G.O.; funding acquisition, N.S.C. All authors have read and agreed to the published version of the manuscript.

Funding: This research was partially funded by the National Science Foundation Grant No. 1852543.

Data Availability Statement: The data presented in this study are available in the Supplementary Material.

Acknowledgments: The authors acknowledge the electron microscopy services provided by Joyce Miller, Technical Manager of the MTSU Interdisciplinary Microscopy and Imaging Center.

Conflicts of Interest: The authors declare no conflict of interest. The funding agency had no role in the design of the study; in the collection, analyses, or interpretation of data; in the writing of the manuscript; or in the decision to publish the results.

References

1. Wong, K.Y.; Ng, J.-H.; Chong, C.T.; Lam, S.S.; Chong, W.T. Biodiesel Process Intensification through Catalytic Enhancement and Emerging Reactor Designs: A Critical Review. *Renew. Sustain. Energy Rev.* **2019**, *116*, 109399. [CrossRef]
2. Efavi, J.K.; Kanbogtah, D.; Apalangya, V.; Nyankson, E.; Tiburu, E.K.; Dodoo-Arhin, D.; Onwona-Agyeman, B.; Yaya, A. The Effect of NaOH Catalyst Concentration and Extraction Time on the Yield and Properties of Citrullus Vulgaris Seed Oil as a Potential Biodiesel Feed Stock. *S. Afr. J. Chem. Eng.* **2018**, *25*, 98–102. [CrossRef]
3. Ling, J.; Tan, Y.; Mujawar, M.; Kansedo, J.; Saptoro, A.; Nolasco-Hipolito, C. A Review of Heterogeneous Calcium Oxide Based Catalyst from Waste for Biodiesel Synthesis. *SN Appl. Sci.* **2019**, *1*, 810. [CrossRef]
4. Banerjee, N.; Barman, S.; Saha, G.; Jash, T. Optimization of Process Parameters of Biodiesel Production from Different Kinds of Feedstock. *Mater. Today: Proc.* **2018**, *5*, 23043–23050. [CrossRef]
5. Yang, C.; He, K.; Xue, Y.; Li, Y.; Lin, H.; Han, S. Factors Affecting the Cold Flow Properties of Biodiesel: Fatty Acid Esters. *Energy Sources Part A Recovery Util. Environ. Eff.* **2018**, *40*, 516–522. [CrossRef]
6. Etim, A.O.; Musonge, P.; Eloka-Eboka, A.C. Effectiveness of Biogenic Waste-derived Heterogeneous Catalysts and Feedstock Hybridization Techniques in Biodiesel Production. *Biofuels Bioprod. Bioref.* **2020**, *14*, 620–649. [CrossRef]
7. Nayak, S.N.; Bhasin, C.P.; Nayak, M.G. A Review on Microwave-Assisted Transesterification Processes Using Various Catalytic and Non-Catalytic Systems. *Renew. Energy* **2019**, *143*, 1366–1387. [CrossRef]
8. Arumugam, A.; Ponnusami, V. Production of Biodiesel by Enzymatic Transesterification of Waste Sardine Oil and Evaluation of Its Engine Performance. *Heliyon* **2017**, *3*, e00486. [CrossRef] [PubMed]
9. Van Gerpen, J.; Shanks, B.; Pruszko, R.; Clements, D.; Knothe, G. *Biodiesel Analytical Methods: August 2002–January 2004*; NREL/SR-510-36240; National Renewable Energy Lab. (NREL): Golden, CO, USA, 2004; p. 15008800. [CrossRef]
10. Leung, D.Y.C.; Wu, X.; Leung, M.K.H. A Review on Biodiesel Production Using Catalyzed Transesterification. *Appl. Energy* **2010**, *87*, 1083–1095. [CrossRef]
11. Ashine, F.; Kiflie, Z.; Prabhu, S.V.; Tizazu, B.Z.; Varadharajan, V.; Rajasimman, M.; Joo, S.-W.; Vasseghian, Y.; Jayakumar, M. Biodiesel Production from Argemone Mexicana Oil Using Chicken Eggshell Derived CaO Catalyst. *Fuel* **2023**, *332*, 126166. [CrossRef]
12. Attari, A.; Abbaszadeh-Mayvan, A.; Taghizadeh-Alisaraei, A. Process Optimization of Ultrasonic-Assisted Biodiesel Production from Waste Cooking Oil Using Waste Chicken Eggshell-Derived CaO as a Green Heterogeneous Catalyst. *Biomass Bioenergy* **2022**, *158*, 106357. [CrossRef]
13. Mekonnen, K.D.; Sendekie, Z.B. NaOH-Catalyzed Methanolysis Optimization of Biodiesel Synthesis from Desert Date Seed Kernel Oil. *ACS Omega* **2021**, *6*, 24082–24091. [CrossRef]
14. Sharma, A.; Kodgire, P.; Kachhwaha, S.S. Investigation of Ultrasound-Assisted KOH and CaO Catalyzed Transesterification for Biodiesel Production from Waste Cotton-Seed Cooking Oil: Process Optimization and Conversion Rate Evaluation. *J. Clean. Prod.* **2020**, *259*, 120982. [CrossRef]
15. Mishra, V.; Goswami, R. A Review of Production, Properties and Advantages of Biodiesel. *Biofuels* **2017**, *9*, 273–289. [CrossRef]

16. Singh, D.; Sharma, D.; Soni, S.L.; Sharma, S.; Kumar Sharma, P.; Jhalani, A. A Review on Feedstocks, Production Processes, and Yield for Different Generations of Biodiesel. *Fuel* **2020**, *262*, 116553. [CrossRef]
17. El-sherif, A.A.; Hamad, A.M.; Shams-Eldin, E.; Mohamed, H.A.A.E.; Ahmed, A.M.; Mohamed, M.A.; Abdelaziz, Y.S.; Sayed, F.A.-Z.; El Qassem Mahmoud, E.A.A.; Abd El-Daim, T.M.; et al. Power of Recycling Waste Cooking Oil into Biodiesel via Green CaO-Based Eggshells/Ag Heterogeneous Nanocatalyst. *Renew. Energy* **2023**, *202*, 1412–1423. [CrossRef]
18. Chen, G.-Y.; Shan, R.; Yan, B.-B.; Shi, J.-F.; Li, S.-Y.; Liu, C.-Y. Remarkably Enhancing the Biodiesel Yield from Palm Oil upon Abalone Shell-Derived CaO Catalysts Treated by Ethanol. *Fuel Process. Technol.* **2016**, *143*, 110–117. [CrossRef]
19. Gaide, I.; Makareviciene, V.; Sendzikiene, E.; Kazancev, K. Snail Shells as a Heterogeneous Catalyst for Biodiesel Fuel Production. *Processes* **2023**, *11*, 260. [CrossRef]
20. Kedir, W.M.; Wondimu, K.T.; Weldegrum, G.S. Optimization and Characterization of Biodiesel from Waste Cooking Oil Using Modified CaO Catalyst Derived from Snail Shell. *Heliyon* **2023**, *9*, e16475. [CrossRef] [PubMed]
21. Karkal, S.S.; Rathod, D.R.; Jamadar, A.S.; Mamatha, S.S.; Kudre, T.G. Production Optimization, Scale-up, and Characterization of Biodiesel from Marine Fishmeal Plant Oil Using Portunus Sanguinolentus Crab Shell Derived Heterogeneous Catalyst. *Biocatal. Agric. Biotechnol.* **2023**, *47*, 102571. [CrossRef]
22. Nahas, L.; Dahdah, E.; Aouad, S.; El Khoury, B.; Gennequin, C.; Abi Aad, E.; Estephane, J. Highly Efficient Scallop Seashell-Derived Catalyst for Biodiesel Production from Sunflower and Waste Cooking Oils: Reaction Kinetics and Effect of Calcination Temperature Studies. *Renew. Energy* **2023**, *202*, 1086–1095. [CrossRef]
23. Hangun-Balkir, Y. Green Biodiesel Synthesis Using Waste Shells as Sustainable Catalysts with *Camelina Sativa* Oil. *J. Chem.* **2016**, *2016*, 1–10. [CrossRef]
24. Nakatani, N.; Takamori, H.; Takeda, K.; Sakugawa, H. Transesterification of Soybean Oil Using Combusted Oyster Shell Waste as a Catalyst. *Bioresour. Technol.* **2009**, *100*, 1510–1513. [CrossRef] [PubMed]
25. Aigbodion, V.S. Modified of CaO-Nanoparticle Synthesized from Waste Oyster Shells with Tin Tailings as a Renewable Catalyst for Biodiesel Production from Waste Cooking Oil as a Feedstock. *Chem. Afr.* **2023**, *6*, 1025–1035. [CrossRef]
26. Hu, S.; Wang, Y.; Han, H. Utilization of Waste Freshwater Mussel Shell as an Economic Catalyst for Biodiesel Production. *Biomass Bioenergy* **2011**, *35*, 3627–3635. [CrossRef]
27. Kumar, D.; Ali, A. Transesterification of Low-Quality Triglycerides over a Zn/CaO Heterogeneous Catalyst: Kinetics and Reusability Studies. *Energy Fuels* **2013**, *27*, 3758–3768. [CrossRef]
28. Chong, N.S.; Okejiri, F.U.; Abdulramoni, S.; Perna, S.; Ooi, B.G. Evaluation of Shell-Derived Calcium Oxide Catalysts for the Production of Biodiesel Esters from Cooking Oils. *AJC* **2021**, *6*, 20–27. [CrossRef]
29. Chong, N.S.; Abdulramoni, S.; Patterson, D.; Brown, H. Releases of Fire-Derived Contaminants from Polymer Pipes Made of Polyvinyl Chloride. *Toxics* **2019**, *7*, 57. [CrossRef]
30. Romano, P.; Fabritius, H.; Raabe, D. The Exoskeleton of the Lobster Homarus Americanus as an Example of a Smart Anisotropic Biological Material. *Acta Biomater.* **2007**, *3*, 301–309. [CrossRef]
31. Mergelsberg, S.T.; Ulrich, R.N.; Xiao, S.; Dove, P.M. Composition Systematics in the Exoskeleton of the American Lobster, Homarus Americanus and Implications for Malacostraca. *Front. Earth Sci.* **2019**, *7*, 69. [CrossRef]
32. Rodriguez-Navarro, C.; Ruiz-Agudo, E.; Luque, A.; Rodriguez-Navarro, A.B.; Ortega-Huertas, M. Thermal Decomposition of Calcite: Mechanisms of Formation and Textural Evolution of CaO Nanocrystals. *Am. Miner.* **2009**, *94*, 578–593. [CrossRef]
33. Boßelmann, F.; Romano, P.; Fabritius, H.; Raabe, D.; Epple, M. The Composition of the Exoskeleton of Two Crustacea: The American Lobster Homarus Americanus and the Edible Crab Cancer Pagurus. *Thermochim. Acta* **2007**, *463*, 65–68. [CrossRef]
34. Jacobsson, T.J.; Pazoki, M.; Hagfeldt, A.; Edvinsson, T. Goldschmidt's Rules and Strontium Replacement in Lead Halogen Perovskite Solar Cells: Theory and Preliminary Experiments on CH3NH3SrI3. *J. Phys. Chem. C* **2015**, *119*, 25673–25683. [CrossRef]
35. Kesić, Ž.; Lukić, I.; Brkić, D.; Rogan, J.; Zdujić, M.; Liu, H.; Skala, D. Mechanochemical Preparation and Characterization of CaO·ZnO Used as Catalyst for Biodiesel Synthesis. *Appl. Catal. A Gen.* **2012**, *427–428*, 58–65. [CrossRef]
36. Gheisari, H.; Karamian, E.; Abdellahi, M. A Novel Hydroxyapatite –Hardystonite Nanocomposite Ceramic. *Ceram. Int.* **2015**, *41*, 5967–5975. [CrossRef]
37. Mohan, K.; Muralisankar, T.; Jayakumar, R.; Rajeevgandhi, C. A Study on Structural Comparisons of α-Chitin Extracted from Marine Crustacean Shell Waste. *Carbohydr. Polym. Technol. Appl.* **2021**, *2*, 100037. [CrossRef]
38. Samantaray, S.; Pradhan, D.K.; Hota, G.; Mishra, B.G. Catalytic Application of CeO2–CaO Nanocomposite Oxide Synthesized Using Amorphous Citrate Process toward the Aqueous Phase One Pot Synthesis of 2-Amino-2-Chromenes. *Chem. Eng. J.* **2012**, *193–194*, 1–9. [CrossRef]
39. Laskar, I.B.; Rajkumari, K.; Gupta, R.; Chatterjee, S.; Paul, B.; Rokhum, S.L. Waste Snail Shell Derived Heterogeneous Catalyst for Biodiesel Production by the Transesterification of Soybean Oil. *RSC Adv.* **2018**, *8*, 20131–20142. [CrossRef] [PubMed]
40. Dinatha, I.K.H.; Jamilludin, M.A.; Supii, A.I.; Wihadmadyatami, H.; Partini, J.; Yusuf, Y. Characteristics of Bioceramic Hydroxyapatite Based on Sand Lobster Shells (Panulirus Homarus) as Sources of Calcium with Optimal Calcination Temperature. *Mater. Sci. Forum* **2023**, *1090*, 39–44. [CrossRef]
41. Widiarti, N.; Lailun Ni'mah, Y.; Bahruji, H.; Prasetyoko, D. Development of CaO From Natural Calcite as a Heterogeneous Base Catalyst in the Formation of Biodiesel: Review. *J. Renew. Mater.* **2019**, *7*, 915–939. [CrossRef]
42. Rizwanul Fattah, I.M.; Ong, H.C.; Mahlia, T.M.I.; Mofijur, M.; Silitonga, A.S.; Rahman, S.M.A.; Ahmad, A. State of the Art of Catalysts for Biodiesel Production. *Front. Energy Res.* **2020**, *8*, 101. [CrossRef]

43. Castro, L.D.S.; Barañano, A.G.; Pinheiro, C.J.G.; Menini, L.; Pinheiro, P.F. Biodiesel Production from Cotton Oil Using Heterogeneous CaO Catalysts from Eggshells Prepared at Different Calcination Temperatures. *Green Process. Synth.* **2019**, *8*, 235–244. [CrossRef]
44. Lee, H.; Juan, J.; Yun Hin, T.-Y.; Ong, H. Environment-Friendly Heterogeneous Alkaline-Based Mixed Metal Oxide Catalysts for Biodiesel Production. *Energies* **2016**, *9*, 611. [CrossRef]
45. Kaewdaeng, S.; Sintuya, P.; Nirunsin, R. Biodiesel Production Using Calcium Oxide from River Snail Shell Ash as Catalyst. *Energy Procedia* **2017**, *138*, 937–942. [CrossRef]
46. Toledo Arana, J.; Torres, J.J.; Acevedo, D.F.; Illanes, C.O.; Ochoa, N.A.; Pagliero, C.L. One-Step Synthesis of CaO-ZnO Efficient Catalyst for Biodiesel Production. *Int. J. Chem. Eng.* **2019**, *2019*, 1–7. [CrossRef]
47. Awofeso, N. Generator Diesel Exhaust: A Major Hazard to Health and the Environment in Nigeria. *Am. J. Respir. Crit. Care Med.* **2011**, *183*, 1437. [CrossRef] [PubMed]
48. "Hot Spots" Stationary Diesel Engine Screening Risk Assessment Tables | California Air Resources Board. Available online: https://ww2.arb.ca.gov/hot-spots-stationary-diesel-engine-screening-risk-assessment-tables (accessed on 28 May 2023).
49. Pereira, R.G.; Oliveira, C.D.; Oliveira, J.L.; Oliveira, P.C.P.; Fellows, C.E.; Piamba, O.E. Exhaust Emissions and Electric Energy Generation in a Stationary Engine Using Blends of Diesel and Soybean Biodiesel. *Renew. Energy* **2007**, *32*, 2453–2460. [CrossRef]
50. IRIS Advanced Search. United States Environmental Protection Agency. Available online: https://iris.epa.gov/AdvancedSearch/ (accessed on 4 June 2023).

ARTICLES FOR FACULTY MEMBERS

ELUCIDATING THE CALCIUM OXIDE DERIVED FROM THE WASTE SHELLS OF MUD CLAM (GELOINA EXPANSA) AS A CATALYST FOR BIODIESEL PRODUCTION

Progress on modified calcium oxide derived waste-shell catalysts for biodiesel production / Ooi, H. K., Koh, X. N., Ong, H. C., Lee, H. V., Mastuli, M. S., Taufiq-Yap, Y. H., Alharthi, F. A., Alghamdi, A. A., & Mijan, N. A.

Catalysts
Volume 11 Issue 2 (2021) 194 Pages 1–26
https://doi.org/10.3390/catal11020194
(Database: MDPI)

catalysts

MDPI

Review

Progress on Modified Calcium Oxide Derived Waste-Shell Catalysts for Biodiesel Production

Hui Khim Ooi [1], Xin Ning Koh [1], Hwai Chyuan Ong [2,*], Hwei Voon Lee [3], Mohd Sufri Mastuli [4,5], Yun Hin Taufiq-Yap [6,7], Fahad A. Alharthi [8], Abdulaziz Ali Alghamdi [8] and Nurul Asikin Mijan [1,*]

1 Chemical Sciences, Faculty of Science and Technology, Universiti Kebangsaan Malaysia (UKM), Bangi 43600, Selangor, Malaysia; A170358@siswa.ukm.edu.my (H.K.O.); A170752@siswa.ukm.edu.my (X.N.K.)
2 School of Information, Systems and Modelling, Faculty of Engineering and Information Technology, University of Technology, Sydney, NSW 2007, Australia
3 Nanotechnology and Catalysis Research Centre (NanoCat), Institute of Advanced Studies, Universiti Malaya, Kuala Lumpur 50603, Selangor, Malaysia; leehweivoon@um.edu.my
4 School of Chemistry and Environment, Faculty of Applied Sciences, Universiti Teknologi MARA, Shah Alam 40450, Selangor, Malaysia; mohdsufri@uitm.edu.my
5 Centre for Functional Materials and Nanotechnology, Institute of Science, Universiti Teknologi MARA, Shah Alam 40450, Selangor, Malaysia
6 Faculty of Science and Natural Resources, Universiti Malaysia Sabah, Kota Kinabalu 88400, Sabah, Malaysia; taufiq@upm.edu.my
7 Catalysis Science and Technology Research Centre (PutraCat), Faculty of Science, Universiti Putra Malaysia, UPM Serdang 43400, Selangor, Malaysia
8 Chemistry Department Science College, King Saud University, P.O. Box 2455, Riyadh 11451, Saudi Arabia; fharthi@ksu.edu.sa (F.A.A.); aalghamdia@ksu.edu.sa (A.A.A.)
* Correspondence: HwaiChyuan.Ong@uts.edu.au (H.C.O.); nurul.asikin@ukm.edu.my (N.A.M.)

Citation: Ooi, H.K.; Koh, X.N.; Ong, H.C.; Lee, H.V.; Mastuli, M.S.; Taufiq-Yap, Y.H.; Alharthi, F.A.; Alghamdi, A.A.; Asikin Mijan, N. Progress on Modified Calcium Oxide Derived Waste-Shell Catalysts for Biodiesel Production. *Catalysts* **2021**, *11*, 194. https://doi.org/10.3390/catal11020194

Academic Editor: Diego Luna
Received: 2 January 2021
Accepted: 26 January 2021
Published: 2 February 2021

Abstract: The dwindling of global petroleum deposits and worsening environmental issues have triggered researchers to find an alternative energy such as biodiesel. Biodiesel can be produced via transesterification of vegetable oil or animal fat with alcohol in the presence of a catalyst. A heterogeneous catalyst at an economical price has been studied widely for biodiesel production. It was noted that various types of natural waste shell are a potential calcium resource for generation of bio-based CaO, with comparable chemical characteristics, that greatly enhance the transesterification activity. However, CaO catalyzed transesterification is limited in its stability and studies have shown deterioration of catalytic reactivity when the catalyst is reused for several cycles. For this reason, different approaches are reviewed in the present study, which focuses on modification of waste-shell derived CaO based catalyst with the aim of better transesterification reactivity and high reusability of the catalyst for biodiesel production. The catalyst stability and leaching profile of the modified waste shell derived CaO is discussed. In addition, a critical discussion of the structure, composition of the waste shell, mechanism of CaO catalyzed reaction, recent progress in biodiesel reactor systems and challenges in the industrial sector are also included in this review.

Keywords: biodiesel; transesterification; waste-shell; heterogenous catalyst; green catalyst; alternative fuel

1. Introduction

The drastic depletion of fossil fuels and continuous anthropogenic greenhouse gas emissions have prompted the search for alternative renewable and sustainable fuels with efficiency similar to the conventional fuels being used today [1,2]. In this regard, renewable and sustainable biofuels had been seen as an alternative in order to reduce fossil fuel usage [3,4]. Biofuels are generally referred to as liquid or gaseous fuels that are produced from renewable sources [5], which are typically generated from biological material or living organisms, such as plants, animal by-products, or microorganisms [6]. In the past

10 years, the biofuel industry has experienced an enormous growth, and the main regions contributing to this development are Europe, Brazil and the United States [7]. Currently, the main application of biofuels is as a liquid transportation fuel [8]. In general, biofuels can be divided into four generations, which depend on the raw materials used. First-generation biofuels are mostly derived from subsistence crops. Second-generation biofuels come from non-food biomass or lignocellulosic crops [9]. This is sustainable, cost-effective, and highly available, which will be advantageous for the biorefinery industry. Noteworthy, the use of lignocellulosic crops lead to a zero net carbon dioxide emission and environmental friendliness [10]. The third generation of biofuels come from algae-sources [11,12]. The best means of utilizing raw materials for second and third generation biofuel production is to avoid the issue of food competition. Besides, there are many advantages in producing biofuels from algae, where the triglyceride-based oil extracted from microalgae is 15 to 300 times higher than that of conventional crops in terms of area [13,14]. Production of biofuels from genetically modified algae is considered as the fourth-generation of biofuels [15]. The growing interest in fourth-generation biofuel usage strives to lower environmental impact, especially on land usage for crop plantation [16].

Typically, the liquid-based biofuels that widely apply to transportation purposes are biodiesel and bioethanol [17,18]. Bioethanol is produced through starch or sugar fermentation, while biodiesel is obtained via the transesterification reaction of oil crops [9]. Biodiesel is used to replace diesel, while bioethanol is used to substitute for petrol [19]. It is noteworthy that the majority of biofuel usage is from biodiesel (76%) (Figure 1a), followed by bioethanol (~20%). Malaysia is one of the most important palm oil producers in the world. The country is experiencing a robust development in new oil palm plantations and palm oil mills. According to a Malaysian Palm Oil Board (MPOB) report [20], the total biodiesel production projected to 2019 in Malaysia shows an increasing trend (Figure 1b), which suggests that Malaysia has an important role to play in fulfilling the growing global need for palm oil-derived biofuels. Biodiesel is generated by esterification of fatty acids (FAs) or transesterification of triacylglycerol (TAG) with alcohol in the presence of a catalyst. Water is co-generated in the esterification reaction of fatty acid, and glycerol is transesterified from TAG (Figure 1c) [21]. Commonly, biodiesel is used in engines with compression ignition with little or no modification [22]. The characteristics of biodiesel are similar but not the same as petroleum diesel. Biodiesel has a high flash point, thus making it safe to store and handle [23]. Biodiesel can be used directly as engine fuel (B100) or blended with diesel in a certain proportion (B20, B50, etc.) [24,25]. Noteworthy, biodiesel has a higher cetane number compared to bioethanol, efficient for engine ignition, while bioethanol has a high-octane number with anti-knocking properties in engines. Earlier literature has discovered that biodiesel exhibited better engine performance than bioethanol, because bioethanol has higher miscibility to water and organic solvent that will contaminate the automotive lubricant parts with resulting corrosion to the engine [26–28].

Generally, there are differences between the esterification and transesterification process. Esterification occurs when a carboxylic acid reacts with alcohol by adding an acid catalyst and produces water as a by-product. Transesterification is the reaction between the vegetable oil or animal fat and alcohol in the presence of a basic catalyst to form ester and glycerol as a by-product [29,30].

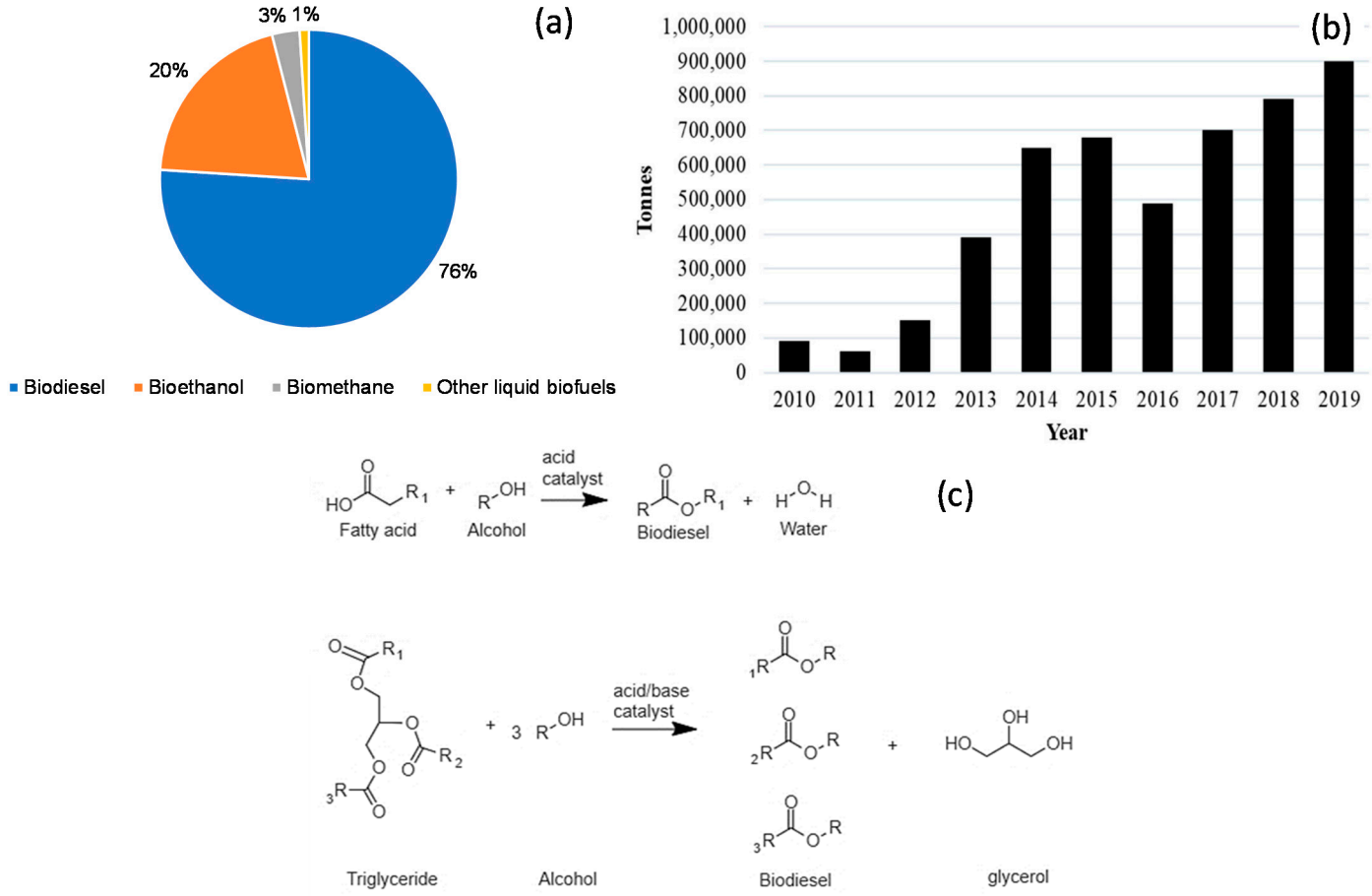

Figure 1. (**a**) Share of each type of biofuel consumed in the EU transport sector in 2011 (adapted from [31]) (**b**) Biodiesel production from palm oil from 2010 to 2019 in Malaysia [20] (**c**) Esterification of fatty acid and transesterification of vegetable oils/ animal fats.

Based on various physicochemical properties of the catalysts, both acid and base catalysts can be classified as homogeneous, heterogeneous or enzymatic catalysts [32–34]. Homogeneous acid and base catalysts such as H_2SO_4, HCl, NaOH and KOH are the most common homogeneous catalysts used in esterification and transesterification reactions [35]. Compared with homogeneous type catalytic transesterification and esterification, heterogeneous catalytic systems have several advantages, including the ease of the biodiesel separation process, catalyst recycling or reuse, lower energy requirements and minimal water consumption. Due to these advantages, processing costs can be reduced significantly [18]. In addition, the use of heterogeneous acid catalysts is the most suitable when the feedstock contains high free fatty acid (FFA) and high water content, as the catalyst has a high tolerance for both of the compounds [36]. Solid acid catalysts such as SO_4^{2-}/SnO^{2-}- SiO_2, carbon-supported solid acid catalyst, sulfated zirconia, etc., have been extensively studied for transesterification of high FFA feedstock with high biodiesel yield of 94.8–97.0% [18]. However, a longer reaction time makes this unattractive compared to the short reaction time from the base-catalysed transesterification process [37,38]. Several types of solid base catalysts have been utilized for biodiesel production such as alkaline metal oxide, alkaline metal carbonates or hydro-carbonates, anionic resins and basic zeolites [39]. Among these catalysts, alkaline metal oxides (AMOs) are the most well-known and effective metal group for base-catalysed transesterification reaction [40]. Many reports have been published on AMO catalysts (e.g., CaO) for transesterification in various types of feedstock-based biodiesel production, due to the high basicity of active sites that enhance kinetic reactivity during the transesterification process. Currently, CaO can be generated

directly from natural waste shell/limestone/chemical Ca salt, which reported comparable characteristics to conventional CaO [41–43]. The high availability of calcium resources makes it a cheap material for various applications.

It was discovered that the waste shells are beneficial for the production of a wide range of value-added chemicals and products, such as 1,2,3-triazoles [44], cyclopentanone [45], 7,8-dihydro-4H-chromen-5(6H)-one [46], dimethyl carbonate [47], steam gasification [48], wastewater treatment [49], soil improvement [50], Portland cement replacement [51] and artificial stone [52]. Xiong et al. [44] studied the synthesis of 1,2,3-triazoles catalyzed by waste oyster shell powders (OSPs)-supported CuBr catalyst (OSPs-CuBr). The copper(I) content of the OSPs-CuBr catalyst was found to have the ability to be reused consistently for eight runs. The authors reported that the prepared OSPs-CuBr catalysts showed high catalytic activity with cost-effectiveness for the larger-scale synthesis of 1,4-disubstituted 1,2,3-triazoles. Sheng et al. [45] investigated the multiple characteristics of the *Scapharca Broughtonii* shell, conch shell and oyster shell derived catalyst for cyclopentanone self-aldol condensation. Dimer obtained from the self-aldol condensation pathway of cyclopentanone can be used as a high-density fuel or perfume precursor.

The synthesis of 7,8-dihydro-4H-chromen-5(6H)-one using a one-pot three-component condensation catalysed by eggshell at ambient temperature was reported by Mosaddegh & Hassankhani [46]. Synthesis of 7,8-dihydro-4H-chromen-5(6H)-one and its derivatives contributed to the potential pharmacological activity and as cognitive enhancers for the treatment of neurodegenerative diseases. Based on the high catalytic activity and reusability, the synthesis was completed in a short time with a high yield. The optimum catalyst loading amount to produce the maximum yield was only 0.1 g of eggshell powder. The catalyst was able to be reused in five runs without losing its catalytic activity. In addition, the authors found that benzylidene malononitrile intermediate was generated instead of 7,8-dihydro-4H-chromen-5(6H)-one when condensation occurred without the utilisation of the catalyst.

Gao & Xu [47] examined the viability of eggshell-derived catalyst for the synthesis of dimethyl carbonate (DMC) from the transesterification between methanol and propylene carbonate (PC). DMC is an important methylation and carbonylation agent, which is substituted for dimethyl sulphate and methyl halide in methylation reactions and for harmful phosgene in polycarbonate and isocyanate synthesis. In "green chemistry" and "sustainable societies", the production and chemical applications of DMC are remarkable for its negligible ecotoxicity, low bioaccumulation and persistency. The maximum value of PC conversion and DMC yield were shown after 1 h under the optimum reaction conditions of 0.8 wt.% catalyst amount, with methanol to PC molar ratio 10:1 in 25 °C and 1 atm, which are 80% and 75%, respectively. The eggshell catalyst was able to be reused at least four times with a minimal deactivation.

Note that waste shell is also widely utilized in the steam gasification process [53,54]. Fan et al. [48] studied steam gasification of Indonesian sub-bituminous KPU coal (KPU) using an innovative composite K_2CO_3-eggshell catalyst in a fixed bed reactor. In this study, eggshells were calcined at a temperature range of 700–900 °C under N_2 atmosphere. The mixture of pure K_2CO_3 and calcined eggshells were impregnated with the KPU. The introduction of H_2O and N_2 gasified the resultant char after completion of the pyrolysis process. The primary product gases were H_2, CO, CO_2 and CH_4. The experiment resulted in improved yields of H_2 and CO in the presence of the composite catalyst with a composition of 15% K_2CO_3 and 5% eggshell. H_2 yield with this composite catalyst was increased by 6% and 123%, respectively, compared to that obtained by utilizing pure K_2CO_3 and no-catalyst. Besides, an increase in carbon conversion rate constant of more than three times in the range of 700–900 °C was also achieved by this composite catalyst, as it reduces the activation energy of gasification by about 38% compared to the no-catalyst reaction.

In addition, waste shells can be used for wastewater treatment. Evidently, Luo et al. [49] utilised waste oyster shell in a bio-contact oxidation tank to treat tidal combined river wastewater. Wastewater quality including chemical oxygen demand (COD), five days' biochemical oxygen demand (BOD_5), salinity and ammonia-nitrogen (NH_3-N), total phos-

phorus (TP) and total suspended solids (TSS) was analysed. According to the average removal percentage of these chemicals (80.05%, 85.02%, 86.59%, 50.58% and 85.32%, respectively), it was confirmed the waste oyster shell bio-filler was efficient in pollutant removal. The oyster shell as active filler indirectly improved the recovery ability of the system in the bio-contact oxidation tank by allowing the microbes from the biofilm that decompose pollutants to attach and grow on it. The growth of microbes and the high porosity of oyster shell reduced the sludge amount form in the bio-contact oxidation tank, thereby ensuring accessibility in the one-year experiment.

Soil contamination has impacted on agricultural toxicity, and thereby threatened human and animal health. Noteworthy, agricultural soil improvement was also achieved by mixing the soil with calcined waste oyster shell. This has been successfully implemented by Bi et al. [50]. Moreover, it was discovered that the amount of heavy metal cadmium (Cd) and arsenic (As) in the soil was remarkably reduced. The oyster shells were calcined at various temperatures between 400–800 °C and it was discovered that higher calcination temperature (800 °C) rendered excellent removal of Cd and As. It is noteworthy to state that the vegetables grown in this improved soil are within the C and A categories regarding food safety standards.

In the case of the construction sector, waste shell partially replaced expensive Portland cement and it was discovered that it has the ability to reduce CO_2 emissions. The mixture of cement, sand, water and eggshell powder for mortar production was investigated by Pliya & Cree [51]. The strength, compression and flexural of the mortar decreased as the replacement percentage of eggshells increased. Hence, the authors suggest that eggshells could act as a filler to enhance these properties. Waste shells were also utilised in the production of artificial stone with high mechanical properties artificial. Silva et al. [52] created artificial stone by mixing oyster shell powder with unsaturated polyester resin. The authors reported that flexural strength of oyster shell stone (20 $\pm$ 2 MPa) was higher than marble (natural stone) and even than Aglostone (marble powder plus polyester resin). The authors also inferred that the flexural strength of oyster shell stone might be improved to 50MPa by adding glass microcrystals which are higher than Marmoglass (>32 MPa). Its hardness was also tested an 1216 $\pm$ 120 MPa was obtained which is comparable with marble (1471 MPa). This shell stone is currently is available for countertops and worktops, laboratory benches, etc. Based on the above findings, it can be summarized that waste shells are beneficial for a variety of applications. Since the waste shell is a renewable and cheap alternative, its implementation in a variety of applications will not only simultaneously decrease manufacturing cost, but also reduce the burden on the environment and ecological system.

Based on the above applications of waste shell, obviously it is very promising to be used as catalyst for effective production of biodiesel; hence, this paper focused on a detailed review of natural waste shell as catalyst for biodiesel production [55]. To date, many studies have reported that Ca^{2+} ion from CaO catalyst was easily leached out during the reaction, and hence the CaO-catalysed reaction is still far from using an ideal catalyst. Indeed, the limitation of CaO has been solved chemical modification, such as incorporation of AMO, transition metal oxide (TMO) or metal functionalization approaches. Several reviews focused on commercial CaO and eggshell-derived CaO for biodiesel production [56,57]. In the present study, we aim to discuss the remarkable progress of waste shell-derived CaO for biodiesel production from 2011–2020, besides a comparative study of transesterification activity summarized for conventional CaO, waste shell-derived CaO and modified waste-shell-derived CaO catalysts. The review will highlight the reaction mechanism of both CaO and modified CaO derived from waste shells for biodiesel production. Lastly, the review summarizes the existing technology of reactor systems for advance biodiesel production.

1.1. Solid Base Catalysts

Solid based catalysts are principally referred to as a heterogeneous system in the reaction medium, where the solid surface consists of active sites that act as a Bronsted base

(proton acceptor) or Lewis base (electron-pair donor) [58]. There are a few characteristics for a catalyst to be recognised as a solid base catalyst. First, when the surface is characterised, it shows that the basic sites exist. Secondly, the catalyst shows a correlation effect between catalytic activity and the basicity density as well as the distribution strength of basicity. Thirdly, the reaction pathways are similar to the base-catalysed reactions in a homogeneous system. Lastly, the generation of anionic intermediates during the reaction indicates the presence of a base-catalysed pathway [59]. AMOs including MgO, CaO, SrO, and BaO, have been intensively studied as heterogeneous basic catalysts for transesterification of triglycerides with methanol [60]. The basic strength increased in the order of MgO < CaO < SrO < BaO, which was attributed to the decrease in electro-negativity of the conjugated metal cation of AMO. Note that the catalytic activities of transesterification exhibited in the same sequence. Among these AMOs, CaO exhibited promise as a heterogeneous catalyst for biodiesel production [58,61,62]. It is noteworthy to mention that CaO is less soluble in methanol, stable at high temperature, possesses high reaction activity, is non-toxic, naturally abundant and cheap [63,64]. Faruque et al. (2020) [18] reported that CaO showed high stability and long life span especially for moderate reaction conditions. Similar findings were observed [65–67], where the majority of the CaO catalysts exhibited greater reusable capability (>5 cycles) without undergoing any regeneration process.

1.2. Waste Shell-Derived Catalyst

World aquaculture production is increasing rapidly as seafood demand grows and marine capture production stalls. Commercial mollusk shells (referred to as mollusks or shellfish) are an important food component for the global economy, where the commercialisation of mollusks is in second place at a worldwide level. Annually, about 23% (~16.1 million tons) of mollusks are produced, which is equivalent to 19 billion USD [52,57]. According to the FAO global Fishery and Aquaculture statistics database, there are 79 mollusk species listed as cultured and 93 species considered as captured species. They can be classified into four major groups: clams, oysters, mussels and cockles. The clam and oyster are the most prevalent that contribute, 38% and 33%, respectively, to global production [68]. Based on the overview of mollusk farming, Asia has been the main producer of mollusks, followed by Europe and the Americas. China is the leading producer for mollusks (83.4%) followed by Japan (2.2%), South Korea (1.9%), Thailand (1.4%) and Vietnam (1.2%) [57,69]. In 2016, Asia yielded 158.35 million tonnes out of 171.39 million tonnes for total global production [70]. When considering the mollusks' role as a global food source, one of the most worrying factors is the huge amount of residue generated. Most of the waste shells are deposited in landfills, abandoned on land, or returned to the sea, thus causing incalculable environmental impacts. When the aquaculture wastes are deposited in the soil, it will contaminate the environment and create an unfavorable strong odor [52]. Apart from mollusk shells, eggshells are also widely generated during food processing and manufacturing plants as by-products [71]. Eggs represent the main ingredient in a variety of food products such as cakes, salad dressings and fast foods, whose production results in several daily tons of eggshell waste, and incurs considerable global disposal costs. About 250,000 tons of eggshell waste is produced annually worldwide [72]. Similar to the scenario of mollusk waste shell, improper disposal of waste eggshell will result in environmental odor from biodegradation. Thus, it is strongly suggested that all of the waste shells should be recycled, reused and channeled as a valuable product for different applications. Indeed, utilization of waste shell is a priority for sustainable development achievement. Nowadays, waste shells are reused and refined in various fields, such as water treatments, cosmetics, toiletries, food, agrochemicals, bioenergy and pharmaceuticals [70]. Interestingly, waste shell can be potentially used as a bio-based calcium source of catalyst for biodiesel production. Notably, the use of waste shell in biodiesel production is in line with the purpose of the biodiesel development, which is a greener and environmentally friendly product.

1.3. Composition of Waste Shell

Many invertebrates have produced hard-shells composed of crystallized biogenic minerals to protect and support their soft bodies [73]. The major component in the shells is calcium carbonate (calcite) with a composition of approximately 95–99% [54,57,74]. Other than calcium carbonate, mollusk shells also contain organic matrix proteins as secondary compositions, which are known to be important for the nacreous layer and critical in calcification [73]. Mollusk shells are divided into three main layers which are the periostracum, prismatic and nacreous layers. The periostracum layer is the external layer that is composed mainly of conchiolins. The middle layer is called the prismatic layer, which is mainly made up by oriented calcite crystals. The inner pearlite layer is mainly composed of orientated aragonite crystals [75].

In the case of eggshell, it can be classified as membranous for snakes and lizards; pliable for most turtles; and rigid for certain turtles and geckos and all species of crocodiles, birds and dinosaurs. The eggs of the avian species are the highest grade of amniotic eggs among oviparous vertebrates. Eggshell is a complex bio-ceramic that allows the regulation of metabolic gas and water exchange, and its properties can be finely tuned according to the environmental conditions of a given species. Calcium carbonate (calcite) is the main component in eggshell, and is the major inorganic substance found in an egg that makes up about 98% of the chemical composition [76]. Other minor components in eggshell are Mg (0.9%) and P (0.9%) [77].

There are four main polymorphs of calcium carbonate, which are calcite (b-$CaCO_3$), vaterite (m-$CaCO_3$), aragonite (l-$CaCO_3$) and amorphous calcium carbonate. Calcite, aragonite and vaterite are polymorphs in nature in order of increasing stability and can co-exist in numerous marine organisms [78,79]. Noteworthy, calcite with rhombohedral structures is the most stable polymorph of calcium carbonate followed by orthorhombic Aragonite. It forms elongated structures called columns, palisades or crystallite. The presence of magnesium (Mg) in aragonite creates weaker bonds in the crystal structure; thus, it is more soluble. Vaterite with a hexagonal structure, which is the most unstable polymorph, readily transforms into aragonite or calcite at room temperature. Therefore, only a small amount of vaterite can be found in nature [80–82]. Other than calcium carbonate, some shells are also composed of chitin. For example, the major composition of oyster shells is calcium carbonate with a chitin outer layer, and an inner layer consisting of calcite (90%) and aragonite (10%) [83]. Chitin is one of the most widely abundant biopolymers in the waste shell, next to cellulose. Chitin is made up of α-(1-4)-linked 2-acetamido-2-deoxy-D-glucose with β-(1→4) linkage, known as oligomer. Commercial chitin is mostly extracted from crustacean shells. About 40 wt.% of waste shells is composed mainly of chitin, lipid, meat offcuts, calcium carbonate and pigments [78]. Depending on the species and cultivation condition of the aquaculture, the composition of chitin in shells will differ from 15–40%. Despite this, the highest composition chitin is tightly bound with calcium (20–50%) and proteins (20–40%) that give a structural stiffness to the shell. Hence, multiple steps of pretreatment are required to recover each component [84].

2. Recent Trend in Waste Shell-Derived Catalyst for Biodiesel Production

Valorisation of waste shell rich calcium as natural material for catalyst synthesis is an outstanding topic. It is considered to be environmentally friendly and provides various beneficial impacts on the biodiesel industry. Figure 2a shows that the scientific investigation of biodiesel production in the presence of a catalyst is widely available; here the statistics indicate an increment from 579 publications in 2010 to 950 publications in 2020. The report indicates that within 10 years (2010–2020), China was the country with the highest number of publications in this field, with 1415 out of 8409 publications from around the world, followed by India (1383) and Malaysia (816) (Figure 2b). However, there are only about 205 publications related to waste shell-derived catalyst (Figure 2c). Figure 2d reveals the trend of countries with publications related to waste shell-derived catalyst for biodiesel production from 2010 to 2020. It can be seen that India has published 55 studies

on the subject, which accounts for 3.98% of total publications. Malaysia comes in second with 39 publications, 4.78% of the total. Publications from Thailand (23), China (19) and Indonesia (19) are also relatively high in number when compared to other countries.

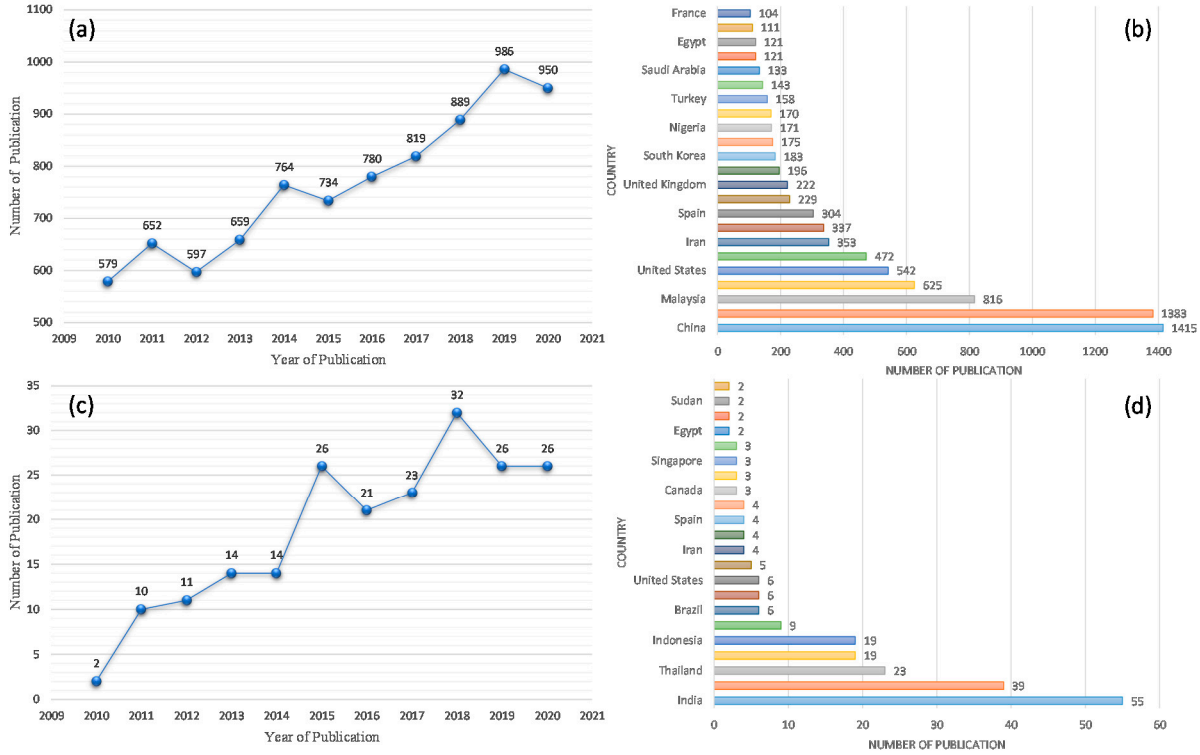

Figure 2. (**a**) Publication trends on biodiesel production in the presence of catalyst from 2010–2020, (**b**) Publications on biodiesel production in the presence of a catalyst based on country from 2010–2020, (**c**) Publication trends on waste shell catalyst in biodiesel production from 2010 to 2020, (**d**) Publications on waste shell catalyst in biodiesel production based on country from 2010–2020 (data collected from SciFinder Database).

3. Waste Shells vs. Modified Waste Shells Catalyst

3.1. Waste Shells-Derived Catalyst for Biodiesel Production

Table 1 presents various types of waste shell-derived catalysts for transesterification of vegetable oil. The majority of the waste shells can be transformed into active CaO after calcination at a temperature within the range of 800–1000 °C. It can be seen that the majority of the pure CaO derived from waste shells successfully converted the low FFA feedstock (palm oil, Camelina Sativa oil, soybean oil and some low FFA waste cooking oil) into biodiesel [74,85–92]. High biodiesel yield (90–97%) was achieved by Hangun-Balkir [74] from transesterification of Camelina sativa oil (FFA: 1.6%) over waste eggshell and lobster shell-derived catalysts. Both waste shells were prepared by calcination at 900 °C. The transesterification was catalysed by 1% (*w*/*w*) catalyst loading with 12:1 MeOH:oil molar ratio at 65 °C for 3 h. The authors compared the biodiesel yield that was catalysed by commercial CaO, waste eggshell and lobster shell. The maximum biodiesel produced was 99%, 97% and 90%, respectively. Buasri et al. (2013) [86] used waste mussel, cockle and scallop shell as a catalyst for transesterification of palm oil (FFA: 0.1%) at 65 °C with MeOH:oil molar ratio of 9:1 within 3 h and 10 wt.% catalyst loading under 1 atm pressure in a glass reactor. The waste mussel shell-derived catalyst with a large surface area of 89.91 m^2/g and pore volume of 0.130 cm^3/g produced 97.23% of biodiesel. However, scallop (74.96 m^2/g, 0.097 cm^3/g) and cockle (59.87 m^2/g, 0.087 cm^3/g) shell-derived catalysts produced 96.68% and 94.47%, respectively. Reusability is the most important feature of heterogeneous catalysts in industrial applications. Based on former literature,

the majority of waste shell-derived CaO catalysts can be reused up to five times without further undergoing regeneration treatment [74,88,93,94]. Notably, Laskar et al. successfully regenerated the CaO derived from snail shell [92]. After being washed with water and dried, the spent catalyst was reactivated at 900 °C for 4 h. The experimental results showed that 91% of biodiesel yields were obtained consistently within the eighth run but dropped to 77% sharply in the ninth cycle over the regenerated catalyst, suggesting that the active sites of pure CaO catalyst could be recovered after undergoing the regeneration process. It is worth mentioning that, based on Table 1, the majority of pure CaO derived from shell still exhibited lower catalyst stability.

When comparing the conventional reflux system with microwave-assisted transesterification, it was observed that the use of a microwave system successfully converts the biodiesel within a shorter reaction time [95]. This fact was in agreement with Khemthong et al. [87], whereby an effective transesterification activity on palm oil (FFA: 0.55%) using CaO derived from waste eggshells using the microwave at 900 W has been achieved within 4 min. This method improved the transesterification rate as compared to the traditional heating method for biodiesel production. Various conditions were tested to obtain the optimum condition in order to carry out transesterification reaction. Overall, the authors produced a maximum biodiesel yield of 96.7% using 15 wt% of catalyst loading amount and MeOH:oil molar ratio of 18:1 at 122 °C. The effectiveness of microwave technology is due to the presence of electromagnetic radiation that transmits energy directly to the molecule of reactants, thus resulting in intense local heating able to accelerate molecular restructuring. Some studies [87,90,93] reported on microwave-assisted biodiesel production and noted that high microwave power could accelerate the reaction and improve product yield in a short time (4–5 min).

Waste cooking oil (WCO) refers mainly to frying oil used at high temperatures, edible fat mixed in kitchen waste and oily wastewater [96] and has been shown to have a high content of acidic compounds (FFA: >3%) [97]. The amount of FFA from feedstock is an important criterion for catalyst selection. WCO with high FFA concentration will result in increased soap formation with an alkaline catalyst, so it needs to be pretreated with an acid catalyst to reduce FFA concentration [98]. Due to this reason, it can be suggested that the WCO with low FFA value will easily trans-esterify to biodiesel. Evidently, Aitlaalim et al. [88], Lin et al. [90] and Sirisomboonchai et al. [91] successfully transesterified the WCO with FFA value within the range of 0.30–0.61%. It was found that the biodiesel yield was within the range of 86–94%. Since the FFA for these WCO is lower than 3%, an undesired saponification reaction would not occur during the transesterification reaction.

Although waste shell-derived CaO are effective catalysts for transesterification of low FFA feedstock with high biodiesel yield (90–99%) and high reusability (3–6 cycles), waste shell-derived CaO shows poor performance in the presence of feedstock with high FFA and moisture. The presence of moisture favors hydrolysis of triglyceride to diglycerides and more FFAs, while the presence of FFA with high acidity favors the reaction with the basic CaO catalyst. Generally, CaO-catalyzed transesterification process renders two plausible pathways; the first preferable step is a partial heterogeneous reaction attributed to basic sites of the Ca-O surface; while the second unfavorable step is a homogeneous reaction that contributes to the Ca^{2+} liquid species that leach into methanol, which causes the loss of active sites. The leached Ca^{2+} further reacts with FFA in oil via a saponification process that forms soap as by-product. The formation of soap during reactions resulted in the poisoning of the catalyst surface, which resulted in the reduction of both transesterification reactivity and reusability. Besides, the presence of catalyst-soap suspension in the reaction medium makes the separation between glycerol and biodiesel product difficult and thus reduces the biodiesel yield [99].

Therefore, further modification of CaO derived from the waste shell is needed as this may enhance the hydrophobicity of the catalyst as well as the generation of new acid sites (Lewis or Bronsted acid sites) in CaO system. The presence of both acid-based properties of the catalyst are crucial for the process of biodiesel production, especially highly adapted to a

wide-range of low-cost and high acid oil feedstock. It was noted that Lewis/Bronsted bases sites (attributed to lattice oxide & OH^- phases) favor transesterification of triglyceride oil to ester, while Lewis/Bronsted acid sites (attributed from metal and H^+ phases) favor the esterification process of FFA in oil into ester. Thus, the presence of acid sites from modified CaO appeared to be insensitive to FFAs and moisture and hindered the saponification reaction, which increased yield [100]. Generally, the basic nature and acid active sites of catalysts can be determined by several types of analysis, such as Hammett's indicators (references), and CO_2/NH_3 desorption from thermal programmed desorption (TPD), or a microcalorimetry instrument that provides the basic/acid density as well as the different strength (weak, medium, and strong) of the adsorption profile. On the other hand, in-depth information of Lewis and Bronsted sites for acid-based profile, usage of model catalytic reactions, and theoretical/modeling approaches to determine acid-base actives site can obtained from other techniques such as Fourier-transform infrared spectroscopy (FTIR), Electron Spin Resonance Spectroscopy (ESR), Nuclear magnetic resonance (NMR), photoluminescence, Raman, UV–Visible Spectroscopy (UV–Vis), and X-Ray Photoelectron Spectroscopy (XPS) [101].

3.2. Modified Waste Shells-Derived Catalyst for Biodiesel Production

As mentioned above, waste shells are natural and renewable resources that can be used for the preparation of CaO-based catalyst. Calcium carbonate in the waste shells can be decomposed to CaO through calcination, which can be used as bio-based material for biodiesel production [74]. Although CaO is highly active for the transesterification process, the CaO is limited in stability and sensitive to FFA content and frequent dissolution and leaching of Ca^{2+} ions. This phenomenon resulted in reduction of catalytic activity during a reusability study, where the leached Ca^{2+} contaminated the biodiesel product at the end of the process [61,102]. Indeed, CaO catalysts have been extensively modified by adding a second or more chemical components to improve its catalytic activity and the stability of the system. Generally, these modified CaO catalysts were prepared via incorporation of AMO, TMO, mesoporous material, and through functionalization approaches.

Based on the previous section, other AMOs including MgO, SrO, and BaO have been intensively studied as heterogeneous basic catalysts for transesterification of triglycerides [60]. Taking into account the superior basicity characteristic for these AMOs [103–105], combining these with CaO derived from waste shell has been focused on. Boro et al. [104] investigated biodiesel production from WCO by using a series concentration of Ba (0.5%, 1.0% 1.5%) doped waste *Turbonilla striatula* shell-derived CaO catalyst. It was found that, as the Ba concentration increased from 0.5% to 1.0%, the basicity properties increased, and reduced when the Ba concentration increased to 1.5%. This author suggested that reduction of basicity is due to reduction in the CaO species. The study revealed that Ba1.0/CaO showed higher biodiesel yield (98%) and the capability to be reused four times. Similarly, Boro's study in transforming Nahor oil (FFA: ~8%) [106] and WCO (FFA: 11%) [104] into biodiesel rich fuel over Ba modified waste shell-derived CaO catalyst and Ba/CaO catalysts, yielded biodiesel of 98%. Mg/CaO synthesized from waste eggshell was also found effective in transesterification of edible waste oil. EDX analyses showed MgO/CaO catalyst consisting of 26.03% calcium, 41.93% oxygen, and 32.04% magnesium. The highest biodiesel yield of 98.37% was produced at the optimum condition of 4.5 wt% catalyst loading amount, 16.7:1 MeOH:oil molar ratio at 69 °C for 7 h with reusability up to six times [105]. Tomano et al. [103] investigated the properties of Sr substituted cuttlebone-derived CaO for the conversion of biodiesel from palm olein. The Sr species were loaded within a range of 1–10 wt.%. Different content of Sr dispersion on CaO surface was indicated by the mapping analysis. However, the rich Sr species on the CaO surface could result in a reduction of BET surface area of the Sr/CaO catalyst. Overall, Sr/CaO with 1 wt.% of Sr loading has the highest BET surface area. The transesterification was carried out in 60 °C with 9:1 methanol/oil ratio and 5 wt.% catalyst loading for 3 h. The 1 wt.% Sr/CaO rendered highest conversion of biodiesel at 95%. Not that the biodiesel

yield produced by AMO doped CaO was mostly >95% and the catalyst can be reused up to >5 times after regeneration treatment.

Transition Metals (TM) such as Zn, Fe, Mn, Al, Mo, Cu, etc., are important materials that have been used in many catalytic reactions. Indeed, TMOs are commonly used in the process of oxidation, dehydrogenation, selective oxidation/reduction, ammoxidation, metathesis, water–gas shift, etc. The unique physicochemical properties of TMOs favour the selective reaction pathways such as surface acidity and basicity, cationic and anionic vacancies, high mobility of lattice oxygen, etc. [107]. Due to the excellent chemical properties of TMOs, the chemical properties of CaO could be tailored through TMO addition. Hence, TMO modified CaO will have both acidic-basic sites, which actively convert high FFA feedstock to biodiesel via both esterification and transesterification processes [108]. Evidently, Joshi et al. [109] successfully converted high FFA feedstocks (Jatropha (6.25%) and Karanja oils (8.75%)) over Zn, Fe, Mn and Al-doped CaO derived from eggshell to biodiesel. Interestingly, the specific surface area and basicity character of TMO doped CaO catalyst are greater than for pure CaO. The high basicity character of TMO modified CaO is possibly due to the existence of synergistic interaction between the multi-metal ions. The authors also stated that the electron-donating property of oxygen anion in the TMO makes the combined metal ions more electropositive, which may lead to the formation of more Lewis base sites on the surface of CaO. As expected, the TMO doped CaO effectively transesterified and esterified the high FFA feedstocks with yield within a range of 76–98% and have the ability to be reused for four cycles with a biodiesel yield within the range 92–95%. Similarly, Rahman et al. reported on the transesterification of eucalyptus oil by using Cu and Zn doped CaO derived from eggshell [110]. Zn doped CaO exhibited excellent basic sites, a larger surface area and pore volume than Cu doped CaO and CaO itself. The transesterification of eucalyptus oil was performed at the optimum condition: 5 wt.% catalyst loading, 6:1 MeOH:oil molar ratio, 65 °C for 2.5 h. The biodiesel yield for catalyzed transesterification of eucalyptus oil was in the sequence of Zn/CaO > Cu/CaO > CaO. The authors reported the reusability of the Zn/CaO up to seven times with the yield of the biodiesel maintained > 85% to the sixth run. The effectiveness of TMO modified CaO was agreed by Kaur and Ali's study, in which the transesterification of jatropha oil occurred over Mo doped CaO at reaction parameter: 12:1 ethanol to oil molar ratio, 65 °C using 5 wt.% of catalyst loading within 4.5 h of reaction time. The results showed that 99% of biodiesel was achieved and the catalyst can be reused up to five times [111]. Das et al. [112] utilised cobalt-doped waste eggshell derived CaO catalyst, in the conversion of lipid extracted from *Scenedesmus quadricauda* species algae to biodiesel. In this work, about 98% of algae oil was successfully converted into biodiesel over Co/CaO catalyst. Note, the Co/CaO exhibited stable activity for at least three reaction runs. The authors remarked that partial leaching of the Co and deposition of reaction products to the catalyst active sites were the possible reasons for lower catalyst stability. More recent studies for biodiesel production using TMO doped CaO derived from waste shell (W-Mo/CaO, Zn/CaO and Fe_3O_4/CaO) have been reported by Mansir et al. [113], Borah et al. [114] and Helwani et al. [115]. In general, the TMO doped catalyst produced high biodiesel yield within the range 90–97% and reported that these catalysts can be reused in up to five consecutive runs. The above findings suggest that TMO modified CaO catalyst has been found to be the most promising technique in overcoming the dissolution of active Ca^{2+} and improving the catalyst stability.

Functionalization is a treatment incorporating other chemical elements or compounds such as alkaline (KOH, NaOH, KF) and acid (H_2SO_4, HCl, HSO_3CI) to tune desirable characteristics in the catalyst [116]. Alkaline functionalisation is an approach to improving the surface area and pore volume of the catalyst [117], while acid functionalisation will improve the acidic properties of the catalyst. Thereby, the acid functionalised CaO catalyst is capable of converting high FFA feed to biodiesel via esterification [118]. This is evinced by Nurhayati et al. finding [118], with sulfonated blood clam shell catalyst (CaO treated by 3M H_2SO_4) effectively converting both FFA and TAG to a high yield of biodiesel

(~97%) under reaction conditions: 12:1 MeOH:oil molar ratio, 60 °C for 3 h using 1 wt.% catalyst loading. Cho and Seo [119] also treated quail eggshell with 0.005 M HCl for 2 h and maximum biodiesel conversion of 89% was obtained by transesterification of palm oil at 65 °C within 2 h using 1 wt.% of catalyst and 12:1 methanol:oil molar ratio. Other cases of high FFA microalgae oil were studied by Syazwani et al. [120] with the utilisation of CaO derived from Angel Wing shell catalyst. The CaO catalyst was modified via sulfuric acid treatment and the result indicated that the CAWS-$_{(x)}SO_4$ catalysts were capable of converting the palm fatty acid distillate (PFAD) (FFA: 92%) to biodiesel rich fuel. The optimal biodiesel conversion (98%) from the PFAD was acquired at the reaction temperature of 80 °C, 15:1 MeOH:PFAD molar ratio and 5wt.% catalyst loading for a 3h reaction time [121].

As discussed previously, the alkaline functionalisation approach has been extensively investigated to improve the textural properties of the CaO [117]. This was confirmed by Nurdin et al. [122] in the transesterification of castor oil. Obviously, KOH/CaO derived from mussel shell shows high surface area and pore volume properties. The authors reported the catalyst's reactivity, capable of maintaining biodiesel yield to ~80% for four reaction runs under optimal condition: 6:1 MeOH:oil molar ratio, 2 wt.% catalyst loading, 60 °C for 3 h. Other than KOH, CaO was also modified by alkaline potassium fluoride (KF). Thi & Myat [123] treated the waste eggshell derived CaO with KF in order to promote stronger active sites formation. KF was functionalized with CaO via a wet-incipient method under microwave irradiation. The authors remarked that the composition of Ca and KF in KF/CaO catalyst influenced the catalytic transesterification activity. The study indicated that the maximum yield of biodiesel was not achieved with the high amount of KF, due to over-coating of the catalyst surface by potassium and fluoride components. Biodiesel production was performed at the optimum condition with 8:1 MeOH:oil molar ratio, 5 wt.% catalyst loading at 65 °C for 2.5 h with maximum biodiesel yield of ~95%, while a reusability study showed that KF/CaO only can be reused for up to four runs with biodiesel yield > 80%. The stability of KF/CaO was further compared with pure CaO, when KF/CaO rendered better stability with less Ca leaching. Beyond that, Komintarachat & Chuepeng functionalised KCl on green mussel-derived CaO (CaO_{waste}) for transesterification of WCO under optimum conditions of 4 wt.% catalyst loading, EtOH:oil molar ratio of 10:1, 80 °C within 3 h [124]. The optimum biodiesel yield obtained was 97%. A comparison study was performed between CaO_{com}, synthesised CaO calcined from green mussel shell (CaO_{waste}) and KCl-impregnated CaO waste (KCl/CaO_{waste}), when KCl/CaO_{waste} catalyst was shown as most effective in facilitating the transesterification reaction.

Instead of metal oxide dopant and acid-alkaline functionalization approaches, the CaO can be modified via a hydration–dehydration technique. The hydration-dehydration of CaO catalyst involves the replacement of CO^{2-} with OH^- form Brønsted basic sites [125]. Ahmad et al. [126] treated waste eggshell-derived CaO with the hydration-dehydration method for the transesterification of algal biomass. With this method, the calcined eggshells were refluxed in the water at 60 °C for 6 h, followed by partial thermal treatment. Noteworthy, hydroxylation reaction occurred during water treatment, which simultaneously promoted the hydroxide surface on CaO. When the water-treated samples were sent for partial dehydration process, the attached water molecules were removed from the catalyst lattice, which led to the fractionation of crystallites to smaller sizes (higher surface area) and generation of higher porosity [100]. Ahmed further reported that the yield of biodiesel obtained was 93% under condition of 2 wt.% catalyst loading, 30:1 MeOH:Algal biomass at 60 °C for 3 h [126]. The authors reported that this catalyst was stable for six cycles with an average yield of >85%. A series of Zn doped CaO derived from eggshell (0.5–2 wt.% Zn^{2+} concentration in CaO) nano-catalysts was prepared and employed in the transesterification of WCO [114]. Maximum biodiesel conversion of 97% was recorded under the reaction conditions of 20:1 MeOH:oil molar ratio, 5 wt.% catalyst loading, 65 °C reaction temperature and 4 h of reaction time. Recently, Niju et al. utilized modified CaO derived from eggshell for transesterification of WCO and the result showed that biodiesel

conversion at94% with reusability > 90% for six runs [127]. Similarly, Niju's research study also discovered a high biodiesel yield (97%) from transesterification of WCO over calcination–hydration–dehydration modified CaO. The CaO was produced from *Tellina tenuis* shells [128]. Based on Niju's observation, an excellent porous structure of the CaO catalyst was obtained from this method, and the large surface area confirmed the enhancement of the transesterification process [54,129]. Although several studies proved that the CaO synthesized from the hydration–dehydration approach exhibited excellent transesterification activity, this catalyst is chemically unstable as it possesses low reusability. This was in accordance with our former research group finding [100], where the modified CaO catalyst from natural waste clamshell (*Meretrix meretrix*) was used for transesterification of palm oil. The CaO modified via hydration–dehydration treatment showed high biodiesel conversion (98%) under a reaction time of 2 h, 1 wt.% catalyst loading and 9:1 methanol: oil molar ratio. Unfortunately, the catalyst was only capable of maintaining two runs of reaction with 98% biodiesel yield. Instability of the catalyst is due to the presence of active $Ca(OH)_2$ phases, which partially decomposed during the transesterification reaction. Interestingly, Chen's group [130] replaced the water medium with an alcohol medium during the catalyst's hydration treatment for the purpose of better $Ca(OH)_2$ stability during transesterification. The modified abalone shell-derived CaO (M-CaO_100) was treated by using ethanol in the hydration–dehydration method. Similarly, the ethanol acted as water that partially hydrated CaO to $Ca(OH)_2$ species, the results showing high basic density and excellent textural properties. The study further reported that a 7 wt.% catalyst loading, 9:1 MeOH:oil molar ratio and a reaction time of 2.5 h is required to obtain a biodiesel yield of 96%. In detail, after the fifth run, the biodiesel yield of the M-CaO_100 catalysed reaction dropped from 95.0% to 88.5%. The loss in activity during the reusability process was due to formation of calcium diglyceroxide on the catalyst surface, which resulted in unfavourable reaction between $Ca(OH)_2$ with the by-product glycerol. Overall, the results suggested that the ethanol treatment did not provide a significant stability effect to reduce Ca^{2+} leaching behaviour for M-CaO_100. Based on the above discussion, it is still a great challenge to identify a highly stable solid CaO derived from waste shell for biodiesel reaction.

It can be noted that not all of the literature studies on modification of CaO showed a significant impact on the stability of the catalyst for transesterification of plant-based oil. However, it has confirmed that the CaO catalysts were ineffective in transforming high FFA feedstock to biodiesel. This is due to the partial homogeneous state of CaO (dissolution of Ca^{2+}) and lead to a big challenge for large scale biodiesel production. The high basicity of CaO catalyst is sensitive to the acid characteristics of FFA and the moisture content in low grade feedstock. Therefore, FFA content in oils needs to be kept as low as possible (0.5–1%) to hinder the saponification reaction, because otherwise it will react with the Ca^{2+} to produce soap as by-product. Excessive soap formation inhibits the biodiesel-glycerol phase separation and thus reduces biodiesel yield drastically. Due to this, modification of CaO is necessary to generate the acid sites in the catalyst system. The presence of Lewis/Bronsted acid sites is able to esterify the presence of FFA in low-grade feedstock into ester product without reducing the transesterification reactivity of the catalyst.

Table 1. Summary of various types of waste shell derived catalysts in transesterification of biodiesel production.

Waste Shells	Feedstocks	FFA (%)	Catalyst	Calcination		Transesterification			Conversion/Yield (%)	Reusability (%)	Ref.
				Temperature (°C)	Duration (h)	MeOH:Oil	Catalyst (wt%)	Duration (h)			
Angel Wing Shell	Microalgae Oil	8.03	CaO	805	2	150:1	9	1	84.11	3	[120]
Blood Clam Shells	Crude Palm Oil	<2	H_2SO_4/CaO	900	5	12:1	3	3	96.69	-	[118]
Capiz Shell	Refined Palm Oil	0.10	CaO	900	2	8:1	3	6	92.83	3	[85]
Chicken Eggshell	Jatropha Oil	6.25	ZnO-CaO	900	4	12:1	5	1	98.20	4	[109]
Cockle Shell	Palm Oil	0.10	CaO	1000	4	9:1	10	4	94.47	4	[86]
Crab Shell	Jatropha Oil	6.25	CaO	900	2	18:1	4	5 (min) (Microwave)	92.11	5	[93]
Cuttle Bone	Palm Oil	0.10	Sr/CaO	1000	5	9:1	1	3	95.47		[103]
Eggshell	Palm Oil	0.55	CaO	800	4	18:1	15	4 (min) (Microwave)	96.70	5	[87]
Eggshell	Camelina Sativa Oil	1.60	CaO	900	3	12:1	1	3	97.20	-	[74]
Eggshell	Nahor Oil	<1	Li Doped CaO	800	2	10:1	5	4	95.00	3	[106]
Eggshell	WCO	-	MgO/CaO	900	4	16.7:1	4.5	7	98.30	6	[105]
Eggshell	Eucalyptus Oil	0.56	ZnO/CuO	900	4	6:1	5	2.5	>90	7	[110]
Eggshell	Microalgal Oil	0.37	Co/CaO	900	4	-	1.5	4	98	3	[112]
Eggshell	Palm Oil	0.10	KF/CaO	900	3	8:1	5	2.5	~95	4	[123]
Eggshell	Algal Biomass	-	HD CaO	900	3	30:1	2.1	3	93.44	6	[126]
Grooved Razor Shell	WCO	0.66	CaO	900	-	15:1	5	3	94.00	6	[88]
Lobster Shell	Camelina Sativa Oil	1.60	CaO	900	3	12:1	1	3	90.00	-	[74]
Mussel Shell	Soybean Oil	0.10	KI-CaO	1000	4	6:1	3.5	4	85.00	-	[89]
Mussel Shell	Palm Oil	0.10	CaO	1000	4	9:1	10	4	97.23	4	[86]
Mussel Shel	Castor Oil	1.00	KOH/CaO	1000	1	6:1	2	3	91.17	5	[122]
Oyster Shell	WCO	1.00	CaO	1000	2	9:1	6	3 (Microwave)	87.30	-	[90]
Quail Eggshell	Jatropha Oil	6.25	CaO	900	2	18:1	4	5 (min) (Microwave)	92.78	5	[93]
Quail Eggshell	Palm Oil	0.10	H_2SO_4/CaO	800	-	12:1	0.01 (g)	2	89	-	[119]
Scallop Shell	Palm Oil	0.10	CaO	1000	4	9:1	10	4	96.68	4	[86]
Scallop Shell	WCO	0.62	CaO	1000	2	6:1	5	2	86.00	4	[91]
Snail Shell	Soybean Oil	0.10	CaO	900	4	6:1	3	7 (28°C)	98.00	9	[92]
***Turbonilla Striatula* Shell**	WCO	<1	Ba Doped CaO	900	3	6:1	1	3	>98%	4	[104]

4. Mechanism of CaO Catalysed Transesterification

The most usual foundations for heterogeneous transesterification mechanisms are Eley-Rideal (ER) and Langmuir-Hinshel (LH) [131]. Both mechanisms are a theoretical model of bimolecular chemical reaction that can take place on a solid surface. In the ER mechanism, an atom or molecule adsorbs onto the surface, followed by direct reaction with another atom or molecule attached to the catalyst's surface. However, in the LH mechanism two atoms or molecules are initially adsorbed on the surface of the catalyst, and diffuse across the surface until they are close enough to interact [132]. The ER mechanism for the transesterification process involves three steps (Figure 3a): (i) methanol (M) is first adsorbed on the active site of the catalyst surface (S); (ii) then the triglyceride (TG) reacts with the methoxide ion to form fatty acid methyl ester (FAME) and glycerol (GL); and (iii) finally the glycerol is desorbed from the surface of the catalyst active site [133]. In the case of the LH mechanism, the reaction involves a five-step process. In the first two steps, the methanol and oil are individually adsorbed on the surface of the catalyst and generate two different active sites for further reaction. Both reactants will further react with each other in the following step, which is known as the determining step. The glycerol and FAME produced from the determining step is then desorbed separately in the last two-step of the transesterification process (Figure 3b) [133].

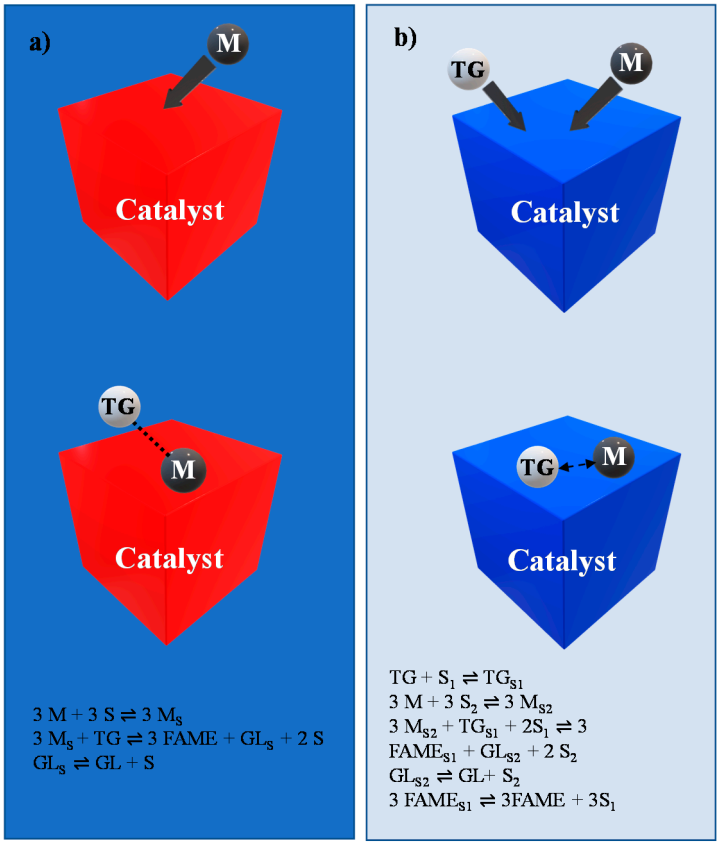

Figure 3. (**a**) Eley-Rideal (ER) mechanism and (**b**) Langmuir-Hinshel (LH) mechanism (data adapted from http://www.chem.ucl.ac.uk/cosmicdust/er-lh.htm).

As mentioned in the previous section, CaO is the most studied alkaline-earth metal oxide catalyst for transesterification. The presence of conjugated oxygen anions on the surface of CaO generates strong Lewis basicity that greatly affects the catalytic activity during the transesterification reaction [134]. The generation of basic sites on the oxide phase of the Ca-O surface plays role in abstracting the protons from the organic matter, which trigger a basic catalytic reaction [135]. Figure 4a illustrates the mechanism of CaO catalysed transesterification. The presence of basic active sites in the CaO catalyst abstracts

the proton from methanol to form a higher catalytic activity methoxide anion (CH_3O^-). The CH_3O^- then carries out a nucleophilic attack on the carbonyl carbon of triglyceride to form the tetrahedral alkoxy carbonyl intermediate. The rearrangement of this unstable intermediate results in the decomposition of the diglyceride anion and the formation of fatty acid methyl ester (biodiesel). Finally, the proton attracts the diglyceride anion to produce diglyceride and regenerate the active site of the CaO catalyst. This mechanism is then repeated twice for another two-carbonyl carbon and glycerol is yielded as a by-product. Both the first and second steps of the complex process of the transesterification of triglycerides and diglycerides with methanol are always much faster than the reaction of monoglycerides, which ultimately produces biodiesel and glycerol [136].

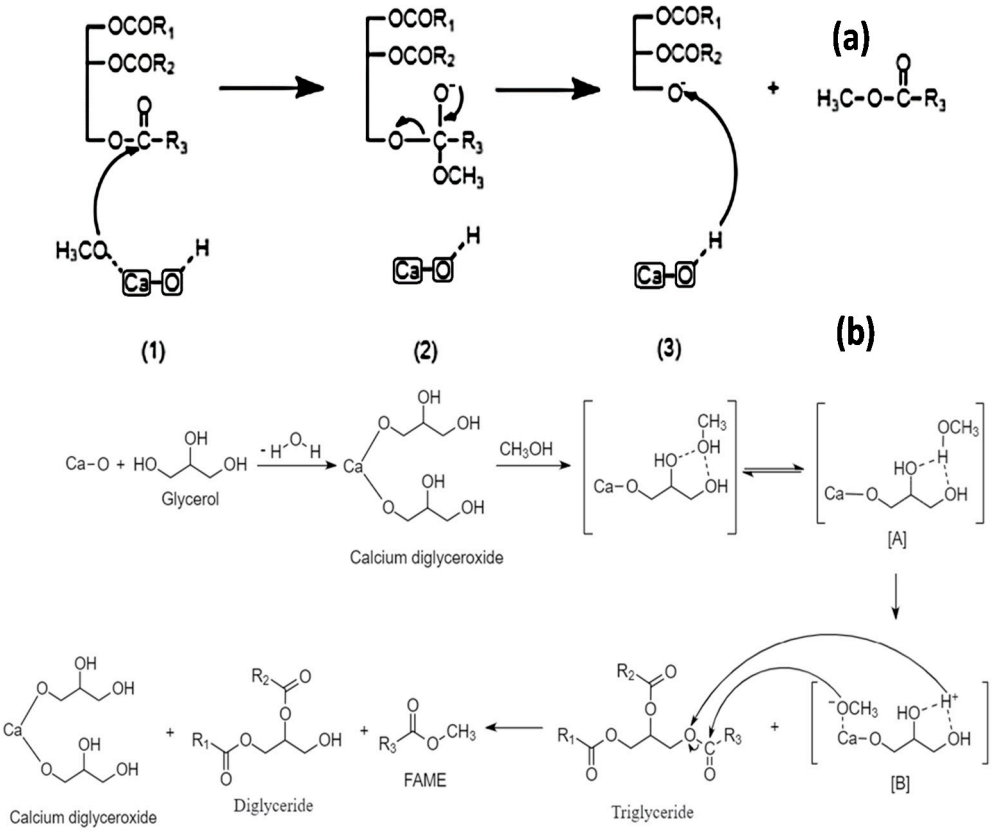

Figure 4. (**a**) Mechanism of CaO catalyzed transesterification (data adapted from [21]) (**b**) Mechanism of CaO reacted with by-produced glycerol in production of fatty acid methyl ester (FAME) (adapted from [137]).

The generated by-product glycerol is a trihydric alcohol, which tend to react with CaO via the dihydroxylation process to form CaO-glycerol complexes, known as calcium diglyceroxide ($Ca[O(OH)_2C_3H_5]_2$). The catalytic activity of these complexes is slightly lower than CaO in transesterification. Figure 4b shows the mechanism of CaO reacted with glycerol. The protons of the methanol are abstracted by two of the –OH groups located next to each other in calcium diglyceroxide and contribute to the establishment of intermolecular hydrogen bonding to generate species A and B. Species B then reacts with triglycerides to yield biodiesel. Calcium diglyceroxide is finally regenerated and makes the process self-repeating, which further enhances the transesterification reaction [131,135,137].

5. Recent Progress of Reactors Used for CaO and Waste Shell Catalyzed Transesterification

Generally, the lab-based transesterification and esterification process is conducted by using a three-neck round-bottom flask fitted with a reflux condenser, magnetic stirrer and a thermometer with water cooling condenser (Figure 5a) [114,138]. Notably, the ma-

jority of the waste shell catalyzed transesterification focused on the reflux distillation system [129,139]. The conventional heating system for biodiesel production has shown some drawbacks. Limitations typically are the dependence on the thermal conductivity of the material, the heterogenic heating of the surface and specific heat. To date, these reflux distillation techniques are being replaced by more advanced systems.

In biodiesel production, proper mixing is critically important to create sufficient contact between oil and alcohol. In this context, ultrasonication helps by facilitating the liquid–liquid interfacial area through emulsification, which can effectively generate vapour bubbles and cavitation bubbles in viscous liquids (Figure 5b) [140,141]. The ultrasound in the chemical processing enhances both the mass transfer and chemical reactions, offering the potential for shorter reaction times, cheaper reagents and less extreme physical conditions [142,143]. In Teixeira et al. [142] on transesterification of beef tallow, it was reported that using ultrasound irradiation shortens the reaction time (70 s). Obviously, the transesterification of beef tallow using ultrasound irradiation had a biodiesel conversion (92%) that was comparable to the conventional method (reflux distillation system) that needed 1 h (91%). Note that the quality of the biodiesel was like biodiesel produced with the conventional method. These finding suggest that the process involving ultrasonic irradiation could be a feasible and effective method for the production of good quality biodiesel from beef tallow. Recently, Wilayat et al. [144] produced biodiesel from WCO by using CaO assisted by ultrasonic wave. About 1–4.4% of catalyst is used for the biodiesel reaction with the presence of an ultrasonic wave generated from an ultrasonic cleaner at 28 and 42 kHz of frequency. The results have shown a highest methyl ester yield at ~90% using 9:1 MeOH:oil molar ratio and a frequency of 40 kHz. Clearly, the increment frequency of the ultrasonic wave causes an increase in the transesterification rate. The ultrasonic-assisted transesterification of palm oil in the presence of CaO was investigated by Mootabadi [145]. The reaction process was carried out with 20 kHz ultrasonic cavitation, reaction time (10–60 min), MeOH to palm oil molar ratio (3:1–15:1), catalysts loading (0.5–3%) and varying of ultrasonic amplitudes (25–100%). At optimum conditions of 60 min, 95% of biodiesel yield was achieved as compared to 2–4 h under the conventional reflux process. A further study on ultrasonic-assisted transesterification of palm oil with the aid of waste ostrich eggshell-derived CaO was reported in the earlier literature [146]. Under ultrasonic conditions, ~93% of biodiesel yield was achieved under the optimal condition: reaction time: 69 min; MeOH:oil to oil ratio of 9:1, catalyst loading of 8 wt.%.

Microwave irradiation provides an alternative energy source suitable for use in heating of the transesterification process. During transesterification of oil-based triglyceride with alcohol, the microwave system is able to activate the smallest variance in degree of polar molecules and ions, such as alcohol (R–OH), with a continuously changing magnetic field. The varying electric field resulted in an interaction between the triglyceride and alcohol ions (R–O–), thereby rapid rotation occurs between the reaction medium, which further generates heat attributed to molecular friction. Hereafter, the microwave-assisted system will accelerate the generation of heat and pressure from the reaction medium, which supports further decomposition and re-structuring of the molecular structure, and increases the mass transfer rate. It can be suggested that the high conversion of triglyceride into desired biodiesel will be attained within a shorter reaction period [147,148]. It is noteworthy that the former literature also revealed that the microwave system might enhance reaction rate, purity and yield of product in biodiesel synthesis [149,150]. Figure 5c shows an example of a modified Samsung 1000 W 2450 Hz household microwave oven. Two holes were drilled in the top of the domestic microwave oven, one to position the stirrer and the other to shift the thermocouple inside the microwave. The microwave was fitted with a mechanical stirrer, which was powered by a motor to replace the carousel. The thermocouple was attached to a USB-5104 4-channel thermocouple logger. For this experiment, a one-litre beaker was supplied and a separation funnel was used to isolate the biodiesel from the reaction mixture. The reaction analysis was conducted by varying microwave power input, catalytic loading and methanol to oil molar ratio. Although the application of a modi-

fied household microwave for biodiesel synthesis is an effective and low-budget study, its application is still not considered as ideal for scientific experiments due the lack safety features such as overpressure guard, temperature control regulator and power control, etc. Due to this concern, researchers continue to discover the potential of a microwave-assisted system for biodiesel synthesis [93,151,152]. The efficiency of the microwave reaction system has been further proved by Liou and Chung in the microwave-assisted transesterification of Jatropha oil over KOH impregnated CaO catalyst [151]. The optimum condition for producing the highest yield of biodiesel was as follows: 8.42 MeOH:oil molar ratio, 3.17% catalyst loading and total reaction time of 67.9 min. The average conversion for three repeated experimental runs at optimum condition was found to be 97.1%. The biodiesel obtained also had properties satisfying the desired standards. Similarly, Zamberi and his partners reported the utilization of CaO derived from waste cockles on the biodiesel production of WCO via a microwave heating system. Within 4 min, more than 95% yield concentration was recorded through the microwave irradiation method [153]. This was based on Buasri and Loryuenyong's findings on biodiesel production from jatropha oil over CaO derived from eggshell via a microwave-assisted reaction system [93]. Apparently, rapid transesterification reaction is observed which yielded a conversion of oil of nearly 94%, reaction time 5 min, microwave power 800 W, MeOH:oil molar ratio 18:1, and catalyst loading 4 wt.%. Overall, based on these studies, it is highly affirmed that the transesterification assisted by the microwave-assisted method improved biodiesel yield, quality and reaction rate. When comparing the technology effectiveness of biodiesel production by using the ultrasound irradiation, ultrasonic wave and microwave reaction systems, it was observed that the transesterification process under ultrasound irradiation is much faster. This is due to a collapse of the cavitation bubbles and ultrasonic jets that impinge feedstock to methanol, disrupting the phase boundary and causing emulsification. Overall, the ultrasound irradiation method is the most promising alternative heating source for the biodiesel industry.

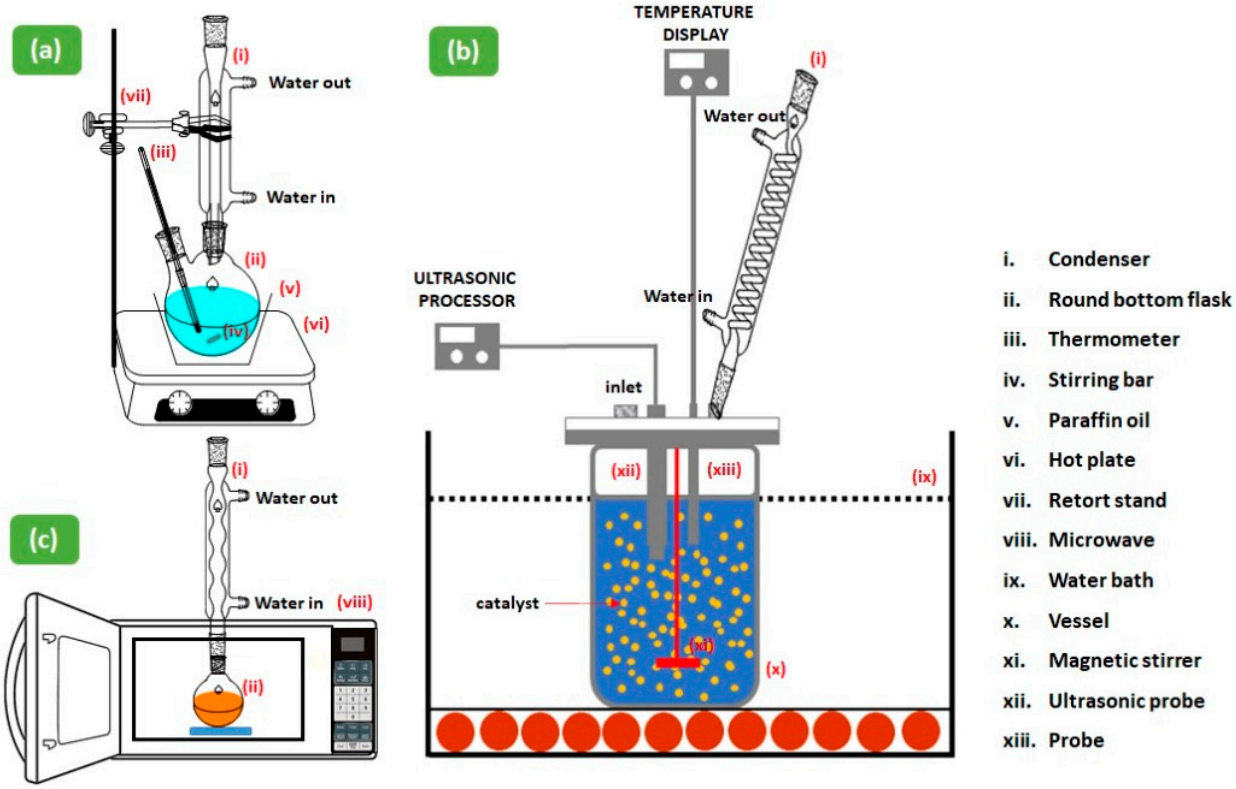

Figure 5. (**a**) Set up of transesterification reaction, (**b**) Component part of ultrasonic-assisted transesterification (adapted from [141]) (**c**) Transesterification by using a batch process within a modified Samsung 1000 W 2450 Hz household microwave oven (adapted from [152]).

6. The Challenge of Waste Shell-Derived Catalyst and Advance Reactors for the Biodiesel Industry

Calcium-rich waste shell materials as a low-cost green resource are readily available around the world. Utilization of the waste shell modified catalyst is a tremendous prospect for the biodiesel industry. Yet, there are still challenges for further improvement on an industrial scale. This is due to the instability of CaO catalyst which commonly suffers from Ca^{2+} leaching problem [135]. Other problems such as low surface area, water sensibility, leaching of active sites by glycerol, and competing with soap-forming side reactions have afflicted the utilization of waste shell-derived CaO catalysts. According to the research work done by Kouzu and Hidaka, the leached Ca^{2+} is increased when there is excess water content in the reaction medium [135]. This is noteworthy to mention, since Ca^{2+} easily dissolves and leaches into the reaction product; hence, additional advance separation and purification are needed to extract Ca^{2+} ions from the biodiesel. Thus, it will produce a significant volume of wastewater during the purification process. Furthermore, the CaO catalyst was often easily deactivated by water or CO_2 [154]. Due to the adsorption of CO_2 and humidity, the CaO surface is readily contaminated by moisture attachments and transforms to $CaCO_3$ and $Ca(OH)_2$, respectively. This $Ca(OH)_2$ phase will apparently act as a partial homogenous catalyst in the transesterification reaction, hence leading to the increment of Ca^{2+} leaching species. Based on the above discussion, the instability of CaO derived from waste shells can be resolved by combining the CaO with other chemical compounds such as AMOs, TMOs and functionalization approaches. Moreover, alkaline metal and transition metal are considered inexpensive materials, which do not significantly contribute to the overall production cost when the catalyst can be reuses for many runs under a simple purification process as compared to a homogeneous [154].

In the case of reactor design, although intensification systems such as microwave- and ultrasonication-assisted transesterification offer the opportunity to save operation time as well as improve productivity, one of the limitations of microwave scale-up technology for industrial purposes is the restricted penetration depth of microwave irradiation into absorbing materials. Weissman et al. [155] reported that the penetration depth of microwave irradiation is limited to 2–5 cm and therefore the vessel size cannot be expanded unrestrictedly. High microwave power may also lead to rapid input of energy into the reaction and to overheating. Another issue is related to the homogeneity (inhomogeneity may lead to hot spots and product degradation) and stability of solvents, reagents, and products at temperatures higher than 200 °C. The continuous occurrence of instability and degradation of the reaction mixture will result in safety issues.

As a consequence of microwave input, the system will result in a rise in pressure during the reaction; hence the construction materials for the microwave reactor must be able to withstand high temperatures and high pressure (e.g., 250 °C, 20 bar). Based on this fact, it is believed that the implementation of ultrasonication scale-up technology will face additional issues including the implementation of the ultrasonic homogenization system. This technique is very important in producing chemical and physical effects that arise from the collapse of cavitation bubbles. As reported by Shinde and Kaliaguine, high-frequency ultrasound (~40 kHz) will rapidly increase the rate of transesterification reaction and hence increase biodiesel yield [140]. As a consequence, the ultrasound amplitude and power should be carefully controlled for up-scaling purposes. Noteworthy to mention is that, when comparing microwave- and ultrasonication-assisted method, the ultrasound offers a much cheaper process and less extreme physical conditions. Despite the large number of studies that have investigated ultrasonic-assisted biodiesel production [142,156], it appears that there has been no thorough study conducted on the use of ultrasound for improving biodiesel production for scale-up purposes.

7. Conclusions

Natural waste shells are rich in calcium that is potentially convertible into Ca-based catalyst for biodiesel synthesis via transesterification/esterification pathways. Generally,

the calcium is present in the form of calcium carbonate (95–99%), and further treatment is required in order to expose the calcium active phases (e.g., oxide or hydroxide phases) for further reaction. The waste shell-derived CaO or $Ca(OH)_2$ shows similar characteristics to the conventional form, such as basicity and surface area. It was noted that both properties, especially the high basicity density and strong basic strength of catalyst, greatly enhance the transesterification rate for biodiesel production. However, the present form of waste shell-derived catalysts is still limited in use for feedstock with high free fatty acid or high moisture content found in non-edible oil and waste cooking oil. Unfavorable side reactions occurred between Ca from waste shell-derived catalysts with FFA or moisture to form unwanted soap product, and the ease of dissolution of catalyst by Ca leaching, respectively. Thus, further modification of waste shell-derived catalysts has been extensively studied by researchers to improve the stability of catalyst, as well as resist FFA/moisture in the feedstock. The modification can be performed via incorporation of alkaline metal oxide, transition metal oxide, and functionalization with chemicals (KOH, NaOH, KF, H_2SO_4, HCl, HSO_3CI) to tune the acidity-basicity of active sites and textural properties of waste shell-derived catalysts. The findings show that the transesterification reactivity significantly improves with higher biodiesel yield, as well as a better reusability profile. Other than modifying the waste shell-derived catalyst, intensification of transesterification was performed by using microwave- or ultrasonic-assisted technology to replace the conventional reflux heating, with short operation time as well as clean biodiesel product. However, implementation of this technology for scale up biodiesel production must meet the challenge of construction and operating cost. Thus, continuous development of reactor technology for biodiesel production is in progress to strive for better ecological processes.

Author Contributions: Conceptualization, N.A.M.; validation, H.V.L.; data curation, M.S.M.; writing—original draft preparation, H.K.O., X.N.K.; writing—review and editing, N.A.M., H.V.L., H.C.O., M.S.M. and Y.H.T.-Y.; supervision, N.A.M.; funding acquisition, N.A.M., A.A.A., F.A.A. and H.V.L. All authors have read and agreed to the published version of the manuscript.

Funding: This research was funded by Galakan Penyelidik Muda (GGPM) (GGPM-2020-015), University of Malaya's Research Grant:MOHE-Top 100 (IIRG)-IISS (IIRG002A-2020IISS), International Scientific Partnership Program ISPP at King Saud University for funding this research work through ISPP-142.

Institutional Review Board Statement: Not applicable.

Informed Consent Statement: Not applicable.

Acknowledgments: We are grateful to the financial support from Galakan Penyelidik Muda (GGPM) (GGPM-2020-015), University of Malaya's Research Grant:MOHE-Top 100 (IIRG)-IISS (IIRG002A-2020IISS) and International Scientific Partnership Program ISPP at King Saud University for funding this research work through ISPP-142.

Conflicts of Interest: The authors declare no conflict of interest.

References

1. Lee, S.Y.; Sankaran, R.; Chew, K.W.; Tan, C.H.; Krishnamoorthy, R.; Chu, D.-T.; Show, P.-L. Waste to bioenergy: A review on the recent conversion technologies. *BMC Energy* **2019**, *1*, 1–22. [CrossRef]
2. Rathore, D.; Nizami, A.S.; Singh, A.; Pant, D. Key issues in estimating energy and greenhouse gas savings of biofuels: Challenges and perspectives. *Biofuel Res. J.* **2016**, *3*, 380–393. [CrossRef]
3. Sharvini, S.R.; Noor, Z.Z.; Chong, C.S.; Stringer, L.C.; Yusuf, R.O. Energy consumption trends and their linkages with renewable energy policies in East and Southeast Asian countries: Challenges and opportunities. *Sustain. Environ. Res.* **2018**, *28*, 257–266. [CrossRef]
4. Ong, H.C.; Chen, W.-H.; Farooq, A.; Gan, Y.Y.; Lee, K.T.; Ashokkumar, V. Catalytic thermochemical conversion of biomass for biofuel production: A comprehensive review. *Renew. Sustain. Energy Rev.* **2019**, *113*, 109266. [CrossRef]
5. Ong, Y.K.; Bhatia, S. The current status and perspectives of biofuel production via catalytic cracking of edible and non-edible oils. *Energy* **2010**, *35*, 111–119. [CrossRef]
6. Lee, H.; Wu, W.-H.; Chen, B.-H.; Liao, J.-D. Heterogeneous Catalysts Using Strontium Oxide Agglomerates Depositing upon Titanium Plate for Enhancing Biodiesel Production. *Catalysts* **2021**, *11*, 30. [CrossRef]

7. Chownk, M.; Thakur, K.; Purohit, A.; Vashisht, A.; Kumar, S. *Applications and Future Perspectives of Synthetic Biology Systems*; Elsevier, B.V.: Amsterdam, The Netherlands, 2018; ISBN 9780444640857.
8. Roberts, L.G.; Patterson, T.J. Biofuels. *Encycl. Toxicol. Third Ed.* **2014**, *1*, 469–475. [CrossRef]
9. Sindhu, R.; Binod, P.; Pandey, A.; Ankaram, S.; Duan, Y.; Awasthi, M.K. *Biofuel Production from Biomass: Toward Sustainable Development*; Elsevier B.V.: Amsterdam, The Netherlands, 2019; ISBN 9780444640833.
10. Adav, S.S.; Sze, S.K. *Trichoderma Secretome: An Overview*; Elsevier: Amsterdam, The Netherlands, 2014; ISBN 9780444595768.
11. Muhammad, G.; Alam, M.A.; Mofijur, M.; Jahirul, M.I.; Lv, Y.; Xiong, W.; Ong, H.C.; Xu, J. Modern developmental aspects in the field of economical harvesting and biodiesel production from microalgae biomass. *Renew. Sustain. Energy Rev.* **2021**, *135*, 110209. [CrossRef]
12. Goh, B.H.H.; Ong, H.C.; Cheah, M.Y.; Chen, W.-H.; Yu, K.L.; Mahlia, T.M.I. Sustainability of direct biodiesel synthesis from microalgae biomass: A critical review. *Renew. Sustain. Energy Rev.* **2019**, *107*, 59–74. [CrossRef]
13. Rather, M.A.; Bano, P. Third Generation Biofuels: A Promising Alternate Energy Source. *Integr. Green Chem. Sustain. Eng.* **2019**, 1–21. [CrossRef]
14. Chia, S.R.; Ong, H.C.; Chew, K.W.; Show, P.L.; Phang, S.-M.; Ling, T.C.; Nagarajan, D.; Lee, D.-J.; Chang, J.-S. Sustainable approaches for algae utilisation in bioenergy production. *Renew. Energy* **2017**. [CrossRef]
15. Abdullah, B.; Syed Muhammad, S.A.F.; Shokravi, Z.; Ismail, S.; Kassim, K.A.; Mahmood, A.N.; Aziz, M.M.A. Fourth generation biofuel: A review on risks and mitigation strategies. *Renew. Sustain. Energy Rev.* **2019**, *107*, 37–50. [CrossRef]
16. Mat Aron, N.S.; Khoo, K.S.; Chew, K.W.; Show, P.L.; Chen, W.H.; Nguyen, T.H.P. Sustainability of the four generations of biofuels—A review. *Int. J. Energy Res.* **2020**, *44*, 9266–9282. [CrossRef]
17. Hassan, M.H.; Kalam, M.A. An overview of biofuel as a renewable energy source: Development and challenges. *Procedia Eng.* **2013**, *56*, 39–53. [CrossRef]
18. Faruque, M.O.; Razzak, S.A.; Hossain, M.M. Application of heterogeneous catalysts for biodiesel production from microalgal oil—A review. *Catalysts* **2020**, *10*, 1025. [CrossRef]
19. Demirbas, A. Biofuels sources, biofuel policy, biofuel economy and global biofuel projections. *Energy Convers. Manag.* **2008**, *49*, 2106–2116. [CrossRef]
20. *Reuter Malaysia Palm Oil Output, Exports Forecast to Rise in—MPOB*; Thomson Reuters Corporation: Toronto, ON, Canada, 2017.
21. Boey, P.-L.; Maniam, G.P.; Hamid, S.A. Performance of calcium oxide as a heterogeneous catalyst in biodiesel production: A review. *Chem. Eng. J.* **2011**, *168*, 15–22. [CrossRef]
22. Luna, C.; Luna, D.; Calero, J.; Bautista, F.M.; Romero, A.A.; Posadillo, A.; Verdugo-Escamilla, C. *Biochemical Catalytic Production of Biodiesel*; Elsevier Ltd.: Amsterdam, The Netherlands, 2016; Volume 3, ISBN 9780081004562.
23. Basu, P. Production of synthetic fuels and chemicals from biomass. In *Biomass Gasification, Pyrolysis Torrefaction. Practical Design and Theory*; Elsevier: Amsterdam, The Netherlands, 2018; pp. 415–443.
24. Aydogan, H.; Hirz, M.; Brunner, H. The current use and the future of biofuels. *Int. J. Soc. Sci.* **2014**, *3*, 12–21.
25. Ong, H.C.; Masjuki, H.H.; Mahlia, T.M.I.; Silitonga, A.S.; Chong, W.T.; Leong, K.Y. Optimization of biodiesel production and engine performance from high free fatty acid Calophyllum inophyllum oil in CI diesel engine. *Energy Convers. Manag.* **2014**, *81*. [CrossRef]
26. Khuong, L.S.; Zulkifli, N.W.M.; Masjuki, H.H.; Mohamad, E.N.; Arslan, A.; Mosarof, M.H.; Azham, A. A review on the effect of bioethanol dilution on the properties and performance of automotive lubricants in gasoline engines. *RSC Adv.* **2016**, *6*, 66847–66869. [CrossRef]
27. Hamza, M.; Ayoub, M.; Shamsuddin, R.B.; Mukhtar, A.; Saqib, S.; Zahid, I.; Ameen, M.; Ullah, S.; Al-sehemi, A.G.; Ibrahim, M. Jou rna lP. *Environ. Technol. Innov.* **2020**, 101200. [CrossRef]
28. Xue, J.; Grift, T.E.; Hansen, A.C. Effect of biodiesel on engine performances and emissions. *Renew. Sustain. Energy Rev.* **2011**, *15*, 1098–1116. [CrossRef]
29. Boro, J.; Deka, D.; Thakur, A.J. A review on solid oxide derived from waste shells as catalyst for biodiesel production. *Renew. Sustain. Energy Rev.* **2012**, *16*, 904–910. [CrossRef]
30. Chaveanghong, S.; Smith, S.M.; Smith, C.B.; Luengnaruemitchai, A.; Boonyuen, S. Simultaneous transesterification and esterification of acidic oil feedstocks catalyzed by heterogeneous tungsten loaded bovine bone under mild conditions. *Renew. Energy* **2018**, *126*, 156–162. [CrossRef]
31. Bórawski, P.; Bełdycka-Bórawska, A.; Szymańska, E.J.; Jankowski, K.J.; Dubis, B.; Dunn, J.W. Development of renewable energy sources market and biofuels in The European Union. *J. Clean. Prod.* **2019**, *228*, 467–484. [CrossRef]
32. Thangarasu, V.; Anand, R. *Comparative Evaluation of Corrosion Behavior of Aegle Marmelos Correa Diesel, Biodiesel, and Their Blends on Aluminum and Mild Steel Metals*; Elsevier Ltd.: Amsterdam, The Netherlands, 2019; ISBN 9780081027912.
33. Ong, H.C.; Tiong, Y.W.; Goh, B.H.H.; Gan, Y.Y.; Mofijur, M.; Fattah, I.M.R.; Chong, C.T.; Alam, M.A.; Lee, H.V.; Silitonga, A.S.; et al. Recent advances in biodiesel production from agricultural products and microalgae using ionic liquids: Opportunities and challenges. *Energy Convers. Manag.* **2020**, 113647. [CrossRef]
34. Amini, Z.; Ilham, Z.; Ong, H.C.; Mazaheri, H.; Chen, W.-H. State of the art and prospective of lipase-catalyzed transesterification reaction for biodiesel production. *Energy Convers. Manag.* **2017**, *141*. [CrossRef]
35. Román-Martínez, M.C.; Salinas-Martínez de Lecea, C. *Heterogenization of Homogeneous Catalysts on Carbon Materials*; Elsevier, B.V.: Amsterdam, The Netherlands, 2013; ISBN 9780444538765.

36. Endalew, A.K.; Kiros, Y.; Zanzi, R. Inorganic heterogeneous catalysts for biodiesel production from vegetable oils. *Biomass Bioenergy* **2011**, *35*, 3787–3809. [CrossRef]
37. Zabeti, M.; Wan Daud, W.M.A.; Aroua, M.K. Activity of solid catalysts for biodiesel production: A review. *Fuel Process. Technol.* **2009**, *90*, 770–777. [CrossRef]
38. Khurshid, S.N.A. Biodiesel Production by Using Heterogeneous Catalysts. Master's Thesis, Royal Institute of Technology (KTH), Stockholm, Sweden, 2014; pp. 1–64.
39. Mat, R.; Samsudin, R.A.; Mohamed, M.; Johari, A. Solid catalysts and their application in biodiesel production. *Bull. Chem. React. Eng. Catal.* **2012**, *7*, 142–149. [CrossRef]
40. Lee, H.V.; Juan, J.C.; Taufiq-Yap, Y.H.; Kong, P.S.; Rahman, N.A. Advancement in heterogeneous base catalyzed technology: An efficient production of biodiesel fuels. *J. Renew. Sustain. Energy* **2015**, *7*. [CrossRef]
41. Sahu, G.; Gupta, N.K.; Kotha, A.; Saha, S.; Datta, S.; Chavan, P.; Kumari, N.; Dutta, P. A Review on Biodiesel Production through Heterogeneous Catalysis Route. *ChemBioEng Rev.* **2018**, *5*, 231–252. [CrossRef]
42. Lee, H.V.; Juan, J.C.; Taufiq-Yap, Y.H. Preparation and application of binary acid–base CaO–La_2O_3 catalyst for biodiesel production. *Renew. Energy* **2015**, *74*, 124–132. [CrossRef]
43. Taufiq-Yap, Y.H.; Lee, H.V.; Lau, P.L. Transesterification of jatropha curcas oil to biodiesel by using short necked clam (orbicularia orbiculata) shell derived catalyst. *Energy Explor. Exploit.* **2012**, *30*. [CrossRef]
44. Xiong, X.; Cai, L.; Jiang, Y.; Han, Q. Eco-efficient, green, and scalable synthesis of 1,2,3-triazoles catalyzed by Cu(I) catalyst on waste oyster shell powders. *ACS Sustain. Chem. Eng.* **2014**, *2*, 765–771. [CrossRef]
45. Sheng, X.; Xu, Q.; Wang, X.; Li, N.; Jia, H.; Shi, H.; Niu, M.; Zhang, J.; Ping, Q.W. Waste seashells as a highly active catalyst for cyclopentanone self-aldol condensation. *Catalysts* **2019**, *9*, 661. [CrossRef]
46. Mosaddegh, E.; Hassankhani, A. Application and characterization of eggshell as a new biodegradable and heterogeneous catalyst in green synthesis of 7,8-dihydro-4H-chromen-5(6H)-ones. *Catal. Commun.* **2013**, *33*, 70–75. [CrossRef]
47. Gao, Y.; Xu, C. Synthesis of dimethyl carbonate over waste eggshell catalyst. *Catal. Today* **2012**, *190*, 107–111. [CrossRef]
48. Fan, S.; Yuan, X.; Zhao, L.; Xu, L.H.; Kang, T.J.; Kim, H.T. Experimental and kinetic study of catalytic steam gasification of low rank coal with an environmentally friendly, inexpensive composite K_2CO_3-eggshell derived CaO catalyst. *Fuel* **2016**, *165*, 397–404. [CrossRef]
49. Luo, H.; Huang, G.; Fu, X.; Liu, X.; Zheng, D.; Peng, J.; Zhang, K.; Huang, B.; Fan, L.; Chen, F.; et al. Waste oyster shell as a kind of active filler to treat the combined wastewater at an estuary. *J. Environ. Sci. (China)* **2013**, *25*, 2047–2055. [CrossRef]
50. Bi, D.; Yuan, G.; Wei, J.; Xiao, L.; Feng, L. Conversion of Oyster Shell Waste to Amendment for Immobilising Cadmium and Arsenic in Agricultural Soil. *Bull. Environ. Contam. Toxicol.* **2020**, *105*, 277–282. [CrossRef] [PubMed]
51. Pliya, P.; Cree, D. Limestone derived eggshell powder as a replacement in Portland cement mortar. *Constr. Build. Mater.* **2015**, *95*, 1–9. [CrossRef]
52. Silva, T.H.; Mesquita-Guimarães, J.; Henriques, B.; Silva, F.S.; Fredel, M.C. The potential use of oyster shell waste in new value-added by-product. *Resources* **2019**, *8*, 13. [CrossRef]
53. Huang, Q.; Lu, P.; Hu, B.; Chi, Y.; Yan, J. Cracking of Model Tar Species from the Gasification of Municipal Solid Waste Using Commercial and Waste-Derived Catalysts. *Energy Fuels* **2016**, *30*, 5740–5748. [CrossRef]
54. Hart, A. Mini-review of waste shell-derived materials' applications. *Waste Manag. Res.* **2020**, *38*, 514–527. [CrossRef] [PubMed]
55. Mazaheri, H.; Ong, H.C.; Masjuki, H.H.; Amini, Z.; Harrison, M.D.; Wang, C.-T.; Kusumo, F.; Alwi, A. Rice bran oil based biodiesel production using calcium oxide catalyst derived from Chicoreus brunneus shell. *Energy* **2018**, *144*. [CrossRef]
56. Mansir, N.; Teo, S.H.; Rashid, U.; Saiman, M.I.; Tan, Y.P.; Alsultan, G.A.; Taufiq-Yap, Y.H. Modified waste egg shell derived bifunctional catalyst for biodiesel production from high FFA waste cooking oil. A review. *Renew. Sustain. Energy Rev.* **2018**, *82*, 3645–3655. [CrossRef]
57. Morris, J.P.; Backeljau, T.; Chapelle, G. Shells from aquaculture: A valuable biomaterial, not a nuisance waste product. *Rev. Aquac.* **2019**, *11*, 42–57. [CrossRef]
58. Guo, F.; Fang, Z. Biodiesel Production with Solid Catalysts. In *Biodiesel Feedstocks Processing and Technologies*; IntechOpen: London, UK, 2011. [CrossRef]
59. Hattori, H. Solid base catalysts: Fundamentals and their applications in organic reactions. *Appl. Catal. A Gen.* **2015**, *504*, 103–109. [CrossRef]
60. Su, M.; Yang, R.; Li, M. Biodiesel production from hempseed oil using alkaline earth metal oxides supporting copper oxide as bi-functional catalysts for transesterification and selective hydrogenation. *Fuel* **2013**, *103*, 398–407. [CrossRef]
61. Papargyriou, D.; Broumidis, E.; de Vere-Tucker, M.; Gavrielides, S.; Hilditch, P.; Irvine, J.T.S.; Bonaccorso, A.D. Investigation of solid base catalysts for biodiesel production from fish oil. *Renew. Energy* **2019**, *139*, 661–669. [CrossRef]
62. Rizwanul Fattah, I.M.; Ong, H.C.; Mahlia, T.M.I.; Mofijur, M.; Silitonga, A.S.; Rahman, S.M.A.; Ahmad, A. State of the Art of Catalysts for Biodiesel Production. *Front. Energy Res.* **2020**, *8*, 1–17. [CrossRef]
63. Roschat, W.; Siritanon, T.; Yoosuk, B.; Promarak, V. Biodiesel production from palm oil using hydrated lime-derived CaO as a low-cost basic heterogeneous catalyst. *Energy Convers. Manag.* **2016**, *108*, 459–467. [CrossRef]
64. Latchubugata, C.S.; Kondapaneni, R.V.; Patluri, K.K.; Virendra, U.; Vedantam, S. Kinetics and optimization studies using Response Surface Methodology in biodiesel production using heterogeneous catalyst. *Chem. Eng. Res. Des.* **2018**, *135*, 129–139. [CrossRef]

65. Granados, M.L.; Poves, M.D.Z.; Alonso, D.M.; Mariscal, R.; Galisteo, F.C.; Moreno-Tost, R.; Santamaría, J.; Fierro, J.L.G. Biodiesel from sunflower oil by using activated calcium oxide. *Appl. Catal. B Environ.* **2007**, *73*, 317–326. [CrossRef]
66. Liu, X.; He, H.; Wang, Y.; Zhu, S.; Piao, X. Transesterification of soybean oil to biodiesel using CaO as a solid base catalyst. *Fuel* **2008**, *87*, 216–221. [CrossRef]
67. Yusuff, A.S.; Adeniyi, O.D.; Olutoye, M.A.; Akpan, U.G. A Review on Application of Heterogeneous Catalyst in the Production of Biodiesel from Vegetable Oils. *J. Appl. Sci. Process. Eng.* **2017**, *4*, 142–157. [CrossRef]
68. Food and Agriculture Organization of the United Nation. *Globefish Highlights Issue 4 2018*; Food and Agriculture Organization of the United Nation: Rome, Italy, 2018; ISBN 9789251312001.
69. Jović, M.; Mandić, M.; Šljivić-Ivanović, M.; Smičiklas, I. Recent trends in application of shell waste from mariculture. *Stud. Mar.* **2019**, *32*, 47–62. [CrossRef]
70. FAO. *The State of World Fisheries and Aquaculture 2018—Meeting the Sustainable Development Goals*; FAO: Rome, Italy, 2018.
71. Viriya-empikul, N.; Krasae, P.; Puttasawat, B.; Yoosuk, B.; Chollacoop, N.; Faungnawakij, K. Waste shells of mollusk and egg as biodiesel production catalysts. *Bioresour. Technol.* **2010**, *101*, 3765–3767. [CrossRef]
72. Faridi, H.; Arabhosseini, A. Application of eggshell wastes as valuable and utilizable products: A review. *Res. Agric. Eng.* **2018**, *64*, 104–114. [CrossRef]
73. Miyamoto, H.; Miyoshi, F.; Kohno, J. The carbonic anhydrase domain protein nacrein is expressed in the epithelial cells of the mantle and acts as a negative regulator in calcification in the mollusc Pinctada fucata. *Zoolog. Sci.* **2005**, *22*, 311–315. [CrossRef] [PubMed]
74. Hangun-Balkir, Y. Green biodiesel synthesis using waste shells as sustainable catalysts with Camelina sativa oil. *J. Chem.* **2016**, *2016*. [CrossRef]
75. Chen, B.; Fan, J.; Wang, J.; Peng, X.; Wu, X. Research of nanostructure of bivalva shell. *J. Metastable Nanocrystalline Mater.* **2005**, *23*, 83–86. [CrossRef]
76. Abdulrahman, I.; Tijani, H.I.; Mohammed, B.A.; Saidu, H.; Yusuf, H.; Ndejiko Jibrin, M.; Mohammed, S. From Garbage to Biomaterials: An Overview on Egg Shell Based Hydroxyapatite. *J. Mater.* **2014**, *2014*, 1–6. [CrossRef]
77. Abdel-Salam, Z.A.; Abdou, A.M.; Harith, M.A. Elemental and ultrastructural analysis of the eggshell: Ca, Mg and Na distribution during embryonic development via LIBS and SEM techniques. *Int. J. Poult. Sci.* **2006**, *5*, 35–42. [CrossRef]
78. Hou, Y.; Shavandi, A.; Carne, A.; Bekhit, A.A.; Ng, T.B.; Cheung, R.C.F.; Bekhit, A.E.-d.A. Marine shells: Potential opportunities for extraction of functional and health-promoting materials. *Crit. Rev. Environ. Sci. Technol.* **2016**, *46*, 1047–1116. [CrossRef]
79. Chen, X.; Yang, H.; Yan, N. Shell Biorefinery: Dream or Reality? *Chem. A Eur. J.* **2016**, *22*, 13402–13421. [CrossRef]
80. Yang, T.; Fu, J.; Ma, L.; Du, H.; Yue, X.; Zhao, B.; Wang, C. Biomimetic synthesis of calcium carbonate under phenylalanine: Control of polymorph and morphology. *Mater. Sci. Eng. C* **2020**, *114*, 111019. [CrossRef]
81. Oral, Ç.M.; Ercan, B.; Kapusuz, D. Calcium carbonate polymorph dictates in vitro osteoblast proliferation. *J. Aust. Ceram. Soc.* **2020**. [CrossRef]
82. Barclay, K.M.; Gingras, M.K.; Packer, S.T.; Leighton, L.R. The role of gastropod shell composition and microstructure in resisting dissolution caused by ocean acidification. *Mar. Environ. Res.* **2020**, *162*, 105105. [CrossRef]
83. Ramakrishna, C.; Thenepalli, T.; Han, C.; Ahn, J.W. Synthesis of aragonite-precipitated calcium carbonate from oyster shell waste via a carbonation process and its applications. *Korean J. Chem. Eng.* **2017**, *34*, 225–230. [CrossRef]
84. Suryawanshi, N.; Jujjavarapu, S.E.; Ayothiraman, S. Marine shell industrial wastes–an abundant source of chitin and its derivatives: Constituents, pretreatment, fermentation, and pleiotropic applications-a revisit. *Int. J. Environ. Sci. Technol.* **2019**, *16*, 3877–3898. [CrossRef]
85. Suryaputra, W.; Winata, I.; Indraswati, N.; Ismadji, S. Waste capiz (*Amusium cristatum*) shell as a new heterogeneous catalyst for biodiesel production. *Renew. Energy* **2013**, *50*, 795–799. [CrossRef]
86. Buasri, A.; Chaiyut, N.; Loryuenyong, V.; Worawanitchaphong, P.; Trongyong, S. Calcium oxide derived from waste shells of mussel, cockle, and scallop as the heterogeneous catalyst for biodiesel production. *Sci. World J.* **2013**, *2013*. [CrossRef] [PubMed]
87. Khemthong, P.; Luadthong, C.; Nualpaeng, W.; Changsuwan, P.; Tongprem, P.; Viriya-Empikul, N.; Faungnawakij, K. Industrial eggshell wastes as the heterogeneous catalysts for microwave-assisted biodiesel production. *Catal. Today* **2012**, *190*, 112–116. [CrossRef]
88. Aitlaalim, A.; Ouanji, F.; Benzaouak, A.; El Mahi, M.; Lotfi, E.M.; Kacimi, M.; Liotta, L.F. Utilization of waste grooved razor shell (Grs) as a catalyst in biodiesel production from refined and waste cooking oils. *Catalysts* **2020**, *10*, 703. [CrossRef]
89. Jairam, S.; Kolar, P.; Sharma-Shivappa Ratna, R.; Osborne, J.A.; Davis, J.P. KI-impregnated oyster shell as a solid catalyst for soybean oil transesterification. *Bioresour. Technol.* **2012**, *104*, 329–335. [CrossRef]
90. Lin, Y.C.; Amesho, K.T.T.; Chen, C.E.; Cheng, P.C.; Chou, F.C. A cleaner process for green biodiesel synthesis from waste cooking oil using recycled waste oyster shells as a sustainable base heterogeneous catalyst under the microwave heating system. *Sustain. Chem. Pharm.* **2020**, *17*, 100310. [CrossRef]
91. Sirisomboonchai, S.; Abuduwayiti, M.; Guan, G.; Samart, C.; Abliz, S.; Hao, X.; Kusakabe, K.; Abudula, A. Biodiesel production from waste cooking oil using calcined scallop shell as catalyst. *Energy Convers. Manag.* **2015**, *95*, 242–247. [CrossRef]
92. Laskar, I.B.; Rajkumari, K.; Gupta, R.; Chatterjee, S.; Paul, B.; Rokhum, L. Waste snail shell derived heterogeneous catalyst for biodiesel production by the transesterification of soybean oil. *RSC Adv.* **2018**, *8*, 20131–20142. [CrossRef]

93. Buasri, A.; Loryuenyong, V. Application of waste materials as a heterogeneous catalyst for biodiesel production from Jatropha Curcas oil via microwave irradiation. *Mater. Today Proc.* **2017**, *4*, 6051–6059. [CrossRef]
94. Colombo, K.; Ender, L.; Barros, A.A.C. The study of biodiesel production using CaO as a heterogeneous catalytic reaction. *Egypt J. Pet.* **2017**, *26*, 341–349. [CrossRef]
95. Milano, J.; Ong, H.C.; Masjuki, H.H.; Silitonga, A.S.; Chen, W.H.; Kusumo, F.; Dharma, S.; Sebayang, A.H. Optimization of biodiesel production by microwave irradiation-assisted transesterification for waste cooking oil-Calophyllum inophyllum oil via response surface methodology. *Energy Convers. Manag.* **2018**, *158*, 400–415. [CrossRef]
96. Zhang, H.; Wang, Q.; Mortimer, S.R. Waste cooking oil as an energy resource: Review of Chinese policies. *Renew. Sustain. Energy Rev.* **2012**, *16*, 5225–5231. [CrossRef]
97. Oldham, D.; Rajib, A.; Dandamudi, K.P.R.; Liu, Y.; Deng, S.; Fini, E.H. Transesterification of Waste Cooking Oil to Produce A Sustainable Rejuvenator for Aged Asphalt. *Resour. Conserv. Recycl.* **2020**, 105297. [CrossRef]
98. Gaur, A.; Mishra, S.; Chowdhury, S.; Baredar, P.; Verma, P. A review on factor affecting biodiesel production from waste cooking oil: An Indian perspective. *Mater. Today Proc.* **2020**. [CrossRef]
99. Elias, S.; Rabiu, A.M.; Okeleye, B.I.; Okudoh, V.; Oyekola, O. Bifunctional heterogeneous catalyst for biodiesel production from waste vegetable oil. *Appl. Sci.* **2020**, *10*, 3153. [CrossRef]
100. Asikin-Mijan, N.; Lee, H.V.; Taufiq-Yap, Y.H. Synthesis and catalytic activity of hydration-dehydration treated clamshell derived CaO for biodiesel production. *Chem. Eng. Res. Des.* **2015**, *102*, 368–377. [CrossRef]
101. Védrine, J.C. Acid-base characterization of heterogeneous catalysts: An up-to-date overview. *Res. Chem. Intermed.* **2015**, *41*, 9387–9423. [CrossRef]
102. Endalew, A.K.; Kiros, Y.; Zanzi, R. Heterogeneous catalysis for biodiesel production from Jatropha curcas oil (JCO). *Energy* **2011**, *36*, 2693–2700. [CrossRef]
103. Tomano, N.; Prokaew, A.; Boonyuen, S.; Ummartyotin, S. Development of Sr/Cao catalyst derived from cuttlebone (Sepia officinalis) for biodiesel production. *J. Met. Mater. Miner.* **2020**, *30*, 40–47. [CrossRef]
104. Boro, J.; Konwar, L.J.; Thakur, A.J.; Deka, D. Ba doped CaO derived from waste shells of T striatula (TS-CaO) as heterogeneous catalyst for biodiesel production. *Fuel* **2014**, *129*, 182–187. [CrossRef]
105. Foroutan, R.; Mohammadi, R.; Esmaeili, H.; Mirzaee Bektashi, F.; Tamjidi, S. Transesterification of waste edible oils to biodiesel using calcium oxide@magnesium oxide nanocatalyst. *Waste Manag.* **2020**, *105*, 373–383. [CrossRef] [PubMed]
106. Boro, J.; Konwar, L.J.; Deka, D. Transesterification of non edible feedstock with lithium incorporated egg shell derived CaO for biodiesel production. *Fuel Process. Technol.* **2014**, *122*, 72–78. [CrossRef]
107. He, Z.; Wang, X. Renewable energy and fuel production over transition metal oxides: The role of oxygen defects and acidity. *Catal. Today* **2014**, *240*, 220–228. [CrossRef]
108. Lee, H.V.; Juan, J.C.; Binti Abdullah, N.F.; Nizah Mf, R.; Taufiq-Yap, Y.H. Heterogeneous base catalysts for edible palm and non-edible Jatropha-based biodiesel production. *Chem. Cent. J.* **2014**, *8*, 30. [CrossRef]
109. Joshi, G.; Rawat, D.S.; Lamba, B.Y.; Bisht, K.K.; Kumar, P.; Kumar, N.; Kumar, S. Transesterification of Jatropha and Karanja oils by using waste egg shell derived calcium based mixed metal oxides. *Energy Convers. Manag.* **2015**, *96*, 258–267. [CrossRef]
110. Rahman, W.U.; Fatima, A.; Anwer, A.H.; Athar, M.; Khan, M.Z.; Khan, N.A.; Halder, G. Biodiesel synthesis from eucalyptus oil by utilizing waste egg shell derived calcium based metal oxide catalyst. *Process. Saf. Environ. Prot.* **2019**, *122*, 313–319. [CrossRef]
111. Kaur, N.; Ali, A. Biodiesel production via ethanolysis of jatropha oil using molybdenum impregnated calcium oxide as solid catalyst. *RSC Adv.* **2015**, *5*, 13285–13295. [CrossRef]
112. Das, V.; Tripathi, A.M.; Borah, M.J.; Dunford, N.T.; Deka, D. Cobalt-doped CaO catalyst synthesized and applied for algal biodiesel production. *Renew. Energy* **2020**, *161*, 1110–1119. [CrossRef]
113. Mansir, N.; Hwa Teo, S.; Lokman Ibrahim, M.; Yun Hin, T.Y. Synthesis and application of waste egg shell derived CaO supported W-Mo mixed oxide catalysts for FAME production from waste cooking oil: Effect of stoichiometry. *Energy Convers. Manag.* **2017**, *151*, 216–226. [CrossRef]
114. Borah, M.J.; Das, A.; Das, V.; Bhuyan, N.; Deka, D. Transesterification of waste cooking oil for biodiesel production catalyzed by Zn substituted waste egg shell derived CaO nanocatalyst. *Fuel* **2019**, *242*, 345–354. [CrossRef]
115. Helwani, Z.; Ramli, M.; Saputra, E.; Bahruddin, B.; Yolanda, D.; Fatra, W.; Idroes, G.M.; Muslem, M.; Mahlia, T.M.I.; Idroes, R. Impregnation of CaO from eggshell waste with magnetite as a solid catalyst (Fe_3O_4/CaO) for transesterification of palm oil off-grade. *Catalysts* **2020**, *10*, 164. [CrossRef]
116. Dorozhkin, S.V. Functionalized calcium orthophosphates ($CaPO_4$) and their biomedical applications. *J. Mater. Chem. B* **2019**, *7*, 7471–7489. [CrossRef] [PubMed]
117. Hawa, K.A.; Helwani, Z.; Amri, A. Synthesis of Heterogeneous Catalysts NaOH/CaO/C From Eggshells for Biodiesel Production Using Off-Grade Palm Oil. *J. Rekayasa Kim. Lingkung.* **2020**, *15*, 31–37. [CrossRef]
118. Nurhayati; Amri, T.A.; Annisa, N.F.; Syafitri, F. The Synthesis of Biodiesel from Crude Palm Oil (CPO) using CaO Heterogeneous Catalyst Impregnated H_2SO_4,Variation of Stirring Speed and Mole Ratio of Oil to Methanol. *J. Phys. Conf. Ser.* **2020**, *1655*. [CrossRef]
119. Cho, Y.B.; Seo, G. High activity of acid-treated quail eggshell catalysts in the transesterification of palm oil with methanol. *Bioresour. Technol.* **2010**, *101*, 8515–8519. [CrossRef]

120. Nur Syazwani, O.; Rashid, U.; Taufiq Yap, Y.H. Low-cost solid catalyst derived from waste Cyrtopleura costata (Angel Wing Shell) for biodiesel production using microalgae oil. *Energy Convers. Manag.* **2015**, *101*, 749–756. [CrossRef]
121. Syazwani, O.N.; Rashid, U.; Mastuli, M.S.; Taufiq-Yap, Y.H. Esterification of palm fatty acid distillate (PFAD) to biodiesel using Bi-functional catalyst synthesized from waste angel wing shell (*Cyrtopleura costata*). *Renew. Energy* **2019**, *131*, 187–196. [CrossRef]
122. Nurdin, S.; Rosnan, N.A.; Ghazali, N.S.; Gimbun, J.; Nour, A.H.; Haron, S.F. *Economical Biodiesel Fuel Synthesis from Castor Oil Using Mussel Shell-Base Catalyst (MS-BC)*; Elsevier B.V.: Amsterdam, The Netherlands, 2015; Volume 79.
123. Thi, T.; Myat, M. Synthesis and Characterization of CaO and KF Doped CaO (KF/CaO) Derived from Chicken Eggshell Waste as Heterogeneous Catalyst in Biodiesel Production. *Am. Sci. Res. J. Eng. Technol. Sci.* **2017**, *38*, 134–151.
124. Komintarachat, C.; Chuepeng, S. Catalytic enhancement of calcium oxide from green mussel shell by potassium chloride impregnation for waste cooking oil-based biodiesel production. *Bioresour. Technol. Reports* **2020**, 100589. [CrossRef]
125. Yoosuk, B.; Udomsap, P.; Puttasawat, B.; Krasae, P. Modification of calcite by hydration-dehydration method for heterogeneous biodiesel production process: The effects of water on properties and activity. *Chem. Eng. J.* **2010**, *162*, 135–141. [CrossRef]
126. Ahmad, S.; Chaudhary, S.; Pathak, V.V.; Kothari, R.; Tyagi, V.V. Optimization of direct transesterification of Chlorella pyrenoidosa catalyzed by waste egg shell based heterogenous nano—CaO catalyst. *Renew. Energy* **2020**, *160*, 86–97. [CrossRef]
127. Niju, S.; Meera Sheriffa Begum, K.M.; Anantharaman, N. Enhancement of biodiesel synthesis over highly active CaO derived from natural white bivalve clam shell Enhancement of biodiesel synthesis over highly active CaO. *Arab. J. Chem.* **2016**, *9*, 633–639. [CrossRef]
128. Niju, S.; Indhumathi, J.; Begum, K.M.M.S.; Anantharaman, N. Tellina tenuis: A highly active environmentally benign catalyst for the transesterification process. *Biofuels* **2017**, *8*, 565–570. [CrossRef]
129. Niju, S.; Rabia, R.; Sumithra Devi, K.; Naveen Kumar, M.; Balajii, M. Modified Malleus malleus Shells for Biodiesel Production from Waste Cooking Oil: An Optimization Study Using Box–Behnken Design. *Waste Biomass Valorization* **2020**, *11*, 793–806. [CrossRef]
130. Chen, G.Y.; Shan, R.; Yan, B.B.; Shi, J.F.; Li, S.Y.; Liu, C.Y. Remarkably enhancing the biodiesel yield from palm oil upon abalone shell-derived CaO catalysts treated by ethanol. *Fuel Process. Technol.* **2016**, *143*, 110–117. [CrossRef]
131. Marinković, D.M.; Stanković, M.V.; Veličković, A.V.; Avramović, J.M.; Miladinović, M.R.; Stamenković, O.O.; Veljković, V.B.; Jovanović, D.M. Calcium oxide as a promising heterogeneous catalyst for biodiesel production: Current state and perspectives. *Renew. Sustain. Energy Rev.* **2016**, *56*, 1387–1408. [CrossRef]
132. Irvine, W.M. Eley–Rideal Mechanism. In *Encyclopedia of Astrobiology*; Gargaud, M., Amils, R., Quintanilla, J.C., Cleaves, H.J., Irvine, W.M., Pinti, D.L., Viso, M., Eds.; Springer: Berlin/Heidelberg, Germany, 2011; p. 485. ISBN 978-3-642-11274-4.
133. Al-Sakkari, E.G.; El-Sheltawy, S.T.; Attia, N.K.; Mostafa, S.R. Kinetic study of soybean oil methanolysis using cement kiln dust as a heterogeneous catalyst for biodiesel production. *Appl. Catal. B Environ.* **2017**, *206*, 146–157. [CrossRef]
134. Widiarti, N.; Ni'mah, Y.L.; Bahruji, H.; Prasetyoko, D. Development of CaO from natural calcite as a heterogeneous base catalyst in the formation of biodiesel: Review. *J. Renew. Mater.* **2019**, *7*, 915–939. [CrossRef]
135. Kouzu, M.; Hidaka, J. Transesterification of vegetable oil into biodiesel catalyzed by CaO: A review. *Fuel* **2012**, *93*, 1–12. [CrossRef]
136. Kesic, Z.; Lukic, I.; Zdujic, M.; Mojovic, L.; Skala, D. Calcium oxide based catalysts for biodiesel production: A review. *Chem. Ind. Chem. Eng. Q.* **2016**, *22*, 391–408. [CrossRef]
137. Pasupulety, N.; Gunda, K.; Liu, Y.; Rempel, G.L.; Ng, F.T.T. Production of biodiesel from soybean oil on CaO/Al_2O_3 solid base catalysts. *Appl. Catal. A Gen.* **2013**, *452*, 189–202. [CrossRef]
138. Tshizanga, N.; Aransiola, E.F.; Oyekola, O. Optimisation of biodiesel production from waste vegetable oil and eggshell ash. *S. Afr. J. Chem. Eng.* **2017**, *23*, 145–156. [CrossRef]
139. Niju, S.; Begum, M.M.M.S.; Anantharaman, N. Modification of egg shell and its application in biodiesel production. *J. Saudi Chem. Soc.* **2014**, *18*, 702–706. [CrossRef]
140. Shinde, K.; Kaliaguine, S. A comparative study of ultrasound biodiesel production using different homogeneous catalysts. *ChemEngineering* **2019**, *3*, 18. [CrossRef]
141. Changmai, B.; Vanlalveni, C.; Ingle, P. Widely used catalysts in biodiesel production: A review. *RSC Adv.* **2020**, 41625–41679. [CrossRef]
142. Teixeira, L.S.G.; Assis, J.C.R.; Mendonça, D.R.; Santos, I.T.V.; Guimarães, P.R.B.; Pontes, L.A.M.; Teixeira, J.S.R. Comparison between conventional and ultrasonic preparation of beef tallow biodiesel. *Fuel Process. Technol.* **2009**, *90*, 1164–1166. [CrossRef]
143. Tan, S.X.; Lim, S.; Ong, H.C.; Pang, Y.L. State of the art review on development of ultrasound-assisted catalytic transesterification process for biodiesel production. *Fuel* **2019**, *235*, 886–907. [CrossRef]
144. Widayat, W.; Darmawan, T.; Rosyid, R.A.; Hadiyanto, H. Biodiesel Production by Using CaO Catalyst and Ultrasonic Assisted. *J. Phys. Conf. Ser.* **2017**, *877*. [CrossRef]
145. Mootabadi, H.; Salamatinia, B.; Bhatia, S.; Abdullah, A.Z. Ultrasonic-assisted biodiesel production process from palm oil using alkaline earth metal oxides as the heterogeneous catalysts. *Fuel* **2010**, *89*, 1818–1825. [CrossRef]
146. Chen, G.; Shan, R.; Shi, J.; Yan, B. Ultrasonic-assisted production of biodiesel from transesterification of palm oil over ostrich eggshell-derived CaO catalysts. *Bioresour. Technol.* **2014**, *171*, 428–432. [CrossRef] [PubMed]
147. Jaliliannosrati, H.; Amin, N.A.S.; Talebian-Kiakalaieh, A.; Noshadi, I. Microwave assisted biodiesel production from Jatropha curcas L. seed by two-step in situ process: Optimization using response surface methodology. *Bioresour. Technol.* **2013**, *136*, 565–573. [CrossRef] [PubMed]

148. Kant Bhatia, S.; Kant Bhatia, R.; Jeon, J.M.; Pugazhendhi, A.; Kumar Awasthi, M.; Kumar, D.; Kumar, G.; Yoon, J.J.; Yang, Y.H. An overview on advancements in biobased transesterification methods for biodiesel production: Oil resources, extraction, biocatalysts, and process intensification technologies. *Fuel* **2021**, *285*, 119117. [CrossRef]
149. Geuens, J.; Kremsner, J.M.; Nebel, B.A.; Schober, S.; Dommisse, R.A.; Mittelbach, M.; Tavernier, S.; Kappe, C.O.; Maes, B.U.W. Microwave-assisted catalyst-free transesterification of triglycerides with 1-butanol under supercritical conditions. *Energy Fuels* **2008**, *22*, 643–645. [CrossRef]
150. Zhang, S.; Zu, Y.G.; Fu, Y.J.; Luo, M.; Zhang, D.Y.; Efferth, T. Rapid microwave-assisted transesterification of yellow horn oil to biodiesel using a heteropolyacid solid catalyst. *Bioresour. Technol.* **2010**, *101*, 931–936. [CrossRef]
151. Liao, C.C.; Chung, T.W. Optimization of process conditions using response surface methodology for the microwave-assisted transesterification of Jatropha oil with KOH impregnated CaO as catalyst. *Chem. Eng. Res. Des.* **2013**, *91*, 2457–2464. [CrossRef]
152. Zamberi, M.M.; Ani, F.N.; Abdollah, M.F. The application of calcium oxide from waste cockle for biodiesel production from used cooking oil via microwave heating system. *J. Adv. Res. Fluid Mech. Therm. Sci.* **2018**, *49*, 92–100.
153. Peng, Y.P.; Amesho, K.T.T.; Chen, C.E.; Jhang, S.R.; Chou, F.C.; Lin, Y.C. Optimization of biodiesel production from waste cooking oil using waste eggshell as a base catalyst under a microwave heating system. *Catalysts* **2018**, *8*, 81. [CrossRef]
154. Shan, R.; Zhao, C.; Lv, P.; Yuan, H.; Yao, J. Catalytic applications of calcium rich waste materials for biodiesel: Current state and perspectives. *Energy Convers. Manag.* **2016**, *127*, 273–283. [CrossRef]
155. Weissman, A.M.; Yang, Y.; Kitagaki, J.; Sasiela, C.A.; Beutler, J.A. Scale-Up in Microwave-Accelerated Organic Synthesis. *Cancer* **2007**, *3*, 133–149. [CrossRef]
156. Almasi, S.; Ghobadian, B.; Najafi, G.H.; Yusaf, T.; Soufi, M.D.; Hoseini, S.S. Optimization of an ultrasonic-assisted biodiesel production process from one genotype of rapeseed (Teri (OE) R-983) as a novel feedstock using response surface methodology. *Energies* **2019**, *12*, 2656. [CrossRef]

ARTICLES FOR FACULTY MEMBERS

ELUCIDATING THE CALCIUM OXIDE DERIVED FROM THE WASTE SHELLS OF MUD CLAM (GELOINA EXPANSA) AS A CATALYST FOR BIODIESEL PRODUCTION

Snail shells as a heterogeneous catalyst for biodiesel fuel production / Gaide, I., Makareviciene, V., Sendzikiene, E., & Kazancev, K.

Processes
Volume 11 Issue 1 (2023) 260 Pages 1-13
https://doi.org/10.3390/pr11010260
(Database: MDPI)

processes

Article

Snail Shells as a Heterogeneous Catalyst for Biodiesel Fuel Production

Ieva Gaide, Violeta Makareviciene *, Egle Sendzikiene and Kiril Kazancev

Agriculture Academy, Vytautas Magnus University, K. Donelaicio Str. 58, LT-44248 Kaunas, Lithuania
* Correspondence: violeta.makareviciene@vdu.lt

Abstract: Homogeneous catalysis is relevant for biodiesel fuel synthesis; however, it has the disadvantage of difficult separation of the catalyst. In the present work, heterogeneous catalysis was applied for rapeseed oil transesterification with methanol, while snail shells were used as a catalyst. CaO content in the catalyst was investigated. Transesterification reactions were carried out in a laboratory reactor, ester yield was analyzed using gas chromatography. Response surface methodology was used for process optimization. It was found that the optimum transesterification conditions when the reaction temperature is 64 °C are the following: a catalyst amount of 6.06 wt%, a methanol-to-oil molar ratio of 7.51:1, and a reaction lasting 8 h. An ester yield of 98.15 wt% was obtained under these conditions.

Keywords: biodiesel; oil; methanol; snail shells; heterogeneous catalysis; optimization

check for updates

Citation: Gaide, I.; Makareviciene, V.; Sendzikiene, E.; Kazancev, K. Snail Shells as a Heterogeneous Catalyst for Biodiesel Fuel Production. *Processes* **2023**, *11*, 260. https://doi.org/10.3390/pr11010260

Academic Editors: Muhammad Zafar and Cherng-Yuan Lin

Received: 6 December 2022
Revised: 6 January 2023
Accepted: 11 January 2023
Published: 13 January 2023

1. Introduction

Global warming has been a big challenge in recent decades. With the aim of reducing it, the global demand for clean energy is growing, resulting in an increasing search for ways to replace fossil fuels with less polluting and more environmentally friendly fuels. This transformation into cleaner fuels is crucial for achieving the commitments made in the Paris Agreement and the Glasgow Climate Pact [1], where it was decided to reduce emissions 50% by 2030 and to reach net zero by mid-century. In addition to this, the Lithuanian energy independence strategy envisages that the transport sector must reach 15% of consumed energy being from renewable sources by 2030 [2].

One of the main reasons for greenhouse gas emissions is the use of mineral diesel in transport engines, which not only pollutes the environment, but is also produced from a non-renewable resource. One of the alternatives to mineral diesel is the production and use of biofuels made from renewable energy sources. Sustainable biofuel production is crucial in the context of the Green Course in Europe. Biodiesel, which can be used in a mixture with mineral diesel, is one type of biofuel.

Biomass that can be used for biodiesel production absorbs CO_2 from the atmosphere through photosynthesis. Biodiesel is biodegradable, which is a positive property for the environment [3]. Biodiesel or its mixtures with mineral diesel in vehicles reduces CO, SO_2, particulate matter and unburnt hydrocarbon emissions when compared to mineral diesel [4].

Biodiesel can be obtained both in homogeneous and heterogeneous ways. Usually, chemical catalysts are used in homogeneous synthesis, which has good catalytic activity. However, there are some disadvantages, including the inevitable production of wastewater during the washing process, which cannot be reused, and, when using homogeneous catalysts, a one-step process is usually not sufficient to obtain biodiesel of high quality [5–7]. In this context, heterogeneous catalysis has the advantage of using biocatalysts and chemical catalysts [8–10], allowing a one-step process that can be used more than once [11,12].

CaO is the heterogeneous catalyst that has been most widely studied for biodiesel production. It has many advantages, including high activity, low solubility in methanol,

and the possibilities of regeneration and reuse. The reaction of transesterification catalyzed by CaO take place under moderate conditions [13,14]. Natural sources rich in calcium carbonate can be used as cheap raw material for catalyst preparation through the conversion of calcium carbonate to oxide [15]. Various shells rich in $CaCO_3$ are contained in waste derived from the food industry. Oyster shells [16], egg shells, crab shells [17], mussel shells [18], clam shells [19], shrimp shells [20], and crab shells [21] have been used as heterogeneous catalysts for biodiesel production.

Snails belong to the class Gastropoda and the Phylum Mollusca. The edible snail global market is worth EUR 1 billion, corresponding to 300,000 tonnes, per year. Annually, 100,000 tonnes of edible snails are consumed in Europe [22]. After snails are consumed, snail shells remain as waste. They are rich in $CaCO_3$ which can be converted into CaO and used for the heterogeneous transesterification reaction from which biodiesel is obtained.

This study aimed to investigate the catalytic activity of snail shells in the transesterification of rapeseed oil with methanol and to optimize the process conditions.

2. Materials and Methods

2.1. Determination of CaO in Snail Shells

Snail shells were decomposed using royal water. After snail shell decomposition, the water, ammonia buffer solution and the dark blue chromogen indicator were added, and trilon B (EDTA) was used for titration [23]. Equation (1) was used for the calculation of the CaO content:

$$\mathrm{CaO} = \frac{V_1 \times K \times 0.0014 \times 250}{m \times 25} \times 100\% \quad (1)$$

where:

V_1—volume of trilon B used for Ca titration, mL;
m—mass of the snail shell sample, g;
K—trilon B correction factor.

2.2. Snail Shell Preparation

Snail shells from a member of the Helicidae family of Helix Aspersa Maxima were used. Catalyst preparation is a very important step to perform before using it for the transesterification reaction. Snail shells were sieved, and a fraction of 0.315–0.1 mm was obtained [23]. Calcination was performed under the same conditions as described by Gaide et al., who determined 5 h at a temperature of 850 °C to be optimum for dolomite preparation [23]. Laskar et al. investigated snail shell preparation for transesterification reaction and determined that a temperature of at least 800 °C was needed to reach the best catalytic activity (>85%) [24]. Kaewdaeng et al. [25] calcined snail shells at 800 °C, the same as Laskar et al. [24]. Other researchers crushed snail shells calcinated for 3.5 h at 900 °C [26]. Trisupakitti et al. investigated a few methods for snail shell preparation and determined that 1 h at 1050 °C was enough [27].

2.3. Transesterification of Rapeseed Oil

Rapeseed oil was purchased in a local supermarket, and met the national requirements for edible oil. Transesterification reactions were conducted using a laboratory reactor containing a reflux condenser, a thermometer heating device, a temperature controller, and stirrers. Twenty grams of rapeseed oil was placed in a reactor and heated. When the required temperature was reached, the determined amount of catalyst was charged to the reactor, and alcohol was added. The process was carried out at the intended temperature for a set time. At the end of the reaction, the mixture was filtered, and the glycerol phase was removed by using a separation funnel. Rapeseed oil methyl esters were washed with 10% by volume of H_3PO4 (5%) solution, and twice with 10% distilled water, with evaporation of the residual water at 110 °C.

2.4. Ester Yield Evaluation Using Gas Chromatography

The glyceride contents (glycerol, monoglycerides, diglycerides, triglycerides) were investigated and used to determine ester yield in the samples. The contents of glycerides were determined by gas chromatography and a Perkin Elmer Clarus 500 (detector—FID) (Boston, MA, USA) gas chromatographer was used according to the requirements of the EN 14105 standard. First, 100 mg of test sample was dissolved in 200 µL of pyridine. Then 80 µL of 1,2,4-butantriol and 200 µL of standard glyceride stock solution containing monononadecanoate, dinonadecanoate, trinonadecanoate and 200 µL of MSTFA were added to the sample solution. The mixture was shaken for about 30 s, and after 25 min, 8 mL of heptane was added. The received mixture was analyzed using gas chromatography. Analysis was performed under programmed temperature conditions: the initial temperature of 50 °C was maintained for 1 min; then, the temperature was increased at a rate of 15 °C/min to 180 °C, then at a rate of 7 °C/min to 230 °C, and further at a rate of 10 °C/min to 370 °C. After a temperature of 370 °C was reached, it was maintained for 7 min. The injector temperature was greater than oven temperature by 5 °C (detector temperature was constant at 380 °C), the injection volume of the sample was 1 µL, and hydrogen gas was used as carrier gas (at constant pressure—80 kPa).

The ester yield was calculated according to the glyceride levels using Equation (2) [28]:

$$EY = 100 \cdot \left(1 - \frac{0.2411 \cdot MG + 0.1426 \cdot DG + 0.1012 \cdot TG}{10.441}\right) \quad (2)$$

where:

EY—ester yield, %;

MG, DG, and TG—the concentrations of monoglyceride, diglyceride, and triglycerides, respectively, %;

0.2411, 0.1426, and 0.1012—the respective conversion indicators for the glycerides;

10.441—the amount of glycerol obtained from 1 kg of rapeseed oil.

2.5. Analysis of Response Surface

In order to set the experimental plan and analyze results, the response surface methodology (RSM) was used.

Process optimization was performed depending on three variables: the amount of methanol, the snail shell content, and the process duration. The response surface methodology was used to optimize the process based on actual experiments. A laboratory reactor was used to carry out the transesterification reaction under different conditions. The parameters mentioned above were varied as follows: methanol-to-oil molar ratio (mol:mol) (from 4 to 12), catalyst amount (from 2 to 8 wt%), and reaction duration (from 2 to 8 h). The performance of twenty assays concluded the experimental plan.

RSM was used for the creation of a mathematical model. For the determination of the interaction between the transesterification reaction parameters and the biodiesel yield, a quadratic reaction surface model was used.

Three parameters were involved in this study; therefore, Equation (3) can be used to show the mathematical relationship between the factors and the response:

$$Y = \beta_0 + \sum_{i=1}^{3} \beta_i X_i + \sum_{i=1}^{3} \beta_{ii} X_i^2 + \sum_{i=1}^{2} \sum_{j=i+1}^{3} \beta_{ij} X_i X_j \quad (3)$$

where:

y—predicted response;

β_0—the offset term;

β_i—the linear coefficients;

β_{ii} and β_{ij}—the interaction coefficients;

x_i and x_j—the independent variables [29].

The final model was applied, and the results of the performed experiments were analyzed. The selected model gave the values of variables on which maximum ester yield can be determined.

3. Results

3.1. CaO Content in Snail Shells

CaO is known to be a good heterogeneous catalyst for oil transesterification [13–15]. The process of the transesterification reaction using calcium oxide as a heterogeneous base catalyst consists of two stages. In the first stage, reactants are adsorbed on the surface of the catalyst, and the reaction takes place; in the second stage, the reaction products are desorbed from the surface of the catalyst. During the transesterification process, methanol protons are transformed by the base site of CaO surface with the formation of methoxide anion, which reacts with the carbonyl group of triglycerides to form one molecule of fatty acid alkyl esters and an intermediate compound—diglyceride. In the next stage, the anion reacts with the diglyceride molecule, forming ester and monoglyceride molecules, and in the third stage, the monoglyceride molecule reacts in the same way, forming the third ester molecule and glycerol.

It was determined that the calcinated snail shells used for biodiesel synthesis contained 91.69 ± 0.43% of CaO, meaning that the content of Ca was 65.49%. Other researchers have investigated calcium content in snail shells, and determined results differing from ours: Birla et al. [26] obtained 98.35 wt% of calcium in the form of oxide in calcinated snail shells; Laskar et al. [24], 98.017 wt% of CaO; Kaewdaeng et al. [25], 70.113 wt% of CaO; Roschat et al. [30] 98.5% Ca. Parveen et al. [31] investigated the properties of three freshwater snail shells, namely, Pila globosa, Bellamya bengalensis and Brotia costul, and determined that the amount of $CaCO_3$ ranged between 87 and 96% of the total weight.

3.2. Optimal Reaction Condition Modeling and Determination Using Response Surface Methodology

The experimental design was planned using ANOVA. The predicted ester yield responses and experimental values are shown in Table 1. The highest methyl ester yield obtained was 99.10 wt%, using a methanol-to-oil molar ratio of 12:1, a catalyst content of 8 wt%, and a reaction duration of 8 h. However, a similar methyl ester yield (98.1 wt%) was determined when the alcohol-to-oil molar ratio was 8:1, the catalyst content was 5 wt% and the reaction duration was 9.2 h.

Table 1. Central composite design matrix and observed and modeled results.

No	A: Methanol-to-Oil Molar Ratio, mol/mol	B: Catalyst Amount, wt%	C: Reaction Duration, h	Predicted Methyl Ester Yield, wt%	Experimental Methyl Ester Yield, wt%
1	4.00	2.00	2.00	29.54	25.00± 0.71
2	12.00	2.00	2.00	3.39	8.12 ± 0.25
3	4.00	8.00	2.00	21.40	23.12 ± 0.69
4	12.00	8.00	2.00	14.45	15.50 ± 0.34
5	4.00	2.00	8.00	74.81	79.15 ± 0.69
6	12.00	2.00	8.00	58.86	62.26 ± 0.98
7	4.00	8.00	8.00	86.57	86.70 ± 0.67
8	12.00	8.00	8.00	89.82	99.10 ± 0.64
9	2.40	5.00	5.00	66.65	67.60 ± 0.46
10	13.60	5.00	5.00	50.62	40.36 ± 0.56
11	8.00	0.80	5.00	31.35	28.87 ± 0.36
12	8.00	9.20	5.00	47.33	41.62 ± 0.69
13	8.00	5.00	0.80	23.66	24.34 ± 0.65
14	8.00	5.00	9.20	99.12	98.10 ± 0.84
15	8.00	5.00	5.00	68.32	69.45 ± 0.75
16	8.00	5.00	5.00	68.32	72.47 ± 0.69
17	8.00	5.00	5.00	68.32	71.56 ± 0.67
18	8.00	5.00	5.00	68.32	68.14 ± 0.34
19	8.00	5.00	5.00	68.32	67.47 ± 0.77
20	8.00	5.00	5.00	68.32	70.36 ± 0.63

The F value of the quadratic model is 55.67 and the p value < 0.0001. These values show that the model is statistically significant (Table 2). Values < 0.0500 were considered significant; insignificant (>0.0500) elements were removed. Equation (4) describes the ester yield after it was modified and only significant components were left:

$$EY = 67.74 - 5.48A + 5.60B + 29.82C + 4.29AB + 4.46BC - 4.57A2 - 15.18B2 \quad (4)$$

where:

EY—the ester yield (%);
A—the methanol-to-oil molar ratio;
B—the catalyst (snail shells) amount (wt%);
C—the process duration (h).

Table 2. Analysis of variance of quadratic model.

Source	Sum of Squares	Df	Mean Square	F Value	p-Value Prob > F	
Model	13,981.41	9	1553.49	55.67	<0.0001	Significant
A—Methanol-to-oil molar ratio	358.16	1	358.16	12.84	0.0050	
B—Temperature	373.23	1	373.23	13.38	0.0044	
C—Catalyst	10,598.79	1	10,598.79	379.84	<0.0001	
AB	147.06	1	147.06	5.27	0.0446	
AC	33.21	1	33.21	1.19	0.3009	
BC	159.31	1	159.31	5.71	0.0380	
A2	161.40	1	161.40	5.78	0.0370	
B2	1890.44	1	1890.44	67.75	<0.0001	
C2	32.22	1	32.22	1.15	0.3078	
Residual	279.04	10	27.90			
Lack of Fit	263.04	5	52.61	16.44	0.0040	Not significant
Pure Error	16.00	5	3.20			
Cor Total	14,260.44	19	1553.49			

The "Pred R-Squared" of 0.8555 is in agreement with the "Adj R-Squared" of 0.9628. "Adeq Precision" measures the signal-to-noise ratio. A ratio greater than four is desirable. In our case, the ratio is 27.308 is almost seven times higher than the desirable value, which indicates an adequate signal (Table 3).

Table 3. Statistical parameters determined using ANOVA.

Variable	Value	Variable	Value
Std. Dev.	5.28	R-Squared	0.9804
Mean	55.97	Adj R-Squared	0.9628
C.V. %	9.44	Pred R-Squared	0.8555
PRESS	2061.16	Adeq Precision	27.308

Figure 1 presents a graph comparing the experimental and predicted values of ester yield (wt%). It can be seen that the differences were not significant.

3.3. Effect of the Interaction of Independent Variables on the Effectiveness of Transesterification

3.3.1. The Effect of Methanol-to-Oil Molar Ratio and Amount of Catalyst on FAME Conversion

Figure 2 demonstrates the catalyst content and the impact of the methanol-to-oil molar ratio on the ester yield with a reaction duration of 8 h. A higher catalyst content had a positive effect on ester yield; however, when the catalyst content reached around 6 wt%, the ester yield started decreasing. A higher methanol-to-oil molar ratio also had a positive impact on the ester yield until a certain point. A methanol-to-oil molar ratio greater than

around 8:1 was not found to be desirable for achieving higher ester yield in the present study. Birla et al. [26] obtained similar results when waste frying oil and calcinated snail shells were used as catalysts. When increasing the methanol-to-oil molar ratio, oil conversion increased until a certain point—the highest conversion (95%) was reached at 6.03:1—while when adding a methanol-to-oil molar ratio of 9.65:1, oil conversion was 86.02%. A similar tendency was observed with increasing amount of catalyst: oil conversion increased until 2 wt% catalyst, and after this point, conversion started to decrease [26]. Rochat et al. [30] investigated the process of palm oil transesterification with methanol using heterogeneous catalyst derived from river snail shells and obtained a FAME yield of 98.5% ± 1.5 under an optimal catalyst-to-oil ratio of 5 wt%, an optimal methanol-to-oil molar ratio of 12:1, a reaction temperature of 65 °C, and a reaction time of 90 min. Tendencies were observed whereby when increasing the methanol-to-oil molar ratio from 9:1 to 12:1, the biodiesel yield increased, but when increasing the molar ratio to 15:1, the ester yield did not change. Furthermore, when a methanol-to-oil molar ratio of 18:1 was reached, the ester yield started to decrease. It is believed that this may be due to glycerol being soluble in methanol and inhibiting the mixing of methanol with oil and heterogeneous catalyst [30].

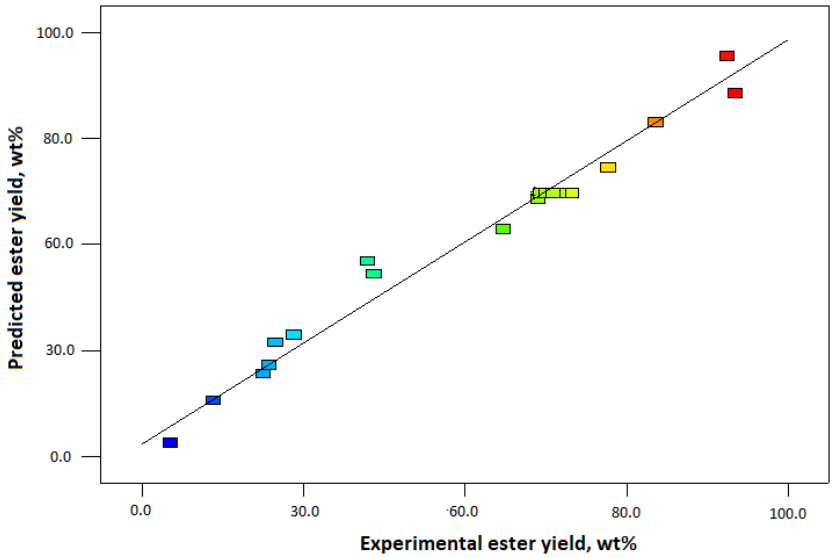

Figure 1. Experimental and predicted values of ester yield (wt%).

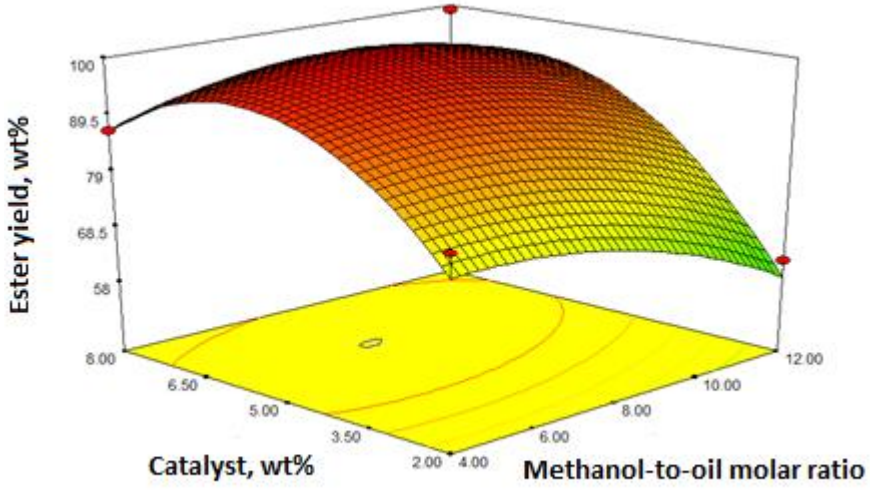

Figure 2. Response surface contour plot for the interaction between the catalyst content and the methanol-to-oil molar ratio with a process duration of 8 h and at a temperature of 64 °C.

When using palm oil for biodiesel synthesis, the optimum amount of catalyst (snail shells) was determined to be 10 wt%, with a methanol-to-oil molar ratio of 12:1 [32]. Under these conditions, a 93.2 wt% ester yield was obtained. These results show that more catalyst and methanol are needed to achieve an ester yield (93.2 wt%) that is even lower that that obtained in our study. However, there is a study in which 3 wt% catalyst and a methanol-to-oil molar ratio of 6:1 was enough to reach an ester yield of 98 wt% [24]. These differences can be explained by the fact that different oils were used, and the reaction durations were different.

Similar tendencies were observed by other researchers, who investigated the oil transesterification process with methanol and heterogeneous catalyst with a high content of CaO. The researchers analyzed the transesterification of different oils (rapeseed, soybean, sunflower) with methanol using eggshells as a catalyst and determined that a high methanol-to-oil molar ratio is not desirable for obtaining high ester yield, as it is believed that a high alcohol-to-oil molar ratio increases reversible reaction [33–35].

3.3.2. Effect of Process Duration and Methanol Content on FAME Conversion

The methanol-to-oil molar ratio and the process duration have a great influence on the methyl ester yield (the snail shells amount is 5 wt%), as shown in Figure 3. As mentioned previously, higher methanol-to-oil molar ratios have a positive effect until around 8:1, whereas longer process times lead to higher methyl ester yields. When the process duration was 6 h, and the methanol-to-oil molar ratio was 6:1, an ester yield of around 80 wt% was achieved, while after 8 h, the yield increased to more than 92 wt%. Birla and colleagues [26] determined the optimal process duration for waste frying oil transesterification to be 8 h, with a methanol-to-oil molar ratio of 6.03:1; under these conditions, a methyl ester yield of 87.28 wt% was obtained.

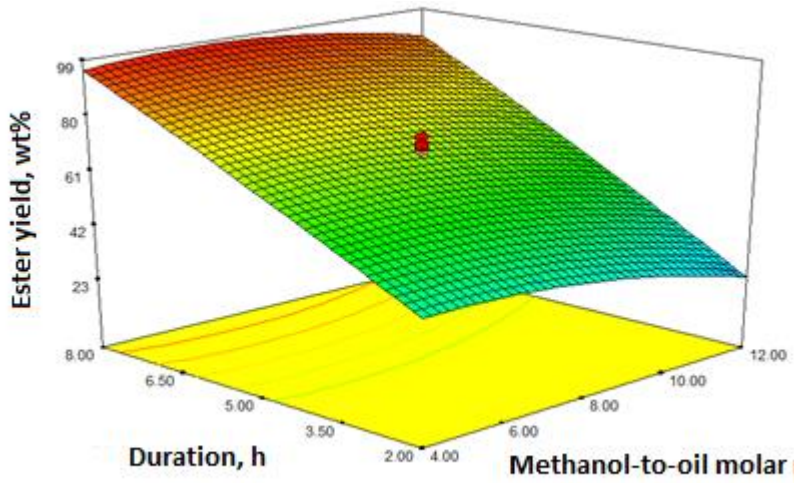

Figure 3. Response surface contour plot for the interaction between the methanol-to-oil molar ratio and the process duration at a temperature of 64 °C with a catalyst content of 5 wt%.

Other researchers have obtained similar results: a soybeen oil methyl ester yield of 98 wt% was achieved with a methanol-to-oil molar ratio of 6:1 and a reaction duration of 7 h [24]. Viriya-empikul et al. [32] and Trisupakitti et al. [27] analyzed palm oil transesterification using methanol and snail shells, whereby the optimal amount of alcohol was determined to be 12:1; however, the reaction durations were very different. Viriya-empikul et al. [32] obtained an ester yield of 93.2 wt% after 2 h, while Trisupakitti et al. [27] obtained similar results (92.5 wt%) after 6 h (catalyst amount 0.8 wt%).

When using different heterogeneous catalysts (dolomite, eggshells, oyster shells) in oil transesterification reactions with methanol, there are tendencies showing that ester yield increases with increasing process duration. It is possible to obtain a similar ester yield

using less alcohol when the reaction takes longer, or with a higher alcohol amount and a shorter duration [23,30,36].

3.3.3. Effect of Process Duration and Heterogeneous Catalyst Amount on FAME Conversion

Figure 4 shows the influence of the catalyst content and the process duration on the yield of rapeseed oil methyl ester when the methanol-to-oil molar ratio is 8:1.

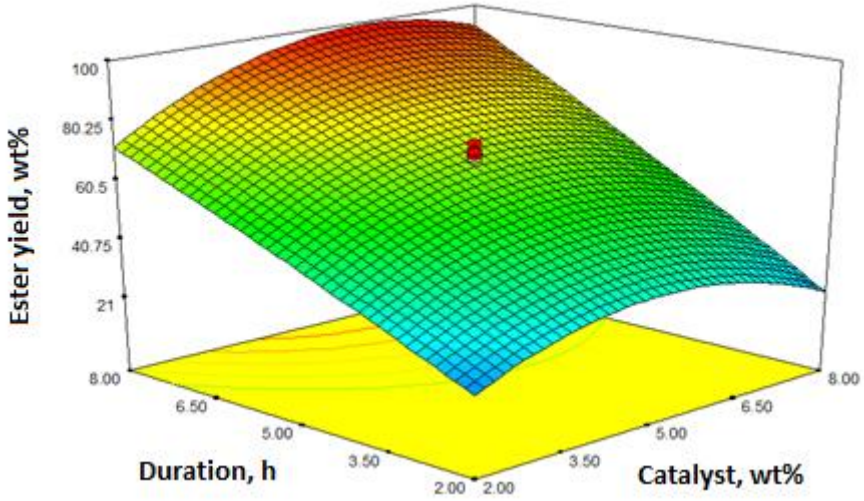

Figure 4. Response surface contour plot for the interaction between the processing time and the catalyst at 64 °C with a methanol-to-oil molar ratio of 8:1.

Longer process times and higher snail shell contents had a positive effect on methyl ester yield; however, when the catalyst amount exceeded around 6 wt%, the ester yield started to decrease. With a process duration of 8 h and a catalyst amount of 3.5 wt%, an ester yield of around 85 wt% was obtained, while when the catalyst amount was increased to 6 wt%, the yield increased to more than 92 wt%. Results obtained by other researchers are very different. Viriya-empikul and colleagues (2012) determined that the optimum catalyst amount was 10 wt%, with a very short optimum duration of 2 h [32]. Other researchers have obtained optimum catalyst amounts of 2–3 wt%, with the process duration varying between 1 and 8 h [24–26]. Trisupakitti and colleagues achieved an ester yield of 92.5 wt% with a reaction duration of 6 h and a snail shell amount of 0.8 wt% [27].

Gaide et al. (2021) investigated oil transesterification using calcinated dolomite and obtained results showing that longer process durations and higher catalyst content lead to a higher methyl ester yield. An ester yield of less than 62 wt% was obtained after 2 h with 6 wt% of catalyst, while after 5 h, ester yield increased to more than 96 wt% [23]. Kumar et al. [36] and Gaide et al. [33] investigated biodiesel production by means of transesterification with methanol, using calcinated eggshells as catalyst, and noticed that increased process duration and catalyst amount had positive effects on ester yield. Nakatani and colleagues [37] investigated soybean oil transesterification using methanol and calcinated oyster shells, and identified a positive effect of reaction duration and catalyst amount on FAME content. The optimal reaction conditions of catalyst concentration and reaction time were determined to be 25 wt% and 5 h, respectively. Under the optimal conditions obtained, the biodiesel yield, relative to the amount of soybean oil, was 73.8%, with high biodiesel purity (98.4 wt%) [37].

3.4. Optimization of the Fatty Acid Methyl Ester Synthesis Process

In this research, three independent variables that influence the synthesis of rapeseed oil methyl esters were investigated. Aiming to determine the optimum conditions for biodiesel production, an optimization step was performed. The predicted and experimental ester yields are presented in Table 4. The optimal conditions at a process temperature of

64 °C are as follows: snail shell concentration, 6.06 wt%; methanol-to-oil molar ratio, 7.51:1; and reaction duration, 8 h.

Table 4. Optimum parameters for rapeseed oil methyl ester production, and predicted and experimental ester yield.

Methanol-to-Oil Molar Ratio, mol/mol	Snail Shells Concentration, wt% (From Oil Mass)	Reaction Duration, h	Predicted Ester Yield, wt%	Experimental Ester Yield, wt%
7.51:1	6.06	8	98.87	98.15 ± 0.35

The results of other studies in which methanol and snail shells have been used as a heterogeneous catalyst are presented in Table 5. The results show ester yields ranging from 87.28 to 98 wt%.

Table 5. Comparison of optimal conditions for fatty acid methyl ester production using snail shells as a heterogeneous catalyst.

Oil	Temperature, °C	Snail Shells Amount	Reaction Duration, h	Methanol-to-Oil Molar Ratio, mol/mol	Ester Yield, wt%	Reference
Waste frying oil	60	2 wt%	8	6.03:1	87.28	[26]
Palm olein oil	60	10 wt%	2	12:1	93.2	[31]
Used cooking oil	65	3 wt%	1	9:1	92.5	[25]
Palm oil	65	0.8 wt%	6	12:1	92.5	[27]
Soybean oil	28	3 wt%	7	6:1	98	[24]

Other researchers have investigated the possibility of using calcinated snail shells for biodiesel synthesis when using methanol. Different results have been obtained, with ester yields varying from 87.28 wt% to 98 wt%. Some studies have been conducted using an optimal temperature of 60 °C [26,31]. In our study, a temperature of 64 °C was used, which is close to methanol's boiling point. Some other transesterification reactions have been investigated at a similar temperature, 65 °C [25,27]. Only Laskar et al. was able to obtain an ester yield of 98 w% using a temperature of 28 °C (7 h, 6:1, 3 wt%) [24]. Birla et al. [26] used waste frying oil for biodiesel production and obtained an ester yield of 87.28 wt% under the following conditions: process temperature, 60 °C; catalyst amount, 2 wt%; process duration, 8 h; methanol-to-oil molar ratio, 6.03:1. Kaewdaeng et al. [25] performed transesterification using cooking oil with a process temperature of 65 °C, a catalyst amount of 3 wt%, a process duration of 1 h, and a methanol-to-oil molar ratio of 9:1, was achieving an ester yield of 92.5 wt%. Using palm oil, Viriya-empikul et al. [31] obtained a 93.2 wt% ester yield (2 h, 12:1, 10 wt%), while a similar ester yield of 93.2 wt% (6 h, 12:1, 0.8 wt%) was obtained by Trisupakitti et al. [27].

3.5. Physical and Chemical Properties of the Obtained Fatty Acid Methyl Esters

In order to use the transesterification product in the transport sector, the physical and chemical properties of the obtained rapeseed oil methyl esters have to meet the requirements of the international standard for biodiesel fuel. The results of the quality analysis are presented in Table 6.

Table 6. The physical and chemical properties of rapeseed oil methyl esters.

Parameter	Units	Requirements of Standard EN 14214	Rapeseed Oil Methyl Esters
Ester content	%	min 96.5	98.15 ± 0.35
Density at 15 °C	kgm^{-3}	min 860 max 900	883 ± 2.50
Viscosity at 40 °C	mm^2s^{-1}	min 3.50 max 5.00	4.78 ± 0.02
Acid value	mg $KOHg^{-1}$	max 0.5	0.25 ± 0.01
Sulfur content	$mgkg^{-1}$	max 10	7.3 ± 0.21
Moisture content	$mgkg^{-1}$	max 500	305 ± 2.10
Iodine value	g $J_2100^{-1}g^{-1}$	max 120	114 ± 0.15
Linolenic acid methyl esters content	%	max 12.0	9.5 ± 0.10
Monoglyceride content	%	max 0.8	0.51 ± 0.09
Diglyceride content	%	max 0.2	0.10 ± 0.02
Triglyceride content	%	max 0.2	0.05 ± 0.01
Free glycerol content	%	max 0.2	0.02 ± 0
Total glycerol content	%	max 0.25	0.21 ± 0.11
Methanol content	%	max 0.2	0.05 ± 0.01
Phosphorus content, ppm		10	7.1 ± 0.09
Metals II (Ca/Mg)	mg kg^{-1}	max 5	4 ± 0.12
Oxidation stability 110 °C	H	min 8	8.3 ± 0.1
Cetane number	-	min 51	53.8 ± 0.15
Cold filter plugging point	°C	−5 °C (in summer) −32 °C (in winter)	−9.5 ± 0.06

An important indicator of biodiesel quality is the ester content, i.e., how many esters were formed from triglycerides. According to the requirements of the standard EN 14214, the fatty acid methyl ester content must be at least 96.5%. It was determined that the ester content of the produced biodiesel was 98.15 ± 0.35 wt%, which is higher than the minimum value indicated in the standard.

The amounts of monoglycerides, diglycerides and triglycerides, and free and total glycerol in biofuels depend on both the production and product purification processes. According to the requirements of the standard, the amounts of monoglycerides, diglycerides and triglycerides, and free and total glycerol in the product cannot exceed 0.8%, 0.2%, 0.2%, 0.2% and 0.25%, respectively. These indicators in the obtained fatty acids methyl esters met the requirements of the standard.

The purity of the biodiesel and the composition of fatty acids in the raw material have an influence on the product density. The density of the triglycerides is reduced with their transesterification; however, the density of the obtained product was higher than that of mineral diesel. This higher fuel density leads to higher fuel consumption and a lower calorific value. The density of the produced biofuel was 883 ± 2.50 kg m^{-3}, which meets the requirements of the standard.

The content of free fatty acids in biodiesel depends on the acidity of the oil used to produce the fatty acid methyl esters and the applied production process, as free fatty acids are formed during production and storage. The standard establishes that the number of acids must not exceed 0.5 mg $KOHg^{-1}$, and the acidity of the obtained and analyzed biofuels was 0.25 ± 0.01 mg $KOHg^{-1}$.

According the EN 14214 standard, the moisture content in biodiesel must not exceed more than 500 mg kg^{-1}. Water can appear during the production process, so it must be removed by drying the biodiesel. In addition, biofuels must be stored in closed containers, as they are hygroscopic and can absorb moisture during storage. The moisture content of the obtained methyl esters reached 305 ± 2.10 mg kg^{-1}.

The amount of sulfur in the fuel has a negative effect on engines, the environment, and living organisms. The sulfur content in biodiesel must not exceed 10 mg kg^{-1}. The sulfur content in the obtained biodiesel was 7.3 ± 0.21 mg kg^{-1}.

In the product, the methanol content must not exceed 0.2% (from mass). The amount of methanol is limited, because excess methanol is used for the transesterification of triglycerides. Therefore, the unreacted alcohol must be removed. The amount of methanol produced in biodiesel is only $0.05 \pm 0.01\%$.

The amount of linolenic acid esters and the iodine number do not depend on the biodiesel production process or its purification. These indicators depend on the fatty acid composition of the oil used. The maximum content of linolenic acid methyl ester must be 12%; in the obtained biofuel it was $9.5 \pm 0.10\%$. The iodine number cannot exceed 120 g $J_2$100-1g^{-1}, and it was 114 ± 0.15 g $J_2100^{-1}g^{-1}$ in the obtained biodiesel.

Since calcium is the main element of the snail shells used for the transesterification reaction, the content of metals II (Ca/Mg) in the biodiesel must be investigated, with these being limited by the standard to 5 mg kg^{-1}; a value of 4 ± 0.12 mg kg^{-1} was obtained in the produced fuel.

Storing biofuels can increase their acidity and reduce their oxidation resistance, i.e., during oxidation processes, fuel stability decreases, which is important in order to store fuels. The esters obtained in this research meet the requirements of the standard (i.e., a minimum resistance of 8 h); their resistance to oxidation was 8.3 ± 0.12 h.

Since fuel is used both in summer and winter, low-temperature properties are very important. Depending on the climatic conditions, there are different requirements for the limits of CFPP value. During the summer in Lithuania, the CFPP of fuel must not be higher than minus 5 °C (class C in the moderate climate zone). The CFPP of the obtained biodiesel was minus 9 ± 0.06 °C.

The fatty acid methyl esters obtained in biodiesel synthesis using rapeseed oil, methanol and snail shells as catalysts were able to meet the requirements of standard EN 14214 for biodiesel.

4. Conclusions

The snail shells selected for heterogeneous biodiesel synthesis contained $91.69 \pm 0.43\%$ CaO. Catalyst preparation is a very important step prior to use for the transesterification reaction. A fraction size of 0.315–0.1 mm was obtained and calcinated for 5 h at a temperature of 850 °C.

Three independent parameters (the methanol-to-oil molar ratio, the snail shell content, and the duration of the reaction) were selected to determine their influence on the efficiency of the transesterification process. It was determined that a larger catalyst amount and a larger methanol-to-oil molar ratio led to a higher ester yield. However, when it reaches a certain point (around 6 wt% of snail shell content and around 8:1 methanol-to-oil molar ratio), the yield of rapeseed oil methyl ester starts to decrease. Longer process duration has a positive effect on the ester yield. Response surface analysis was applied to optimize the rapeseed oil transesterification process with methanol when snail shells are used as a heterogeneous catalyst. The following optimal conditions for rapeseed oil methyl ester synthesis were determined: a methanol-to-oil molar ratio of 7.51:1, a snail shell content of 6.06 wt%, and a reaction time of 8 h at a temperature of 64 °C. Under the determined optimal conditions, rapeseed oil methyl ester yield reached 98.15 wt%. The analysis of the physical and chemical properties of the produced rapeseed oil methyl ester proved that physical and chemical properties of the biodiesel were able to meet the requirements of the EN 14214 standard, and the obtained product was suitable for use in diesel engines during the summer period.

Author Contributions: Conceptualization, V.M. and E.S.; methodology, I.G., V.M. and K.K.; software, I.G.; validation, I.G., V.M. and E.S.; formal analysis, investigation, I.G., V.M. and K.K.; resources, E.S.; data curation, I.G. and V.M.; writing—original draft preparation, I.G., V.M. and E.S.; writing—review and editing, I.G., V.M. and E.S.; visualization, I.G. and E.S.; supervision, V.M. All authors have read and agreed to the published version of the manuscript.

Funding: This research received no external funding.

Data Availability Statement: Not applicable.

Conflicts of Interest: The authors declare no conflict of interest.

References

1. Fransen, T.; Ross, K.; Srouji, J. 5 Ways the Glasgow Climate Pact Aims to Reduce Greenhouse Gas Emissions. 2022. Available online: https://www.wri.org/insights/glasgow-climate-pact-reduce-ghg-emissions (accessed on 27 April 2022).
2. Lithuanian Energy Agency. Available online: https://www.ena.lt/aei-transporte/ (accessed on 27 December 2021).
3. Sendzikiene, E.; Makareviciene, V.; Janulis, P.; Makareviciute, D. Biodegradability of biodiesel fuel of animal and vegetable origin. *Eur. J. Lipid Sci. Technol.* **2007**, *109*, 493–497. [CrossRef]
4. Garcia-Martin, J.F.; Barrios, C.C.; Ales-Alvarez, F.J.; Dominiguez-Saez, A.; Alvarez-Mateos, P. Biodiesel production from waste cooking oil in a oscillatory flow reactor. Performance as a fuel on a TDI diesel engine. *Renew. Energy.* **2018**, *125*, 546–556. [CrossRef]
5. Karciauskiene, D.; Sendzikiene, E.; Makareviciene, V.; Zaleckas, E.; Repšienė, R.; Ambrazaitienė, D. False flax (*Camelina sativa* L.) as an alternative source for biodiesel production. *Agriculture.* **2014**, *101*, 161–168.
6. Mohandass, R.; Ashok, K.; Selvaraju, A.; Rajagopan, S. Homogeneous Catalysts used in Biodiesel Production: A Review. *Int. J. Eng. Res. Technol. (IJERT)* **2016**, *5*, 264–268. [CrossRef]
7. Hariprasath, P.; Selvamani, S.T.; Vigneshwar, M.; Palanikum, K.; Jayaperumal, D. Comparative analysis of cashew and canola oil biodiesel with homogeneous catalyst by transesterification method. *Mater. Today Proc.* **2019**, *16*, 1357–1362. [CrossRef]
8. Quayson, E.; Amoah, J.; Hama, S.; Kondo, A.; Ogino, C. Immobilized lipases for biodiesel. production: Current and future greening opportunities. *Renew. Sust. Energ. Rev.* **2020**, *134*, 110355. [CrossRef]
9. Pratika, R.A.; Wijaya, K.; Trisunaryanti, W. Hydrothermal treatment of SO_4/TiO_2 and TiO_2/CaO as heterogeneous catalysts for the conversion of Jatropha oil into biodiesel. *J. Environ. Chem. Eng.* **2021**, *9*, 106547. [CrossRef]
10. Dasta, P.; Singh, A.P.; Singh, A.P. Zinc oxide nanoparticle as a heterogeneous catalyst in generation of biodiesel. *Mater. Today Proc.* **2022**, *52*, 751–757. [CrossRef]
11. Ilgen, O. Dolomite as a heterogeneous catalyst for transesterification of canola oil. *Fuel Process. Technol.* **2011**, *92*, 452–455. [CrossRef]
12. Marín-Suárez, M.; Méndez-Mateos, D.; Guadix, A.; Guadix, E.M. Reuse of immobilized lipases in the transesterification of waste fishoil for the production of biodiesel. *Renew. Energ.* **2019**, *140*, 1–8. [CrossRef]
13. Roschat, W.; Siritanon, T.; Yoosuk, B.; Promarak, V. Biodiesel production from palm oil using hydrated lime-derived CaO as a low-cost basic heterogeneous catalyst. *Energy Convers. Manag.* **2016**, *108*, 459–467. [CrossRef]
14. Latchubugata, C.S.; Kondapaneni, R.V.; Patluri, K.K.; Virendra, U.; Vedantam, S. Kinetics and optimization studies using response surface methodology in biodiesel production using heterogeneous catalyst. *Chem. Eng. Res. Des.* **2018**, *135*, 129–139. [CrossRef]
15. Correia, L.M.; Sousa Campelo, N.D.; Novaes, D.S.; Cavalcante, C.L.; Cecilia, J.A.; Rodrıguez-Castellon, E.; Vieira, R.S. Characterization and Application of Dolomite as Catalytic Precursor for Canola and Sunflower Oils for Biodiesel Production. *Chem. Eng. J.* **2015**, *269*, 35–43. [CrossRef]
16. Shobana, R.; Vijayalakshmi, S.; Deepanraj, B.; Ranjitha, J. Biodiesel production from Capparis spinosa L seed oil using calcium oxide as a heterogeneous catalyst derived from oyster shell. *Mater. Today Proc.* 2021; *in press*. [CrossRef]
17. Correia, L.M.; Saboya, R.M.A.; de Sousa Campelo, N.; Cecilia, J.A.; Rodrguez-Castelln, E.; Cavalcante, C.L.; Vieira, R.S. Characterization of calcium oxide catalysts from natural sources and their application in the transesterification of sunflower oil. *Bioresour. Technol.* **2014**, *151*, 207–213. [CrossRef]
18. Rezaei, R.; Mohadesi, M.; Moradi, G.R. Optimization of biodiesel production using waste mussel shell catalyst. *Fuel* **2013**, *109*, 534–541. [CrossRef]
19. Asikin-Mijan, N.; Lee, H.V.; Taufiq-Yap, Y.H. Synthesis and catalytic activity of hydration—Dehydration treated clamshell derived CaO for biodiesel production. *Chem. Eng. Res. Des.* **2015**, *102*, 368–377. [CrossRef]
20. Sun, Y.; Sage, V.; Sun, Z. An enhanced process of using direct fluidized bed calcination of shrimp shell for biodiesel catalyst preparation. *Chem. Eng. Res. Des.* **2017**, *12*, 142–152. [CrossRef]
21. Boey, P.L.; Maniam, G.P.; Abd Hamid, S. Biodiesel production via transesterification of palm olein using waste mud crab (*Scylla serrata*) shell as a heterogeneous catalyst. *Bioresour. Technol.* **2009**, *100*, 6362–6368. [CrossRef]
22. Massari, S.; Pastore, S. *Helciculture and Snail Caviar: New Trends in the Food Sector*; Monograph: Future Trends and Challenges in the Food Sector; Polish Society of Commodity Science: Cracow, Poland, 2014; pp. 79–90.
23. Gaide, I.; Makareviciene, V.; Sendzikiene, E.; Kazancev, K. Natural Rocks–Heterogeneous Catalysts for Oil Transesterification in Biodiesel Synthesis. *Catalysts* **2021**, *11*, 384. [CrossRef]
24. Laskar, I.B.; Rajkumari, K.; Gupta, R.; Chatterjee, S.; Paul, B.; Rokhum, S.L. Waste snail shell derived heterogeneous catalyst for biodiesel production by the transesterification of soybean oil. *RSC Adv.* **2018**, *8*, 20131. [CrossRef] [PubMed]
25. Kaewdaeng, S.; Sintuya, P.; Nironsin, R. Biodiesel production using calcium oxide from river snail shell ash as catalyst. *Energy Procedia.* **2017**, *138*, 937–942. [CrossRef]
26. Birla, A.; Singh, B.; Upadhyay, S.N.; Sharma, Y.C. Kinetics studies of synthesis of biodiesel from waste frying oil using a heterogeneous catalyst derived from snail shell. *Bioresour. Technol.* **2012**, *106*, 95–100. [CrossRef]

27. Trisupakitti, S.; Ketwong, C.; Senajuk, W.; Phukapak, C.; Wiriyaumpaiwong, S. Golden apple cherry snail shell as catalyst for heterogeneous transesterification of biodiesel. *Braz. J. Chem. Eng.* **2018**, *35*, 1283–1291. [CrossRef]
28. Bailer, J.; Hödl, P.; de Hueber, K.; Mitelbach, M.; Plank, C.; Schindlbauer, H. *Handbook of Analytical Methods for Fatty Acid Methyl Esters Used as Biodiesel Fuel Substitutes*; Fichte, Research Institute for Chemistry and Technology of Petroleum Products, University of Technology: Vienna, Austria, 1994; pp. 36–38.
29. Montgomery, D. *Design and Analysis of Experiments*; John Wiley & Sons: New York, NY, USA, 2001.
30. Roschat, W.; Siritanon, T.; Kaewpuang, T.; Yoosuk, B.; Promarak, V. Economical and green biodiesel production process using river snail shells-derived heterogeneous catalyst and co-solvent method. *Bioresour. Technol.* **2016**, *209*, 343–350. [CrossRef]
31. Parveen, S.; Chakraborty, A.; Chanda, D.K.; Pramanik, S.; Barik, A.; Aditya, G. Microstructure Analysis and Chemical and Mechanical Characterization of the Shells of Three Freshwater Snails. *ACS Omega.* **2020**, *5*, 25757–25771. [CrossRef]
32. Viriya-empikul, N.; Krasae, P.; Nualpaeng, W.; Yoosuk, B.; Faungnawakij, K. Biodiesel production over Ca-based solid catalysts derived from industrial wastes. *Fuel* **2012**, *92*, 239–244. [CrossRef]
33. Gaide, I.; Makareviciene, V.; Sendzikiene, E. Effectiveness of Eggshells as Natural Heterogeneous Catalysts for Transesterification of Rapeseed Oil with Methanol. *Catalysts* **2022**, *12*, 246. [CrossRef]
34. Goli, J.; Sahu, O. Development of heterogeneous alkali catalyst fromwaste chicken eggshell for biodiesel production. *Renew. Energy* **2018**, *128*, 142–154. [CrossRef]
35. Correia, L.M.; Cecilia, J.A.; Rodríguez-Castellón, E.; Cavalcante, C.L.; Vieira, R.S. Relevance of the Physicochemical Properties of Calcined Quail Eggshell (CaO) as a Catalyst for Biodiesel Production. *J. Chem.* **2017**, *2017*, 5679512.
36. Kumar, H.; Renita, A.A.; Anderson, A. Response surface optimization for biodiesel production from waste cooking oil utilizing eggshells as heterogeneous catalyst. *Mater. Today Proc.* **2021**, *47*, 1054–1058. [CrossRef]
37. Nakatani, N.; Takamori, H.; Takeda, K.; Sakugawa, H. Transesterification of soybean oil using combusted oyster shellwaste as a catalyst. *Bioresour. Technol.* **2009**, *100*, 1510–1513. [CrossRef] [PubMed]

ARTICLES FOR FACULTY MEMBERS

ELUCIDATING THE CALCIUM OXIDE DERIVED FROM THE WASTE SHELLS OF MUD CLAM (GELOINA EXPANSA) AS A CATALYST FOR BIODIESEL PRODUCTION

Synthesis of green biodiesel using heterogeneous catalyst derived from snail shells / Chaib, A., Benammar, S., Hamitouche, A. E., Bachari, K., & Boudjemaa, A.

Environmental Progress and Sustainable Energy
(2025) e70084 Pages 1- 13
https://doi.org/10.1002/ep.70084
(Database: Wiley Online Library)

Received: 5 February 2025 | Revised: 24 June 2025 | Accepted: 8 July 2025

DOI: 10.1002/ep.70084

ORIGINAL RESEARCH

ENVIRONMENTAL PROGRESS & SUSTAINABLE ENERGY

Synthesis of green biodiesel using heterogeneous catalyst derived from snail shells

Assia Chaib[1,2,3] | Souad Benammar[1,4] | Adhya-Eddine Hamitouche[1] | Khaldoun Bachari[1] | Amel Boudjemaa[1]

[1]Environmental Chemistry Division, Centre de Recherche Scientifique et Technique en Analyses Physico-Chimiques, BP 384, Siège ex-Pasna Zone Industrie, Bouismail 42004, Tipaza, Algeria

[2]Laboratoire de recherche d'Environnement, Santé et Production Animale (LESPEA) Université Batna 1, Algeria

[3]Environmental Chemistry Division, Plateau Technique d'Analyses Physco-Chimiques, Batna, Algeria

[4]Laboratoire des Sciences de Génie des Procédés Industriels (LSGPI), USTHB, Algiers, BP, Algeria

Correspondence
Amel Boudjemaa, Centre de Recherche Scientifique et Technique en Analyses Physico-Chimiques, BP 384, Siège ex-Pasna Zone Industrielle, Bou-Ismail CP 42004, Tipaza, Algérie.
Email: amel_boudjemaa@yahoo.fr

Abstract

A promising sustainable biofuel was successfully produced from waste frying oils using a calcium oxide (CaO) catalyst derived from Mourgueta snail shell waste, representing a renewable and low-cost resource. The transesterification reaction was conducted at room temperature by varying the methanol to oil molar ratios (6.4:1, 7.7:1, 9:1, 10.25:1) and catalyst loading (0.5–3 wt%). Additionally, the effect of calcination temperature on catalytic activity was investigated at 700°C, 800°C, and 900°C. Under optimal conditions, specifically, 1.5 wt% catalyst calcined at 900°C with a methanol to oil molar ratio of 9:1, the high conversion efficiency of 99.8% was achieved. This reactivity highlights the effectiveness of the biogenic CaO as a solid base catalyst for biodiesel production. The fatty acid methyl ester (FAME) content of the biodiesel product was confirmed by FTIR, ^{1}H-NMR, ^{13}C-NMR, and GC–MS analyses. The identified methyl esters included key components such as methyl linolelaidate, methyl palmitate, methyl oleate, and methyl stearate, indicating a high-quality biodiesel composition. These results demonstrate the viability of converting agro-waste into efficient heterogeneous catalysts, contributing to green chemistry, waste valorization, and the advancement of sustainable biofuel technologies.

KEYWORDS
^{13}C-NMR, ^{1}H-NMR, biodiesel, frying oil, GC–MS, heterogeneous catalysis, mourgueta snail shells

1 | INTRODUCTION

The search for other energy resources to complement or substitute fossil fuels has been increasing in the current years because of the increase in environmental worries, energy safety, and rapid depletion of fossil resources.[1–3] In this respect, biodiesel is an emerging alternative to diesel fuel derived from renewable and locally available resources,[4] it has become more attractive due to its characteristics of being bio-degradable, renewable, and non-toxic.[5]

Actually, biodiesel is technologically formed by the transesterification of triglycerides in methanol or ethanol, frequently methanol because it is inexpensive and its encouraging physical and chemical characteristics (polar and short chain alcohol).[6]

Across the world, biodiesel is prepared from many sources of comestible oil such as soybean, safflower, sunflower, rapeseed, palm, canola etc.[2] Usage of very good quality vegetable oil, as raw material, upsurges biodiesel manufacture cost. Raw material donates about 75–85% of the aggregate biodiesel manufacture cost.[7] A practice method to decrease the cost of biodiesel manufacture is to use cheap vegetable oil[8] such as waste frying oil as feedstock.[9,10] The excessive consumption of frying in the world has generated a large volume of waste frying oil. Application of waste frying oil into production of biodiesel also minimizes the environmental impacts produced by the discarding of these waste oils. The catalyst can be supplied for the reaction in either a homogeneous or heterogeneous phase.[11]

The transesterification reaction uses acid or basic catalysts (homogeneous catalysis) for the production of biodiesel given a very significant conversion rate of biodiesel even at moderate temperature, atmospheric pressure, and with a very short reaction time. These homogeneous catalysts dissolve entirely in the glycerine film and partly in the biodiesel, which makes the separation and washing of the biodiesel difficult.[12] In addition, homogeneous catalysts like the example of sodium hydroxide and potassium hydroxide are dangerous, corrosive, and hygroscopic.[13] In order to find solutions to the problems of homogeneous catalysts, research has been oriented towards heterogeneous catalysis. Heterogeneous catalysts minimize the problems of homogeneous catalysis in terms of catalyst regeneration and the possibility of being reused in continuous processes. It is reported in the literature that the economic potential of the heterogeneous catalytic process is better than that of the homogeneous one, for example. The heterogeneous catalysts acquire 4–20% lower refining costs than the homogeneous catalysts.[14] Therefore, many heterogeneous catalysts suitable for biodiesel production from various oils have been developed and evaluated in biodiesel production processes. Calcium oxide (CaO) is one of the widely used catalysts due to its abundant availability in nature, its high activity, and low cost[15]; it is non-corrosive and non-hazardous to the environment.[16,17]

Many research articles have reported the study of natural materials from renewable sources such as biomass or waste, such as egg shells,[18,19] river snail shells,[20] mollusk shells,[21] and mussel shell,[22] sea shells,[23] as starting materials for CaO preparation via calcination process. These materials are green heterogeneous catalysts used in sustainable biodiesel production, the degradation reagent, and lubricant production.[24–27]

Snail shell-derived calcium oxide (CaO) catalyst presents several notable advantages that make it highly attractive for sustainable biodiesel production. So, it is a low-cost, eco-friendly catalyst ideal for sustainable biodiesel production. Sourced from biowaste, it offers high catalytic efficiency due to its strong basicity and enables high-yield transesterification under mild conditions. Unlike homogeneous catalysts, it is non-toxic, easily recoverable, and reusable with minimal activity loss. These features make it a promising green alternative for efficient, low-impact biofuel synthesis.[28]

Despite their advantages, snail shell-derived CaO catalysts face several limitations. Ca^{2+} ion leaching—especially in the presence of methanol or moisture—can reduce fuel purity and complicate product separation. Additionally, exposure to air and water leads to catalyst deactivation through carbonation (forming $CaCO_3$) and hydration (forming $Ca(OH)_2$), reducing catalytic efficiency over time.[29,30] High free fatty acid content in feedstock also promotes soap formation via saponification, further hindering biodiesel separation. Addressing these challenges requires careful feedstock pretreatment, optimized reaction conditions, and potential surface modifications to improve catalyst stability and reusability.[31]

To enhance the stability and longevity of snail shell-derived CaO catalysts in biodiesel production, several strategies can be employed. Catalyst surface modification or doping with metal oxides such as Al_2O_3, ZnO, MgO, Fe_3O_4 or SiO_2 can significantly improve structural stability and reduce ion leaching[32–34] Supporting CaO on inert or mesoporous materials like silica, activated carbon, zeolites, or biochar enhances dispersion and minimizes direct contact with methanol, thereby increasing thermal and chemical resistance. Proper pretreatment through high-temperature calcination (e.g., 900°C) ensures complete transformation into reactive CaO and eliminates residual carbonates[35]; post-calcination, catalysts should be stored in dry, airtight conditions to prevent hydration or carbonation. Maintaining a controlled reaction environment is also essential; using anhydrous methanol and pretreated oils with low free fatty acid content helps avoid hydration and saponification. Encapsulating CaO particles with protective layers, such as silica coatings, can further limit leaching by regulating ion diffusion. Optimizing reaction parameters such as avoiding excess methanol and using appropriate catalyst loading also contributes to improved performance. Lastly, spent catalysts can be regenerated by washing, drying, and re-calcining at high temperatures to restore activity and reduce waste.

In this paper, the green heterogeneous based catalysts are derived from snail shells waste "Mourgueta snail shells" to produce the biodiesel from waste frying oil. The novelty of this study is in the use of snail shell-derived catalysts for the transesterification of vegetable oils into biodiesel. The ability of snail shells to act as an efficient catalyst has not been thoroughly explored in the context of biodiesel production. This novel catalyst not only provides a sustainable alternative but also shows superior reusability and effectiveness compared to other commonly used catalysts, making it a promising solution for large-scale biodiesel synthesis.

The major component inside the snail shells, calcium carbonate, $CaCO_3$ was converted to calcium oxide, CaO, under elevated calcination temperatures of 900°C. The CaO heterogeneous base catalysts obtained were then used as catalysts in the biodiesel production. The heterogeneous base catalyst was investigated, and the optimum conditions of the transesterification process were identified. The percentage of conversion was 98%, much better compared to other studies using CaO resulting from different catalysts, e.g.; waste mollusk shell,[21] egg shells,[36] mussel shells.[22]

2 | MATERIALS AND METHODS

2.1 | Material elaboration

Waste frying oil was purchased from the local market in Batna, Algeria. Physicochemical properties of frying oil are regrouped in Table 1. Waste mourgueta snail shells were procured from a restaurant (Batna). Methanol of analytical reagent (Merck) grade was acquired from Merck.

TABLE 1 Physicochemical properties of waste frying oil.

Properties	Measured values
Density at 25°C (g/cm^3)	0.923
Kinematic viscosity at 25°C (mm^2/s)	61.57
Acid value (mg of KOH/g of oil)	1.1

The material used in the present work is mourgueta snail shells Eobaniavermiculta (MSS) or hedge snails, forest garden Cepaea Hartensis (Figure 1). These are edible molucca waste procured from restaurants. Brown or light pink color with saws no earthworm. The snail shells were washed thoroughly in tap water to remove any unwanted material adhered to their surfaces and then rinsed with distilled water. Then the shells were dried under air for several days. After that, they are crushed agate mortar (diameter around 45 μm). The obtained material was calcined at 700°C (MSS1), 800°C (MSS2), 900°C (MSS3) in a muffle furnace for 3 hours and under static air with a heating rate of 2.5°C/min.[36–39] Finally, all calcined samples were stored in a desiccator.

2.2 | Characterization techniques

XRD, FTIR, XRF, TGA, CHNS analysis, and SEM analyses were performed to evaluate the structure and morphology of the calcined snail shells. Structural data were collected using powder X-ray diffraction (XRD) with a Brüker D8-Diffractometer using monochromate Cu-Kα ($\lambda = 1.54056$ Å) radiation with 2θ values ranging from 5 to 80° with a scanning rate of 0.05° (2θ) steps. Fourier transform infrared (FTIR) spectra were recorded on a Perkin-Elmer spectrometer (Spectrum one) within the range of 4000–400 cm^{-1}. X-ray fluorescence (XRF, M4 TORNADO S) was used to determine the chemical composition, while elemental analysis of the samples was performed using an attached X-ray microanalyzer. The thermal behavior and the stability of the catalysts were evaluated through thermogravimetric analysis (TGA) was carried out using SDT Q600 instrumentation. The typical organic elements, including carbon, hydrogen, nitrogen, and sulfur, (CHNS analysis) were identified through a 2400 Series II CHNS/O Elemental Analyzer. The surface morphology of the catalysts was analyzed using a Thermo Fisher APERO 2C scanning electron microscope (SEM).

2.3 | Biodiesel synthesis via transesterification reactions

Transesterification of frying oil was carried out by mixing an appropriate amount (10 mL) of the waste frying oil with alcohol (methanol) in the presence of an elaborated material. The reaction was conducted in a 50 mL three-neck round-bottom batch reactor under magnetic stirring. Reaction parameters such as the calcination temperature of catalyst ($T = 700$, 800, 900°C), the molar ratios of methanol to oil (6.4:1, 7.7:1, 9:1, 10.25:1), and the catalyst amount (0.5–3 wt%) were investigated; all reactions were carried out at room temperature (25°C) and atmospheric pressure (Schema 1). The yield of biodiesel was calculated using the following equation.[40]

$$\text{Biodiesel yield}\,(\%) = \left(1 - \frac{0.2411\,MG + 0.1426\,TG + 0.1012\,TG}{10.441}\right) \times 100 \quad (1)$$

where *MG*, *DG*, and *TG* represent the concentrations of monoglyceride, diglyceride, and triglycerides, respectively. 0.2411, 0.1426, and 0.1012 are the respective conversion indicators for the glycerides; 10.441, and the amount of glycerol obtained from 1 kg of rapeseed oil (Scheme 1).

2.4 | Biodiesel product analysis

The samples taken from the oily phase were analyzed using gas chromatography–mass spectrometry (GC–MS) and Nuclear Magnetic Resonance spectroscopy (NMR). The transformation of oil to fatty acid methyl esters (biodiesel) was determined by 1H and 13C NMR using a Bruker Avance III HD 400 MHz corresponding to a magnetic field of 9.4 Tesla. Deuterated chloroform (CDCl3) was

FIGURE 1 Mourgueta snail shells *Eobania vermiculta*.

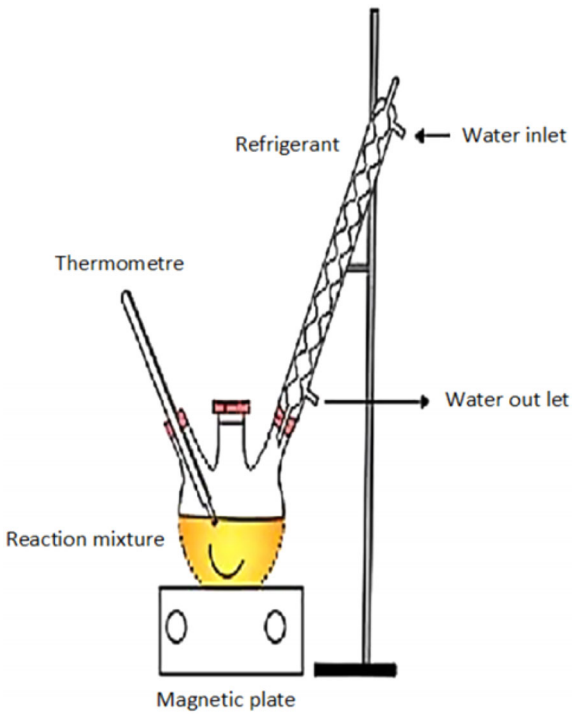

SCHEME 1 Design of experiment approach for transesterification reaction.

used as a solvent. The percent conversion (C) to methyl ester was calculated using the equation (Equation 2)[41,42]

$$C = 100 \times \left(\frac{2A_{ME}}{3A_{\alpha-CH_2}}\right) \quad (2)$$

where A_{ME} is the integration value of protons of the methyl esters (the singlet peak) appearing at 3.64 ppm, and $A_{\alpha-CH_2}$ is the integration value of methylene protons on carbons next to the glycerol moiety appearing at 2.3 ppm. The factors 2 and 3 were derived from the fact that the methylene carbon possesses two protons and the alcohol (methanol-derived) carbon has three attached protons.[43]

The biodiesel obtained was identified and quantified by GC–MS using Hewlett Packard Agilent 6890 plus Gas chromatography equipped with a Hewlett Packard Agilent 5973 mass selective detector, HP-5MS capillary column (30 m × 0.25 mm, 0.25 µm); the auto-injector was operated in the splitless mode at 250°C using helium as a carrier gas (flow rate of 1 mL/min). 1 µL of sample was injected; the oven temperature was programmed between 70°C and 220°C.

3 | RESULTS AND DISCUSSIONS

3.1 | Catalyst characterization

XRD patterns of different materials are shown in Figure 2. For MSS1, the diffraction peaks at 23°, 29.5°, 31.5, 39.8°, 43.5°, 47.5°, 49.5°, 48.5°, and 57.4° are attributed to the calcium carbonates ($CaCO_3$) in accordance with JCPDS card N° 47–1743.[36] When the temperature increases to 800°C, the same peaks of calcium carbonates persist but with lower intensities. On the other hand, there is an appearance of peaks characteristic of calcium hydroxide $Ca(OH)_2$ at 18°, 22°, 34°, 47°, and 50.5° (JCPDS N° 01–073-5492) and calcium oxide (CaO). At 900°C, calcium oxide (CaO) becomes the dominant phase observed at 2θ = 32.5°, 37.5°, 54°, 64.8°, and 67.7° (JCPDS N° 00–37-149).[44] Although $CaCO_3$ peaks remain detectable at this stage, their low intensity indicates a minimal presence of residual carbonate. To further verify the presence of unconverted $CaCO_3$ and associated carbonate species, CHNS elemental analysis was conducted (Table 2). The results show a marked decrease in carbon content with increasing temperature: from 12.03% at 700°C to 10% at 800°C and down to 7.15% at 900°C.

These findings align with the XRD results and confirm that, while the decomposition of $CaCO_3$ is largely achieved at higher temperatures, small quantities of carbonate residues remain in the material.

Figure 3 illustrates the FTIR spectra MSS1, MSS2, and MSS3 calcined at 700°C, 800°C, and 900°C, respectively. For MSS1, the main absorption bands showed at 1442, 875, and 712 cm^{-1}, which are assigned to asymmetric stretching, out-of-plane bending and in-plane bending vibrational modes of carbonates CO_3^{2-}, respectively. Increasing the calcination temperature to 800°C and 900°C, a sharp OH^- stretching band begins to appear at 3638 cm^{-1} characteristic of surface hydroxyl groups OH— bonded to Ca^{2+} ions in CaO. This band arises due to the interaction of freshly formed CaO with atmospheric moisture, leading to partial surface hydration.[45]

As expected, XRF results indicated that snail shells and the synthesized catalysts were composed of more than 99% Ca (Table 3). It should be noted that light elements with atomic numbers below 11, such as carbon (C) and oxygen (O), are not detected by XRF and are therefore excluded from the quantitative analysis.

TABLE 2 CHNS analysis.

Sample	T (°C)	C (%)	H (%)	N (%)	S (%)
MSS1	700	12.03	0.00	0.09	0.00
MSS2	800	10.00	0.22	0.04	0.00
MSS3	900	7.15	0.78	0.04	0.03

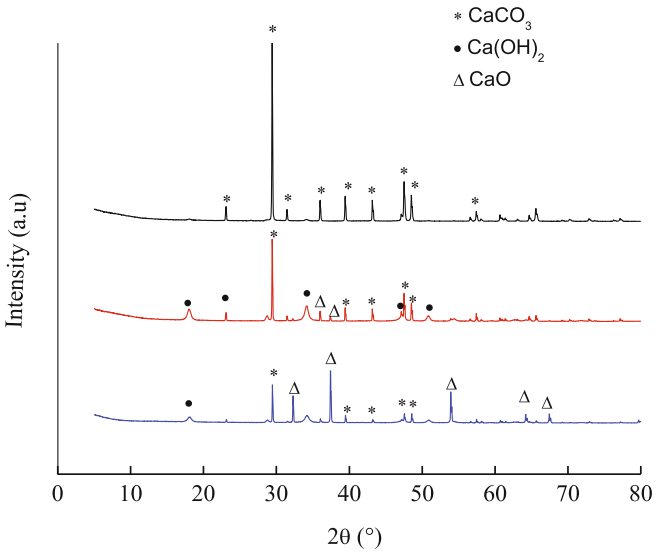

FIGURE 2 XRD patterns of MSS materials calcined at different temperatures. (–) MSS1, (–) MSS2, and (–) MSS3.

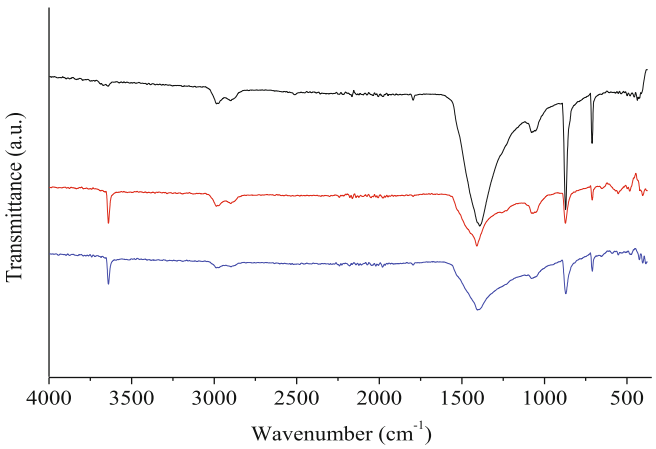

FIGURE 3 FTIR spectra of MSS materials calcined at different temperatures (–) MSS1, (–) MSS2 and (–) MSS3.

The TGA/DTG analysis of snail shell (MSS1) calcined at 700°C (Figure 4a) shows a major weight loss of approximately 45% occurring between 650°C and 780°C, corresponding to the thermal decomposition of calcium carbonate ($CaCO_3$) into calcium oxide (CaO) and CO_2[18] with a relatively broad DTG peak, indicating a slower decomposition process, likely due to insufficient thermal activation at this temperature.[46] The TGA curves of the MSS2 and MSS3 snail shell samples calcined at 800°C and 900°C exhibit two distinct weight loss stages, each associated with specific thermal events (Figure 4b, 4c). The first stage, occurring between approximately 100 and 400°C, corresponds to the loss of physically adsorbed moisture and the decomposition of residual organic matter. The second and most significant weight loss stage appears between 600°C and 800°C (35, 94% for MSS2, 23% for MSS3) attributed to the thermal decomposition of calcium carbonate ($CaCO_3$) into calcium oxide (CaO) and carbon dioxide (CO_2).[47,48] The MSS2 undergoes significant but not complete thermal decomposition; the loss of mass corresponds mainly to the elimination of moisture, organic matter degradation, and partial decomposition of calcium carbonate ($CaCO_3$). The DTG peak around 728°C indicates the onset of $CaCO_3$ decomposition, but some unconverted carbonate may still be present. The decomposition process for MSS3 ($T = 900$°C) is more advanced. Two distinct DTG peaks at 667.5°C and 705°C indicate a more complete and possibly multi-step decomposition of $CaCO_3$ into calcium oxide (CaO). The total weight loss

TABLE 3 Elemental analysis XRF analysis of MSS1, MSS2, and MSS3.

	MSS1		MSS2		MSS3	
Element	**wt%**	**at%**	**wt%**	**at%**	**wt%**	**at%**
Si	0	0	0.07	0.09	0.06	0.09
P	0.09	0.12	0.09	0.12	0.09	0.12
Ca	99.11	99.10	99.47	99.51	99.75	99.72
Fe	0.05	0.03	0.33	0.24	0.09	0.06
Al	0.19	0.28	0	0	0	0
S	0.02	0.02	0.02	0.02	0.01	0.02
K	0.1	0.1	0	0	0	0
Mg	0.11	0.18	0	0	0	0
Mn	0.02	0.01	0.02	0.01	0	0
Sr	0.32	0.15	0	0	0	0

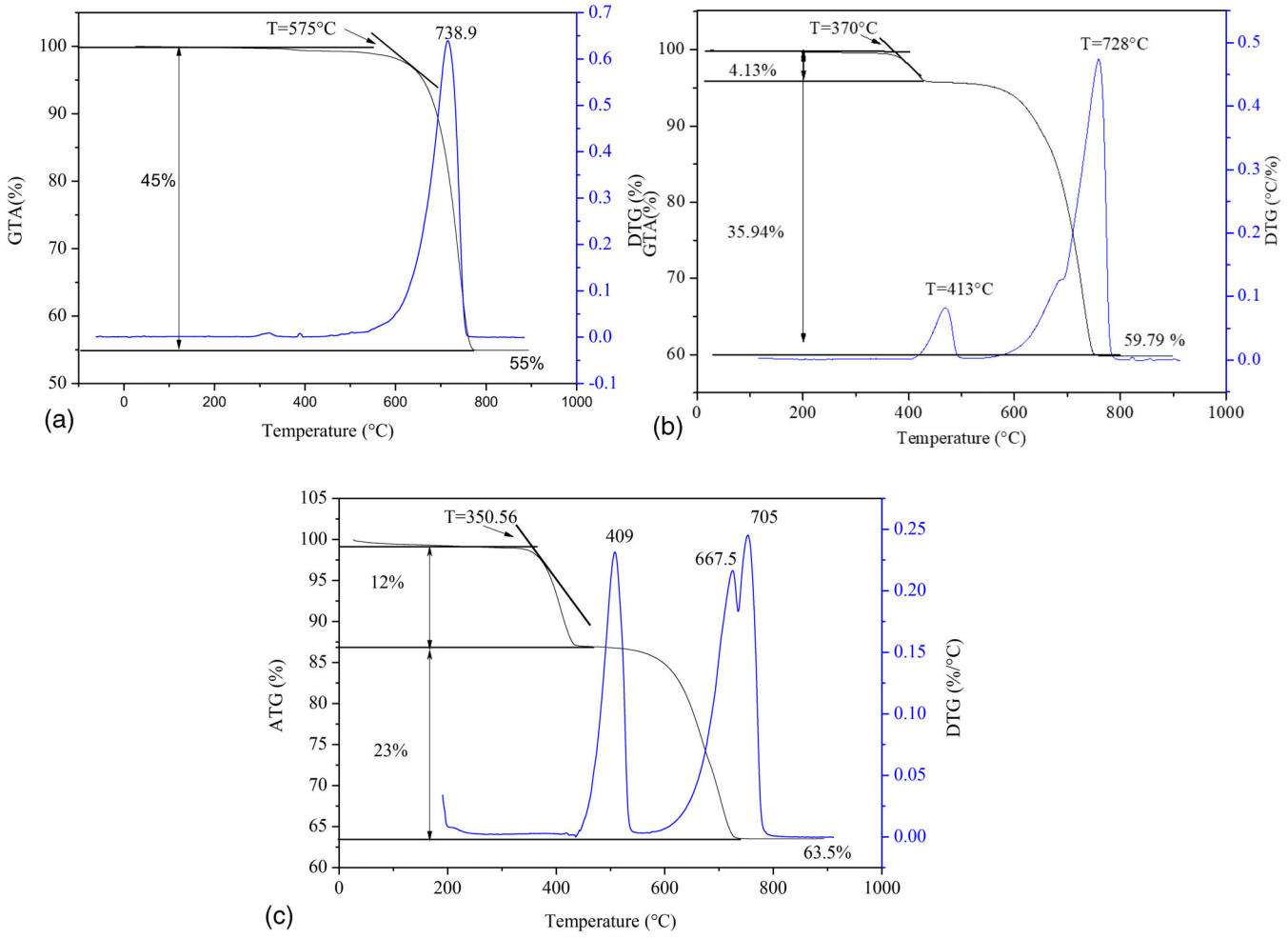

FIGURE 4 TGA/DTA curve of the as-prepared material.

reaches 63.5%, confirming a higher degree of thermal degradation and mineral transformation compared to MSS2. These findings demonstrate that calcination at 900°C ensures a more complete conversion of $CaCO_3$ into CaO, which is crucial for applications such as catalysis where the active phase is CaO.

The SEM images of the catalysts presented in Figure 5 reveal the morphological evolution of MSS1, MSS2, and MSS3. MSS1 exhibits an irregular and porous surface with loosely packed particles, indicating incomplete decomposition and limited structural development. In contrast, MSS2 shows significant morphological transformation, characterized by enhanced crystallinity and surface reorganization, as evidenced by the formation of more defined and interconnected porous structures; this may be due to the release of water and gaseous CO_2 during decomposition of $CaCO_3$ to CaO.[30]

However, MSS3 displays a denser and more compact morphology, with smoother surfaces that suggest the formation of a well-developed crystalline CaO phase. High-temperature calcination promotes particle agglomeration, ultimately resulting in sintered powders; the obtained result is close to Mohammed et al.[49]

3.2 | Parametric study of transesterification

3.2.1 | Effect of the calcination temperature

Using MSS1 in transesterification, a 10% yield of white biodiesel was obtained, where the glycerol phase did not appear. Washing with citric acid (1 N) was unsuccessful, thus enhancing emulsion formation. Even in the case of MSS2, the glycerol phase did not appear; the biodiesel yield achieved 20%, and the wash with citric acid was successful. Whereas using MSS3, three phases appeared; the biodiesel obtained was of an orange-yellow color. In this case, the yield of biodiesel exceeded 93.89% (Figure 6) due to the significant amount of CaO present in MSS3. A similar result was obtained by Ikbal Bahar Laskar et al. in their study on the treatment of waste snail shell-derived heterogeneous catalyst for biodiesel production via transesterification of soybean oil.[30]

3.2.2 | Effect of catalyst amount on biodiesel yield

The influence of the catalyst amount on the frying oil conversion is explored by changing the catalyst amount from 0.5 to 3 wt% using MSS3 catalyst and methanol/oil to volume ratio of 7.7:1 (Figure 7). The reaction happened at room temperature (20°C) for 48 h. It was noticed that the oil conversion to biodiesel increases as the catalyst amount increases from 0.5 to 1.5 wt% (60 to 99.8%); beyond 1.5 wt%, the conversion of the oil reaches the plateau or may even slightly decline. The optimal catalyst amount was 1.5 wt % with a conversion of 99.8%; at a higher catalyst amount, the reaction mixture is likely to become more viscous, which can cause resistance to mass transfer in the liquid–liquid–solid system and, subsequently, cause the conversion rate of the catalyst to drop methyl ester.[50] The results obtained in this work are better than those obtained using the golden apple snail shell and the came Meretrix snail shells as catalysts.[21]

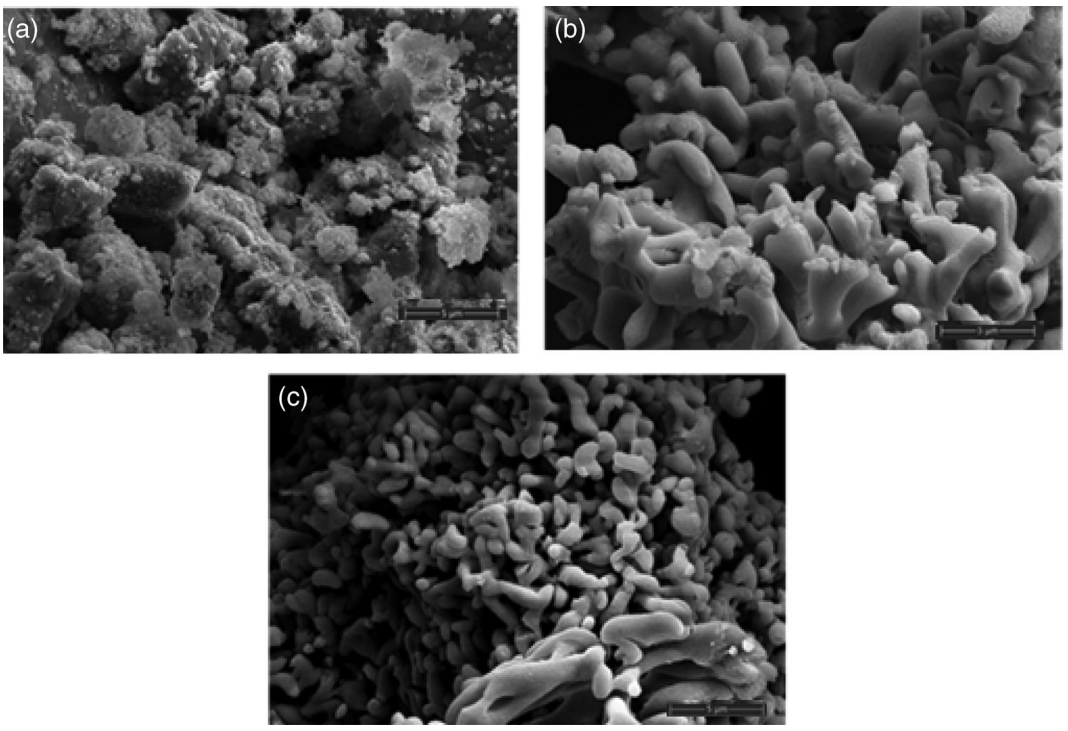

FIGURE 5 SEM images of the catalysts: (a) MSS1, (b) MSS2, and (c) MSS3 at a magnification of ×7500.

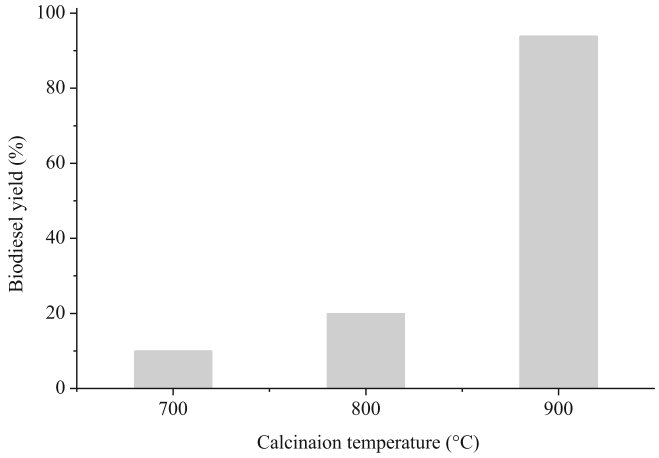

FIGURE 6 Effect of the calcination temperature on the biodiesel yield using MSS catalysts under the reaction conditions: (methanol/oil molar ratio 7.7:1, catalyst amount 1 wt. %).

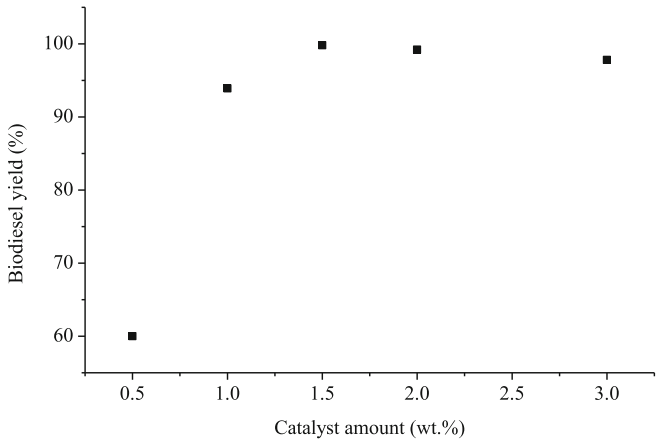

FIGURE 7 Effect of catalyst amount on the biodiesel yield using MSS3 catalyst under the reaction condition: Methanol/ oil molar ratio 7.7:1.

3.2.3 | Effect of methanol/oil ratio on biodiesel yield

The influence of the molar ratio oil to methanol on the conversion of frying waste oils to biodiesel was studied in the range (6.4:1, 7.7:1, 9:1, 10.25:1) (Figure 8). It is shown that the molar ratio of oil to methanol influences the conversion of oil to biodiesel. Figure 8 clearly shows the influence of the methanol/oil molar ratio on the yield of biodiesel obtained from the transesterification of frying waste oils using a heterogeneous catalyst derived from the shells of murguta snails. Increasing the methanol/oil molar ratio from 6.4:1 to 9:1 significantly increases biodiesel yield. More by increasing the amount of methanol more by requiring the formation of methoxy species on the surface of CaO, and this will divert the balance of the transesterification reaction towards the formation of biodiesel. However, further increases in the methanol/oil ratio up to 10.25:1 have a negative effect on the transesterification reaction. Because according to

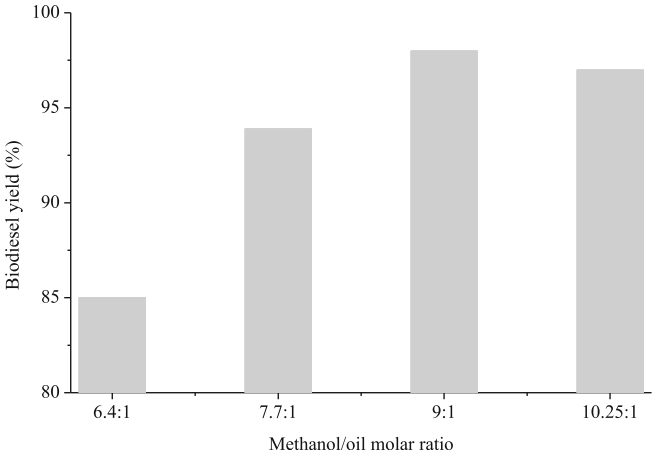

FIGURE 8 Effect of oil to methanol molar ratio on biodiesel yield using 1 wt. % MSS3.

Refs. [51–53], a high methanol content promotes the reverse reaction. Probably the reverse reaction can occur between biodiesel and glycerol formed to give monoglycerides and diglycerides behaving as a co-solvent. This would lead to a decrease in yield and will inhibit the transesterification reaction.[51]

High feedstock cost is a serious economic disadvantage of biodiesel. Meanwhile, the final properties of the biodiesel are affected greatly by the qualities of the iodine value, the water content, and the free fatty acid content of the feedstock. Thus, the feedstock used for biodiesel production is needed to be analyzed and controlled.

FTIR analysis was carried out to identify the main functions in biodiesel produced under the transesterification reaction using MSS3 catalyst with a methanol/oil molar ratio equal to 7.7:1 (Figure 9). The change between the oil and the biodiesel spectra was observed in the region of 1000-1500 m^{-1}. This region is known as the fingerprint region for the produced biodiesel, where a new peak appeared during the transesterification reaction.[54] So, the peak at 1437 cm^{-1} in the biodiesel spectrum corresponds to the asymmetric stretching –CH3, whereas this peak is not observed in the frying oil spectrum[55] indicated the transformation of frying oil into biodiesel.[56] The glycerol group O–CH2 stretching was attributed to the absorbance peak at 1370 cm^{-1} which was found in frying oil but absent in the biodiesel spectrum.[57] The peak obtained at 1195 cm^{-1}, attributed to the stretching of O—CH_3, confirmed the formation of biodiesel. The C—H (sp^2) elongating band located at 3011 cm^{-1} in both frying oil and biodiesel. The bands located at 2921 and 2852 cm^{-1} were characteristic of asymmetric and symmetric stretching and bending C—H alkyl, respectively. The strong intensity of elongating vibrations at 1742 cm^{-1} attributed to the stretching of —C═O in both oil and biodiesel.[58] The peak located at 1460 cm^{-1} confirms the existence of the alkane group (C—H).

The peaks at 1447 cm^{-1} for —CH3 asymmetric bending and 1200 cm^{-1} for O—CH_3 stretching confirmed the conversion of used frying oil into biodiesel, whereas these IR peaks did not exist in the IR spectrum of the oil,[59] as shown in the figure. The out-of-plane C—H (sp^3) band was found at 722 cm^{-1}. The differences between the oil and

the biodiesel spectrum can be summed up in the appearance of the methyl ester functional groups in the biodiesel. After its transformation to biodiesel, novel bands appeared at 1437, 1196, and 1160 cm^{-1} attributed to the methyl ester (—O—CH_3) group. These bands originated from the alcohol C—O group at 1158 cm^{-1} (Figure 9a).[60] The IR band in the range 1370–1400 cm^{-1} gives information about the existence of O—CH_2 groups in glycerol such as moiety of triglycerides, diglycerides, and monoglycerides.[59] Stretching vibration of C—O from ester is observed at 1234, 1119, and 1026 cm^{-1}.[61]

3.3 | Analysis transesterification products

3.3.1 | ^{1}H-NMR and ^{13}C-NMR analysis

Biodiesel produced from frying oil using a catalyst MSS3 is also characterized by ^{1}H-NMR and ^{13}C-NMR spectroscopies (Figures 10 and Figure 11). It is observed that the major difference between the ^{1}H-NMR spectra of oil and biodiesel is the disappearance of signals characteristic of glyceridic protons and olefinic hydrogen at multiple peaks 4.21 and 5.31 ppm[62,63]. The appearance of a single signal at 3.66 ppm represents the methoxy protons of the ester functionality during the conversion of oil to methyl ester (—CO_2CH_3).[64] The signal at 3.49 ppm is bound to methanol, which is a reactant in the transesterification reaction.[65]

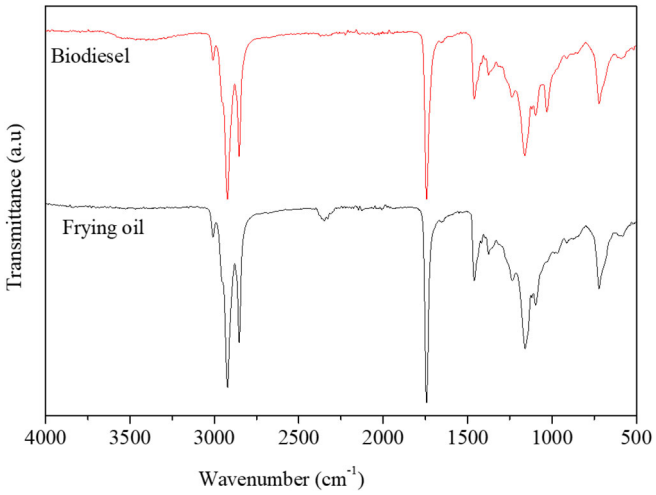

FIGURE 9 FTIR spectra of waste frying oil and biodiesel using a catalyst MSS3 (1 wt%) with methanol/oil molar ratio 7.7:1.

The signals at 2.28 ppm result from protons on CH1 groups adjacent to the methyl or glyceryl ester fragments ($CH_2CO_2CH_3$ for the methyl esters). These signals can be used for quantification using Equation (2) as described above. The yield of triglycerides to the corresponding methyl esters was 94%. —CH_2 protons related to the glyceride of waste oil, which appeared in the range of δ[4.00–4.5] ppm (Figure 10a), completely disappeared after reaction (Figure 10b), in agreement with the result of Moawia et al.[66] The results of ^{13}C-NMR technique of biodiesel (Figure 10b) demonstrated the presence of peaks at 173.96 and 51.17 ppm characteristic of carbonyl ester (COO) and CO, respectively. The same results have been confirmed by other studies.[67–69] Whereas, for the waste frying oil (Figure 11a), the peaks located at 62 and 68 ppm attributed to glyceryl carbon atoms in the triglyceride molecules disappeared, and the appearance of a new one at 51.38 (Figure 11b) due to the methoxy carbon is indicative enough for the desired transformation.[62]

3.3.2 | GC/MS results

The GC/MS results revealed the presence of hexadecanoic acid methyl ester, methyl 11-octadecenoate, eicosanoic acid methyl ester, methyl butanoate, docosanoic acid methyl ester, 11,14-eicosadienoic acid methyl ester, and tetracosanoic acid methyl ester as the methyl esters present in the biodiesel. The major methyl ester is the hexadecanoic acid methyl ester. The methyl ester profile of biodiesel prepared from used cooking oil and the fatty acid of this oil are

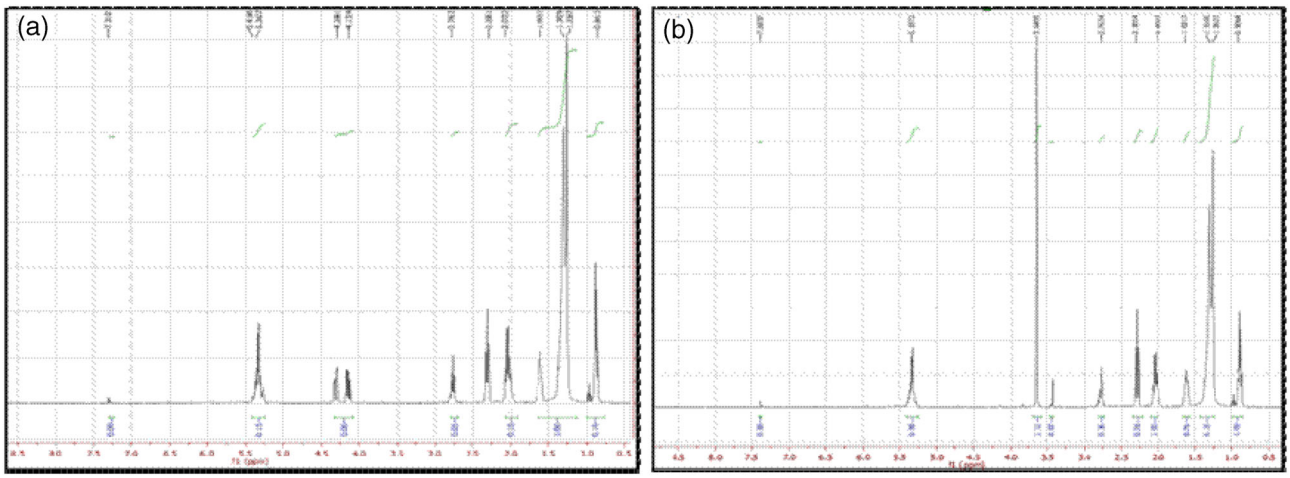

FIGURE 10 ^{1}H-NMR spectrum of (a) waste frying oil and (b) biodiesel spectra using 1 wt% MSS3 catalyst and a molar ratio methanol/oil = 7.7:1.

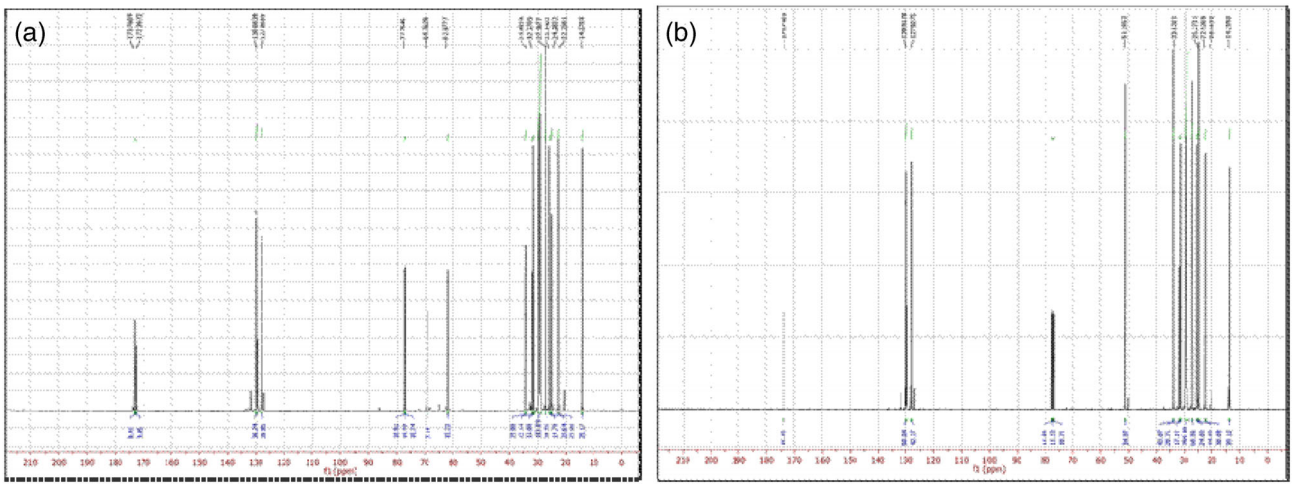

FIGURE 11 ^{13}C-NMR of (a) waste frying oil (b) produced biodiesel using 1 wt% MSS3 catalyst under methanol/oil molar ratio = 7.7:1.

TABLE 4 Compounds detected from waste frying oil.

Compounds identified	Acids	Molecular formula	Area (%)
Octanoic acid	Caprylic acid	$C_8H_{16}O_2$(C8:0)	0.06
Tetradecanoic acid	Myristic acid	$C_{14}H_{28}O_2$(C14:0)	0.08
9-Hexadecenoic acid	Palmitelaidic acid	$C_{16}H_{30}O_2$ (C16:0)	12.22
Heptadecanoic acid	Margaric acid	$C_{17}H_{34}O_2$(C17:0)	0.22
9-Octadecenoic acid (Z)-, methyl ester	Oleique acid	$C_{18}H_{34}O_2$(C18:1)	1.36
9,12-Octadecadienoic acid	Linoleic acid	$C_{18}H_{32}O_2$(C18:2)	66.18
Octadecanoic acid	Stearic acid	$C_{18}H_{36}O_2$(C18:0)	5.47
9,12,15-Octadecatrienoic acid	Linolenic acid	$C_{18}H_{30}O_2$(C18:3)	1.45
10-Nonadecenoic acid		$C_{19}H_{36}O_2$(C19:1)	0.17
2(1H)-Naphthalenone, octahydro-4a-methyl-7-(1-methylethyl)		$C_{13}H_{22}O$	1.99
11-Eicosenoic acid	Gondoicacid	$C_{20}H_{38}O_2$ (C20:1)	1.29
Eicosanoic acid	Arachidic acid	$C_{20}H_{40}O_2$ (C20:0)	2.18
Cycloheptanone, 2-isopropylidene Semicarbazone		$C_9H_{15}N_3O$	1.40
Naphthalene, decahydro-2,3-dimethyl		$C_{12}H_{22}$	1.95
Heneicosanoic acid	Heneicosylic	$C_{21}H_{42}O_2$(C21:0)	0.15
1-Cyclohexene-1-acetaldehyde, trimethyl	β-Cyclohomocitral	$C_{11}H_{18}O$(C11:1)	1.40
Docosanoic acid	Behenic acid	$C_{22}H_{44}O_2$(C22:0)	1.69
Tricosanoic acid	Tricosylic acid	$C_{23}H_{46}O_2$(C23:0)	0.21
Tetracosanoic acid	Lignocerique acid	$C_{24}H_{48}O_2$ (C24:0)	0.60

presented in Tables 3 and 4. The main methyl esters are as follows: linolelaidic acid, methyl ester $C_{19}H_{34}O_2$ (C18:2) 57.02%, Palmitic acid methyl ester $C_{17}H_{34}O_2$ (C16:0) 13.73%, Oleic acid methyl ester, methyl 11-octadecenoate (Methyl Octadecanoate) $C_{19}H_{36}O_2$ (C18:1) 11.60%, and Stearic acid methyl ester $C_{19}H_{38}O_2$ (C18:0) 6.17%. Linolenate acid methyl ester $C_{19}H_{32}O_2$ (C18:3) has a low percentage (~1.51%). Long-chain fatty acids are present as minor constituents. This result is consistent with that of Leung and Guo,[70] where the synthesized biodiesel from used frying oil was collected from Chinese restaurants. The study conducted by Huseyin Sanli et al.[71] carried out on frying oils gave rise to equivalent FAME profiles in our study with a low percentage of linolenate acid methyl ester. These components are able to improve not only some important fuel properties like cetane number, heat of combustion, oxidative stability, and kinematic viscosity (C18:1, C16:0) but also the cold flow properties of biodiesel (C18:2) as shown in the work of Knothe.[72]

To determine the composition of fatty acids, the produced biodiesel was examined by GC–MS. There were four main characteristic peaks of fatty acid methyl esters (FAME) for biodiesel production. Each peak corresponds to a fatty acid methyl ester component. The

TABLE 5 Compounds detected from biodiesel.

Compounds identified	Fatty Acid Methyl Ester (FAMEs)	Molecular formula	Area%
Hexadecanoic acid methyl ester	Palmitic acid methyl ester	$C_{17}H_{34}O_2$ (C16:0)	13.73
9-Hexadecenoic acid, methyl ester	Methylpalmitoleate	$CH_3OCO(CH_2)_7CH=CH–(CH_2)_5CH$ (C16:1)	0.1
11-Hexadecenoic acid, 15-methyl-, methyl ester	Methylisoheptade canoate	$C_{18}H_{34}O_2$ (17:1)	0.15
9,12-Octadecadienoic acid, methyl ester	Linolelaidic acid, methyl ester	$C_{19}H_{34}O_2$ (C18:2)	57.02
9-Octadecenoic acid (Z)-, methyl ester	Oleic acid, methyl ester	$C_{19}H_{36}O_2$ (C18:1)	11.60
Octadecanoic acid methyl ester	Stearic acid, methyl ester	$C_{19}H_{38}O_2$ (C18:0)	6.17
2(1H)-Naphthalenone, octahydro-4a methyl-7-(1-methylethyl)-(4aalpha, 7beta, 8abeta)-	Jatamansone	$C_{14}H_{24}O$	1.62
11-Eicosenoic acid, methyl ester	Gondoicacid Methyleicosenoate	$C_{21}H_{40}O_2$ (C20:1)	1.19
Eicosenoic acid, methyl ester	Arachidic acid methyl ester	$C_{21}H_{42}O_2$ (C20:0)	1.99
2-Propionyl-6-methyl-3,4-dihydropyran	(6-Methyl-3,4-dihydro-2H-pyran-2-yl)-1-propanone	$C_9H_{14}O_2$	0.48
9,12,15-Octadecatrienoic acid, methyl ester	Linolenate acid methyl ester elaidolinolenate	$C_{19}H_{32}O_2$(C18:3)	1.51
13-Docosenoic acid, methyl ester	Methylbrassidate	$C_{23}H_{44}O_2$	0.03
Docosanoic acid, methyl ester	Behenicacid, methyl ester	$C_{23}H_{46}O$ (C22:0)	1.50
13-Docosenoic acid, methyl ester	Methylbrassidate	$C_{23}H_{44}O_2$ (C22:1)	0.03
Tricosanoic acid, methyl ester	Methyl tricosanoate	$C_{24}H_{48}O_2$ (C23:0)	0.18
Tetracosanoic acid, methyl ester	Lignoceric acid methyl ester	$C_{25}H_{50}O$ (C24:0)	0.66

chemical composition for GC–MS result is regrouped in the Table 5. The major component present in the biodiesel is 9,12-octadecanoic acid methyl ester. The main methyl esters are as follows: linolelaidic acid methyl ester $C_{19}H_{34}O_2$ (C18:2) 57.02%, Palmitic acid methyl ester $C_{17}H_{34}O_2$ (C16:0)13.73%, Oleic acid, methyl ester $C_{19}H_{36}O_2$ (C18:1) 11.60% and Stearic acid methyl ester $C_{19}H_{38}O_2$ (C18:0) 6.17%. Linolenate acid methyl ester $C_{19}H_{32}O_2$ (C18:3) has a low percentage (∼1.51%). This result is consistent with that of Leung and Guo[70] who synthesized biodiesel from used frying oil collected from Chinese restaurants. The study conducted by Huseyin Sanli et al.[71] carried out on frying oils gave rise to equivalent FAME profiles in our study with a low percentage of linolenic acid methyl ester.

From the GCMS analysis the saturated fatty acids include methyl butanoate, tetracosanoic acid methyl ester, docosanoic acid methyl ester, hexadecanoic acid methyl ester and eicosanoic acid methyl ester which account for 71.1% of the biodiesel makeup. Similarly, 11,14-eicosadienoic acid methyl ester and methyl 11-octadecenoate (elaidic acid methyl ester) are unsaturated fatty acids and make up 28.59% of the biodiesel make up while 2H-1-benzopyran6-ol accounts for 0.31% of the biodiesel makeup. According to Ref. [73], the presence of low level of unsaturated fatty acids is desirable as these unsaturated fatty acids results in poor oxidative stability of the fuel while a high presence of saturated fatty acids enhances the biodiesel fuel oxidative capacity. Similarly, Mu Kaisan et al.,[73] reported that higher degree of unsaturation in the fatty acid methyl esters limits its suitability for use as a fuel due to high polymerization tendency which is caused by peroxidation. Therefore, since the predominant methyl ester is methyl hexadecanoate which is a saturated fatty acid and as such has an affinity for oxygen therefore the tendency for peroxidation to occur in the car engine leading to engine failure would not occur.

4 | CONCLUSION

A biodegradable, economical, and ecofriendly catalyst was successfully developed by simple calcination of waste mourguetas snail shells. CaO derived from these mourgueta snail shells demonstrated excellent catalytic activity for the transesterification of used frying oil, achieving a biodiesel yield of 99.8% under optimal conditions: room temperature, a reaction time of 24 hours, 1.5% MSS3 loading (relative to oil weight), and a methanol-to-oil molar ratio of 9:1. The high catalytic efficiency of MSS3 is directly linked to its purity, as confirmed by XRF, TGA, and CHNS elemental analysis. The results highlight the potential of mourguetas snail shells derived CaO as an efficient and sustainable catalyst for biodiesel production. The produced biodiesel was identified by ^{1}H-NMR and ^{13}C-NMR, GC/MS, FTIR analysis. Additionally, GC/MS analysis confirmed the presence of major fatty acid methyl esters (FAMEs), including methyl linolelaidate, methyl palmitate, methyl oleate, and methyl stearate. These results demonstrate that calcination at 900°C ensures a more complete conversion of $CaCO_3$ into CaO, which is crucial for applications such as catalysis where the active phase is CaO.

ACKNOWLEDGMENTS

This work was supported by the Directorate General for Scientific Research and Technological Development DGRSDT.

CONFLICT OF INTEREST STATEMENT

The authors declare no competing interests.

DATA AVAILABILITY STATEMENT

The data that support the findings of this study are available on request from the corresponding author. The data are not publicly available due to privacy or ethical restrictions.

ORCID

Amel Boudjemaa https://orcid.org/0000-0001-7429-6922

REFERENCES

1. Ngadi N, Hamdan NF, Hassan O, Putra Jaya R. Production of biodiesel from palm oil using eggshell waste as heterogeneous catalyst. *J Teknol*. 2016;78(9):9. doi:10.1016/j.Sc.2010.00372
2. Ameen M, Zafar M, Ahmad M, et al. Cleaner biofuel production via process parametric optimization of nonedible feedstock in a membrane reactor using a titania-based heterogeneous nanocatalyst: an aid to sustainable energy development. *Membranes*. 2023;13(12):889.
3. Abbasi TU, Ahmad M, Asma M, et al. High efficient conversion of *Cannabis sativa* L. biomass into bioenergy by using green tungsten oxide nano-catalyst towards carbon neutrality. *Fuel*. 2023;336:126796.
4. Lang X, Dalaia AK, Bakhshia NN, Reaney MJ, Hertz BP. Preparation and characterization of bio-diesels from various bio-oils. *Bioresour Technol*. 2001;80(1):53-62. doi:10.1016/s0960-8524(01)00051-7
5. Zhang WB. Review on analysis of biodiesel with infrared spectroscopy. *Renew Sustain Energy Rev*. 2012;16(8):6048-6058.
6. Bibi H, Ahmad M, Osman AI, et al. Green synthesis of highly active and recyclable chromium oxide nanocatalyst for biodiesel production from novel nonedible oil seeds. *GCB Bioenergy*. 2024;16(5):e13140.
7. Siddiquee MN, Rohani S. Experimental analysis of lipid extraction and biodiesel production from wastewater sludge. *Fuel Process Technol*. 2011;92(12):2241-2251. doi:10.1016/j.fuproc.2011.07.018
8. Wang R, Zhou WW, Hanna MA, et al. Biodiesel preparation, optimization, and fuel properties from non-edible feedstock, *Datura stramonium* L. *Fuel*. 2012;91(1):182-186.
9. Zhang Y, Dubé M, McLean D, Kates M. Biodiesel production from waste cooking oil: 2. Economic assessment and sensitivity analysis. *Bioresour Technol*. 2003;90(3):229-240. doi:10.1016/s0960-8524(03)00150-0
10. Math MC, Kumar SP, Chetty SV. Technologies for biodiesel production from used cooking oil – a review. *Energy Sustain Dev*. 2010;14(4):339-345. doi:10.1016/j.esd.2010.08.001
11. Van Gerpen J, Knothe G. Basics of the transesterification reaction. *The Biodiesel Handbook*; 2005:26-41. AOCS Press.
12. Graboski MS, McCormick RL. Combustion of fat and vegetable oil derived fuels in diesel engines. *Prog Energy Combust Sci*. 1998;24:125-164. doi:10.1016/S0360-1285(97)00034-8
13. Helwani Z, Othman MR, Aziz N, Fernando WJN, Kim J. Technologies for production of biodiesel focusing on green catalytic techniques: a review. *Fuel Process Technol*. 2009;90(12):1502-1514.
14. Tan YH, Abdullah MO, Hipolito CN. Comparison of biodiesel production between homogeneous and heterogeneous base catalysts. *Appl Mech Mater*. 2016;833(2016):71-77. doi:10.4028/www.scientific.net/AMM.833.71
15. Wong YC, Ang RX. Study of calcined eggshell as potential catalyst for biodiesel formation using used cooking oil. *Open Chem*. 2018;16:1166-1175.
16. Boey PL, Maniam GP, Hamid SA. Performance of calcium oxide as a heterogeneous catalyst in biodiesel production: a review. *Chem Eng J*. 2011;168(1):15-22.
17. Sivasamy A, Cheah KY, Fornasiero P, Kemausuor F, inoviev S, Miertus S. Catalytic applications in the production of biodiesel from vegetable oils. *ChemSusChem*. 2009;2(4):278-300. doi:10.1002/cssc.20080025
18. Wei Z, Xu C, Li B. Application of waste eggshell as low-cost solid catalyst for biodiesel production. *Bioresour Technol*. 2009;100(11):2883-2885. doi:10.1016/j.biortech.2008.12.039
19. Erchamo YS, Mamo TT, Workneh GA, Mekonnen YS. Improved biodiesel production from waste cooking oil with mixed methanol–ethanol using enhanced eggshell-derived CaO nano-catalyst. *Sci Rep*. 2021;11:6708. doi:10.1038/s41598-021-86062-z
20. Roschat W, Siritanon T, Kaewpuang T, Yoosuk B, Promarak V. Economical and green biodiesel production process using river snail shells-derived heterogeneous catalyst and co-solvent method. *Bioresour Technol*. 2016;209(2016):343-350. doi:10.1016/j.biortech.2016.03.03
21. Viriya-empikul N, Krasae P, Puttasawat B, Yoosuk B, Chollacoop N, Faungnawakij K. Waste shells of mollusk and egg as biodiesel production catalysts. *Bioresour Technol*. 2010;101(10):3765-3767. doi:10.1016/j.biortech.2009.12.079
22. Rezaei R, Mohadesi M, Moradi GR. Optimization of biodiesel production using waste mussel shell catalyst. *Fuel*. 2013;109:534-541.
23. Nakatani N, Takamori H, Takeda K, Sakugawa H. Transesterification of soybean oil using combusted oyster shell waste as a catalyst. *Bioresour Technol*. 2009;100(3):1510-1513. doi:10.1016/j.biortech.2008.09.007
24. Asuquoa AJ, Zhanga X, Linb L, Lia J. Green heterogeneous catalysts derived from fermented kola nut pod husk for sustainable biodiesel production. *International Journal of Green Energy*. 2024;21(10):2218-2227.
25. Izquierdo S, Silvero G, DuránValle CJ, LópezCoca IM. Green heterogeneous catalysts for cleaner solvent-free production of acetates. *J Porous Mater*. 2023;30:847-858.
26. Li Y, Huang K-H, Morato NM, Cooks RG. Glass surface as strong base, green heterogeneous catalyst and degradation reagent. *Chem Sci*. 2021;12:9816-9822.
27. Almasi S, Ghobadian B, Soufi MD, Kakavandi B, Aubin J. Calcium oxide anchored on magnetic waste-based activated carbon (MAC@CaO): a sustainable green heterogeneous catalyst for bio-based fuel and lubricant production. *Biomass Bioenergy*. 2024;182(1):107071. doi:10.1016/j.biombioe.2024.107071
28. Buasri A, Chaiyut N, Loryuenyong V, Worawanitchaphong P, Trongyong S. Calcium oxide derived from waste shells of mussel, cockle, and scallop as the heterogeneous catalyst for biodiesel production. *Scientific World Journal*. 2013;2013(1):460923.
29. Das S, Anal JMH, Kalita P, Saikia L, Rokhum SL. Process optimization of biodiesel production using waste snail shell as a highly active nanocatalyst. *Int J Energy Res*. 2023;2023(1):6676844.
30. Laskar IB, Rajkumari K, Gupta R, Chatterjee S, Paul B, Rokhum SL. Waste snail shell derived heterogeneous catalyst for biodiesel production by the transesterification of soybean oil. *RSC Adv*. 2018;8(36):20131-20142.
31. Hadiyanto H, Lestari SP, Abdullah A, Widayat W, Sutanto H. The development of fly ash-supported CaO derived from mollusk shell of Anadara granosa and Paphia undulata as heterogeneous CaO catalyst in biodiesel synthesis. *Int J Energy Environ Eng*. 2016;7:297-305.
32. Arenas-Quevedo MG, Manríquez ME, Wang JA, et al. ZnO-doped CaO binary Core–Shell catalysts for biodiesel production via Mexican palm oil transesterification. *Inorganics*. 2024;12(2):51.

33. Helwani Z, Ramli M, Saputra E, et al. Impregnation of CaO from eggshell waste with magnetite as a solid catalyst (Fe_3O_4/CaO) for transesterification of palm oil off-grade. *Catalysts*. 2020;10:164.
34. Moradi G, Mohadesi M, Hojabri Z. Biodiesel production by CaO/SiO_2 catalyst synthesized by the sol–gel process. *Reaction Kinetics, Mechanisms and Catalysis*. 2014;113:169-186.
35. Alsaiari RA, Musa EM, Rizk MA. Effects of calcination temperature of eggshell-derived CaO as a catalyst for biodiesel production from waste cooking oil. *S Afr J Chem*. 2023;77(1):30-35.
36. Buasri A, Chaiyut N, Loryuenyong V, Wongweang C, Khamsrisuk S. Application of eggshell wastes as a heterogeneous catalyst for biodiesel production. *Sustainable Energy*. 2013;1(2):7-13. doi:10.12691/rse-1-2-1
37. Gaide I, Makareviciene V, Sendzikiene E, Kazancev K. Snail shells as a heterogeneous catalyst for biodiesel fuel production. *Processes*. 2023;11:260. doi:10.3390/pr11010260
38. Birla A, Singh B, Upadhyay SN, Sharma YC. Kinetics studies of synthesis of biodiesel from waste frying oil using a heterogeneous catalyst derived from snail shell. *Bioresour Technol*. 2012;106:95-100.
39. Trisupakitti S, Ketwong C, Senajuk W, Phukapak C, Wiriyaumpaiwong S. Golden apple cherry snail shell as catalyst for heterogeneous transesterification of biodiesel. *Braz J Chem Eng*. 2018;35:1283-1291.
40. Bailer J, Hödl P, de Hueber K, Mitelbach M, Plank C, Schindlbauer H. *Handbook of Analytical Methods for Fatty Acid Methyl Esters Used as Biodiesel Fuel Substitutes*. Fichte, Research Institute for Chemistry and Technology of Petroleum Products, University of Technology; 1994:36-38.
41. Naureen R, Tariq M, Yusoff I, Chowdhury AJK, Ashraf MA. Synthesis, spectroscopic and chromatographic studies of sunflower oil biodiesel using optimized base catalyzed methanolysis. *Saudi J Biol Sci*. 2015;22(3):332-339. doi:10.1016/j.sjbs.2014.11.010
42. Sustaita-Rodríguez A, Ramos-Sánchez VH, Camacho-Dávila AA, Zaragoza-Galán G, Espinoza-Hicks JC, Chávez-Flores D. Lipase catalyzed epoxidation of fatty acid methyl esters derived from unsaturated vegetable oils in absence of carboxylic acid. *Chem Cent J*. 2018;12:39. doi:10.1186/s13065-018-0409-2
43. Kara K, Ouanji F, El Mahi M, Lotfi EM, Kacimi M, Mahfoud Z. Biodiesel synthesis from vegetable oil using eggshell waste as a heterogeneous catalyst. *Biofuels*. 2021;12(9):1083-1089.
44. Navajas A, Issariyakul T, Arzamendi G, Gandía LM, Dalai AK. Development of eggshell derived catalyst for transesterification of used cooking oil for biodiesel production. *Asia-Pacific J Chem Eng*. 2013;8(5):742-748. doi:10.1002/apj.1715
45. Mar WW, Somsook E. Methanolysis of soybean oil over KCl/CaO solid base catalyst for biodiesel production. *Sci Asia*. 2012;38:90-94. doi:10.2306/scienceasia1513-1874.2012.38.090
46. Karaoui M, Hsissou R, Alami M, Assouag M. Physico-chemical characterization of snail shells powder prepared by mechanochemical processes and thermal treatment. *J Met Mater Miner*. 2023;33(2):139-147.
47. Karunadasa KS, Manoratne CH, Pitawala HMTGA, Rajapakse RMG. Thermal decomposition of calcium carbonate (calcite polymorph) as examined by in-situ high-temperature X-ray powder diffraction. *J Phys Chem Solid*. 2019;134:21-28.
48. Zhuang D, Chen Z, Sun B. Thermal decomposition of calcium carbonate at multiple heating rates in different atmospheres using the techniques of TG, DTG, and DSC. *Crystals*. 2025;15(2):108.
49. Mohammed AK, Alkhafaje ZA, Rashid IM. Heterogeneously catalyzed transesterification reaction using waste snail shell for biodiesel production. *Heliyon*. 2023;9(6):e17094.
50. Madhuvilakku R, Piraman S. Biodiesel synthesis by TiO_2–ZnO mixed oxide nanocatalyst catalyzed palm oil transesterification process. *Bioresour Technol*. 2013;150(2013):55-59. doi:10.1016/j.biortech.2013.09.083
51. Teng G, Gao L, Xiao G, Liu H. Transesterification of soybean oil to biodiesel over heterogeneous solid base catalyst. *Energy Fuel*. 2009;23(9):4630-4634.
52. Kim HJ, Kang BS, Kim MJ, et al. Transesterification of vegetable oil to biodiesel using heterogeneous base catalyst. *Catal Today*. 2004;93-95:315-320. doi:10.1016/j.cattod.2004.06.007
53. Siatis NG, Kimbaris AC, Pappas CS, Tarantilis PA, Polissiou MG. Improvement of biodiesel production based on the application of ultrasound: monitoring of the procedure by FTIR spectroscopy. *J Am Oil Chem Soc*. 2006;83:53-57.
54. Mahamuni NN, Adewuyi YG. Fourier transform infrared spectroscopy (FTIR) method to monitor soy biodiesel and soybean oil in transesterification reactions, petrodiesel – biodiesel blends, and blend adulteration with soy oil. *Energy Fuel*. 2009;23(7):3773-3782.
55. Yadav M, Singh V, Sharma YC. Methyl transesterification of waste cooking oil using a laboratory synthesized reusable heterogeneous base catalyst: process optimization and homogeneity study of catalyst. *Energ Conver Manage*. 2017;148:1438-1452. doi:10.1016/j.enconman.2017.06.024
56. Mello VM, Oliveira FC, Fraga WG, do Nascimento CJ, Suarez PA. Determination of the content of fatty acid methyl esters (FAME) in biodiesel samples obtained by esterification using 1H NMR spectroscopy. *Magn Reson Chem*. 2008;46:1051-1054.
57. Dubé MA, Zheng S, McLean DD, Kates M. A comparison of attenuated total reflectance-FTIR spectroscopy and GPC for monitoring biodiesel production. *J Am Oil Chem Soc*. 2004;81(6):599-603. doi:10.1007/s11746-006-0948-x
58. Soares IP, Rezende TF, Silva RC, Castro EVR, Fortes ICP. Multivariate calibration by variable selection for blends of raw soybean oil/biodiesel from different sources using Fourier transform infrared spectroscopy (FTIR) spectra data. *Energy Fuel*. 2008;22(3):2079-2083. doi:10.1021/ef700531n
59. Mumtaz MW, Adnan A, Anwar F, et al. Response surface methodology: an emphatic tool for optimized biodiesel production using rice bran and sunflower oils. *Energies*. 2012;5(9):3307-3328. doi:10.3390/en5093307
60. Lamichhane G, Khadka S, Adhikari S, Koirala N, Poudyal DP. Biofuel production from waste cooking oils and its physicochemical properties in comparison to petrodiesel. *Nepalese J Biotechnol*. 2020;8(3):87-94. doi:10.3126/njb.v8i3.33661
61. Abdullah RNRS, Sianipar DA, Nata IF. Conversion of palm oil sludge to biodiesel using alum and KOH as catalysts. *Sustain Environ Res*. 2017;27(6):315-319. doi:10.1016/j.serj.2017.07.002
62. Deka DC, Basumatary S. High quality biodiesel from yellow oleander (*Thevetia peruviana*) seed oil. *Biomass Bioenergy*. 2011;35(5):1797-1803.
63. Park SH, Khan N, Lee S, et al. Biodiesel production from locally sourced restaurant waste cooking oil and grease: synthesis, characterization, and performance evaluation. *ACS Omega*. 2019;4:7775-7784. doi:10.1021/acsomega.9b00268
64. Rana S, Haque M, Poddar S, Sujan S, Hossain M, Jamal MS. Biodiesel production from non-edible Mahoganyseed oil by dual step process and study of its oxidation stability. *Bangladesh J Sci Ind Res*. 2015;50:77-86. doi:10.3329/bjsir.v50i2.24348
65. Abdullah RF, Rashid U, Hazmi B, Ibrahim ML, Tsubota T, Alharthi FA. Potential heterogeneous nano-catalyst via integrating hydrothermal carbonization for biodiesel production using waste cooking oil. *Chemosphere*. 2022;28:131913. doi:10.1016/j.chemosphere.2021.131913
66. Moawia RM, Nasef MM, Mohamed NH, Ripin A, Farag H. Production of biodiesel from cottonseed oil over aminated flax fibres catalyst: kinetic and thermodynamic behaviour and biodiesel properties. *Adv Chem Eng Sci*. 2019;9:281-298. doi:10.4236/aces.2019.94021
67. Doudin KI. Quantitative and qualitative analysis of biodiesel by NMR spectroscopic methods. *Fuel*. 2021;284:119114. doi:10.1016/j.fuel.2020.119114
68. Do Rego T, Kpoviessi DSS, Gbaguidi F, et al. Transestérification de la tributyrine catalysée par la montmorillonite K10 en présence de l'éthanol. *Int J Biol Chem Sci*. 2010;4(5):1501-1508.

69. Tariq M, Ali S, Ahmad F, et al. Identification, FT-IR, NMR (1H and 13C) and GC/MS studies of fatty acid methyl esters in biodiesel from rocket seed oil. *Fuel Process Technol*. 2011;92(3):336-341. doi:10.1016/j.fuproc.2010.09.02
70. Leung DYC, Guo Y. Transesterification of neat and used frying oil: optimization for biodiesel production. *Fuel Process Technol*. 2006;87(10):883-890.
71. Sanli H, Canakci M, Alptekin E. Predicting the higher heating values of waste frying oils as potential biodiesel feedstock. *Fuel*. 2014;115:850-854. doi:10.1016/j.fuel.2013.01.015
72. Knothe G. "Designer" biodiesel: optimizing fatty Ester composition to improve fuel properties. *Energy Fuel*. 2008;22(2):1358-1364. doi:10.1021/ef700639e
73. Koria L, Nithya G. Analysis of Datura stramonium Linn. Biodiesel by gas chromatography – mass spectrometry (GC-MS) and influence of fatty acid composition on the fuel related characteristics. *J Phytology*. 2012;4(1):6-9.

How to cite this article: Chaib A, Benammar S, Hamitouche A-E, Bachari K, Boudjemaa A. Synthesis of green biodiesel using heterogeneous catalyst derived from snail shells. *Environ Prog Sustainable Energy*. 2025;e70084. doi:10.1002/ep.70084

ABOUT UMT FACULTY

SDI

Selective Dissemination of Information (SDI) service is a current-awareness service offered by the PSNZ for UMT Faculty Members. The contents selection criteria include current publications (last 5 years), highly cited and most viewed/downloaded documents. The contents with pdf full text from subscribed databases are organized and compiled according to a monthly theme which is determined based on the topics of specified interest.

For more information or further assistance, kindly contact us at 09-6684185/4298 or email to psnz@umt.edu.my/sh_akmal@umt.edu.my

Thank you.

Perpustakaan Sultanah Nur Zahirah
Universiti Malaysia Terengganu
21030 Kuala Nerus, Terengganu.

Tel. : 09-6684185 (Main Counter)
Fax : 09-6684179
Email : psnz@umt.edu.my